APPLICATION OF SEQUENCE STRATIGRAPHY TO THE NONMARINE UPPER CRETACEOUS TWO MEDICINE FORMATION, WILLOW CREEK ANTICLINE, NORTHWESTERN, MONTANA

by

Jessica Anne Shelton

A thesis submitted in partial fulfillment
of the requirements for the degree

of

Master of Science

in

Earth Sciences

MONTANA STATE UNIVERSITY
Bozeman, Montana

April 2007

© COPYRIGHT

by

Jessica Anne Shelton

2007

All Rights Reserved

APPROVAL

of a thesis submitted by

Jessica Anne Shelton

This thesis has been read by each member of the thesis committee and has been found to be satisfactory regarding content, English usage, format, citations, bibliographic style, and consistency and is ready for submission to the Division of Graduate Education.

Dr. David W. Bowen

Approved for the Department of Earth Sciences

Dr. Stephan G. Custer

Approved for the Division of Graduate Education

Dr. Carl A. Fox

STATEMENT OF PERMISSION TO USE

In presenting this thesis in partial fulfillment of the requirements for a master's degree at Montana State University, I agree that the Library shall make it available to borrowers under rules of the Library.

If I have indicated my intention to copyright this thesis by including a copyright notice page, copying is allowable only for scholarly purposes, consistent with "fair use" as prescribed by the U.S. Copyright Law. Requests for permission for extended quotation from or reproduction of this thesis in whole or in parts may be granted only by the copyright holder.

Jessica Anne Shelton

April 2007

ACKNOWLEDGEMENTS

I would like to thank my committee members, Dr. David Bowen, Dr. Jim Schmitt, and Dr. David Varricchio for all of their help in the research involved in, and in the writing of this thesis. I would like to thank Dr. Schmitt for helping keep this thesis on track, and Dr. Varricchio and Dr. Bowen for their assistance in the field. I would like to thank the Soot and Dust Group and NASA Montana Space Grant Consortium, and primarily Dr. Varricchio and Russell Raven for their funding for bentonite dating. I would also like to thank the NASA Montana Space Grant Consortium for the 2004-2005 fellowship I received. I would like to thank Dan Miggins of the USGS Denver Geochronology Laboratory and Dr. Carl Swisher of Rutgers University for their help with bentonite dating.

Additionally, I want to thank a number of fellow graduate students including: Josh Bonde, Adriana Fernandez, Luke Wilson, Robert Kambic, Julie Reisner, Bryan Turner, and Eric Williams for their suggestions and continuing encouragement. Finally, I would like to thank the Montana State University Earth Sciences Department for allowing me to conduct this research.

TABLE OF CONTENTS

1. INTRODUCTION…… 1

Purpose……... 1
Location…….… 2
Geologic Setting…….....4
Previous Work……..... 6

2. BACKGROUND: NONMARINE SEQUENCE STRATIGRAPHY……... 7

3. BACKGROUND: CONTROLS ON SEQUENCE DEVELOPMENT…….....10

Introduction.…….…….....10
Campanian Sea Level Change…….. 10
Global Sea Level Change…….....10
Cretaceous Western Interior Seaway……. 13
Eagle Regression…….....15
Claggett Transgression…….....17
Claggett Regression……. 19
Bearpaw Transgression…….....19
Campanian Climate Change……. 22
Campanian Climate Summary……... 22
Campanian Tectonism in Northwestern Montana……. 26
Introduction…….....26
Lewis-Eldorado-Hoadley Thrust Slab…….… 27
Late Cretaceous Igneous Activity in Montana…….…….....30

4. BACKGROUND: IMPORTANT TWO MEDICINE FORMATION ASSOCIATIONS…….....33

Two Medicine Formation Type Section Upper Discontinuity……. 33
Two Medicine Formation Type Section Lower Discontinuity…. 36

5. METHODS…… 39

6. RESULTS: WILLOW CREEK ANTICLINE LITHOFACIES…… 42

Introduction…… .....…42
Bentonite Layer (B)…….. 43
Description……..…… 43
Hydrodynamic Conditions…….… 43

TABLE OF CONTENTS - CONTINUED

Laminated Sandstone, Siltstone, & Mudstone (Fl)..... 46
Description.....46
Hydrodynamic Conditions.....46

Massive Mudstone (Fm).....47
Description.....47
Hydrodynamic Conditions.....47

Carbonate-Rich, Color Mottled Massive Mudstone (Fmc)..... ..49
Description.....49
Hydrodynamic Conditions.....49

Charophytiferous Limestone (Lc).....49
Description.....49
Hydrodynamic Conditions.....50

Horizontally-Bedded Sandstone (Sh).....51
Description.....51
Hydrodynamic Conditions.....52

Massive Sandstone (Sm).....53
Description.....53
Hydrodynamic Conditions.....54

Carbonate Cemented Sandstone with Pupal Cases (Sw)..... 55
Description.....55
Hydrodynamic Conditions.....55

Ripple Cross-Laminated Sandstone (Sr).....57
Description.....57
Hydrodynamic Conditions.....57

Trough Cross-Bedded Sandstone (St).....58
Facies Assemblages.....58
Hydrodynamic Conditions.....59

Non-Lacustrine Carbonates 60
Light Grey, Well-Indurated Carbonate (C)..... 62
Description.....62
ModeFormation.....62

TABLE OF CONTENTS - CONTINUED

Nodular to Discontinuously-Bedded Oxidized Carbonate (P).. ……..…63
Description…….....63
ModeFormation…….....….63

7. RESULTS: WILLOW CREEK ANTICLINE LITHOFACIES ASSOCIATIONS…….66

Introduction…….....…66
Upward Transition from Trough Cross-bedded (St) to Horizontally-Bedded (Sh) to Ripple Cross-Laminated (Sr) Sandstone …….....……..66
Upward Transition from Horizontally-bedded (Sh) to Ripple Cross-Laminated (Sr) Sandstone……..69
Upward Transition from Horizontally-Bedded (Sh) to Trough Cross-Bedded (St) Sandstone…….……..…71
Alternating Massive Mudstone (Fm) and Charophytiferous Limestone (Lc)… …….74
Carbonate-rich, Color Mottled Massive Mudstone (Fmc) and Light Grey, Well-Indurated Carbonate (C)……...…..75

8. WILLOW CREEK ANTICLINE SANDSTONE BODY CHARACTERISTICS.....81

Introduction……..81
Stratigraphically Lower Fluvial Deposits…… 81
Minor Sandstones……...…81
Major Sandstones……...…83
Stratigraphically Higher Fluvial Deposits…… ..…..84
Minor Sandstones……...…….84
Major Sandstones……...…….84

9. DISCUSSION: DEPOSITIONAL ENVIRONMENT OF THE TWO MEDICINE FORMATION, WILLOW CREEK ANTICLINE…… …..87

Introduction……..87
Fluvial Deposits…… …88
Anastomosing River Systems…… …88
Introduction……88
Channel Morphology and Migration…… ..89
Avulsion.....91
Floodplain Vegetation…….……93
Summary……...96
Ephemeral Fluvial Systems……...…97
Introduction……...…97

TABLE OF CONTENTS - CONTINUED

Thin, Horizontally-Bedded Sandstones, with Mudstone Rip-Up Clasts… ……100
Massive, Structureless Sandstones……..….103
Semi-Arid Climate…….…..104
Textural and Compositional Maturity, and Crevasse Splay Deposits…..…… 104
Other Lithofacies…… ….105
Sandbody Width:Thickness Ratios……..…105
Summary…….…106
Lacustrine Deposits……107
Ancient Analogues……..110
Summary……112
Non-Lacustrine Carbonate Deposits…….…..113

10. DISCUSSION OF RESULTS…… .....…120

Introduction…….....…..120
Change from Fluvial and Floodplain to Lacustrine Facies….…….….…120
Introduction…….....…….120
Possible Autocyclic Cause……...……...121
Possible Allocyclic Causes…… ...……..122
Eustatic Sea Level Controls…….....122
Tectonic Controls……...……..123
Climatic Controls……...…..129
Summary……...……129
Change from Lacustrine to Fluvial and Floodplain Facies……....……131
Introduction…….....131
Possible Autocyclic Cause……...…...133
Possible Allocyclic Causes…… ...……..133
Eustatic Sea Level Controls…….....…133
Tectonic Controls…….....…135
Summary…….....…137
Autocyclic Versus Allocyclic Causes……...….138

11. SIGNIFICANCE TO DINOSAUR PALEONTOLOGY…….....140

12. SIGNIFICANCE TO THE MANSON IMPACT EVENT……..…… 143

13. SUMMARY…….....…..145

REFERENCES CITED……..…...…..149

APPENDICES..……...…… .....……..163

TABLE OF CONTENTS - CONTINUED

APPENDIX A: WILLOW CREEK ANTICLINE MEASURED SECTIONS……..……..……..… 164

TABLE OF CONTENTS - CONTINUED

APPENDIX B: WILLOW CREEK ANTICLINE MEASURED SECTION DESCRIPTIONS……..…… 189

APPENDIX C: CORRELATION OF WILLOW CREEK ANTICLINE, TWO MEDICINE FORMATION TYPE SECTION, AND SEVEN MILE HILL AREA MEASURED SECTION DISCONTINUITIES…… ….216

APPENDIX D: SE-NW STRATIGRAPHIC CROSS SECTION MEASURED SECTIONS…….218

APPENDIX E: S/SW-N/NE STRATIGRAPHIC CROSS SECTION THROUGH WILLOW CREEK ANTICLINE MEASURED SECTIONS……...220

LIST OF FIGURES

Figure Page

1. Map showing location of present day Two Medicine Formation and Judith River Formation exposures …… .....…….3

2. View of southeastern portion of Willow Creek anticline taken from top of Thunder Dome…….....……3

3. View of northwestern portion of Willow Creek anticline taken from top of Thunder Dome…….....……4

4. Map showing divisions of a foreland basin…… ....……5

5. Generalized stratigraphic relationships between the Two Medicine Formation and adjacent formations…… .....….5

6. Chart summarizing global eustatic sea level cycles and Western Interior Seaway cycles for the Upper Coniacian through Lower Maastrichtian…….....11

7. Chart summarizing the three main controls on sequence development in northwestern Montana during the Campanian…….....….12

8. Location of Cretaceous Western Interior Seaway during the Campanian…… 13

9. Diagram of present day state of Montana, USA showing the approximate changeing position of the western paleoshoreline of the Cretaceous Western Interior Seaway during the early Early Campanian Eagle Regression (R7)…… 16

10. Diagram of present day state of Montana, USA showing the approximate changeing position of the western paleoshoreline of the Cretaceous Western Interior Seaway during the late Early Campanian Claggett Transgression (T8)…… .....…18

11. Diagram of present day state of Montana, USA showing the approximate changeing position of the western paleoshoreline of the Cretaceous Western Interior Seaway during the early Late Campanian Claggett Regression (R8)…….....…20

LIST OF FIGURES - CONTINUED

Figure Page

12. Diagram of present day state of Montana, USA showing the approximate changeing position of the western paleoshoreline of the Cretaceous Western Interior Seaway during the middle Late Campanian Bearpaw Transgression (T9)…….....21

13. Diagram of present day state of Montana, USA showing approximate present location of the main thrusts that would have effected Two MedicineFormation sedimentation and deposition…….....27

14. Chart summarizing the major tectonic events and volcanic episodes occurring in northwestern and west-central Montana during the Upper Coniacian through Lower Maastrichtian…… .....….28

15. Diagram of present day state of Montana, USA showing rotation of the LEH thrust between 74-59 Ma…… .....…29

16. Diagram of present day state of Montana, USA showing approximate location of the Boulder Batholith and the associated extrusive Elkhorn Mountains Volcanics…… .....……..32

17. Stratigraphic position of the upper discontinuity at the Two Medicine Formation type section…….....…..…34

18. Picture of Two Medicine Formation type section upper discontinuity……....…..35

19. Picture of Two Medicine Formation type section upper discontinuity…….....35

20. Stratigraphic position of the lower discontinuity at the Two Medicine Formation type section……..….....37

21. Correlation of Willow Creek anticline, Two Medicine Formation Type Section, and Seven Mile Hill area measured section discontinuities; Appendix C…….....…213

22. Location of stratigraphic sections measured in this study at the Willow Creek antilcine…… .....…..……...41

23. Summary of lithofacies and depositional conditions……..……42

LIST OF FIGURES - CONTINUED

Figure Page

24. Lithofacies B at Nose Cone Site, Willow Creek anticline, Choteau, MT…… .....….44

25. Lithofacies B at Nose Cone Site, Willow Creek anticline, Choteau, MT .....….44

26. SE-NW stratigraphic cross section through Willow Creek anticline measured sections; Appendix D……..…215

27. S/SW-N/NE stratigraphic cross section through Willow Creek anticline measured sections; Appendix E……..…217

28. Lithofacies Fl at Fault Mountain 2 Site, Willow Creek anticline Choteau, MT..…...46

29. Lithofacies Fm at Nose Cone Site, Willow Creek anticline Choteau, MT……48

30. Lithofacies Lc at Thunder Dome bentonite measured section Site, Willow Creek anticline Choteau, MT…… ……..50

31. Lithofacies Sh near Thunder Dome Site, Willow Creek anticline Choteau, MT …...52

32. Lithofacies Sm at Justin's Peak measured section Site, Willow Creek anticline Choteau, MT…….. 53

33. Lithofacies Sp at Pete's Pupa Peninsula measured section Site, Willow Creek anticline Choteau, MT 56

34. Lithofacies Sp at Pete's Pupa Peninsula measured section Site, Willow Creek anticline Choteau, MT……..… 56

35. Lithofacies Sr near Children's Dig measured section Site, Willow Creek anticline Choteau, MT …… 58

36. Lithofacies St at Flaming Cliffs measured section Site, Willow Creek anticline Choteau, MT …… 59

37. Mudstone rip-up clasts in lithofacies St at Flaming Cliffs measured section Site, Willow Creek anticline Choteau, MT……..60

38. Chart contrasting characteristics of pedogenic calcretes versus groundwater calcretes…….....61

LIST OF FIGURES - CONTINUED

Figure Page

39. Lithofacies P near Fault Mountain 2 Site, Willow Creek anticline Choteau, MT … .....…63

40. Summary of lithofacies associations, associated hydrodynamic conditions, and stratigraphic positions for Willow Creek anticline measured sections …….....67

41. Measured section of lower portion of Nest in the Wall site showing upward transition of sedimentary structures from trough cross-beds to horizontal-bedding and finally to ripple cross-lamination …… 68

42. Measured section of lower portion of Children's Dig site showing upward transition of sedimentary structures from horizontal-bedding to ripple cross-lamination …… .....……70

43. Measured section of Thunder Dome Bentonite site showing upward transition of sedimentary structures from horizontal-bedding to trough cross-bedding……....72

44. Measured section of Justin's Peak site showing alternating massive structureless sandstone and trough cross-bedded sandstone…….…73

45. Measured section of Egg Mountain B site showing alternating charophytiferous limestone and massive mudstone……75

46. Measured section of Nest in the Wall Bentonite site showing alternating Carbonate-rich, color mottled, massive mudstone (lithofacies Fmc) and Light grey, well-indurated carbonate (lithofacies C)…….....77

47. Willow Creek anticline measured section lithofacies associations……...…..78

48. Table showing characteristics of sandstones found in the stratigraphically lower and upper fluvial and floodplain deposits of the Willow Creek anticline…….....…82

49. Measured sections of the Jess Butte and Lake Giardia sites showing major and minor sandstones…….....83

50. Measured sections of the hunder Dome Bentonite and Flaming Cliffs site, showing possible mutlistorey channel relationship…….. 85

LIST OF FIGURES - CONTINUED

Figure Page

51. Criteria for recognition of anastomosing river systems…….....89

52. Simplified cartoon diagram of ephemeral river system depositional environment…… 90

53. Thick trough cross-bedded channel sandstones located at the top of the Thunder Dome Bentonite measured section…… 91

54. Examples of crevasse splay deposits at Jess Butte measured section site…….....93

55. Examples of Willow Creek anticline measured sections showing weakly-developed upward fining trends…….....94

56. A) Cartoon diagram of interpreted depositional environment for stratigraphically lowest Two Medicine Formation strata at the Willow Creek anticline…… 96
B) Cartoon diagram of interpreted depositional environment for stratigraphically highest Two Medicine Formation strata at the Willow Creek anticline…… .....…..97

57. Criteria for ephemeral stream interpretation…….....98

58. Similar lithofacies found in this study and in Dreyer (1993) and Spalletti and Pinol (2005)…….....…….99

59. Measured sections from Children's Dig and Thunder Dome sites showing thin (< 1.7 m thick), repeating sandstone beds that sometimes show normal grading…… 101

60. Measured section of Nest in the Wall Bentonite site showing thin, horizontally-bedded sandstones with basal mudstone rip-up clasts……102

61. Measured section of Nest in the Wall Bentonite site showing interbedded charophytiferous limestone (lithofacies Lc) and massive mudstone (Fm), and alternating carbonate-rich, color mottled massive mudstone (lithofacies Fmc) and light grey, well-indurated carbonate (lithofacies C)…… 109

62. Similar lithofacies in the Jurassic Shuttle Meadow and Campanian Two Medicine Formation…….....…111

LIST OF FIGURES - CONTINUED

Figure Page

63. Simplified cartoon diagram of small, shallow alkaline lake depositional environment ……. 112

64. Cartoon diagram of interpreted depositional environment for lacustrine strata at the Willow Creek anticline…… .....……113

65. Example of measured section showing general change from nodular to bedded groundwater carbonate…….....……116

66. Outcrops of stratigraphically lower rocks exposed near the Egg Mountain area at the Willow Creek anticline Choteau, MT…… .....…..118

67. Outcrops of stratigraphically highest rocks exposed near the Egg Mountain area at the Willow Creek anticline Choteau, MT…… .....…118

68. Schematic cross section showing interval of Two Medicine Formation deposition during Claggett Regression and Bearpaw Transgression…….....123

69. Cartoon cross section through Sevier Thrust Belt foreland basin during time of first change in stratigraphic architecture at the Willow Creek anticline…… .....…..125

70. Simplified diagram of Two Medicine Formation depositional environment interpretations and their associated base level energy cycles…….…. 126

71. Generalized diagram of present day Montana showing the interpreted northward propagation of increased subsidence and stress due to loading in the Helena Salient……..128

72. Cartoon cross section through Sevier Thrust Belt foreland basin during time of second change in stratigraphic architecture at the Willow Creek anticline…… .....…136

73. Location of dinosaur nests in the Egg Mountain area near Choteau, MT…. .....…140

ABSTRACT

The purpose of this research is to create a sequence stratigraphic framework for the Upper Cretaceous Two Medicine Formation exposed on the Willow Creek anticline along the western flank of the Sweetgrass Arch in Montana. The framework developed at this site was then correlated to the framework developed at the type section of the Two Medicine Formation located near Cut Bank, Montana. This research is significant because: 1) it provides a chronostratigraphically-significant framework within which Egg Mountain dinosaur nesting sites can be correlated, providing an important contribution to paleontologists interpreting this site, and 2) within this framework changes in fluvial style are related to relative sea level and a major change in tectonic style in western Montana (emplacement of the Boulder batholith and several volcanic events).

In this study, surface outcrops were used to describe and correlate the Two Medicine Formation. The Willow Creek anticline area demonstrates similar changes in stratigraphic architecture through time as have been described at the upper discontinuity of the Two Medicine Formation type section. A bentonite located 2.8 m (9.2 ft) below this change in architectural style at the Willow Creek anticline has been dated (U-Pb) in this study at approximately 76.5 Ma and gives a new bentonite date for Two Medicine Formation strata, as well as a means of estimating the time of this transition. Similarities in stratigraphic architecture at both areas suggest a shared control on stratigraphic architecture interpreted to be primarily related to loading in the Lombard-Eldorado thrust slab due to the emplacement of the Boulder Batholith (~76-74 Ma). The correlation between the two areas provides additional support for using nonmarine sequence stratigraphy to correlate strata within a Cretaceous nonmarine retroarc foreland basin.

Dinosaur nests located at the Willow Creek anticline are found in the deposits of both high and relatively lower accommodation strata, and can now be relatively dated based on their stratigraphic position above or below the newly dated bentonite. Finally, the new bentonite date suggests that the TM-003 bonebed is too old to be related to the Cretaceous Manson impact in Iowa.

CHAPTER 1

INTRODUCTION

Purpose

The purpose of this research is to: 1) create a sequence stratigraphic framework for the Upper Cretaceous Two Medicine Formation exposed on the Willow Creek anticline along the western flank of the Sweetgrass Arch in Montana, and 2) to evaluate the strata within this framework. Since the concept of sequence stratigraphy was first applied almost 30 years ago (Vail et al., 1977), it has continued to be used as a means of describing, grouping, and spatially characterizing bodies of sedimentary rocks and has been most successfully applied to marine units. Sequence stratigraphy provides a useful mechanism for subdividing the rock record into units bound by unconformities or their correlative conformities. These units are often the stratigraphic response to relative sea level changes, and most often have been used to provide a mechanism for correlation between marine influenced units preserved in different areas of the world. Applying sequence stratigraphy to terrestrial rocks is more difficult. A wide variety of complex and interrelated factors affect sedimentation, and these factors must be recognized and incorporated into the resulting local models generated (Van Wagoner et al., 1988). The consideration of varied sedimentary controls within a sequence stratigraphic framework is useful not only in subdividing the terrestrial rock record, but also in understanding the complex relationships between these factors on a local level. Application of nonmarine

sequence stratigraphic techniques to the Upper Cretaceous Two Medicine Formation would be significant in that it would allow for a more detailed means of subdividing Upper Cretaceous strata of northwestern Montana, and for new interpretations to be made regarding varied controls on the deposition of this strata.

This thesis has two parts. The first is the development of a sequence stratigraphic framework of the section of the Upper Cretaceous Two Medicine Formation that is present in northwestern Montana at outcrop exposures. The second is to use this framework to interpret the stratigraphic architecture of the Two Medicine Formation within this sequence stratigraphic framework in order to ascertain the relative importance of both tectonic evolution of the region and sea level changes on the stratigraphy. This information can then be used to determine the stratigraphic distribution of dinosaur nests in the Willow Creek anticline.

Location

The Two Medicine Formation in north-central Montana is exposed in thrusted outcrops along the Montana Disturbed Belt and across the Sweetgrass Arch to the east (Figures 1,2,3). The type section of the Two Medicine Formation is located along the Two Medicine River near Cut Bank, Montana (Lorenz, 1981). The Willow Creek anticline, a focus of this thesis' field work, is located in northwestern Montana, approximately 19 km (12 mi) west of Choteau, MT and 16 km (10 mi) east of the Northern Rocky Mountain Disturbed Belt (Gavin, 1986).

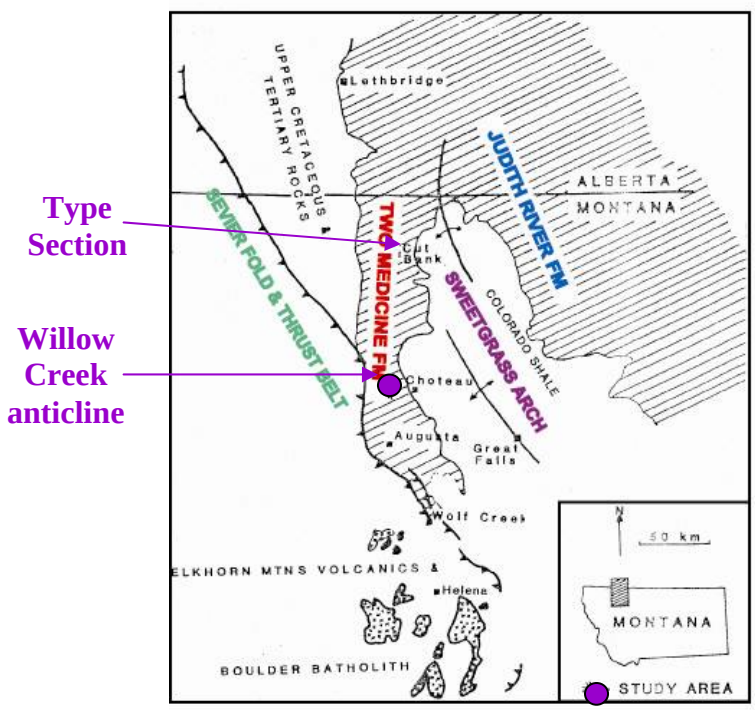

Figure 1: Map showing location of present day Two Medicine Formation and Judith River Formation (stratigraphic equivalent) exposures. (modified from Lorenz, 1981; Gavin, 1986)

Figure 2**:** View of southeastern portion of Willow Creek anticline from top of Thunder Dome (for location please see topographic map in Figure 22). Red arrow denotes axis and plunge (to northwest) of anticline.

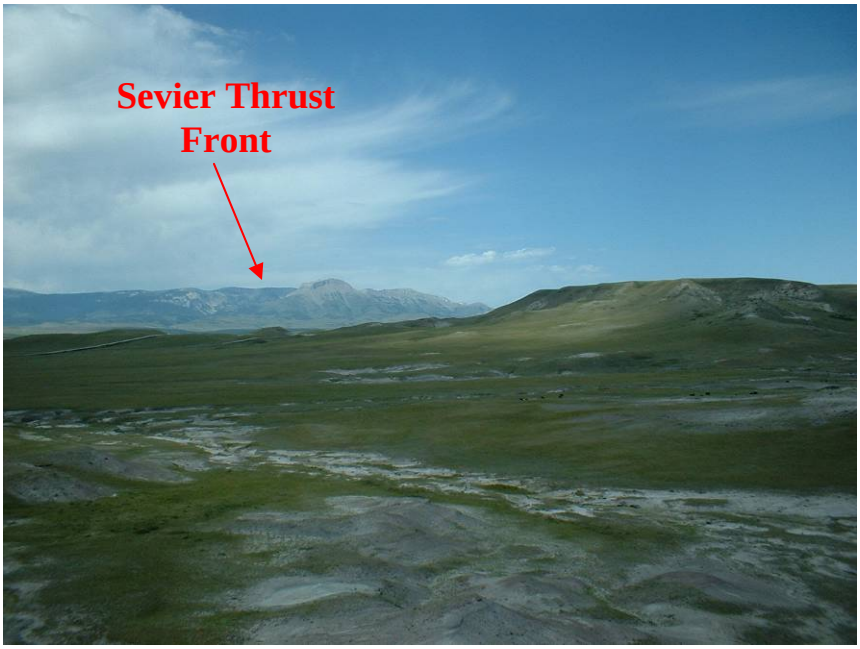

Figure 3**:** View of northwestern portion of Willow Creek anticline from top of Thunder Dome (for location see topographic map in Figure 22).

Geologic Setting

The Two Medicine Formation consists of approximately 600-1500 m of terrestrial molasse deposits that accumulated in the foredeep of the Western Interior foreland basin located in front of the Sevier thrust belt (Lorenz, 1981; Roberts, 1999) (Figures 3,4). Sediments comprising the Two Medicine Formation were derived primarily from sedimentary rocks in the thrust belt located to the west, and from the Elkhorn Mountains Volcanics to the south (Lorenz and Gavin, 1984).

In the Choteau, MT area the Two Medicine Formation is underlain by the regressive Virgelle Sandstone and overlain by the Horsethief Sandstone (Figure 5). Farther to the north and east, it is overlain by the Bearpaw Shale (Figure 5). Dates

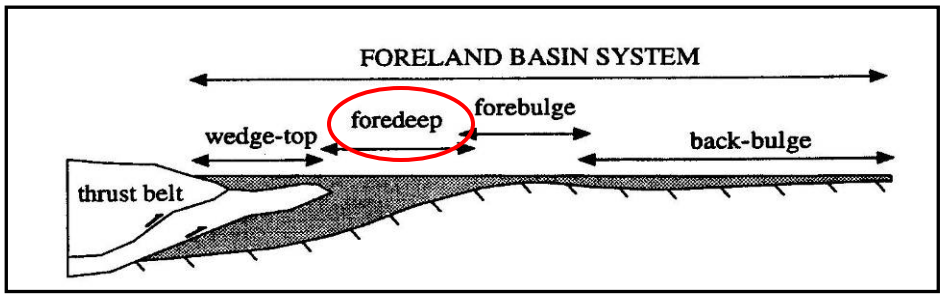

Figure 4: The Two Medicine Formation was deposited in the foredeep in front of the Sevier Fold and Thrust Belt (modified from Currie, 1997).

determined from bentonites and biozone analysis of ammonite fossils found in the marine shales both overlying and underlying the Two Medicine Formation bracket this formation as being deposited during the Campanian of the Upper Cretaceous (~ 82-73 Ma) (Lorenz, 1981).

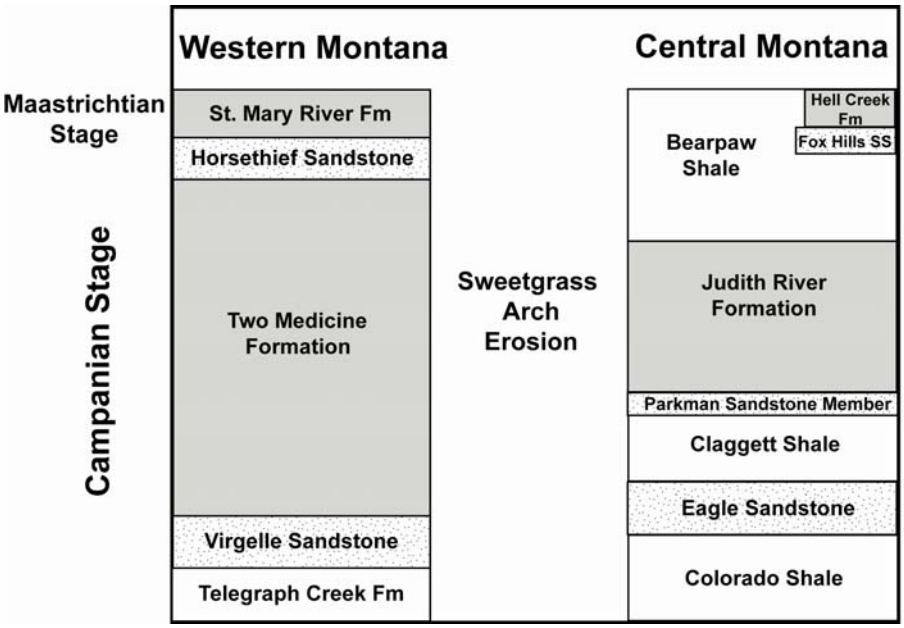

Figure 5**:** Generalized stratigraphic relationships between the Campanian Two Medicine Formation and adjacent formations.

The Canadian equivalent of the Two Medicine Formation is the Belly River Formation (described by Lerbekmo, 1963), with Canadian outcrops of the Two Medicine Formation present in the foothills of southern Alberta (Lorenz, 1981).

Previous Work

Research on Upper Cretaceous strata in north-central Montana began over 90 years ago, with the first studies performed by Stebinger (1914, 1916, and 1917) on the Montana Group. Subsequent studies on the Montana Group were performed by Cobban (1955), Viele and Harris (1965), and Gill and Cobban (1973). Lorenz (1981) completed the first comprehensive study of the Two Medicine Formation in its entirety. Rogers (1994, 1995, and 1998) employed the first use of sequence stratigraphic techniques on the Two Medicine Formation in an attempt to correlate it with the Judith River Formation. Subsequently, Roberts (1999) attempted to trace the lower discontinuity of Rogers (1995) into the Choteau, MT area. Smith (1998), King (1997), and LaBranche (1999) provided studies regarding the effects of the Elkhorn Mountains Volcanics and Adel Mountain Volcanics on Two Medicine Formation sedimentation.

CHAPTER 2

BACKGROUND: NONMARINE SEQUENCE STRATIGRAPHY

The purpose of sequence stratigraphy is to study rock relationships within a chronostratigraphic framework (Posamentier et al., 1988). The basic unit of sequence stratigraphy is the sequence, which is "a relatively conformable succession of genetically related strata bounded at its top and base by unconformities and their correlative conformities" (Vail et al., 1977; p. 53). Application of sequence stratigraphy to marine rocks provides a useful mechanism for subdividing the marine rock record into units correlative with relative sea level changes, thus providing a tool for correlation between marine units preserved in different areas of the world. Sequences form in response to eustasy, subsidence, and changes in sediment supply. All these effects must be addressed before any definite correlations can be made (Van Wagoner et al., 1988).

In addition to studies involving the application of sequence stratigraphy to marine rocks, attempts have been made to apply the same concepts to nonmarine sedimentary rock assemblages (Shanley and McCabe, 1991, 1993, and 1994). Application of sequence stratigraphy to nonmarine units has sometimes been met by skepticism however, in that some scientists shave interpreted sequence stratigraphy to be synonymous with eustasy (Shanley and McCabe, 1994). This is not an accurate view of the objectives of sequence stratigraphy however, in that sequence stratigraphy is not merely used to connect bounding surfaces in rock units to eustasy, but is instead used to consider all of the potential controls on local sedimentation (Shanley and McCabe, 1994).

In applying sequence stratigraphy to terrestrial rocks, a wide variety of complex and interrelated factors affect local sedimentation including sediment supply, local tectonic history, eustasy, changes in fluvial environments, changes in base level, distance inland from paleocoastline, and climate. These factors must be recognized and incorporated into the resulting local models (Van Wagoner et al., 1988). This equal consideration of varied controls makes sequence stratigraphy a useful tool not only in subdividing the terrestrial rock record, but also in understanding the complex relationships between these factors on a local level.

Recent studies demonstrate the usefulness of applying sequence stratigraphy to nonmarine rocks (Shanley and McCabe, 1989, 1991, 1993, and 1994; Legarreta et al., 1993; Wescott, 1993; Wright and Marriott, 1993; Schumm, 1993; Gibling and Bird, 1994; Olsen et al., 1995; Van Wagoner, 1995; Currie, 1997; Rogers, 1998; Roberts, 1999). In these studies, stratigraphic sequences are identified and divided based on vertical changes in rock assemblages due to factors such as change in stratigraphic architecture, and on identification of sequence-bounding unconformities (Shanley and McCabe, 1989, 1991, and 1993; Gibling and Bird, 1994; Van Wagoner, 1995; Rogers, 1998; Roberts, 1999). These studies also suggest that predictable facies assemblages develop within sequences (Shanley and McCabe, 1994). Models by definition are simplifications, and the rock assemblages that result from these complex inputs are highly variable. It is important to understand the range of these assemblages, and thus many studies of the sequence stratigraphy of nonmarine rocks are necessary in order to

better understand these rock assemblage changes, and how diverse controls on sedimentation effect these changes.

CHAPTER 3

CONTROLS ON SEQUENCE DEVELOPMENT

Introduction

Three main processes affect sediment supply into a basin, and thus affect both the type and stacking pattern of sediment that is recorded within the basin. These processes are: climate change, changes in eustatic sea level, and tectonics (Vail, 1987). It is important to note that while each of these processes plays an important role, multiple processes are usually operating at the same time, and it is the balance between these processes that ultimately determines the rocks that will eventually be recorded.

Campanian Sea Level Change

Global Sea Level Change

A chronology of fluctuating sea levels since the Triassic Period has been compiled by Haq et al. (1987), incorporating magnetostratigraphy, chronostratigraphy, biostratigraphy, and sequence stratigraphy in order to reconstruct eustatic sea level curves for the past 250 Ma. Deposition of the Two Medicine Formation (~82-73 Ma) occurred during the Upper Zuni Sloss sequence of the Haq et al. (1987) chronology. Globally, five major short term sea level rises and six major short term sea level falls occurred during this period of time (Haq et al., 1987). These short term changes in sea level were superimposed on a longer term eustatic sea level rise that spanned the beginning of the

Campanian and lasted until approximately 80 Ma, at which time a change toward a long term eustatic sea level fall commenced which lasted throughout the remainder of the Cretaceous Period (Haq et al., 1987) (Figure 6). Global sequence boundaries are recorded in strata of the following ages: 83 Ma, 80 Ma, 75 Ma, and 71 Ma (Haq et al., 1987) (Figure 6). Downlap surfaces, also referred to as marine flooding surfaces, mark the surface of maximum flooding of the continent by relative sea level rise (Van Wagoner et al., 1988) Global downlap surfaces are recorded for strata of the ages: 82 Ma, 79.5 Ma, 78 Ma, 76 Ma, and 73.5 Ma (Haq et al., 1987) (Figure 6). The relationship between Campanian sea level, climate, and tectonics is summarized in Figure 7.

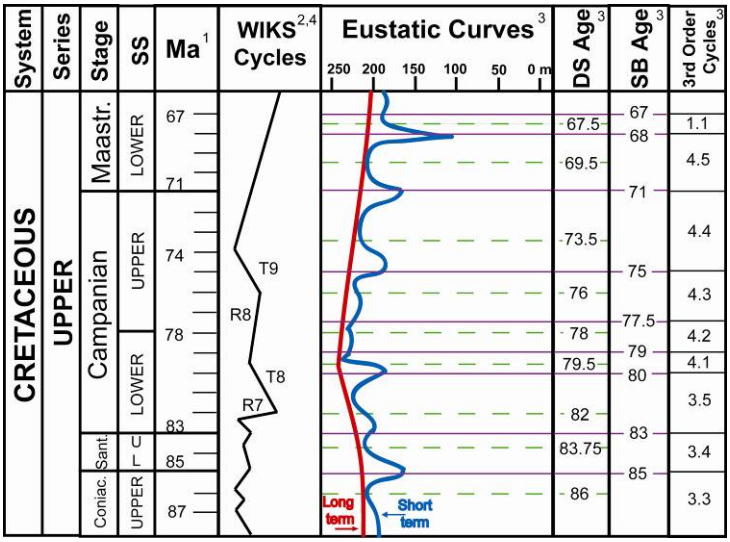

Figure 6**:** Chart summarizing global eustatic sea level cycles and Western Interior Seaway cycles, Upper Coniacian through Lower Maastrichtian. DS Age: downlap surface age. SB Age: sequence boundary age. R7: Eagle Regression. T8: Claggett Transgression. R8: Claggett Regression. T9: Bearpaw Transgression. [1]Time in millions of years before present taken from the International Commission on Stratigraphy's 2004 international stratigraphic chart. [2] WIKS cycles modified from Kauffman (1977). [3] Eustatic sea level curves, downlap surface ages, sequence boundary ages, and third order cycles modified from Haq et al. (1987). [4] Time values for Claggett Regression and Bearpaw Transgression in northwestern Montana from Rogers et al. (1993).

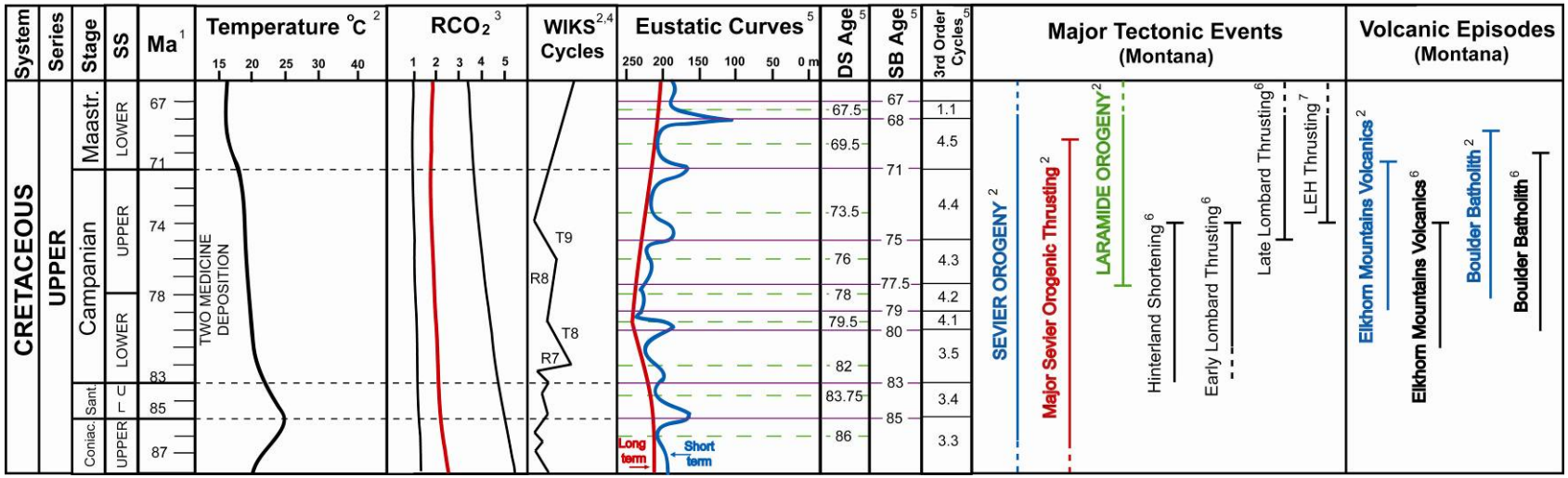

Figure 7**:** Chart summarizing the three main controls on sequence development in northwestern Montana during the Campanian. [1]Time in millions of years before present taken from the International Commission on Stratigraphy's 2004 international stratigraphic chart. [2] Temperature in degrees Celsius and WIKS cycles, and major tectonic events and volcanic episodes dates modified from Kauffman (1977). [3] RCO_2 = mass of atmospheric CO_2 at time t divided by that at present (~ 300 ppmv). RCO_2 values modified from Berner (1994). Red line represents average, while black lines represent extremes. [4] Time values for Claggett Regression and Bearpaw Transgression in northwestern Montana from Rogers et al. (1993). [5] Eustatic sea level curves, downlap surface ages, sequence boundary ages, and third order cycles modified from Haq et al. (1987). [6] Major tectonic events and volcanic episode dates modified from Lageson et al. (2001). [7] LEH timing of thrusting modified from Sears (2001).

Cretaceous Western Interior Seaway

The Cretaceous Western Interior Seaway (WIKS) was an elongate epeiric seaway that, at its maximum development, extended more than 4,827 km (3,000 miles) north to south from Arctic Canada to the Gulf of Mexico, and greater than 1,609 km (1,000 miles) west to east from northeastern Nevada to Iowa and southwestern Minnesota (Kauffman, 1977) (Figure 8). The basin the WIKS occupied during a time of high global sea level in the Cretaceous (Haq et al., 1987) was tectonic in origin, forming and subsiding due to long wavelength flexure resulting from thrust sheet loading of the lithosphere (Jordan, 1981) associated with the Late Jurassic to early Cenozoic Sevier Orogeny and the Late Cretaceous to early Cenozoic Laramide Orogeny (Kauffman, 1977).

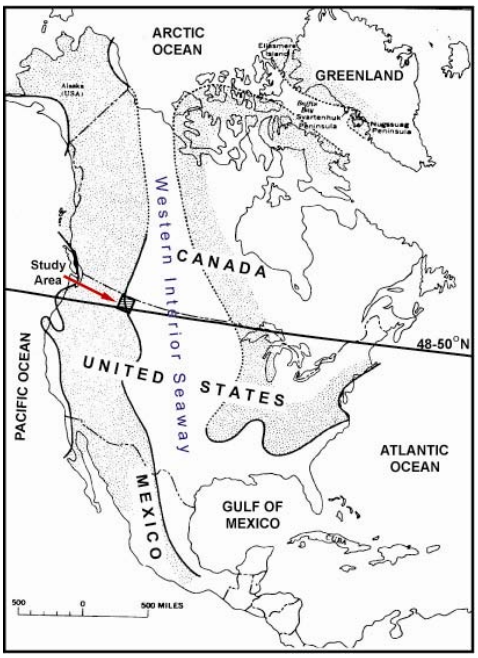

Figure 8**:** Location of Cretaceous Western Interior Seaway (WIKS) during the Campanian. The Two Medicine Formation was deposited on the western edge of the WIKS during the Campanian. (modified from Gill and Cobban, 1973)

During the Cretaceous Period the Western Interior Basin was relatively stable, with the exception of simultaneously occurring subsidence episodes related to thrusting (and the associated lithospheric loading) of the Sevier and Laramide Orogenies (Kauffman, 1977). As a result, global eustatic sea level changes are recorded within the sediments of the Western Interior Basin, and were determined from the study of strandline fluctuations and vertical sedimentary sequences indicating cyclic shallowing and deepening episodes in the stratigraphic record of the basin (Kauffman, 1977). Two major eustatic sea level transgressions (Claggett Transgression (T8) and Bearpaw Transgression (T9)) and two major regressions (Eagle Regression (R7) and Claggett Regression (R8)) are recorded in the Western Interior Basin for the Campanian (Kauffman, 1977) (Figure 7). In addition, Martinson et al. (1998) present evidence for short-term, smaller scale (< 1 m.y.) sea level fluctuations that affected the entire Western Interior Seaway based on foraminiferal data.

Based on biostratigraphy and radiometry, the R7, R8, T8, and T9 sea level changes observed in the WIKS are roughly correlative to major short-term (third order, ~ 0.2-0.5 Ma duration (Church and Coe, 2003; p. 99)) eustatic sea level changes recorded throughout the world for this time as presented by Haq et al. (1987). In contrast, Lillegraven and Ostresh (1990) argue that these four sea level changes observed in the WIKS are not causally related to changes in eustasy, but rather to local, subregional, or continental effects of tectonism (i.e. subsidence). Their data, based on mammalian fauna and ammonite zone correlation used to reconstruct the western paleoshoreline of the WIKS, suggest that a regional regression (first order (~50-200+ Ma duration) or second

order (~0.5-50 Ma duration) (Church and Coe, 2003; p. 99)) of the WIKS, possibly caused by a slow-spreading land surface depression resulting from topographic evolution of the world's mid-oceanic system of ridges and volcanic plateaus, occurred from 84 – 66 Ma (Lillegraven and Ostresh, 1990). The local and regional asynchronous changes in shoreline location (i.e. R7, R8, T8, T9) were therefore superimposed on this longer term regression, and resulted from local tectonic events such as the early phases of the Laramide Orogeny (Lillegraven and Ostresh, 1990). As a result, Lillegraven and Ostresh (1990) argue that the Santonian through Maastrichtian history of the WIKS is inconsistent with third order short term eustatic sea level changes, as well as with the commonly held concept of a high eustatic sea level during the late Campanian.

Eagle Regression (R7). In northwestern Montana, the early Early Campanian Eagle Regression resulted in the deposition of the Eagle/Virgelle Sandstones (Lorenz, 1981). The Eagle Sandstone shoreline regressed diachronously for approximately 5.5 Ma from its initial position west of the present Rocky Mountain front eastward into central Montana (Lorenz, 1981) (Figure 9) at a rate of approximately 80-110 km/m.y. (50-68 mi/m.y) (Gill and Cobban, 1973; Lorenz, 1981). Strandlines within the Eagle Sandstone and Telegraph Creek Formations record lateral eastward movement of the paleoshoreline by approximately 180 miles (290 km) in 2.5 m.y. (Gill and Cobban, 1973). This regression may also have occurred diachronously from south to north (Lorenz, 1981). In addition to the eustatic sea level correlation cited by Kauffman (1977) and Hancock and Kauffman (1979), additional mechanisms cited as potential causes of this regression

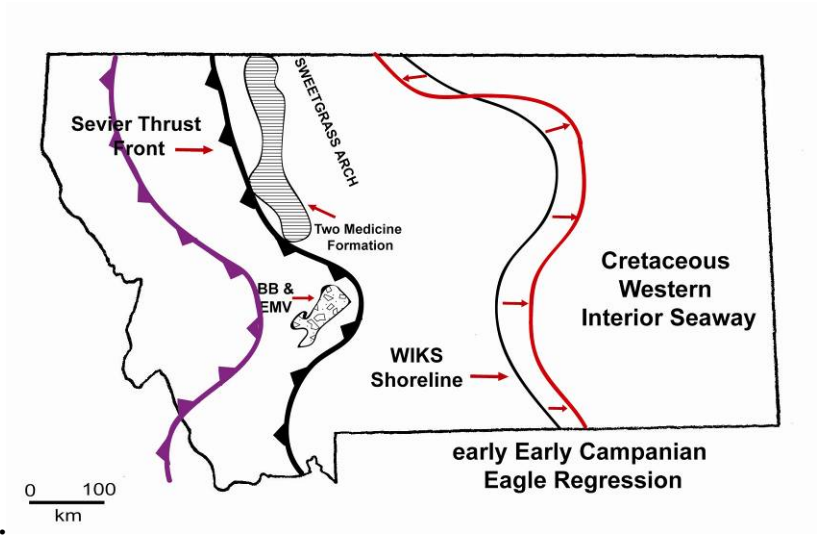

A.

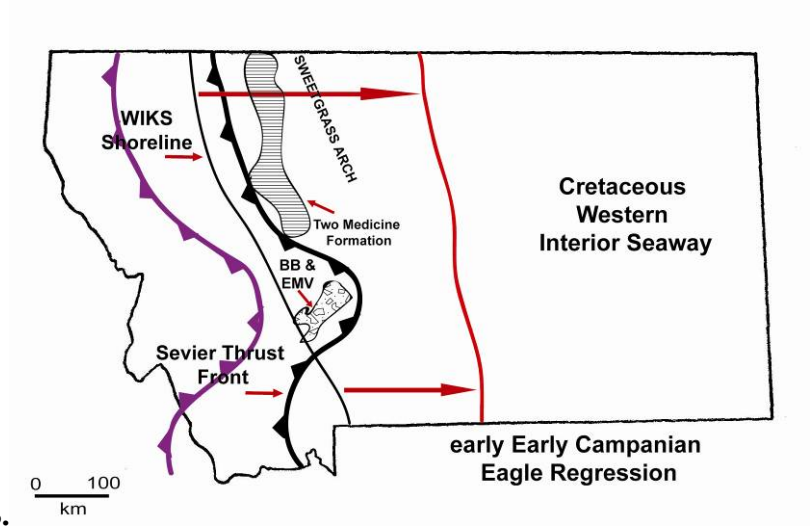

B.

Figure 9: A & B) Diagram of present day state of Montana, USA showing approximate change in position of the western paleoshoreline of WIKS during the early Early Campanian Eagle Regression (R7). Black line represents approximate position of the shoreline at the start of the R7 regression; red line represents its approximate position near the end of the R7 regression. Present day eastern extent of the Sevier fold and thrust belt is denoted by a black line with teeth on the hanging wall; its approximate position during the Campanian (Sears, 2001) is denoted in purple. The filled area to the west of the Sweetgrass Arch represents the present day extent of available Two Medicine Formation outcrops. BB: Boulder Batholith. EMV: Elkhorn Mountains Volcanics. A) Approximate shoreline positions as reconstructed by Gill and Coban (1973) and Lorenz (1981) based on ammonites**.** B) Approximate shoreline positions as reconstructed by Lillegraven and Ostresh (1990) based on mammal fossil distribution.

include: regional uplift (Roberts, 1972), strong, localized uplifts (Jeletzky, 1971), and tectonism and volcanism in western Montana (Gill and Cobban, 1973).

The Eagle Regression marks a distinct change in the character of the transgressive and regressive patterns in the WIKS (Lorenz, 1981). Prior to the Eagle Regression, there was a trend towards transgressions of increasingly larger magnitude, however, subsequent to the Eagle Regression this was followed by an increase in the magnitude of regressions (Jeletzky, 1971). In addition, Kauffman (1977) noted an increase in volcanism related to this event which he attributes to early Laramide orogenic events.

Claggett Transgression (T8). The late Early Campanian Claggett Transgression that followed the Eagle Regression did not extend very far west in Montana, possibly only extending west to the Sweetgrass Arch (Cobban, 1955; Lorenz, 1981) (Figure 10). At the same time as the seaway was transgressing into northwestern Montana, it was retreating in southern Montana (Gill and Cobban, 1973). As a result, there is little record of the Claggett Transgression recorded within the Two Medicine Formation of northwestern Montana. In addition, this transgression extended diachronously (Lorenz, 1981), and may have been rapid (150 km/m.y) (Gill and Cobban, 1973; Lorenz, 1981). Strandlines recorded in the Claggett Shale record a lateral westward change in paleoshoreline position of approximately 140 miles (226 km) in 1.5 m.y. (Gill and Cobban, 1973). Eustasy is the most common mechanism invoked to explain the initiation of the Claggett Trangression (Kauffman, 1977). Interestingly, Kauffman (1977) and Gill

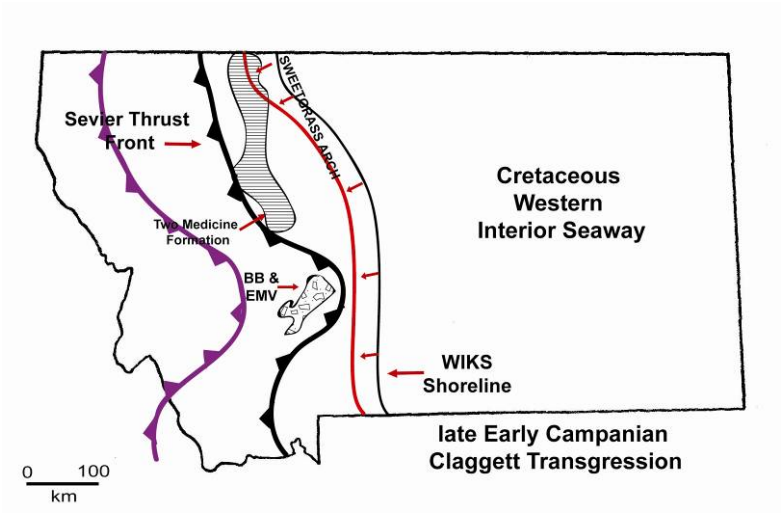

A.

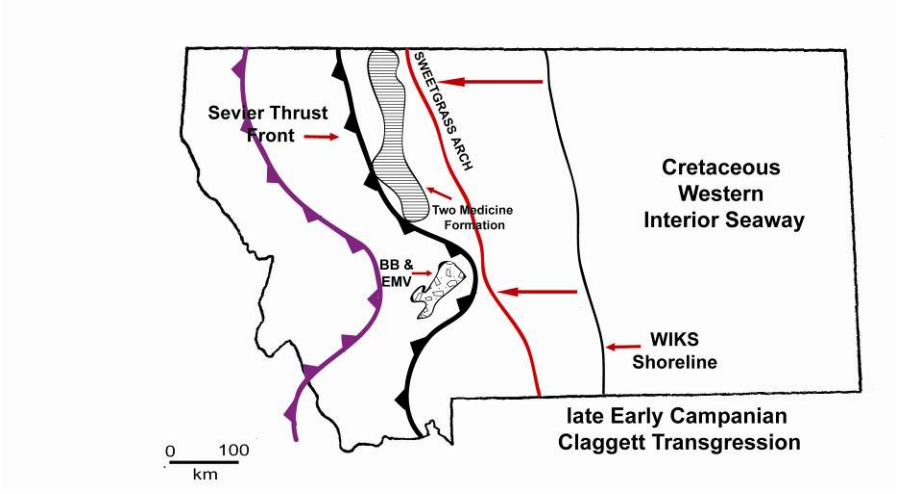

B.

Figure 10: A & B) Diagram of present day state of Montana, USA showing approximate change in position the western paleoshoreline of the WIKS during the late Early Campanian Claggett Transgression (T8). Black line represents approximate position of the shoreline at the start of the T8 transgression; red line represents its approximate position near the end of the T8 transgression. Present day eastern extent of the Sevier fold and thrust belt is denoted by a black line with teeth on the hanging wall; its approximate position during the Campanian (Sears, 2001) is denoted in purple. The filled area to the west of the Sweetgrass Arch represents the present day extent of available Two Medicine Formation outcrops. BB: Boulder Batholith. EMV: Elkhorn Mountains Volcanics. A) Approximate shoreline positions as reconstructed by Gill and Coban (1973) and Lorenz (1981) based on ammonites. B) Approximate shoreline positions as reconstructed by Lillegraven and Ostresh (1990) based on mammal fossil distribution.

and Cobban (1973) note evidence for increase in volcanic activity occurring just prior to and during the early stages of both the Claggett and Bearpaw Transgressions, that they conclude to be related to larger scale tectonism (i.e. plate tectonics or tectonism in western Montana). In contrast, Lillegraven and Ostresh (1990) suggest that the Claggett Transgression was only a localized transgression related to isostatic subsidence following deposition of the Eagle Sandstone and its marine equivalents.

Claggett Regression (R8). The early Late Campanian Claggett Regression (Judith River Regression of Gill and Cobban (1973)) resulted in the diachronous eastward migration (and possibly diachronous north to south migration) of the Judith River shoreline at an estimated rate of 100 km/m.y. (62 mi/m.y.) (Gill and Cobban, 1973; Lorenz, 1981) (Figure 11). The eastward regression of the shoreline therefore also resulted in the eastward progradation of Two Medicine Formation sediments. Strandlines recorded within the Judith River Formation record a lateral eastward change of the paleoshoreline by approximately 190 miles (306 km) in 3 m.y. (Gill and Cobban, 1973). Jeletzky (1971) attributes this regression to a regional tectonic pulse which elevated the whole length of the western shoreline in Canada. Similarly, Gill and Cobban (1973) also attributed it to uplift and volcanism.

Bearpaw Trangression (T9). The middle Late Campanian Bearpaw Transgression marked the last major transgression of the WIKS into the western portion of the North

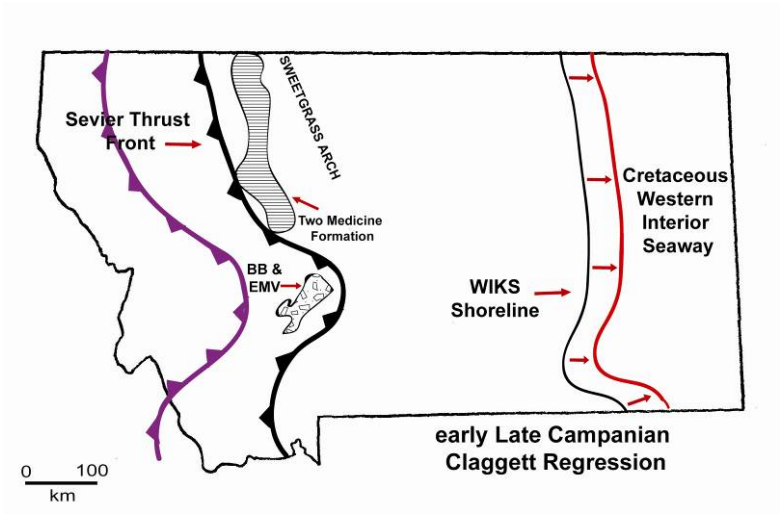

A.

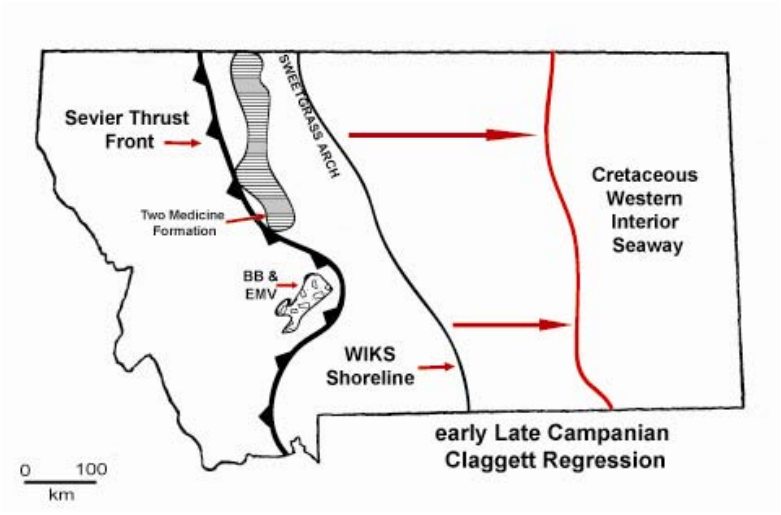

B.

Figure 11: A & B) Diagram of present day state of Montana, USA showing approximate change in position of the western paleoshoreline of the WIKS during the early Late Campanian Claggett Regression (R8). Black line represents approximate position of the shoreline at the start of the R8 regression; red line represents its approximate position near the end of the R8 regression. Present day eastern extent of the Sevier fold and thrust belt is denoted by a black line with teeth on the hanging wall; its approximate position during the Campanian (Sears, 2001) is denoted in purple. The filled area to the west of the Sweetgrass Arch represents the present day extent of available Two Medicine Formation outcrops. BB: Boulder Batholith. EMV: Elkhorn Mountains Volcanics. A) Approximate shoreline positions as reconstructed by Gill and Coban (1973) and Lorenz (1981) based on ammonites. B) Approximate shoreline positions as reconstructed by Lillegraven and Ostresh (1990) based on mammal fossil distribution.

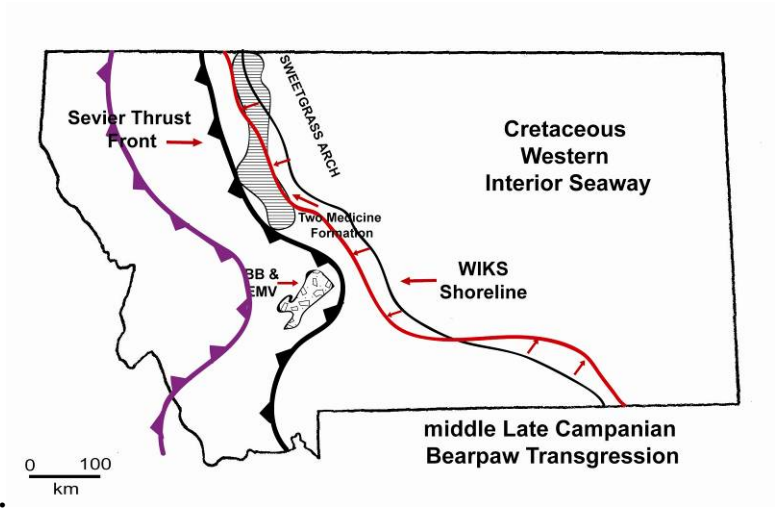

A.

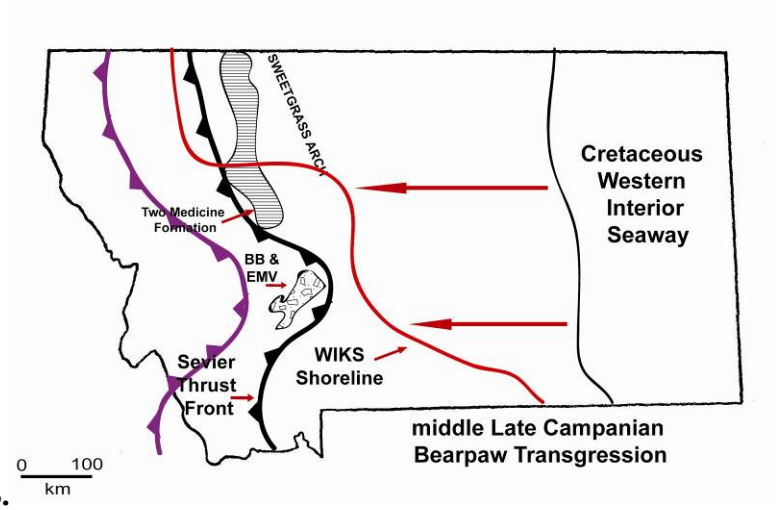

B.

Figure 12: A & B) Diagram of present day state of Montana, USA showing the approximate changing position of the western paleoshoreline of the Cretaceous Western Interior Seaway during the middle Late Campanian Bearpaw Transgression (T9). Black line represents approximate position of the shoreline at the start of the T9 transgression; red line represents its approximate position near the end of the T9 transgression. Present day eastern extent of the Sevier fold and thrust belt is denoted by a black line with teeth on the hanging wall. The filled area to the west of the Sweetgrass Arch represents the present day extent of available Two Medicine Formation outcrops. BB: Boulder Batholith. EMV: Elkhorn Mountains Volcanics. A) Approximate shoreline positions as reconstructed by Gill and Coban (1973) and Lorenz (1981) based on ammonites. B) Approximate shoreline positions as reconstructed by Lillegraven and Ostresh (1990) based on mammal fossil distribution.

American continent, and is generally viewed as an isochronous event (that is, in southern Alberta and northern Montana) (Lorenz, 1981) (Figure 12 above). This transgression progressed at an estimated rate of 110 km/m.y. (Gill and Cobban, 1973; Lorenz, 1981), and is associated with an increase in volcanic activity (Kauffman, 1977). Strandlines recorded in the Bearpaw Shale record lateral westward shoreline migration of approximately 205 miles (331 km) in 3.5 m.y. (Gill and Cobban, 1973). Although the Bearpaw Transgression corresponds to a eustatic transgression of sea level (Kauffman, 1977), McLean and Jerzykiewicz (1978) have proposed that it was initiated by subsidence caused by supracrustal loading in the thrust belt to the west. On the contrary, Lillegraven and Ostresh (1990) suggest that the Bearpaw Transgression resulted from effects of subregional isostatic subsidence caused by resultant sediment loading during deposition of the Two Medicine and Judith River formations and their marine equivalents.

Campanian Climate Change

Campanian Climate Summary

Climate change is a complicated process that involves the interactions of several variables including (Valdes, 2000):

1. Changes in the position of the solar system relative to the galactic center
2. Evolution of the sun and solar variability
3. Changes in Earth's orbit
4. Continental drift and changes in orographic relief
5. Evolution of the atmosphere

6. Volcanic activity
7. Albedo feedbacks and the land surface
8. Ocean and atmospheric circulation

Considering these factors, the Campanian environment of Earth was very different from that of today. The continents were more closely spaced, reflecting the recent break-up of Pangea (DeConto et al., 2000). In addition, sea level was higher than the present day, flooding continental interiors and coastal zones, and resulting in an approximately 20% decrease in land surface area as compared to the present (DeConto et al., 2000). This decrease in land surface is thought to have caused a significant decrease in continentality in the northern hemisphere (DeConto et al., 2000).

Although the Late Cretaceous Earth is generally referred to as a greenhouse world, its climate can be divided into three distinct greenhouse periods (Huber et al., 2002). The Campanian spans the transition from the second greenhouse phase, referred to by Huber et al. (2002) as the "hot greenhouse" phase, to the beginning of the final greenhouse phase of the Late Cretaceous, referred to as the "cool greenhouse" phase beginning in the late early Campanian (Huber et al., 2002). The "hot greenhouse" phase was characterized by terrestrial temperatures ranging from 16-23°C (Francis and Poole, 2002), and by ocean bottom waters reaching temperatures as high as 20°C (Huber et al., 2002). The following "cool greenhouse" phase was characterized by a 4-8 ^{o}C drop in terrestrial temperatures (Francis and Poole, 2002), and by an associated drop in ocean bottom water temperatures below 12°C (Huber et al., 2002). In general, the Campanian is

marked by global mean annual surface temperatures approximately 10°C higher than today (based on climate proxies) (Huber et al., 2002).

The climatic variations during late Cretaceous time most likely resulted from complex interactions among multiple forcing factors. While it is difficult, if not impossible to distinguish the separate effects of each factor on the climate system, some factors appear to have played a more important role than others. These factors include: concentration of atmospheric CO_2, land surface albedo, ocean circulation, and tectonics.

The atmospheric CO_2 concentration (Figure 7) was elevated during the Campanian due to increases in volcanic activity (Arthur et al., 1985) and volcanic degassing (Berner, 1994), as well as a decrease in the total land surface area available for continental weathering (therefore decreasing the holding capacity of this potential CO_2 sink), and decreased CO_2 solubility in the oceans due to warmer ocean temperatures (Barron, 1983).

Earth's albedo was reduced during the Campanian due to a lack of polar ice caps (DeConto et al., 2000) causing Earth's surface to absorb more solar energy. The lack of ice cover would also have subdued the effects of Earth's orbital variations on the climate during this period of time. Additionally, vegetation albedo seems to have played an important role in regulating Earth's Late Cretaceous climate (DeConto et al., 2000).

Ocean General Circulation Models (OGCMs) constructed for the Campanian predict that most of the Campanian ocean heat transport was through meridional (low latitude) overturning, with most deep water formation occurring at high southern latitudes in a process similar to that found in today's North Atlantic (DeConto et al., 2000). In

addition, global cooling and draining of tropical and subtropical epicontinental seas during the mid-late Campanian through early Maastrichtian reduced the production of global hypersaline waters, thus causing a decrease in oceanic heat transport, and a change from low latitude to high latitude production of bottom waters (MacLeod and Huber, 1996). This change is thought to have caused a decline in oceanic heat transport, which led to the increase in latitudinal temperature gradients recorded for the Late Maastrichtian Stage (MacLeod and Huber, 1996).

Early studies addressing Cretaceous climate (Barron and Washington, 1984) asserted that paleogeography could explain a "substantial fraction" of Cretaceous warmth due to the closer configuration of the continents and decreased continentality. However, subsequent General Circulation Models (GCMs) incorporating seasonally varying insolation, and ocean circulation models that capture seasonal thermal cycles have shown that the role of geography was small when compared with climatic forcing from increased atmospheric CO_2 and sea ice distribution (Barron et al., 1993; DeConto et al., 2000).

Campanian climate was therefore affected by numerous interrelated factors, with those listed above playing the most important roles. Together they helped to bring about the most important climatic change associated with the late Campanian: the initiation of a global cooling trend that would ultimately result in Cenozoic glaciation. The relationship between Campanian climate change, sea level change, and tectonics is presented in Figure 7.

It is important to note that at present paleoclimatologists are still not able to reproduce completely accurate climate reconstructions, as some variables (orbital forcing, cloud cover, global paleotopography, etc.) are based on estimations rather than hard data, especially for periods in the distant geologic past. Therefore, further research is needed to more accurately reconstruct the Campanian, as well as other past Earth climates.

Campanian Tectonism in Northwestern Montana

Introduction

During the Campanian, the Sevier orogenic belt exerted the dominant tectonic control influencing Two Medicine Formation deposition. This belt, extending over 6,000 km (3720 mi) from the Canadian Arctic and Alaska to southern Mexico, records the continuous, yet diachronous eastward expansion of orogenic deformation that took place from the Late Jurassic to the Eocene in response to the opening of the North Atlantic Ocean following the rifting of Pangea. Contractional deformation took place along an Andean-style convergent margin in response to the eastward subduction of the Farallon plate, with the timing and style of deformation being highly variable along strike of the orogen (DeCelles, 2004). In western Montana, the Sevier fold and thrust belt roughly follows the trace of the Belt-Purcell Supergroup, a thick siliciclastic sequence of rocks deposited during the Middle Proterozoic (DeCelles, 2004). The Helena salient is located to the south of present day Two Medicine Formation outcrop exposures, while the eastern margin of the Sevier belt borders the Two Medicine Formation to the west. This eastern margin of the Sevier belt consists of six major thrust systems: Moyie, Libby, Pinkham,

Whitefish, and Lewis-Eldorado-Hoadley thrusts, and the frontal imbricate belt of the Sawtooth Range or "Montana Disturbed Belt" (DeCelles, 2004).

Lewis-Eldorado-Hoadley Thrust Slab

The Lewis-Eldorado-Hoadley thrust slab (LEH) and the associated imbricated thrust wedge (Montana Disturbed Belt) in its footwall comprise a massive, eastward-thinning allochthon approximately 70-110 km wide and up to 30 km thick (Figure 13).

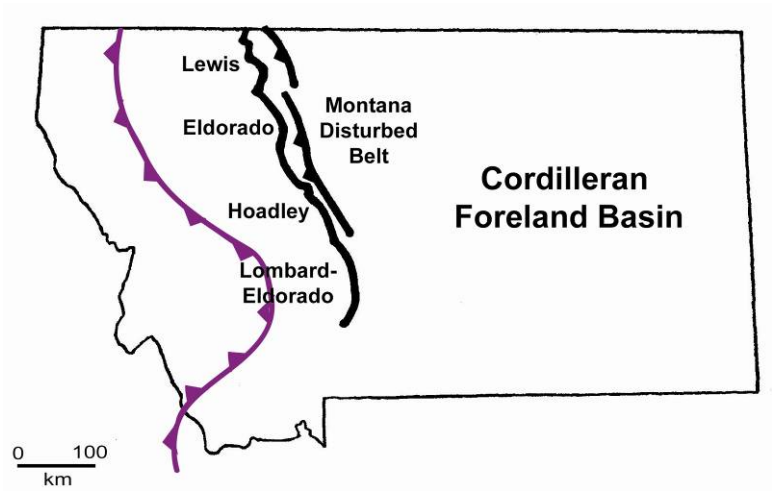

Figure 13) Diagram of present day state of Montana, USA showing approximate Campanian (purple)(modified from Sears, 2001) and present position (black) of the main thrusts that would have effected Two Medicine Formation sedimentation and deposition.

This thrust system extends from the northwest-trending Lewis and Clark shear zone northeast to the Rocky Mountain front and north from west-central Montana to southern Canada (Sears, 2001). The stratigraphy of the LEH slab hanging wall is dominated by the Proterozoic Belt-Purcell Supergroup, with the Montana disturbed belt constituting the exhumed footwall (Sears, 2001; DeCelles, 2004). Within the footwall, the Campanian Two Medicine Formation and the overlying Early Maastrichtian Bearpaw Shale and St.

Mary River Formation comprise the youngest pre-thrust stratigraphic units. The LEH was emplaced over 15 m.y., from approximately 74-59 Ma (based on K-Ar dates), during the Late Cretaceous and early Paleocene Sevier Orogeny (Sears, 2001; DeCelles, 2004) (Figure 14). At approximately 74 Ma, the LEH slab detached from its basement, and in its southern reaches, the leading edge of the slab was imbricated into the Hoadley, Eldorado, and Steinbach thrusts (Sears, 2001). As these imbricated thrusts traveled eastward overriding the adjacent foreland basin, the craton continuously subsided in front of the advancing slab, propagating the associated subsidence approximately 400 km (248 mi) east across the foreland (Sears, 2001). Footwall subsidence was driven by isostatic loading of the wedge-shaped LEH slab, causing it to subside to a stable depth which it

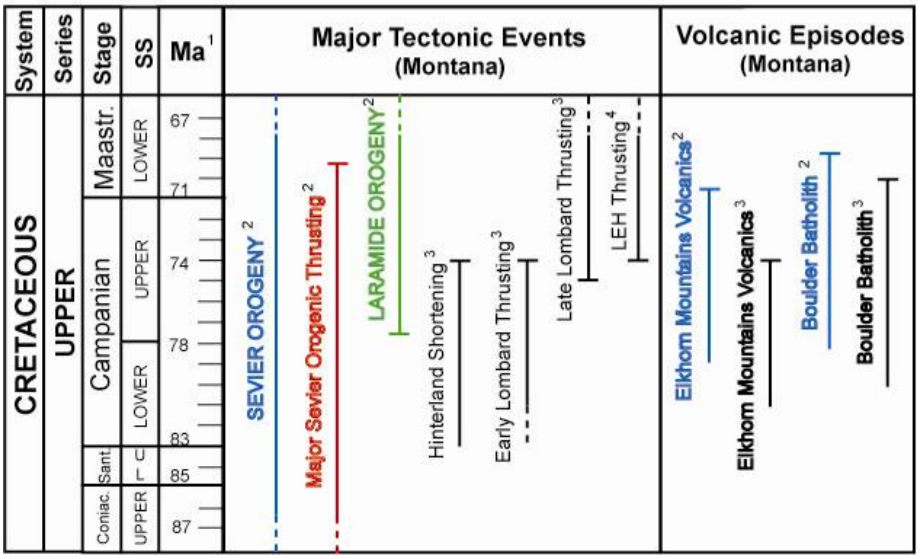

Figure 14) Chart summarizing the major tectonic events and volcanic episodes occurring in northwestern and west-central Montana during the Upper Coniacian through Lower Maastrichtian. [1]Time in millions of years before present taken from the International Commission on Stratigraphy's 2004 international stratigraphic chart. [2] Major tectonic events and volcanic episodes dates modified from Kauffman (1977). [3] Major tectonic events and volcanic episode dates modified from Lageson et al. (2001). [4] LEH timing of thrusting modified from Sears (2001).

maintained until the termination of thrusting (Sears, 2001).

Motion along the length of the slab did not proceed at a uniform rate, as the southern portion moved at an average of approximately 3 km/m.y. (1.9 mi/m.y), while the northern portion near the United States-Canada border moved at approximately 9 km/m.y. (5.6 mi/m.y) (Sears, 2001). As a result, relative horizontal slab displacement increases from south to north along the length of the slab, with the southern portion displaying approximately 40 km (25 mi) of horizontal displacement, and the northern portion at the Unites States-Canada border displaying approximately 140 km (87 mi) (Sears, 2001) (Figure 15). This northern increase in horizontal displacement

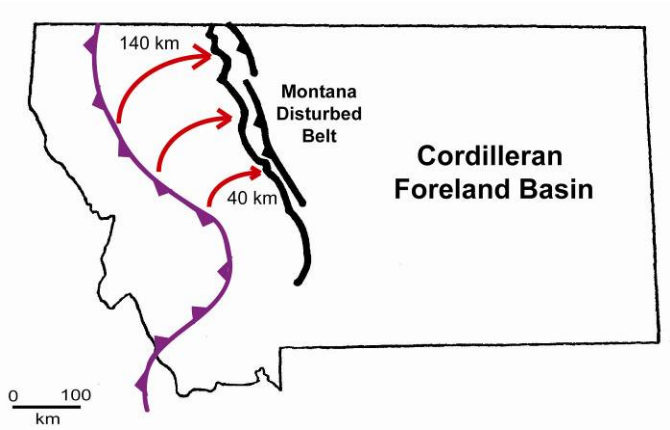

Figure 15) Diagram of present day state of Montana, USA showing rotation of the LEH thrust between 74-59 Ma. The purple line represents the approximate position of the LEH thrust just before approximately 74 Ma. Red lines show clockwise rotation of the thrust as it moved eastward between 74-59 Ma. Relative displacement was greater near the United States-Canada border (~ 140 km displacement), and decreased to the south near the Helena salient (~ 40 km displacement). Black lines represent present location of the LEH and Lombard-Eldorado thrusts. (modified from Sears, 2001)

indicates a general clockwise rotation during slab emplacement (Sears, 2001).

Erosional products sourced primarily from the LEH slab were deposited in the adjacent foreland basin between 74-60 Ma (Sears, 2001). Increased sedimentation occurred in this basin during orogenic pulses of the slab, when greater accommodation was created for sediment deposition as the basin subsided under the increasing load of the orogenic belt (Cantuneau et al., 1999 and 2000; Sears, 2001). Periods of relative tectonic quiescence were characterized primarily by isostatic rebound of the lithosphere and erosional unroofing of the orogenic belt (Cantuneau et al., 1999 and 2000; Sears, 2001). Reciprocal sequence stratigraphy (out of phase sequences developed between the two sides of a hinge line (interpreted foreland basin forebulge) in the Canadian foreland basin as identified by Cantuneau et al. (1999 and 2000), is interpreted as evidence that the orogenic wedge moved in two major pulses (Bearpaw style and post-Bearpaw style) between 74-60 Ma. The reciprocal sequences recorded for this time are further interpreted to indicate the isostatic response of the lithosphere to these orogenic pulses and periods of quiescence (Cantuneau et al., 1999 and 2000; Sears, 2001).

Late Cretaceous Igneous Activity in Montana

During the Campanian, a postulated decrease in the angle of subduction of the Farallon plate beneath the North American plate triggered an inboard sweep of arc magmatism into western Montana causing spatial and temporal overlap of igneous activity and contractional deformation (Lageson et al., 2001; DeCelles, 2004). The general effect of this arc magmatism was an increase in the wedge surface slope angle which created supercritical conditions in the thrust wedge, causing it to migrate

forelandward (eastward), and to change the greatest zone of sediment accumulation in the foreland eastward (Lageson et al., 2001; DeCelles, 2004). Dynamic subsidence in response to this volcanism began to exert a dominant control on regional sediment distribution (DeCelles, 2004). As a consequence of these effects, sediment accumulation rates in western Montana during the Late Cretaceous were among the highest in the Cordilleran foreland (Lageson et al., 2001).

Within west-central Montana, intrusion of the Upper Cretaceous Boulder Batholith and the simultaneous eruption of the Elkhorn Mountains Volcanics, exerted important controls on the development of the Sevier thrust wedge (Lageson et al., 2001) bordering the southwestern portion of the area of Two Medicine Formation deposition, as well as on the deposition of the southern portions of the Two Medicine Formation.

The Boulder Batholith (>6000 km^2 (>3720 mi^2) intrusive complex with thickness estimates ranging from 5-12+ km (3.1-7.4+ mi)) intruded into the hanging wall of the Lombard-Eldorado thrust system between 80-70 Ma, with the major component intruding between 76-70 Ma (Lageson et al., 2001) (Figure 16). The Elkhorn Mountains Volcanics, a sequence of heterogeneous volcanic and volcaniclastic sedimentary rocks roughly 5 km (3.1 mi) thick and representing the extrusive portion of the Boulder batholith, erupted between 81-74 Ma (Lageson et al., 2001). These two igneous events occurred predominantly at the trailing margin of the Lombard-Eldorado allochthon between approximately 80-70 Ma, and had the effect of increasing the wedge surface slope angle, which caused frontal thrust propagation of the allochthon in the area of the Helena salient (Lageson et al., 2001). This thickening caused accelerated basin

subsidence in the adjacent foreland basin (Lageson et al., 2001). The late stage intrusion of the Boulder Batholith into the Elkhorn Mountains Volcanics caused supercritical taper of the orogenic wedge approximately 76-74 Ma, and resulted in eastward thrusting of the Lombard-Eldorado thrust hanging wall (Lageson et al., 2001). A second acquisition of supercritical taper in the hanging wall resulted in a second phase of eastward displacement approximately 74-70 Ma (Lageson et al., 2001).

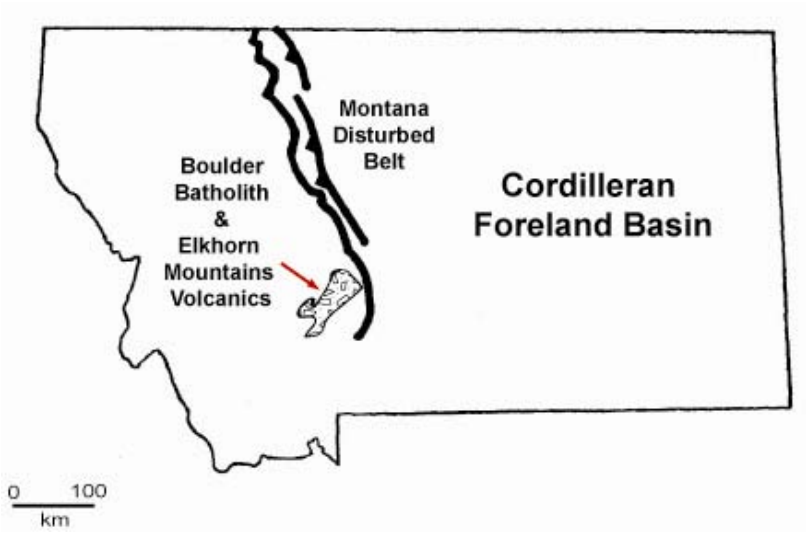

Figure 16) Diagram of present day state of Montana, USA showing approximate present location of the Boulder Batholith and the associated extrusive Elkhorn Mountains Volcanics (modified from Lageson et al., 2001).

The evolution of the Lombard-Eldorado thrust was important in that not only did its associated igneous intrusion and eruptive carapice effect subsidence in the adjacent foreland basin, but sediment eroded from the Elkhorn Mountains Volcanics was continuously deposited in the adjacent foreland basin from approximately 79-54 Ma, where it is now recorded in the stratigraphy of the Two Medicine Formation (Lorenz, 1981).

CHAPTER 4

BACKGROUND: IMPORTANT TWO MEDICINE FORMATION ASSOCIATIONS

Two Medicine Formation Type Section Upper Discontinuity

Two laterally traceable discontinuities, termed the upper and lower discontinuities, (SB2 and SB1 discontinuities of Rogers 1994 and 1998), are present at the type section of the Two Medicine Formation located near Cut Bank, MT (Figure 17). These two surfaces are interpreted by Rogers (1995) to have different origins. The lower discontinuity is present approximately 75 m (246 ft) above the base of the Two Medicine Formation at the type section and has been interpreted to have formed due to a fall in eustatic sea level. The upper discontinuity is present approximately 270 m (886 ft) above the lower discontinuity at the type section, and has been interpreted to have formed due to a tectonically induced increase in the rate of base-level rise. The upper discontinuity is marked by an abrupt change in stratigraphic architecture from fluvial and floodplain facies below to lacustrine carbonate facies above, and as such does not show any evidence of erosional truncation (Rogers, 1995) (Figure 17). This discontinuity is interpreted to have formed at ~ 75.4 Ma based on a bentonite date in correlative Judith River Formation strata, and is interpreted to reflect a regional increase in the rate of base level rise, due to tectonic rejuvenation in the Sevier thrust belt to the east of the study area and subsidence of the foreland basin (Rogers, 1995).

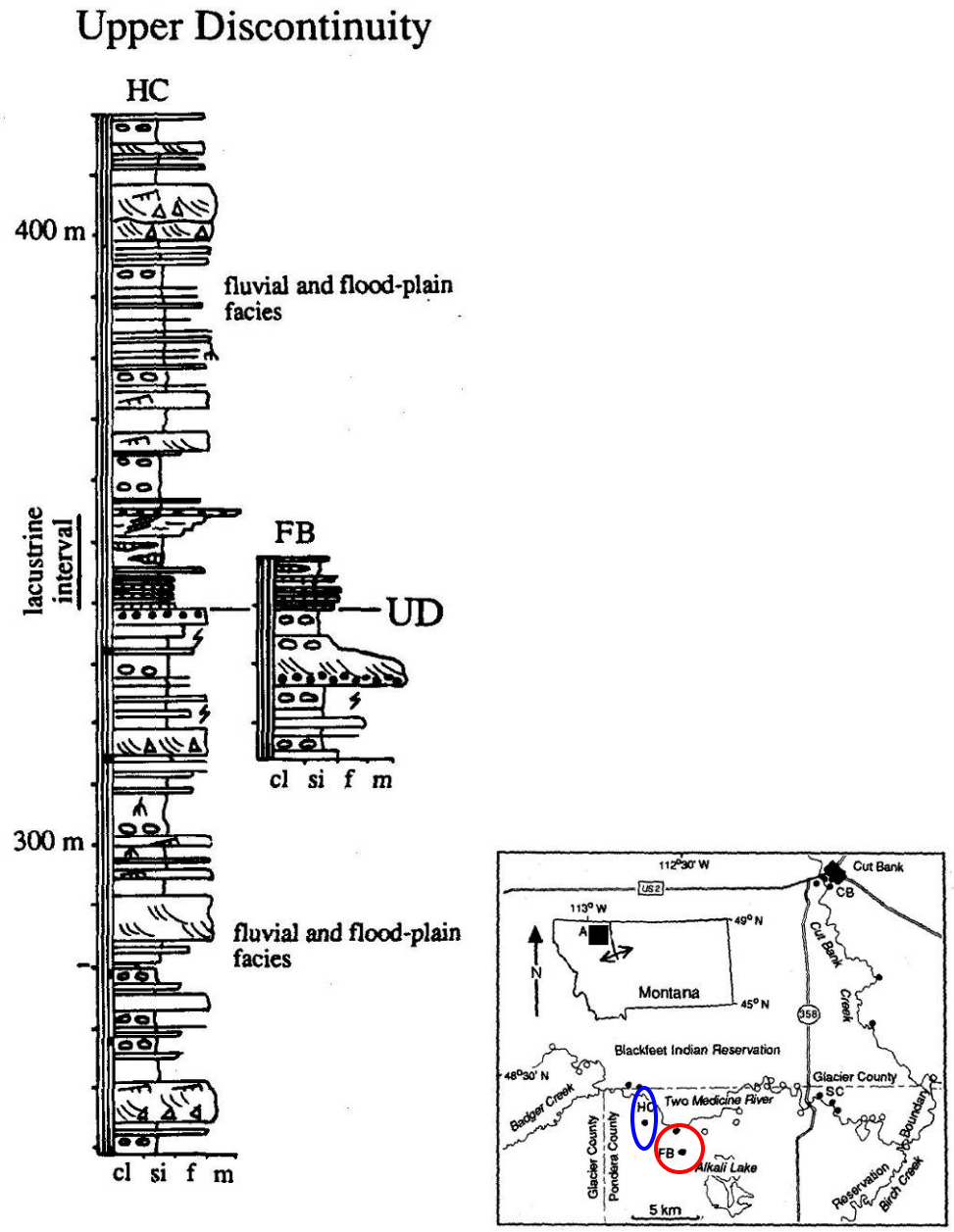

Figure 17: Stratigraphic section showing the position of the Two Medicine Formation upper discontinuity in two sections measured by Rogers (1994). Locations for Hagan's Crossing (HC) and Flag Butte (FB) are shown in the adjacent figure. (modified from Rogers, 1994) (red and blue circles are referred to in figures 18,19) (UD = SB2 in Rogers, 1994,1995)

Figure 18: Two Medicine Formation type section upper discontinuity (denoted by red circle on map in Figure 17). Red arrow denotes base of the interpreted lacustrine interval. Thin bedded lacustrine carbonates change upsection into a siltier and sandier carbonate facies capping the section (location and information from Rogers, 1998).

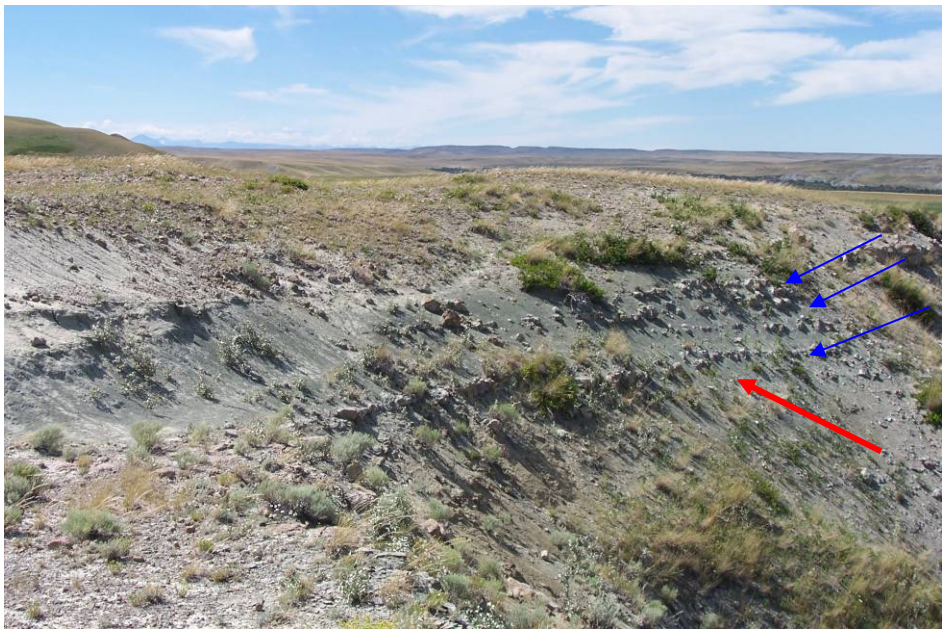

Figure 19: Two Medicine Formation type section upper discontinuity (denoted by blue circle on map in Figure 17). Red arrow denotes base of lacustrine interval. Thin beds of lacustrine carbonates (denoted by blue arrows) are interbedded with mudstone (location and information from Rogers, 1998).

Correlation of the Type Section Lower Discontinuity

In a study similar to Rogers (1998), Roberts (1999) analyzed the stratigraphy of the lower Two Medicine Formation in the Seven Mile Hill, Old Trail, and Robinson areas near Choteau, MT in an attempt to identify a lower discontinuity such as is present in the Two Medicine Formation type area (Figure 20). Although there is no physical disconformity present in the Choteau area, the relative position of the discontinuity was inferred using local dated ash beds and a tuff bed dated to approximately 80 Ma, the same age as the lower discontinuity (SB1) present in the type area (Roberts, 1999) (Figure 21 in Appendix C).

In the Seven Mile Hill area, the interpreted lower discontinuity is marked by a decrease in channel:floodplain ratio, change in degree of paleosol development, and a change from abundant, stacked channel sands to isolated ribbon channel sands packaged in muds (Roberts, 1999). This abrupt change in stratigraphic architecture is inferred to record a change in base level resulting from the phase change from a relative fall to a relative rise in sea level (Roberts, 1999). It is also thought to be correlative with the lower discontinuity present in the type area of the Two Medicine Formation, although in the type area this bounding surface is marked by a disconformity (Roberts, 1999). Another characteristic that is not consistent between the type section and Choteau areas is that in the type area, there is an up section decrease in sandstone body thickness and channel/floodplain ratios beneath the discontinuity, while in the Choteau area there is an

up-section increase in the density and thickness of sandstone bodies (Roberts, 1999). The lack of an erosive surface in the Choteau area, and the differences

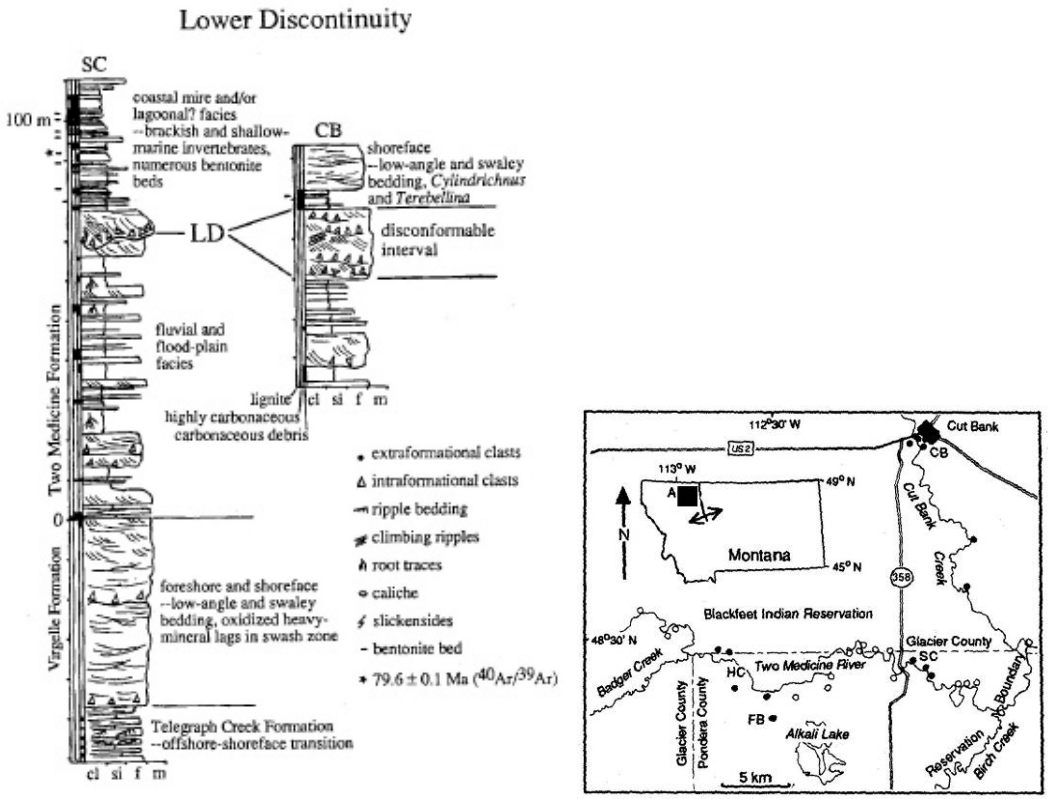

Figure 20: Stratigraphic section showing the position of the Two Medicine Formation lower discontinuity in two sections measured by Rogers (1994). Locations for Shield's Crossing (SC) and Cut Bank (CB) are shown in the adjacent figure. (modified from Rogers, 1994)

between the sandstones may be due to local differences in factors such as subsidence, sediment supply, or tectonics (Roberts, 1999). The potential correlation between discontinuities in both the Choteau and type areas as presented by Roberts (1999) is important in that it provides evidence of the applicability of nonmarine sequence

stratigraphic techniques in tracing discontinuities between nonmarine rock units (Figure 21 in Appendix C).

CHAPTER 5

METHODS

During the summer of 2004, twenty one stratigraphic sections were measured at the Willow Creek anticline using a Brunton compass and a 1.5 m (~ 4.9 ft) Jacob's staff (Figure 22). All measured section descriptions and figures are located in Appendices A and B. For each section, lithology, thickness, color, grain properties, sedimentary and biogenic structures, fossil content, lateral continuity, and the nature of the contacts were recorded. Specific color designation numbers were recorded for each unit using the Munsell Color Chart (2000) numbering system. If applicable, the stratigraphic position of dinosaur nests or egg shell in a measured section was also recorded. In addition, photographs were taken of each measured section. Section descriptions were then converted into stratigraphic columns using Adobe Illustrator. Lithofacies designations were then assigned to the various units using the terminology of Miall (1996) (Appendix A).

Three bentonite samples were collected at the Willow Creek anticline: one from the Nose Cone Site (recorded in the Nest in the Wall Bentonite measured section) (Appendix A), one from the Children's Dig measured section Site (Appendix A), and one from the Justin's Peak measured section site (Appendix A). These samples were subsequently sent to the U.S. Geological Survey Argon Geochronology Laboratory in Denver for U/Pb SHRIMP dating of zircons.

The stratigraphic locations of Willow Creek anticline bentonites, as well as their ages recorded by from U/Pb SHRIMP dating of the zircons were the first datum used to correlate the measured sections of this study. Additional correlations were made using the stratigraphic locations of the lacustrine interval in the measure sections. These measured section correlations were then examined for changes in stratigraphic and stratigraphic architecture by looking for changes in depositional environment and in the nature of channel and floodplain deposits. These findings were then compared to the stratigraphic architectural changes reported by Rogers (1995) at the type section. In addition, in order to more accurately determine similarities between the stratigraphy of the Willow Creek anticline and that of the type section, three trips to the type section of the Two Medicine Formation were also made during the summers of 2004 and 2006. During these trips, observations were concentrated on examining changes in stratigraphic architecture in the rocks spanning the stratigraphic upper discontinuity of Rogers (1995).

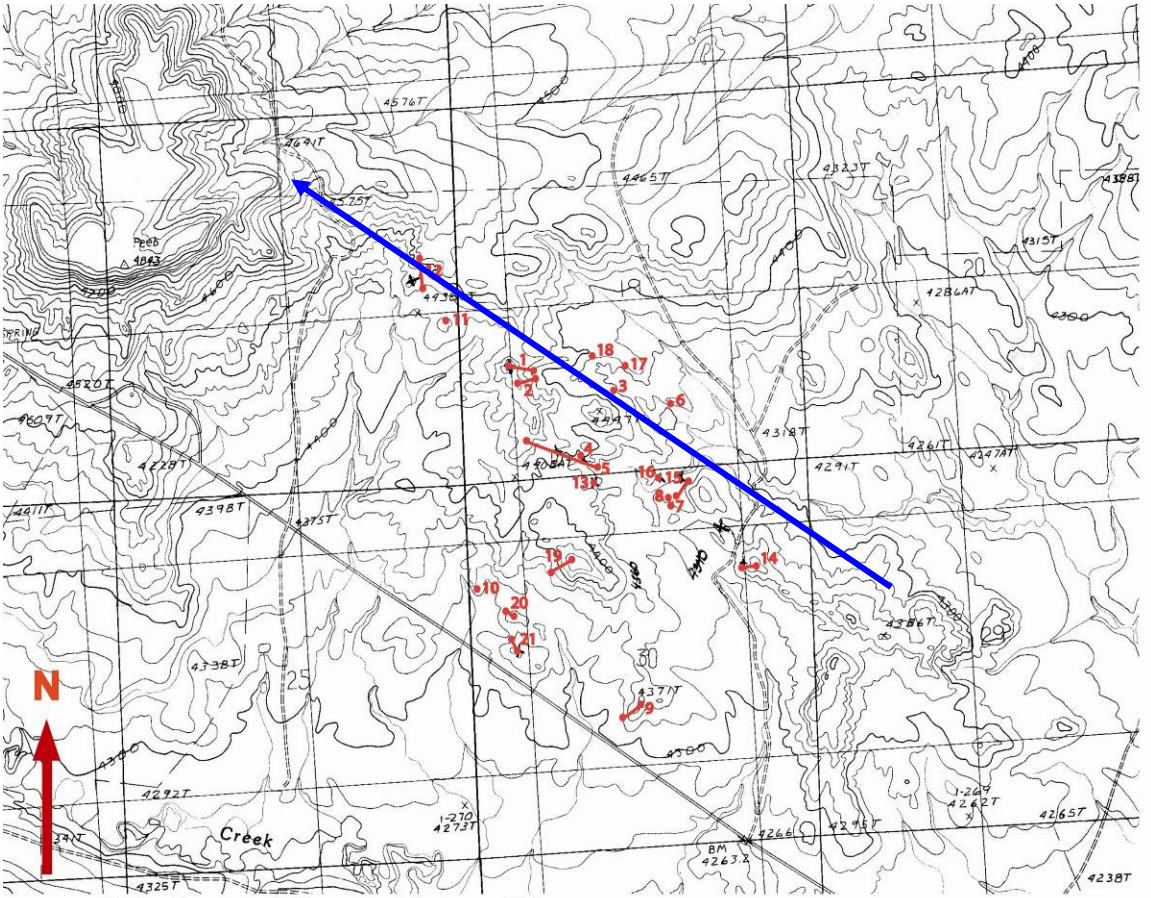

Willow Creek anticline near Choteau, MT
Blow-up of central portion of Watson Flats, MT Quadrangle
Scale 1:24,000
* Measured Sections shown in red

1: Thunder Dome	6: Lake Giardia	11: Egg Island	16: '79 Nest	21: Egg Mountain A
2: T.D. Bentonite	7: Justin's Peak	12: Flaming Cliffs	17: Fault Mountain 1	
3: Pete's Pupa Peninsula	8: Josh's Hill	13: Branvold Site	18: Fault Mountain 2	
4: Nose Cone 2	9: Jess Butte	14: Children's Dig	19: Egg Mountain C	
5: Nest in the Wall Bentonite	10: Frans Site	15: '78 Nest	20: Egg Mountain B	

Figure 22) Location of stratigraphic sections measured in this study at the Willow Creek anticline (axis shown in blue, with arrow pointing in the direction of plunge to NW).

CHAPTER 6

RESULTS: WILLOW CREEK ANTICLINE LITHOFACIES DESCRIPTIONS AND HYDRODYNAMIC INTERPRETATIONS

Introduction

This chapter delineates the specific lithofacies present at the Willow Creek anticline. Each section provides a description and interpretation of hydrodynamic

Lithofacies	Hydrodynamic Conditions / Method of Formation
B Bentonite layer	Clay formed from chemical alteration of ash-fall volcanic ash
C Light grey, well-indurated carbonate	Movement of groundwater (evaporation and capillary groundwater flow or carbon degassing concentrating ions as calcium carbonate near the ground surface during dry periods in climate)
Fl Laminated sand, silt, mud	Suspension and weak traction currents
Fm Massive mud, silt	Suspension settling
Fmc Carbonate-rich, color mottled massive mudstone	Movement of groundwater through mudstone over long periods of time
Lc Charophytiferous limestone	Lacustrine carbonate production
P nodular to discontinuously bedded oxidized carbonate	Soil forming processes
Sh Horizontally bedded sand	Upper flow regime plane bed conditions (fine-med grain size)
Sm Massive sand	Rapid deposition and bioturbation
Sw Carbonate cemented sandstone with pupal cases	Sandstone preserving insect pupal cases and burrows via carbonate cementation due to groundwater table rise
Sr Ripple cross laminated sand	Migration of ripple bedforms
St Trough cross bedded sand	Migration of sinuous crested dunes under lower flow regime unidirectional flow conditions

Figure 23: Summary of lithofacies and depositional conditions.

conditions for a specific lithofacies. Specific color designation numbers for each unit recorded for each lithofacies were determined using the Munsell Color Chart numbering system and are located in the measured section descriptions in Appendix B. The results of this chapter are summarized above in Figure 23. All lithofacies are discussed in alphabetical order except for lithofacies C (light grey, well-indurated carbonate) and lithofacies P (nodular to discontinuously bedded oxidized carbonate) which are discussed together in a section at the end of this chapter.

Lithofacies B: Bentonite Layer

Description

Lithofacies B is characterized by white/reddish white to gray-green bentonite beds ranging from 0.17 m – 1 m (0.56 ft – 3.28 ft) thick, and containing very fine to coarse-grained biotite crystals (Figure 24, 25). No internal stratification or sedimentary structures were observed.

Hydrodynamic Conditions

Bentonite is a soft, plastic light colored rock composed of expandable-layer clay minerals formed by the chemical alteration of volcanic ash. Volcanic ash expelled from a volcanic eruption settles out of the atmosphere and is deposited as a layer of volcanic ash on the ground surface. Over time, the ash is converted via chemical alteration to bentonite composed mainly of montmorillonite and related minerals of the smectite group. The ash layers that were originally deposited were most likely sourced by

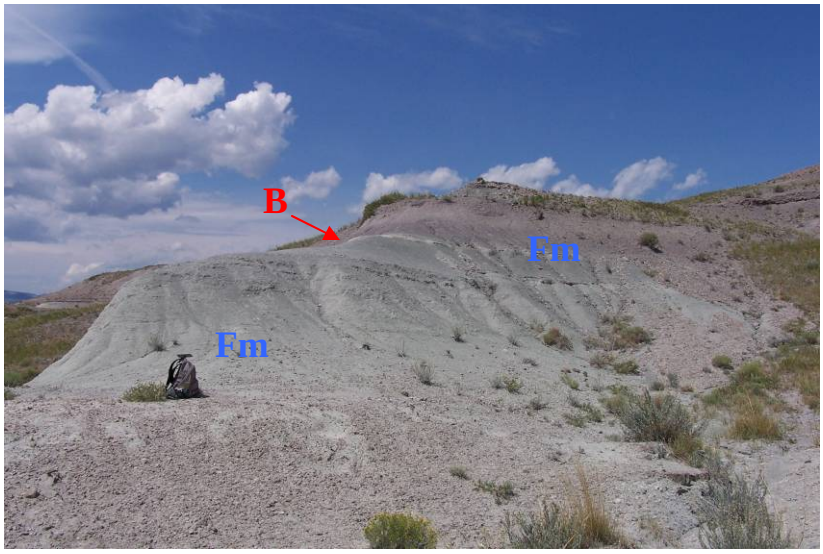

Figure 24: Lithofacies B at Nose Cone Site, Willow Creek anticline, Choteau, MT. Fm: Massive mudstone.

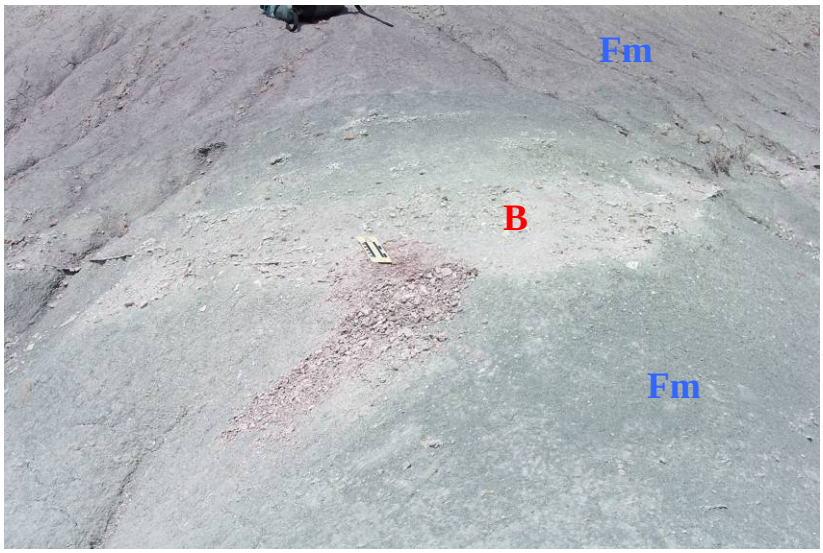

Figure 25: Lithofacies B at Nose Cone Site, Willow Creek anticline, Choteau, MT. Fm: Massive mudstone.

volcanic eruptions from the Elkhorn Mountains Volcanics located in the area south of the Willow Creek anticline (Gavin, 1986).

Two bentonites were dated at the U.S. Geological Survey laboratory in Denver, Colorado using U/Pb SHRIMP radiometric dating techniques on biotite grains found in these bentonite samples. The first, located approximately 3.52 m (11.55 ft) up from the base of the Justin's Peak measured section (Appendix A) records a age of 76.9 +/- 0.5 Ma (Miggins, pers. comm.). The second, located just to the west of the Nose Cone 2 site (Appendix A) is stratigraphically equivalent to the bentonite that is found approximately 3.4 m (11.15 ft) up from the base of the Branvold Site measured section (Appendix A). This bentonite was dated twice using the same methods and records ages of 76.0 +/- 0.6 Ma and 77.0 +/- 0.7 Ma (Miggins, pers. comm.), giving a rough average age of 76.5 Ma. The Branvold Site bentonite, the Nest in the Wall Bentonite bentonite found stratigraphically between the TM-003 bonebed and the beginning of the lacustrine interval, and the bentonite located near Nose Cone 2 (Appendix A) are interpreted to be stratigraphically equivalent and deposited from the same ash fall event, with a date of approximately 76.5 Ma (averaged from 76.0 +/- 0.6 Ma and 77.0 +/- 0.7 Ma) (Figure 26, 27 in Appendices D, E). The Justin's Peak bentonite, Children's Dig bentonite, and '78 Nest bentonite are also interpreted to be stratigraphically equivalent, with a date of approximately 76.9 +/- 0.5 Ma (Figure 26, 27 in Appendices D, E).

Lithofacies Fl: Laminated Sandstone, Siltstone, and Mudstone

Description

Lithofacies Fl is characterized by red-brown, greenish grey, and bluish grey laminated sandstone, siltstone, and mudstone with bed thickness ranging from 5 cm to 1.8 m (1.95 in - 5.9 ft) (Figure 28).

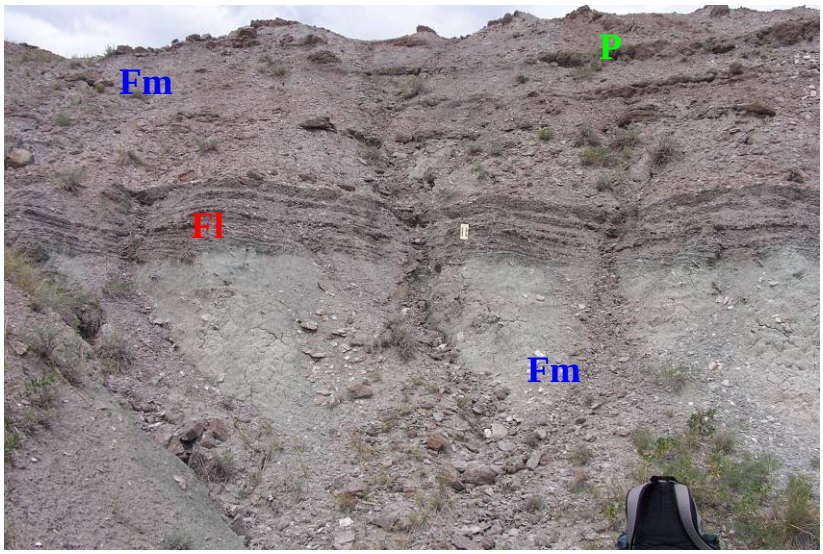

Figure 28: Lithofacies Fl at Fault Mountain 2 Site, Willow Creek anticline Choteau, MT. Fm: Massive mudstone. P: Nodular to discontinuously-bedded oxidized carbonate.

Hydrodynamic Conditions

Laminations reflect differences in grain size and represent deposition from suspension and weak traction currents (Dreyer, 1993; Miall, 1996, p. 123; Spalletti and Pinol, 2005). These deposits are commonly found on floodplains, or in some cases lakes on floodplains (Collinson, 1996, p. 54; Miall, 1996, p. 123). The transition from massive mudstone to Fl reflects a slight increase in depositional energy, but still records

deposition in relatively quiet water as evidenced by the fine-grained nature of the deposits.

Lithofacies Fm: Massive Mudstone

Description

Lithofacies Fm is characterized by massive, dark red-brown to light greenish grey claystone and mudstone to silty mudstone and whitish grey siltstone ranging in thickness from 8 cm to 8.6 m (3.2 in – 28.21 ft) (Figure 29). Many beds contain groundwater carbonate nodules 4 to 7 cm (1.56 in – 2.73 in) in diameter representing the early stages of pedogenesis. Precipitation of calcite crystals is very common in this lithofacies, and calcite may be found as veins or thin layers in the outcrop. Calcite is found forming casts of seeds in the Nest in the Wall Bentonite section (Appendix A). In addition, dinosaur eggshell, dinosaur bone, dinosaur nest sites, and occasional limestone and very fine sandstone clasts are found in this facies.

Hydrodynamic Conditions

Fine-grained mudstones are deposited in low energy, quiet water environments. The massive, structureless bedding of lithofacies Fm can either be attributed to: 1) rapid deposition from a sediment gravity flow, 2) destruction of sedimentary structures through bioturbation, 3) fairly uniform grain size and composition, or 4) liquefaction (Boggs, 2001, p. 97). The position of lithofacies Fm lateral to and between sand deposits and its

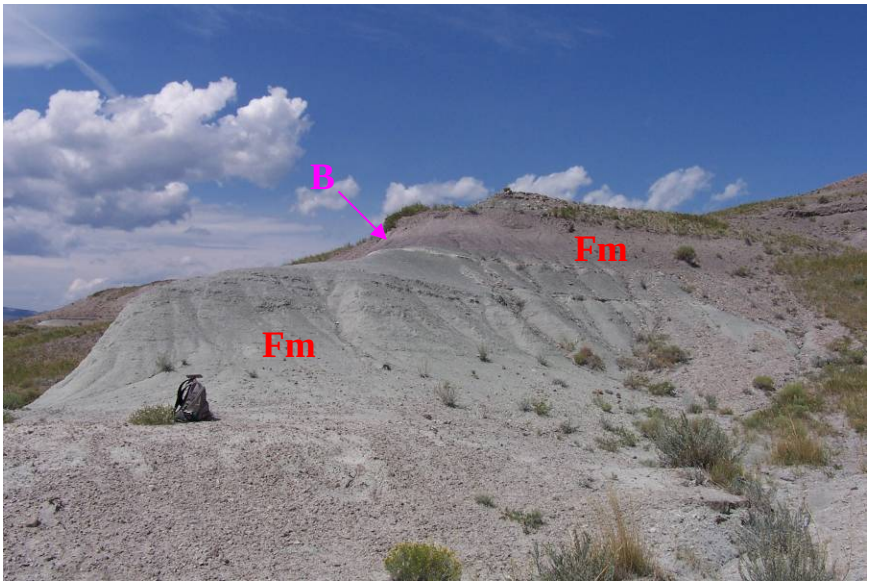

Figure 29**:** Lithofacies Fm at Nose Cone Site, Willow Creek anticline Choteau, MT. B: Bentonite layer.

fairly uniform lateral extent suggests that deposition of lithofacies Fm was not result of a sediment gravity flow, but rather by quiet water suspension deposition. Additionally, there is no evidence for liquefaction or fluidized flow. Through thin section and x-ray analysis, Gavin (1986) identified the presence of pedotubules within many of the mudstones and silty mudstones exposed at the Willow Creek anticline. Thin section analysis shows that these pedotubules are filled with sparry calcite, and x-ray analysis shows that the pedotubules branch and taper, indicating they are most likely root systems (Gavin, 1986). Lithofacies Fm is interpreted to have been deposited through suspension settling in a low energy river floodplain environment (Dreyer, 1993; Spalletti and Pinol, 2005). The massive, structureless nature of lithofacies Fm is therefore attributed to bioturbation, primarily by plant roots.

Lithofacies Fmc: Carbonate-rich, color mottled massive mudstone

Description

Lithofacies Fmc is composed of carbonate-rich mudstone with extensive purple and green color mottling, with thicknesses ranging from 10 cm to 7.5 m (3.9 in – 24.6 ft). Lithofacies Fmc is most commonly found in association with light grey, well-indurated carbonate (lithofacies C) in the stratigraphically highest deposits of the Willow Creek anticline.

Hydrodynamic Conditions

The presence of purple, green, and grey mottling in lithofacies Fmc provides evidence for hydromorphic conditions at the Willow Creek anticline, as strata with grey colors with mottling are interpreted to indicate relatively long periods of a high groundwater level (PiPujol and Buurman, 1994; Djamali et al., 2006). In environments with this characteristic, two important processes in the precipitation of carbonate and the formation of calcretized layers are high evaporation and evapotranspiration (Semeniuk and Meagher, 1981; in Djamali et al., 2006).

Lithofacies Lc Charophytiferous Limestone

Description

Lithofacies Lc consists of light to dark grey argillaceous biomicrite (Folk, 1962) 0.6 m to 2.27 m (1.97 ft – 7.45 ft) thick. Many of the limestone beds contain charophyte fossils (Figure 30).

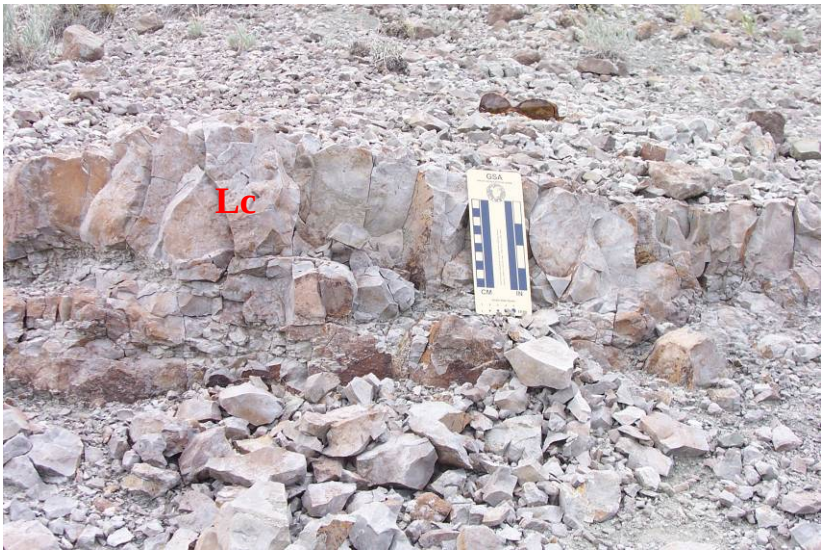

Figure 30: Lithofacies Lc at Thunder Dome bentonite measured section Site, Willow Creek anticline Choteau, MT.

Hydrodynamic Conditions

Analyses of lithofacies Lc were done primarily by Gavin (1986). Through thin section analysis, Gavin (1986) described charophytiferous limestones found in the Willow Creek anticline as being composed mainly of micrite, but also containing 1-10% siliciclastics, primarily very fine sand to silt in size. Some portions of lithofacies Lc also contain possible rhizoliths (calcite casts formed around plant stems) made of sparry calcite (Gavin, 1986).

Lithofacies Lc also contains charophytes, which are a group of aquatic green algae that are very common in freshwater lakes, and that are major producers of carbonate sediment in lakes (Talbot and Allen, 1996, p. 94; Valero Garces et al., 1997; Gierlowski-Kordesch, 1998). Charophytes are found most commonly in shallow, quiet, alkaline water (Peck, 1957; Valero Garces et al., 1997; Gierlowski-Kordesch, 1998), and

they produce calcified female reproductive cells which are usually roughly circular structures 1-2 mm (0.004 in - 0.008 in) in diameter (Talbot and Allen, 1996, p. 94).

Through thin section analysis, Gavin (1986) found three types of preserved charophyte *gyrogonites*, as well as other plant fragments in the deposits of lithofacies Lc. Gavin (1986; p. 32) describes one as "spherical with very thick walls and an almost smooth surface", another as "slightly oblate with nine convex ridges per side (possibly a member of genus *Clavator*)", and the last as "having seven concave grooves per side" and that is relatively rare.

The presence of charophyte fossils within the limestones of lithofacies Lc, suggest it was deposited in a shallow, quiet water, alkaline freshwater lake or system of lakes (Gavin, 1986). The micrite was produced by both organic and physiochemical processes that took place within the lake(s), and accumulated via settling through the water column.

Lithofacies Sh: Horizontally-bedded Sandstone

Description

Lithofacies Sh is characterized by light grey-off-white salt and peppery to light greenish fine to medium-grained sandstone weathering to a rusty color (Figure 31). Grains are subangular-subrounded, moderately to well sorted. Some beds display parting lineations on their surfaces. Lithofacies Sh also often contains fairly abundant burrows 0.5-3 cm (0.2 in – 1.17 in) in diameter and up to 8 cm (3.12 in) in length.

Figure 31: Lithofacies Sh near Thunder Dome Site, Willow Creek anticline Choteau, MT.

Hydrodynamic Conditions

Horizontally-bedded sand occurs under two different conditions: under upper flow regime plane bed conditions and under lower flow regime plane bed conditions (Miall, 1996, p. 120). Lithofacies Sh forms most commonly under upper flow regime plane bed conditions at the transition from subcritical to supercritical flow (Miall, 1996, p. 120; Dreyer, 1993; Spalletti and Pinol, 2005). Plane beds that form under upper flow regime conditions are most commonly composed of very fine to medium-grained sand, and tend to form at flow velocities of 1 m/s (3.28 ft/s) and in water depths between 0.25-0.5 m (.82 ft – 1.64 ft) although they can occur at lower flow velocities and at shallower depth (Miall, 1996, p. 120). Lower flow regime plane beds form under lower flow velocities and are usually composed of coarse to very coarse-grained sand, although this is preserved less often (Miall, 1996, p. 120).

Lithofacies Sh is marked by the presence of parallel lamination and parting lineations on bedding planes (Dreyer, 1993; Spalletti and Pinol, 2005). The fine to medium-grain sizes and parting lineation present in lithofacies Sh indicate that lithofacies Sh was deposited under upper flow regime plane bed conditions most likely found within crevasse splay deposits (Miall, 1996, p. 120).

Lithofacies Sm: Massive Sandstone

Description

Lithofacies Sm is characterized by structureless, massively bedded off-white salt and peppery, well sorted fine to coarse-grained sandstone with subangular to subrounded grains. Bed thickness ranges from to 12 cm to 4.9 m (4.68 in – 16.1 ft) (Figure 32). Burrows 1-2 cm (0.39 in - 0.78 in) in diameter are present throughout some beds. Rarely, small pieces of dinosaur eggshell can also be found.

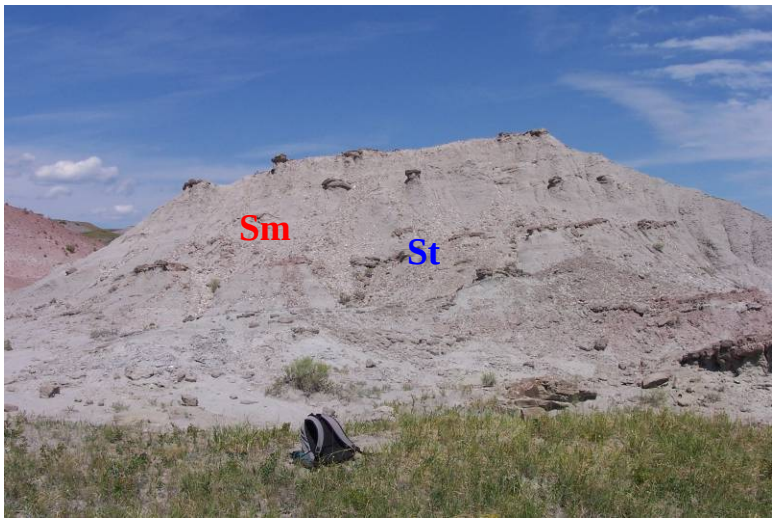

Figure 32: Lithofacies Sm at Justin's Peak measured section Site, Willow Creek anticline Choteau, MT. St: Trough cross-bedded sandstone.

Hydrodynamic Conditions

Massive, structureless beds are produced in one of 3 ways: 1) rapid deposition from a sediment gravity flow, 2) destruction of sedimentary structures through bioturbation, 3) liquefaction (Boggs, 2001, p. 97). Some massive, structureless sandstone beds at the Willow Creek anticline show evidence for extensive bioturbation and these beds therefore may have originally had sedimentary structures such as trough cross-bedding that was subsequently destroyed by later bioturbation. However, other massively bedded sandstones in the area do not contain evidence for bioturbation, and these sandstones are interpreted to have formed under conditions of high rates of suspension settling from currents of moderate to high sediment concentration (Lomas, 1999; and Grecula et al., 2003; in Spalletti and Pinol, 2005). The distinction between these two processes of formation of massive, structureless sandstones is important because bioturbated massive sandstones with possible obscured sedimentary structures may have formed from migration of bedforms (such as sinuous crested dunes) in a river channel at lower flow velocities, as compared to the higher velocities that may have deposited the massive sandstones that do not contain bioturbation.

Some of these beds at the Willow Creek anticline show evidence for extensive bioturbation and these beds therefore may have originally had sedimentary structures such as trough cross-bedding that was subsequently destroyed by later bioturbation. However, other massively bedded sandstones in the area do not contain evidence for bioturbation, and these sandstones are interpreted to have formed under conditions of high rates of suspension settling from currents of moderate to high sediment

concentration (Lomas, 1999; and Grecula et al., 2003; in Spalletti and Pinol, 2005). The distinction between these two processes of formation of massive, structureless sandstones is important because bioturbated massive sandstones with possible obscured sedimentary structures may have formed from migration of bedforms (such as sinuous crested dunes) in a river channel at lower flow velocities, as compared to the higher velocities that may have deposited the massive sandstones that do not contain bioturbation.

Lithofacies Sw: Carbonate Cemented Sandstone with Pupal Cases

Description

Although many of the sandstones preserved at the Willow Creek anticline are cemented with carbonate, Lithofacies Sw is a sandstone distinguished in this study due to its extensive preservation of molds and casts of ellipsoidal-shaped pupal cases. These pupal cases are commonly 1 cm (0.4 in) in width and 2 cm (0.8 in) in length found inside larger vertical burrows (Figures 33, 34). Lithofacies Sw beds range from 35 cm to 2.12 m (13.65 in – 6.95 ft) thick.

Hydrodynamic Conditions

Lithofacies Swp is interpreted as a sandstone formed either on a channel levee or near the shoreline of a lake. These areas would have been sandy initially (when the bees were burrowing into it) and above the water table, but were then cemented with carbonate during a later water table rise. Martin (2001) described pupal cases in the Willow Creek anticline, Upper Two Medicine Formation, and attributed their presence as evidence of

Figure 33: Lithofacies Sw at Pete's Pupa Peninsula measured section Site, Willow Creek anticline Choteau, MT.

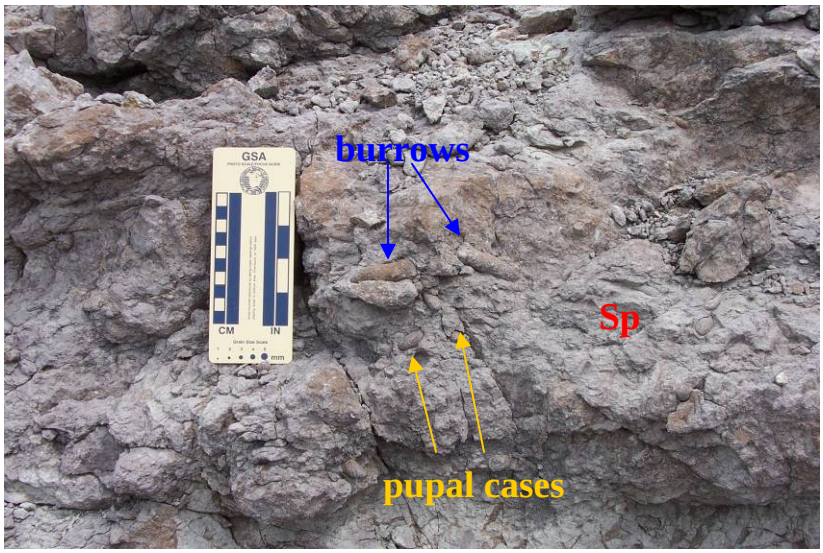

Figure 34: Lithofacies Sw at Pete's Pupa Peninsula measured section Site, Willow Creek anticline Choteau, MT.

insect-on-insect parasitoid behavior. Martin (2001) described the pupal cases as prolate ellipsoids in shape with a mean length of 20.7 mm (0.08 in) and a mean width of 10.4

mm (0.04 in), and as being found inside vertical larger burrows that were made by a different species of insect.

These burrows may have been formed by insects of the order Hymenoptera, such as bees and wasps in areas with arid, well drained soils above the water table (Martin, pers. comm.). Bee pupal cases are smooth walled and flask-shaped with a narrow neck, and tend to occur in clusters, while wasp pupal cases have rough walls, are capsule-shaped, lack a cap, and tend to be solitary (Martin, pers. comm.).

Lithofacies Sr: Ripple Cross-laminated Sandstone

Description

Lithofacies Sr is characterized by light grey-off-white salt and peppery to light greenish very fine to medium-grained sandstone ranging from 20 cm to 50 cm thick (7.8 in – 19.5 in) (Figure 35). Grains are subangular to subrounded and are moderately to well sorted. Lithofacies Sr is also occasionally marked by the presence of burrows 1-2 cm (0.39 in - 0.78 in) in diameter.

Hydrodynamic Conditions

Sand ripples are most commonly composed of fine to medium-grained sand, although they can range from very fine to coarse-grained sand (Miall, 1996, p. 115). Ripples form from the migration of ripple bedforms under lower flow regime conditions at speeds generally less than 1 m/s (3.28 ft/s) (Miall, 1996, p. 115). Sand ripples are most

composed of fine to medium-grained sand, although they can range from very fine to coarse-grained sand (Miall, 1996, p. 115).

Figure 35: Lithofacies Sr near Children's Dig measured section Site, Willow Creek anticline Choteau, MT.

coarse-grained sand (Miall, 1996, p. 115).

Lithofacies St: Trough Cross-bedded Sandstone

Description

Lithofacies St is characterized by off-white salt and peppery to greenish grey medium to coarse-grained sandstone ranging from 60 cm to 3 m (24 in - 9.84 ft) thick (Figure 36). Grains are angular to subrounded and are moderately to well sorted. Purple to green mud rip-up clasts 1 mm – 7 cm (0.04 in – 2.8 in) in diameter are commonly found in the basal-middle portion of the beds (Figure 37). In one section, burrows 1-2 cm (0.04 in – 0.8 in) in diameter are found in the upper portion of the bed.

Hydrodynamic Conditions

Trough cross-bedding forms by the migration of sinuous crested dunes under lower flow regime unidirectional flow conditions and are typically composed of fine to very coarse-grained sand (Miall, 1996, p. 114). Commonly a lag of poorly sorted sand

Figure 36: Lithofacies St at Flaming Cliffs measured section Site, Willow Creek anticline Choteau, MT.

with intraclasts of siltstone or mudstone occurs at the base of the trough (Miall, 1996, p. 115). Trough cross-bed sets form from sand grains avalanching down the lee side of a migrating sinuous crested dune (Boggs, 2001, p. 101). The curved shape characteristic of trough cross-beds results from dunes migrating over and filling in scours formed by eddies that form as a result of water flow over the curved dune crest (Dreyer, 1993; Boggs, 2001, p. 101). Lithofacies St therefore represents deposits left by the migration of sinuous crested dune forms in a river channel. Mudstone rip-up clasts record collapse of

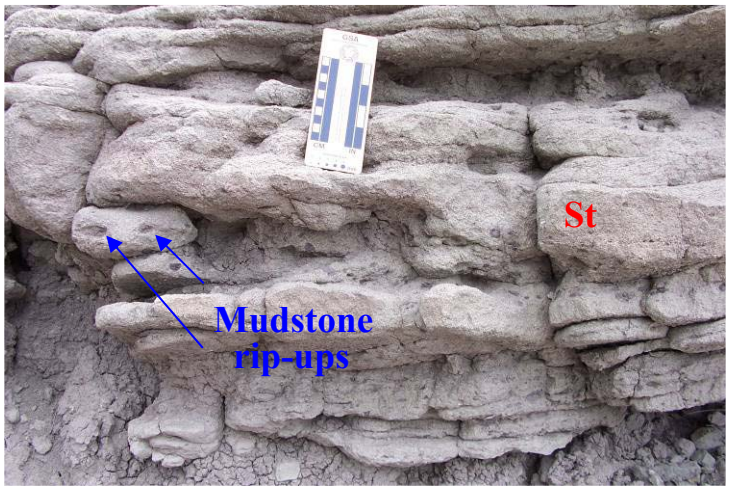

Figure 37: Mudstone rip-up clasts in lithofacies St at Flaming Cliffs measured section Site, Willow Creek anticline Choteau, MT.

cohesive overbank material (Collinson, 1996, p. 66). Paleocurrent data for these sandstones measured by Gavin (1986) record values of $V_0 = 38^o$ with a consistency ratio of 0.91 in the northwestern section of the study area, and $V_0 = 77.65^o$ with a consistency ratio of 0.83 in the central part of the study area. A consistency ratio of 1 represents perfectly preferred orientation and 0 represents totally random orientation (Gavin, 1986).

Non-Lacustrine Carbonate Deposits

Two types of non-lacustrine carbonate deposits are present at the Willow Creek anticline: nodular to discontinuously bedded oxidized carbonate (lithofacies P) and a light grey, well-indurated carbonate (lithofacies C). Calcrete is a term used for non-lacustrine carbonates, and is defined as "a near surface accumulation of predominantly calcium carbonate whose formation within the vadose and phreatic zone is mediated either though pedogenic (soil related) or groundwater processes or a combination of both" (Khadkikar

et al., 1998, p. 254). Two major sinks of calcrete are pedogenic calcrete and groundwater calcrete (Khadkikar et al., 1998). Pimentel et al. (1996) provides information for distinguishing between these two types of calcretes, and this information is summarized in Figure 38. The characteristics listed in Figure 38 above will be used in this section to evaluate method of deposition for the nodular to discontinuously bedded oxidized carbonate lithofacies and the light grey, well-indurated carbonate lithofacies.

Pedogenic Calcretes	**Groundwater Calcretes**
Generally thin, 1-2 m	May reach thicknesses of 10 m or more
Usually display profile with orderly set of horizons. Sharp top and gradational base.	Usually massive throughout. Gradational top and base.
Nodular, massive, laminar, and pisolitic macrostructures	Rarely display laminar horizons. Never prismatic or pisolitic unless at the top of unit.
Microfabric may exhibit beta-fabrics (biogenic microbial / root-related carbonates)	Usually alpha-fabrics (densely crystalline)
Usually finely crystalline	May show wider range of crystal sizes
Low porosity	Porosities locally high (>25%)
Rarely display lateral changes in composition	May show regular mineralogical changes
Usually associated with more stable surfaces on floodplains	Associated with drainage channels, playas, and lake deposits
If present, mottling is minor, reflecting lack of Fe-translocation in generally oxidized setting	Extensive mottling and Fe-translocation in reducing groundwater
Most commonly found in finer units in alluvial cyclothems	More common in more permeable coarser units in alluvial cyclothems

Figure 38: Chart contrasting characteristics of pedogenic calcretes versus groundwater calcretes (modified from Pimentel et al. (1996)).

Lithofacies C: Light Grey, Well-indurated Carbonate

Description

Lithofacies C is characterized by light grey relatively discontinuous beds of well-indurated carbonate 15 cm – 67 cm (5.9 – 26.4 in) thick. Lithofacies C occurs primarily in association with carbonate-rich, color mottled massive mudstone (lithofacies Fmc) in the stratigraphically highest rocks of the Willow Creek anticline (primarily in the Nest in the Wall, Thunder Dome, and Thunder Dome Bentonite measured sections (Appendix A).

Mode of Formation

When compared with Figure 38, the characteristics of lithofacies C noted above suggest that its method of formation was most likely through movement of groundwater. Groundwater carbonate is a non-pedogenic form of calcrete (Khadkikar et al., 1998), and forms from rain infiltration leaching dissolvable ions downward during wet periods, and evaporation and capillary groundwater flow or carbon degassing concentrating ions as calcium carbonate near the ground surface during dry periods (Miall, 1996, p. 127; Khadkikar et al., 1998). Its association with carbonate-rich, color mottled massive mudstone (lithofacies Fmc) also suggests that lithofacies C is a groundwater carbonate, as these green, grey, and purple colors suggests reducing conditions due to a relatively higher groundwater table (Collinson, 1996, p. 68), and the mottling suggests hydromorphic conditions (PiPujol and Buurman, 1994; Djamali et al., 2006).

Lithofacies P: Nodular to Discontinuously Bedded Oxidized Carbonate

Description

Lithofacies P is characterized by brown to red-brown nodular to discontinuously bedded oxidized carbonate 25 cm to 0.95 m (9.75 in – 3.1 ft) thick. Lithofacies P may also be found as nodules aligned in layers within massive mudstones (Figure 39). In addition, lithofacies P is predominantly made of micrite, and contains abundant pedotubules (Gavin, 1986). Lithofacies P in nodular form occurs primarily in the stratigraphically lowermost rocks of the Willow Creek anticline, while the bedded form occurs primarily in the stratigraphically highest rocks (Figure 26; in Appendix D).

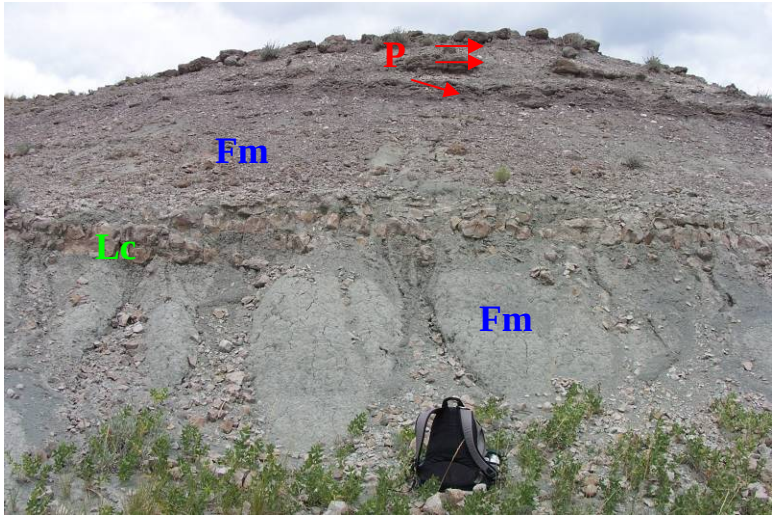

Figure 39: Lithofacies P near Fault Mountain 2 Site, Willow Creek anticline Choteau, MT. Fm: Massive mudstone. Lc: Charophytiferous limestone.

Mode of Formation

When compared with Figure 36, the characteristics of lithofacies P noted above suggest that its method of formation was most likely through pedogenic, or soil forming,

processes. Pedogenic carbonates, or pedogenic calcrete, are calcitic soils that form above the water table in arid to semiarid oxidizing climates where floodplains are exposed to surface weathering processes for extended periods of time (thousands of years) (Miall, 1996, p. 127). Pedogenic carbonate is usually micritic and can be seen to replace and surround clastic grains (Retallack, 1990). Carbonate nodules form through repeated expansion and contraction of clays coupled with rooting activity of plants (Khadkikar et al., 1998) and later these nodules form carbonate beds (Miall, 1996, p. 127). Calcite bearing paleosols form in areas where the rate of water loss due to evaporation is greater than the supply of water to surface by rainfall or flooding (Collinson, 1996, p. 67), and are therefore important components of semi-arid depositional systems and characteristic of regions experiencing a mean annual rainfall of around 500 mm (Wright and Tucker, 1991 in Khadkikar et al., 1998). Soils and paleosols can form because of lengthy episodes of landscape stability. In aggrading terrestrial depositional systems such as is preserved in portions of the Willow Creek anticline, pedogenic carbonates are able to form as long as the rate of sedimentation does not overwhelm the rate of pedogenesis (Kraus, 1999).

In the cases where lithofacies P occurs as nodules (approximately 1-3 in (2.5 – 7.5 cm) in diameter) within massive mudstones at the Willow Creek anticline, it is classified as cornstone (Gavin, 1986). Cornstones are nodular calcareous horizons that develop in less deeply weathered soils in dry climates (Retallack, 1990). Through x-ray analyses, Gavin (1986) determined the cornstones found in the Willow Creek anticline to be

formed of coalescing larger nodules that “seem to follow old root traces”, and that are often penetrated by root traces filled with sparry calcite.

Precipitated calcite is abundant throughout the Willow Creek anticline, especially in the massive mudstone, pedogenic carbonate, laminated sandstone, siltstone, and mudstone, and charophytiferous limestone lithofacies in stratigraphically higher rocks exposed in the area. This precipitated calcite can be found as broken pieces in the float derived from weathering of outcrop exposures, as surfaces of precipitation between sediment layers, and as networks of precipitated calcite in veins that often cut across-beds at sharp angles. Calcite crystals are commonly found in alkaline soils, and can form during burial of a paleosol (e.g. in joints or veins or in cavities formed by dissolution of soluble parts of a paleosol) (Retallack, 1990). More extensive systems of calcite precipitation are thought to represent more mature paleosol deposits (Collinson, 1996, p. 78). Lithofacies P is discussed further in Chapter 9 of this thesis.

CHAPTER 7

RESULTS: WILLOW CREEK ANTICLINE LITHOFACIES ASSOCIATIONS

Introduction

Lithofacies associations are groups of facies that occur together and are genetically or environmentally related (Boggs, 2001, p. 259). This chapter describes groups of specific facies successions which can be found repeated at different stratigraphic intervals at the Willow Creek anticline. Their specific succession and repetitive nature can be used to aid in depositional environment interpretation. The results of this chapter are summarized below in Figure 40. The specific stratigraphic positions for each of the lithofacies associations discussed in this chapter are presented in Figure 47 at the end of the chapter.

Upward Transition from Trough Cross-bedded (St) to Horizontally-bedded (Sh) to Ripple Cross-laminated (Sr) Sandstone

The upward succession of bedforms within a sandstone body from trough cross-beds to horizontal beds and finally to ripple cross-laminations records a change from the deposits of migrating sinuous-crested dunes to plane beds and finally to ripple bedforms (Boggs, 2001, p. 39). At the Willow Creek anticline, the plane beds within this succession record upper flow regime flow velocities because the horizontally-bedded sandstones are fine-medium grained (Southard and Boguchwal, 1990). The resulting deposits therefore record an initial increase in flow velocity from subcritical flow (Froude

Facies Associations	**Hydrodynamic Conditions**	**Stratigraphic Position**
Upward transition from trough cross-bedded (St) to horizontally-bedded (Sh) to ripple cross-laminated (Sr) sandstone	Deposits record an initial increase in flow velocity from subcritical flow to supercritical flow, followed by a later decrease in flow velocity from supercritical flow to subcritical flow.	Lower and Upper Fluvial and Floodplain Intervals
Upward transition from horizontally-bedded (Sh) to ripple cross-laminated (Sr) sandstone	Deposits record a decrease in flow velocity from supercritical upper flow regime to subcritical lower flow regime flow velocities	Lower and Upper Fluvial and Floodplain Intervals
Upward transition from horizontally-bedded (Sh) to trough cross-bedded (St) sandstone	Deposits record deceleration in flow velocity from supercritical flow to subcritical flow.	Upper Fluvial and Floodplain Interval
Alternating massively-bedded (Sm) and trough cross-bedded sandstone (St)	Massive sands may record 1) rapid deposition from a sediment gravity flow. 2) destruction of sedimentary structures through bioturbation. 3) liquefaction. The presence of bioturbation in the measured sections suggests these deposits were most likely once all trough cross-bedded, and certain portions were later bioturbated, obscuring the structures.	Lower and Upper Fluvial and Floodplain Intervals
Alternating massive mudstone (Fm) and charophytiferous limestone (Lc)	Deposits may record changes in lake surface area (movements of the shoreline), changes in clastic influx into the lake, or changes in lake depth.	Lacustrine Interval
Carbonate-rich, color mottled, massive mudstone (lithofacies Fmc) and Light grey, well-indurated carbonate (lithofacies C)	Deposits indicate hydromorphic conditions, with relatively long periods of a high groundwater level that oscillated.	Upper Fluvial and Floodplain Interval

Figure 40: Summary of lithofacies associations, associated hydrodynamic conditions, and stratigraphic positions for Willow Creek anticline measured sections. Hydrodynamic conditions are referenced from Boggs (2001, p. 38-41) and Djamali et al. (2006).

Number < 1) to supercritical flow (Froude Number > 1), followed by a later decrease in flow velocity from supercritical flow to subcritical flow (Boggs, 2001, p. 31). These

deposits form under unidirectional flow conditions, and at the Willow Creek anticline this facies succession is found within thick (> 1 m thick) sandstone units which are interpreted as river channel deposits (to be discussed in Chapters 8 and 9). This facies association is interpreted to have formed from changing flow velocities in a stream channel, which may be part of either an anastomosing or ephemeral river system. This interpretation will be discussed further in Chapter 9.

This lithofacies association is found within both the upper and lower fluvial and floodplain intervals in the Nest in the Wall Bentonite measured section (Figure 41).

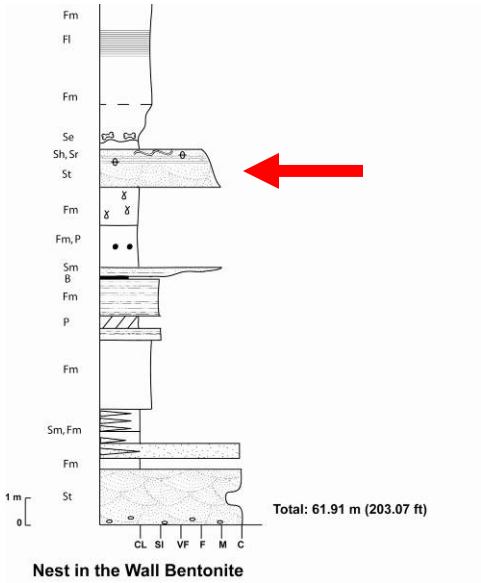

Figure 41: Measured section of lower portion of Nest in the Wall site showing upward transition of sedimentary structures from trough cross-beds to horizontal-bedding and finally to ripple cross-lamination.

This suggests that some of the same unidirectional flow conditions were present in the area of the Willow Creek anticline at the time of deposition of both the lower and upper

deposits, and that the stream processes and type of river system at both times may have been similar. This interpretation will be discussed further in Chapter 9.

Upward Transition from Horizontally-bedded (Sh) To Ripple Cross-laminated (Sr) Sandstone

The upward succession of bedforms within a sandstone body from horizontal beds to ripple cross-laminations records a change from the deposits of plane beds to ripple bedforms (Boggs, 2001, p. 39). At the Willow Creek anticline, the plane beds within this succession record upper flow regime flow velocities because the horizontally-bedded sandstones are fine-medium grained (Southard and Boguchwal, 1990). Deposits record a decrease in flow velocity from supercritical (Froude Number >1) upper flow regime to subcritical (Froude Number < 1) lower flow regime flow velocities (Boggs, 2001, p. 31). These deposits form under unidirectional flow conditions, and at the Willow Creek anticline this facies succession is found in both thin (< 1 m thick) and thick (> 1 m thick) sandstone units. The thinner sandstone units are interpreted to be crevasse splay deposits while the thicker sandstone units are interpreted to be river channel deposits (to be discussed in Chapters 8 and 9). This facies association in the thicker sandstone units is interpreted to have formed from decelerating flow velocities in a stream channel (thicker sandstones) and decelerating flow in crevasse splays associated with these stream channels (thinner sandstones), both of which may be from either an anastomosing or ephemeral river system. This interpretation will be discussed further in Chapters 8 and 9.

This lithofacies association is found within both the upper and lower fluvial and floodplain intervals in the Children's Dig and Nest in the Wall measured sections, and the reverse (ripple cross-laminated sandstone changing to horizontally-bedded sandstone) is found at the Egg Mountain C measured section (Figure 42). This suggests that some of the same unidirectional flow conditions were present in the area of the Willow Creek anticline at the time of deposition of both the lower and upper deposits, suggesting that the stream processes and type of river system at both times may have been similar. This interpretation will be discussed further in Chapter 9.

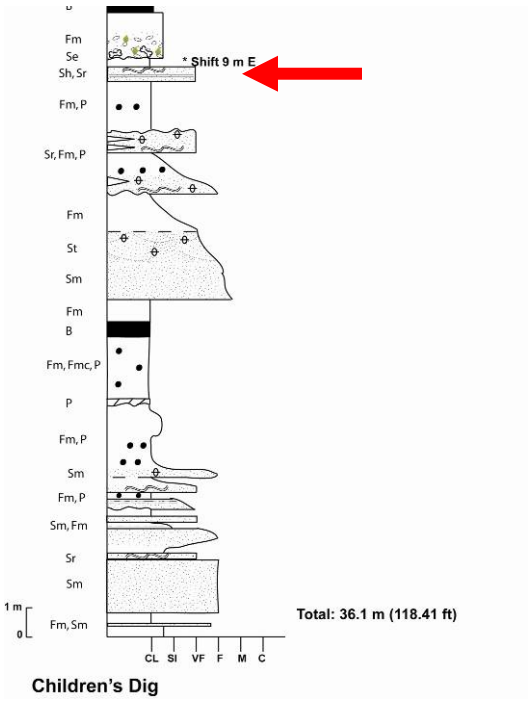

Figure 42: Measured section of lower portion of Children's Dig site showing upward transition of sedimentary structures from horizontal-bedding to ripple cross-lamination.

Upward Transition from Horizontally-bedded (Sh) to Trough Cross-bedded (St) Sandstone

The upward succession of bedforms within a sandstone body from horizontal beds to trough cross-beds records a change from the deposits of plane beds to migrating sinuous-crested dune bedforms (Boggs, 2001, p. 39). The plane beds within this succession record upper flow regime flow velocities because the horizontally-bedded sandstones are fine-medium grained (Southard and Boguchwal, 1990). Deposits record a decrease in flow velocity from supercritical (Froude Number >1) upper flow regime to subcritical (Froude Number < 1) lower flow regime flow velocities (Boggs, 2001, p. 31). These deposits form under unidirectional flow conditions, and at the Willow Creek anticline this facies succession is found as thick (> 1 m thick) sandstone units that are interpreted to be river channel deposits (to be discussed in Chapters 8 and 9). This facies association is interpreted to have formed from decelerating flow velocities in a stream channel, which may be from either an anastomosing or ephemeral river system. This interpretation will be discussed further in Chapter 9.

This lithofacies association is found only in the upper fluvial and floodplain interval in the Thunder Dome Bentonite and Nest in the Wall measured sections (Figure 43). While other deposits recording decelerating flow (i.e. horizontally-bedded sandstone changing to ripple cross-laminated sandstone) are present in the lower fluvial and floodplain interval in the measured sections, this specific facies association is restricted to the upper fluvial and floodplain interval. This interpretation will be discussed further in Chapter 9.

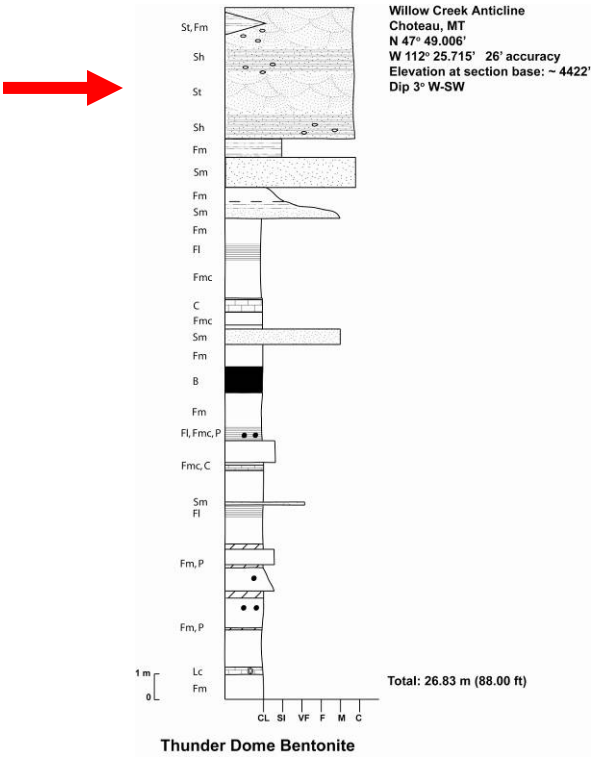

Figure 43: Measured section of Thunder Dome Bentonite site showing upward transition of sedimentary structures from horizontal-bedding to trough cross-bedding.

Alternating Massively-bedded (Sm) and Trough Cross-bedded Sandstone (St)

Massive, structureless beds are produced in one of 3 ways: 1) rapid deposition from a sediment gravity flow, 2) destruction of sedimentary structures through bioturbation, 3) liquefaction (Boggs, 2001, p. 97). In contrast, trough cross-bedding forms by the migration of sinuous crested dunes under lower flow regime unidirectional flow conditions and are typically composed of fine to very coarse-grained sand (Miall, 1996, p. 114). Beds of alternating massively-bedded and trough cross-bedded sandstone at the Willow Creek anticline are often bioturbated, suggesting these deposits were most

likely once all trough cross-bedded, and certain portions were later bioturbated, obscuring the sedimentary structures. These deposits form under unidirectional flow conditions, and at the Willow Creek anticline this facies succession is found as thick (> 1 m thick) sandstone units that are interpreted to be river channel deposits (to be discussed in Chapters 8 and 9). This facies association is interpreted to have formed from decelerating flow velocities in a stream channel, which may be from either an anastomosing or ephemeral river system. This interpretation will be discussed further in Chapter 9.

This lithofacies association is found in both the lower and upper fluvial and floodplain intervals in the Flaming Cliffs, Justin's Peak, and Children's Dig measured sections (Figure 44). This suggests that some of the same unidirectional flow conditions

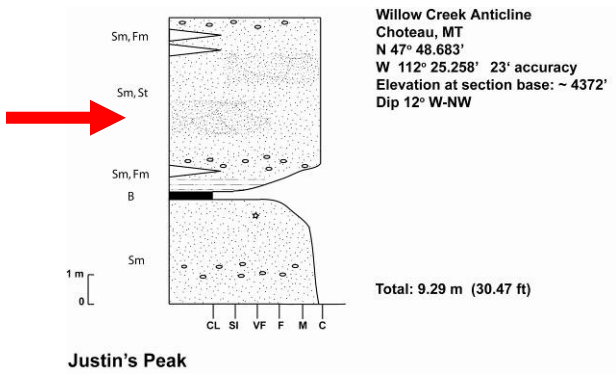

Figure 44: Measured section of Justin's Peak site showing alternating massive structureless sandstone and trough cross-bedded sandstone.

were present in the area of the Willow Creek anticline at the time of deposition of both the lower and upper deposits, suggesting that the stream processes and type of river

system at both times may have been similar. This interpretation will be discussed further in Chapter 9.

Alternating Massive Mudstone (Fm) and Charophytiferous Limestone (Lc)

As discussed in Chapter 6, the charophytes in the limestones are indicative of shallow lakes. No evidence is recorded in the area for the presence of deep lakes. The interbedded nature of the limestone and mudstone deposits may suggest either that the edge of the lake was present in this area, or that the lake occasionally dried up. There are no evaporite minerals interbedded within the lacustrine deposits in this area, suggesting that the lake did not undergo rapid periods of dessication, but instead may have merely fluctuated in size while remaining shallow in depth. The lack of evaporate minerals in an interpreted semi-arid setting (Gavin, 1986), might also be explained if the lake(s) was hydrologically open. If this were the case, then the lake(s) would have had inputs from groundwater and/or surface water which would have prevented the water from evaporating enough to precipitate evaporite minerals (Valero Garces et al., 1997). Additionally, the alternation between mudstone and charophytiferous limestone may record changes in clastic input into the area, with the limestone forming at times of low clastic input into the lake, and the mudstone forming at times of high clastic input.

Deposits reflecting this alteration of lithofacies are found in the Children's Dig, Egg Mountain B, Egg Mountain C, Frans Site, Nest in the Wall Bentonite, Thunder Dome, and Thunder Dome Bentonite measured section sites (Figure 45), suggesting the

lakes were most likely small in size (tens of kilometers wide). This interpretation will be discussed further in Chapter 9.

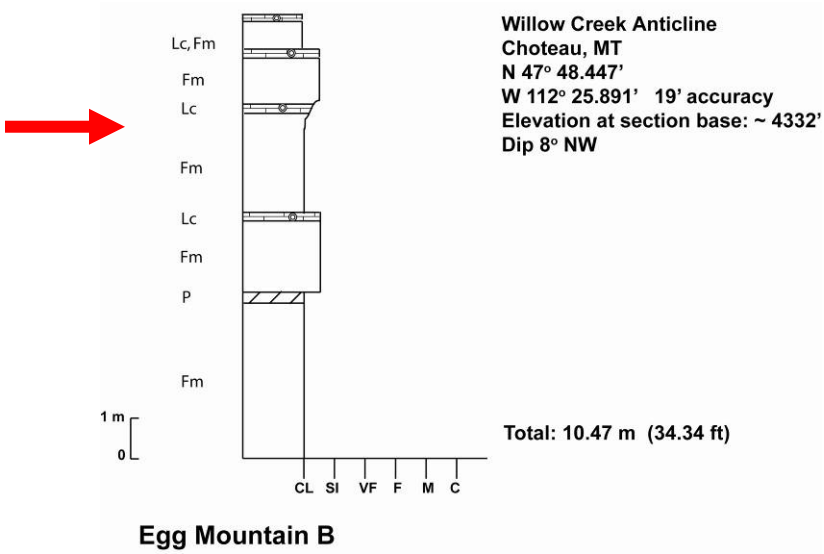

Figure 45: Measured section of Egg Mountain B site showing alternating charophytiferous limestone and massive mudstone.

Carbonate-rich, Color Mottled, Massive Mudstone (Lithofacies Fmc) and Light Grey, Well-indurated Carbonate (Lithofacies C)

The presence of purple, green, and grey mottling in lithofacies Fmc (carbonate-rich, color mottled massive mudstone) provides evidence for hydromorphic conditions at the Willow Creek anticline, as strata with grey colors with mottling are interpreted to indicate relatively long periods of a high groundwater level (PiPujol and Buurman, 1994; Djamali et al., 2006). In environment with this characteristic, two important processes in the precipitation of carbonate and the formation of calcretized layers are high evaporation and evapotranspiration (Semeniuk and Meagher, 1981; in Djamali et al., 2006). These

calcretized zones, also known as groundwater carbonates or groundwater calcretes, most likely formed near an oscillating position of the groundwater table (Djamali et al., 2006). As discussed in Chapter 6, lithofacies C of this study (light grey, well-indurated carbonate) is interpreted to be a groundwater carbonate that probably formed in this manner.

At the Willow Creek anticline, the presence of the lithofacies association of carbonate-rich, color mottled massive mudstone (lithofacies Fmc) and light grey, well-indurated carbonate (lithofacies C) stratigraphically above the lacustrine interval (Figure 46) provides evidence that groundwater tables in the area were rising relative to the stratigraphically lower fluvial and floodplain interval, and were likely near surface and oscillating in the area at the time of deposition of the lacustrine interval and the later, stratigraphically higher fluvial and floodplain strata.

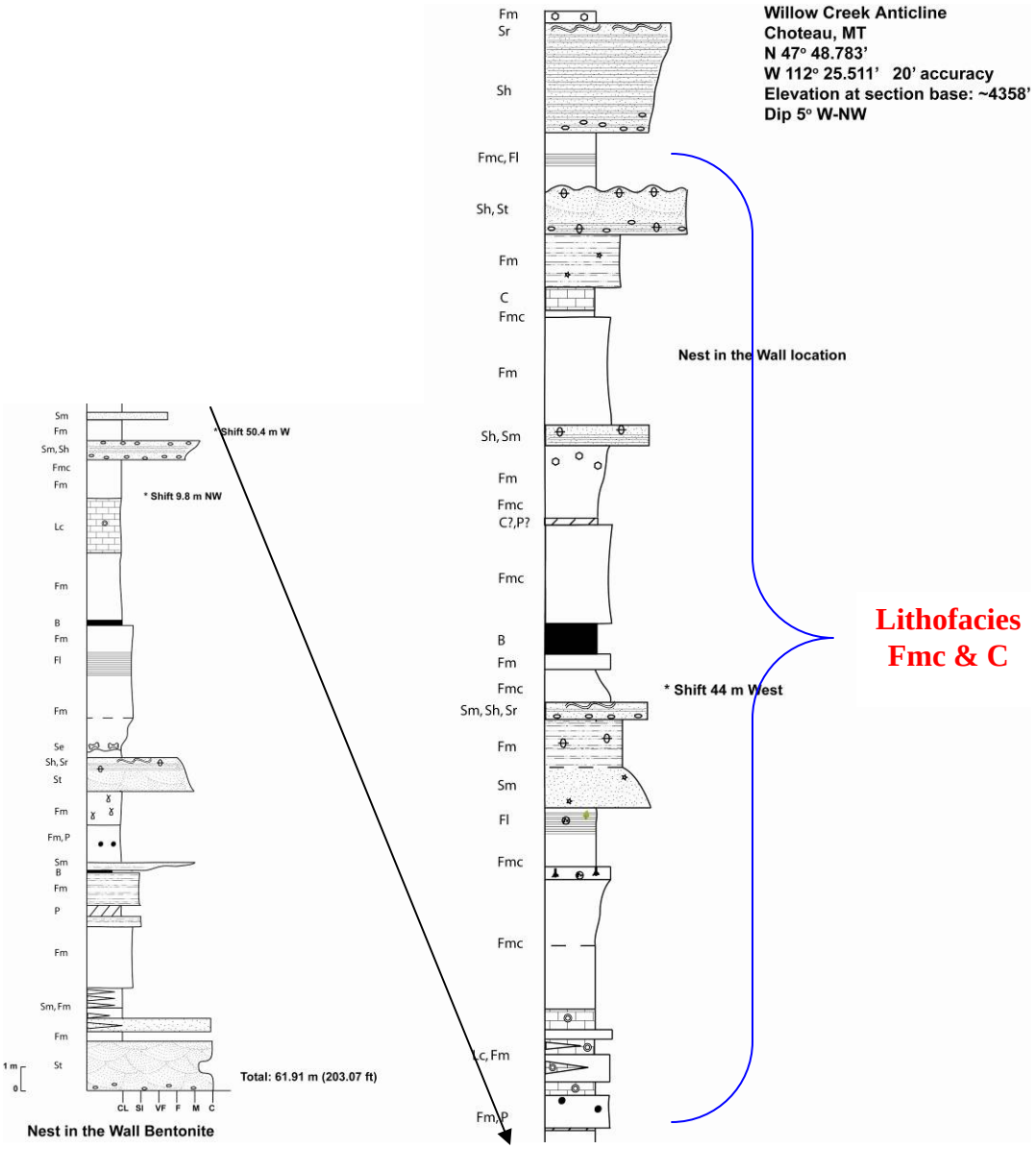

Figure 46: Measured section of Nest in the Wall Bentonite site showing alternating Carbonate-rich, color mottled, massive mudstone (lithofacies Fmc) and Light grey, well-indurated carbonate (lithofacies C).

Measured Section	Willow Creek Anticline Measured Section Lithofacies Associations		
	Lower Fluvial and Floodplain	**Lacustrine Interval**	**Upper Fluvial and Floodplain**
’78 Nest	N/A	N/A	N/A
’79 Nest	Thick massively-bedded sandstone (Sm) units, one with bioturbation and mudstone rip-up clasts.	N/A	N/A
Branvold Site	1. Thin horizontally-bedded and bioturbated sandstone (Sh) unit. 2. Thin massively-bedded sandstone (Sm) unit.	N/A	N/A
Children’s Dig	1. Thick and thin units of massively-bedded sandstone (Sm) 2. Thick sandstone unit changing from massively-bedded (Sm) to trough cross-bedded (St) with mudstone rip-up clasts and bioturbation. 3. Thin ripple cross-laminated and bioturbated sandstone (Sr) changing upwards into massively-bedded sandstone (Sm). 4. Thin sandstone unit changing from horizontally-bedded (Sh) to ripple cross-laminated sandstone (Sr). 4. Thin horizontally-bedded sandstone (Sh) units.	Alternating massive mudstone (Fm) and charophytiferous limestone (Lc).	N/A
Egg Island	N/A	N/A	N/A
Egg Mountain A	N/A	N/A	N/A
Egg Mountain B	N/A	Alternating massive mudstone (Fm) and charophytiferous limestone (Lc).	N/A
Egg Mountain C	1. Thin sandstone unit changing upwards from ripple cross-lamination (Sr) to horizontal-beds (Sh) to bioturbated sandstone. 2. Thick massively-bedded sandstone (Sm), with some bioturbation.	Alternating massive mudstone (Fm) and charophytiferous limestone (Lc).	N/A
Fault Mountain 1	Thick massively-bedded sandstone (Sm) unit.	N/A	N/A
Jess Butte	1. Thin units of horizontally-bedded sandstone (Sh). 2. Thick massively-bedded, bioturbated sandstone (Sm), with some faint ripple cross-lamination (Sr).	N/A	N/A
Josh’s Hill	Thick and thin units of massively-bedded sandstone (Sm).	N/A	N/A

(Figure 47 continued on pages 79-80)

Figure 47 continued.

Justin's Peak	1. Thick unit of massively-bedded sandstone (Sm) with mudstone rip-up clasts. 2. Thick sandstone unit alternating between massively-bedded (Sm) with mudstone rip-up clasts and trough-cross bedded (St).	N/A	N/A
Lake Giardia	1. Thick trough-cross-bedded sandstone units (St) with mudstone rip-up clasts. 2. Thin massive sandstone (Sm) units.	N/A	N/A
Nest in the Wall Bentonite	1. Thick trough cross-bedded sandstone unit with basal mudstone rip-up clasts (St). 2. Thin massively-bedded sandstone unit (Sm). 3. Thick sandstone unit changing upwards from trough cross-beds (St) to horizontal-beds (Sh) to ripple cross-lamination (Sr).	1. Thin horizontally-bedded sandstone (Sh) unit with mudstone rip-ups. 2. Alternating massive mudstone (Fm) and charophytiferous limestone [illegible].	1. Thick horizontally-bedded sandstone (Sh) with basal rip-up clasts changing to ripple cross-laminated sandstone (Sr). 2. Thick sandstone unit changing upwards from horizontally-bedded (Sh) to trough cross-bedded (St) to bioturbated sandstone. 3. Thin horizontally-bedded sandstone unit (Sh) with bioturbated top. 4. Thin sandstone unit changing upwards from massively bedded (Sm) with basal mudstone rip-up clasts, to horizontally-bedded (Sh) to ripple cross-laminated (Sr). 5. Thick massively-bedded sandstone (Sm). 6. Associated carbonate-rich, color mottled massive mudstone (Fmc) and light grey, well-indurated carbonate (C).
Nose Cone 2	N/A	N/A	N/A
Pete's Pupa Peninsula	N/A	N/A	N/A
Thunder Dome	N/A	1. Thin massively-bedded sandstone (Sm) unit. 2. Alternating massive mudstone (Fm) and charophytiferous limestone (Lc).	1. Thin units of massively-bedded sandstone (Sm). 2. Thick sandstone unit changing upward from and alternating between horizontally-bedded (Sh) with basal rip-up clasts to trough cross-bedded (St). 3. Associated carbonate-rich, color mottled massive mudstone (Fmc) and light grey, well-indurated carbonate (C).

Figure 47 continued.

Thunder Dome Bentonite	N/A	Alternating massive mudstone (Fm) and charophytiferous limestone (Lc).	1. Thin units of massively-bedded sandstone. 2. Thick trough cross-bedded sandstone (St) with mudstone rip-up clasts and bioturbation. 3. Thin horizontally-bedded sandstone (Sh) unit. 4. Associated carbonate-rich, color mottled massive mudstone (Fmc) and light grey, well-indurated carbonate (C).
Fault Mountain 2	Thick massively-bedded sandstone units (Sm).	N/A	N/A
Flaming Cliffs	N/A	N/A	1. Thick sandstone unit changing from trough cross-bedded (St) with basal mudstone rip-up clasts to massively-bedded (Sm). 2. Thin massively-bedded sandstone (Sm) units. 3. Associated carbonate-rich, color mottled massive mudstone (Fmc) and light grey, well-indurated carbonate (C).
Frans Site	N/A	Charophytiferous limestone (Lc) unit in between massive mudstone units (Fm).	Associated carbonate-rich, color mottled massive mudstone (Fmc) and light grey, well-indurated carbonate (C).

Figure 47: Willow Creek anticline measured section lithofacies associations. Thin units refer to sandstone units that are less than 1 m thick, while thick units refer to sandstone units greater than 1 m thick.

CHAPTER 8

RESULTS: WILLOW CREEK ANTICLINE SANDSTONE BODY CHARACTERISTICS

Introduction

At the Willow Creek anticline, major packages of sandstone bodies are found in the stratigraphically highest and lowest deposits in the area (Figure 26, 27 in Appendices D, E). An extensive description of these deposits is presented by Gavin (1986). The results of this study regarding sandstone body characteristics will be discussed below and compared to those of Gavin (1986), and this information is summarized in Figure 48. A discussion of the depositional environment for these deposits will be discussed in Chapter 9.

Stratigraphically Lower Deposits

Gavin (1986) distinguishes sandstone deposits of different scales and types at the Willow Creek anticline as “major” and “minor” sandstones, and this same terminology will be used in this study for ease of comparison. The information in this section is summarized in Figure 46.

Minor Sandstones

Minor sandstones of the lower deposits are chert-arenites to sub-chert-arenites (Gavin, 1986), and display a tabular to slightly lenticular geometry with their

Stratigraphic Position	Sandstone Composition / Texture	Sandstone Body Geometry	Sandstone Body Width and Thickness	Other Characteristics
Upper Fluvial and Floodplain	**Minor:** (no data for composition) - Very fine to medium-grained; angular – subangular; poorly – moderately sorted **Major:** feldspathic litharenites or lithic arkoses (Gavin, 1986) -Fine to coarse-grained; angular – subangular; poorly – moderately sorted	**Minor:** planar to slightly lenticular **Major:** concave base, abrupt lateral contacts with minor interfingering (from Gavin, 1986; and this study)	**Gavin (1986)** **Minor:** up to 2 m thick up to 84 m wide (average 15-30 m) **Major:** 7.3 m and 6.4 m thick 49 m and 30 m wide **Width:thickness: 6.7, 4.8** **This Study** **Minor:** up to ~1.5 m thick up to 82 m wide **Major:** 5.1 and 7 m thick 30 m and 50 m wide **Width:thickness: 5.9, 7.1**	**Minor:** tops show bioturbation **Major:** may be multistorey
Lower Fluvial and Floodplain	**Minor:** chert-arenites and sub-chert-arenites (Gavin, 1986) - Very fine to medium-grained; angular – subangular; poorly – moderately sorted **Major:** feldspathic litharenites (Gavin, 1986) - Fine to coarse-grained; angular – subrounded; poorly to moderately sorted	**Minor:** Tabular to slightly lenticular; bases show some evidence of erosion **Major:** abrupt lateral contacts, concave slightly irregular base, minor interfingering on channel margins (from Gavin, 1986; and this study)	**Gavin (1986)** **Minor:** 0.5 – 1.2 m thick up to 43 m wide Average width of 15 m **Major:** Thick: 6 – 10.5 m ~ 30 m wide **Width:Thickness: 3 - 4** **This Study** **Minor:** up to ~1.5 m thick up to 40 m wide **Major:** ~5 - 8 m thick ~ 33 m wide **Width:Thickness 4.1 - 6.6**	**Minor:** tops contain burrows and root traces **Major:** single-storey

Figure 48: Table showing characteristics of sandstones found in the stratigraphically lower and upper fluvial and floodplain deposits of the Willow Creek anticline. The terms “minor” and “major” are used *sensu* Gavin (1986), and refer to sandstones of different scales.

bases showing some evidence of erosion (findings consistent with those of Gavin (1986)). Sandstone bodies are found up to ~1.5 m thick and up to 40 m wide, which is consistent with Gavin's (1986) findings of thicknesses between 0.5 – 1.2 m and widths up to 43 m. In addition, both studies found common bioturbation and root traces in the tops of minor sandstone bodies.

Major Sandstones

Major sandstones of the lower deposits are feldspathic arenites (Gavin, 1986), and display abrupt lateral contacts, concave slightly irregular bases, and minor interfingering on channel margins (findings consistent with Gavin (1986)) (Figure 49).

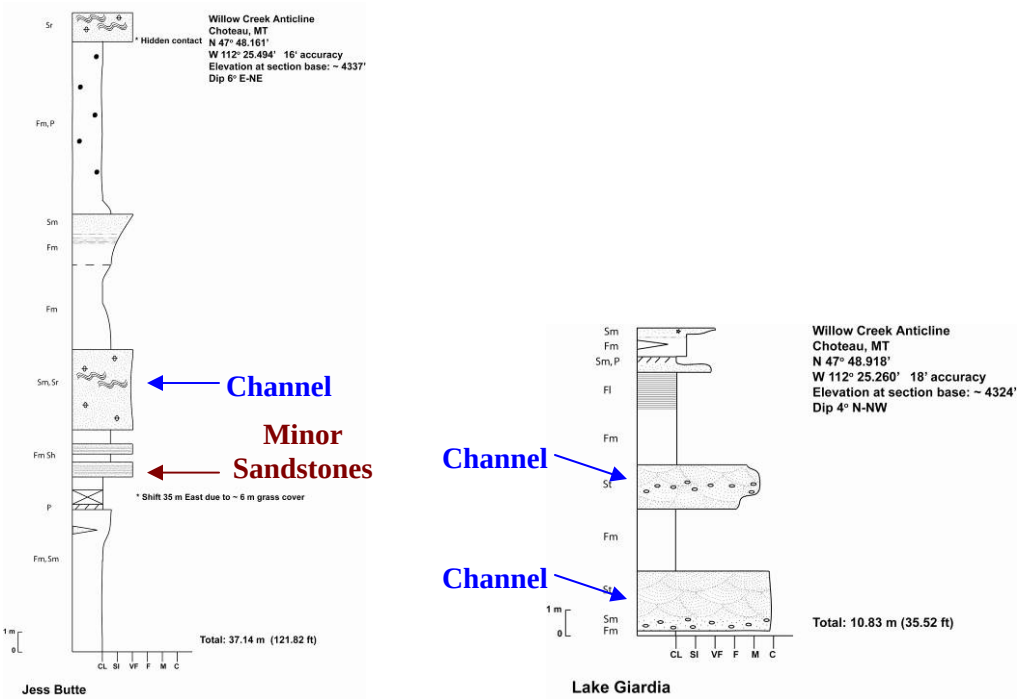

Figure 49: Measured sections of the Jess Butte and Lake Giardia sites showing major and minor sandstones.

Sandstone bodies are ~ 5 – 8 m thick and ~ 33 m wide, which is consistent with Gavin's (1986) findings of thicknesses between 6 – 10.5 m and a width 30 m. Results of this study give a width:thickness ratio of 4.1 – 6.6 versus 3-4 of Gavin (1986). In addition, these channels are single-storey, as there is no evidence of one fluvial channel cutting down into another.

Stratigraphically Higher Deposits

Minor Sandstones

Minor sandstones of the upper deposits are planar to slightly lenticular, with their tops commonly showing bioturbation (findings consistent with Gavin (1986)). Sandstone bodies are found up to ~1.5 m thick and up to 82 m wide, which is consistent with Gavin's (1986) findings of thicknesses up to 2 m and widths up to 84 m (Figure 48).

Major Sandstones

Major sandstones of the upper deposits are feldspathic litharenites or lithic arkoses (Gavin, 1986), and display abrupt lateral contacts, concave slightly irregular bases, and minor interfingering on the edges of sandstone bodies (findings consistent with Gavin (1986)). The major sandstone bodies are 5.1 and 7 m thick, with widths of 30 m and 50 m respectively, which is consistent with Gavin's (1986) findings of thicknesses of 6.4 m and 7.3 m, with widths of 30 m and 49 m respectively. Results of this study give a width:thickness ratio of 5.9 and 7.1 versus 6.7 and 4.8 of Gavin (1986). In addition, these channels appear to be single-storey, but may in fact be multistorey because of upward changes in sandstone body characteristics in the lowermost major

sandstone at the Flaming Cliffs measured section site and the uppermost major sandstone at the Thunder Dome Bentonite measured section site (Figure 50). The changes in sedimentary structures

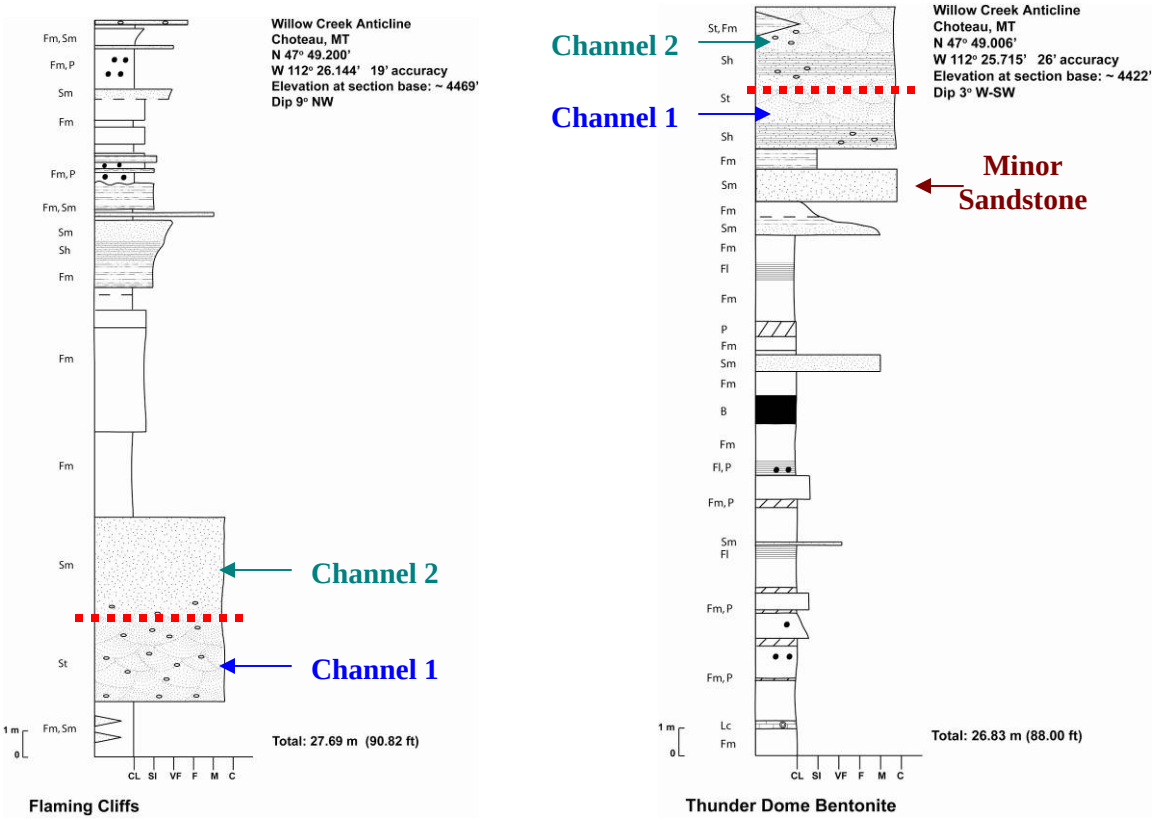

Figure 50: Measured sections of the Thunder Dome Bentonite and Flaming Cliffs site, showing possible multistorey channel relationship.

from horizontally-bedded sandstone with basal mudstone rip-up clasts to trough cross-bedded sandstone to a repeat of this succession at the Thunder Dome Bentonite measured section site, and a change from a thick trough cross-bedded sandstone with mudstone rip-up clasts to a thick massively bedded sandstone at the Flaming Cliffs measured section site, may suggest the presence of two superimposed channels at each site. This transition

is not marked by a clear, well-defined concave boundary at either site making it hard to say with absolute certainty that there are two superimposed channels present, although as previously stated, the changes in sedimentary structures suggests this possibility.

CHAPTER 9

DISCUSSION: DEPOSITIONAL ENVIRONMENT OF THE TWO MEDICINE FORMATION, WILLOW CREEK ANTICLINE

Introduction

Two different depositional environments are interpreted for Two Medicine Formation outcrops present on the Willow Creek anticline: 1) an ephemeral, anastomosing river system, and 2) lacustrine. The ephemeral, anastomosing river system deposits are found in the stratigraphically lowermost rocks on the anticline (located primarily in the southern portions of the Willow Creek anticline (Figures 26, 27 in Appendices D, E), and are overlain by lacustrine deposits approximately 15 m (49 ft) thick. The lacustrine deposits are in turn overlain by ephemeral, anastomosing river system deposits. Deposits become stratigraphically younger going from the south-southeast to the north-northwest across the Willow Creek anticline (Figure 26 in Appendix D). This interpretation for depositional environments recorded on the Willow Creek anticline differs somewhat from of Gavin (1986) in two senses. First, while it is agreed that the river channel pattern at the Willow Creek anticline displays characteristics common to anastomosing fluvial systems, it is further proposed that these fluvial systems were ephemeral in nature. Second, this study found no evidence to support the presence of meandering streams during the interval of lacustrine deposition. Evidence for the interpretations presented in this thesis is described below.

Fluvial Deposits

As previously stated, the fluvial intervals present in Willow Creek anticline strata are interpreted to be the deposits of ephemeral, anastomosing river systems. This interpretation therefore has two components to be discussed: the nature of 1) anastomosing river systems and 2) ephemeral river systems.

Anastomosing River Systems

Introduction. Fluvial deposits interpreted to represent anastomosing river systems (Smith and Putnam, 1980; Nadon, 1994; Valero Garces et al., 1996; Djamali et al., 2006), relatively rare in the geologic record. Present day examples of anastomosing river systems can be found in both temperate and arid climates in areas such as: the Saskatchewan River in western Canada (Smith, 1973, 1983, 1986; Smith and Putnam, 1980; Smith and Smith, 1980; Smith et al., 1997), the Channel Country rivers of central Australia (Rust, 1981; Nanson et al., 1986; Schumm et al., 1996; Knighton and Nanson, 2000, 2002; Fagan and Nanson, 2004), the Okavango Fan in Botswana (Mollard, 1973), and Red Creek in Wyoming (Schumann, 1989). Although some differences exist between anastomosing fluvial systems in arid and temperate areas, their general, shared characteristics include: the presence of large sandstone lenses with concave or steepened margins, abrupt lateral contacts of channel sands with surrounding floodplain fines, low width:thickness ratios of channel sandstone bodies, high percentage of overbank fines, potential presence of crevasse splay deposits, poorly developed upward fining trends, and

lack of sedimentary evidence for lateral channel migration. (Smith and Smith, 1980; Rust, 1981; Smith, 1983, 1986; Friend, 1983; Nadon, 1994; Makaske, 2001) (Figure 51).

Criteria for Anastomosing River System Interpretation	**Applicable to Willow Creek Anticline deposits?**
Large sandstone lenses with concave or steepened margins	Yes
Abrupt lateral contacts of channel sands with surrounding floodplain fines	Yes
Low width:thickness ratios of channel sandstone bodies (~ < 10)	Yes
High percentage of overbank fines	Yes
Crevasse splay deposits	Yes
Poorly developed upward fining trends	Yes
Lack of sedimentary evidence for lateral channel migration	Yes
System in low-relief aggradational basin (for arid-zone systems)	Yes
High (for temperate-zone systems) or low (for arid-zone systems) channel density?	Low (0.9 sand:silt ratio)
Deep dessication cracks (for arid-zone systems)	No
Duricrusts, evaporite horizons, calcretes	Calcretes present
High (for temperate-zone systems) or low (for arid-zone systems) production of plant biomass?	Low (roots tend to be preserved as pedogenic rhizo-concretions rather than organic material)

Figure 51: Criteria for recognition of anastomosing river systems (compiled from Smith and Smith, 1980; Rust, 1981; Smith, 1983; Friend, 1983; Nadon, 1994).

Channel Morphology and Migration. Anastomosing rivers tend to display minimal lateral channel migration, and therefore lack well defined point bar deposits that are an important characteristic associated with meandering streams (Smith and Smith, 1980; Rust, 1981; Nadon, 1994). As a result, anastomosing river channels in both temperate and arid zones are often found as isolated channels within their associated fine-grained floodplain sediments, with the contacts between the channel edges and the floodplain often being fairly sharp and steep (Smith and Smith, 1980; Rust, 1981) (Figure 52). Channel density, however, differs between temperate and arid zones (Rust, 1981).

Based on studies of Cooper Creek in Australia (Rust, 1981), anastomosed river channels in arid zones occupy < 3% of their floodplain, as compared to temperate zone anastomosed river systems which occupy closer to 20% (Smith and Smith, 1980).

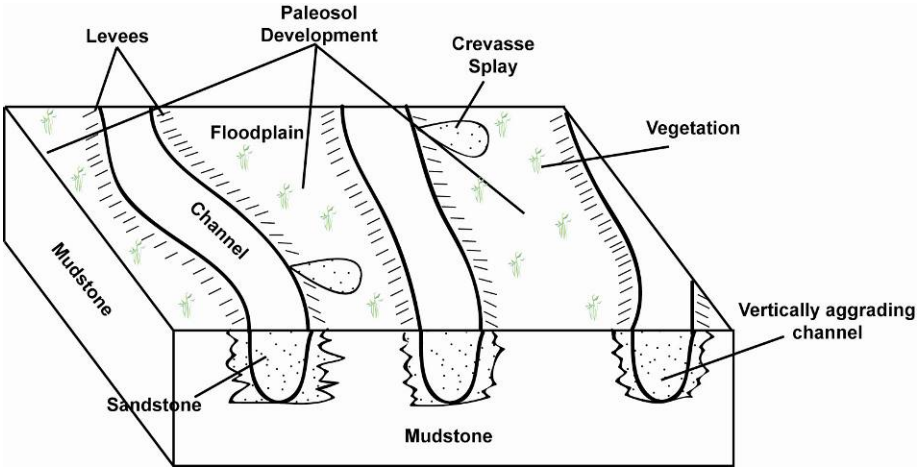

Figure 52**:** Simplified cartoon diagram of ephemeral river system depositional environment.

The presence of isolated channels, the lack of sedimentary evidence for lateral channel migration, and the abrupt lateral contacts of thick lenticular channel sands surrounded by floodplain fines found in Two Medicine Formation rocks at the Willow Creek anticline is consistent with these characteristics of anastomosing streams. Also, as a result of channel confinement (due to their cohesive banks which do not allow channels to migrate very far laterally) channel sandstones in anastomosing river systems can be very thick due to the high rate of vertical sand accretion. These characteristics can be seen in the thick trough cross-bedded (up to 5 m (16.4 ft) thick) sandstones recorded in the Two Medicine Formation deposits on the Willow Creek anticline (Figures 26, 27 in Appendices D, E) (Figure 53).

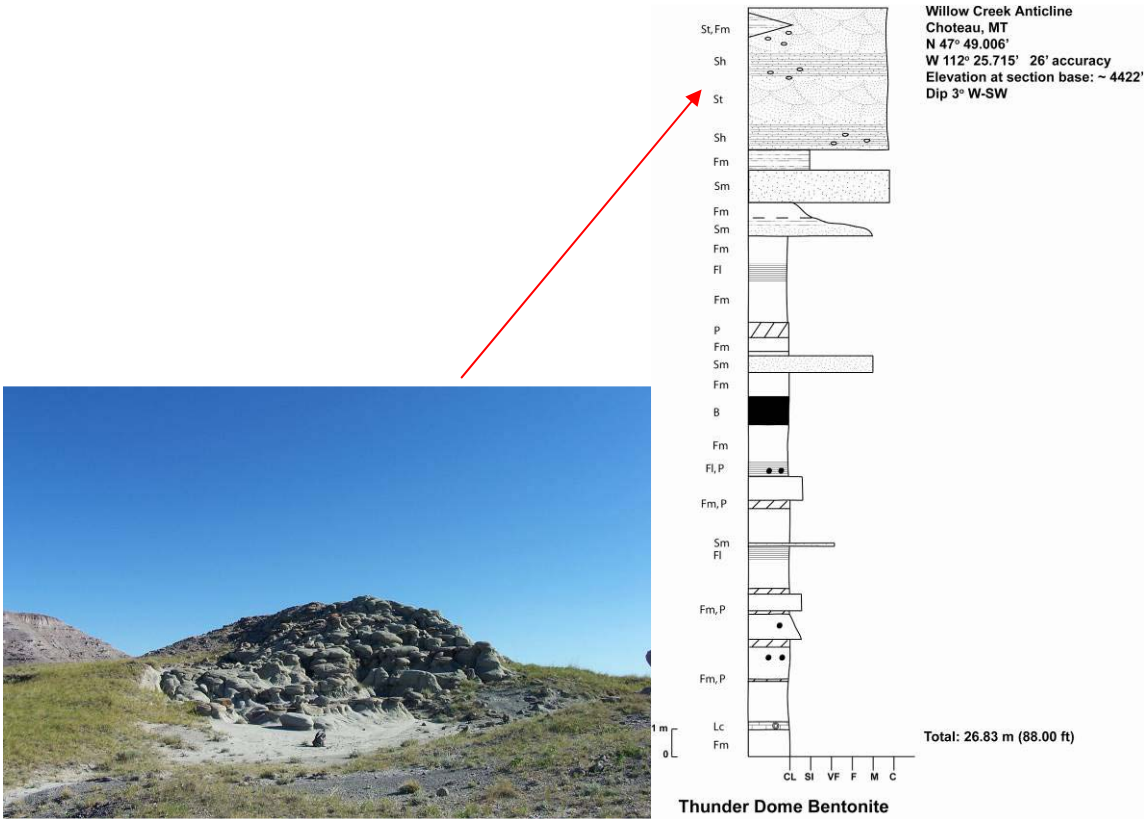

Figure 53: Thick trough cross-bedded channel sandstones located at the top of the Thunder Dome Bentonite measured section (backpack at base of sands for scale). (section location and key are located in Appendix A)

In addition, numerous mudstone rip-up clasts, are commonly found at the base, as well as within both thick and thin sandstone of the Willow Creek anticline (Figure 53), and may record collapse of cohesive channel banks.

Avulsion. New channels form through the process of avulsion in anastomosing river systems in both temperate and arid zones (Rust, 1981; Smith et al., 1989). These avulsions are primarily driven by aggradation of the channel belt and/or the loss of channel capacity by in-channel deposition, both of which are caused by a low floodplain

gradient (Makaske, 2001). While crevasse splays are not restricted to anastomosing river systems, they are a very important characteristic, and the presence of their deposits may still be used to show consistency with the anastomosing river system interpretation. However, Rust (1981) found no evidence for crevassing in the arid-zone Cooper Creek anastomosing fluvial system, and attributed it to discontinuous levees, which allow new channels to form through avulsion without the need for crevasse formation. This suggests that crevasse splay deposits may be more common in deposits of temperate zone anastomosed systems, as compared to arid zone systems. Some evidence of crevassing is recorded at the Willow Creek anticline in the form of thin fine-grained sandstone beds, that are often ripple or horizontally laminated, that are interbedded with siltstone and/or mudstone, and that are sometimes bioturbated (Figure 54; Figures 26, 27 in Appendices D, E). The presence of crevasse splays at the Willow Creek anticline may be related to the semi-arid rather than arid climate of the area versus Cooper Creek, or many be related to the area's position in an active foreland basin, as compared to Cooper Creek, whose origin is interpreted as climatically driven, rather than tectonically driven in nature (Rust, 1981). In addition, deposits of anastomosing river systems also commonly display poor upward fining trends due to their general lack of lateral migration (Nadon, 1994). This characteristic can also be seen in deposits of the Willow Creek anticline (Figure 55).

Floodplain Vegetation. Another important aspect of anastomosing streams is the presence of floodplain vegetation which serves to anchor the floodplains and resist lateral

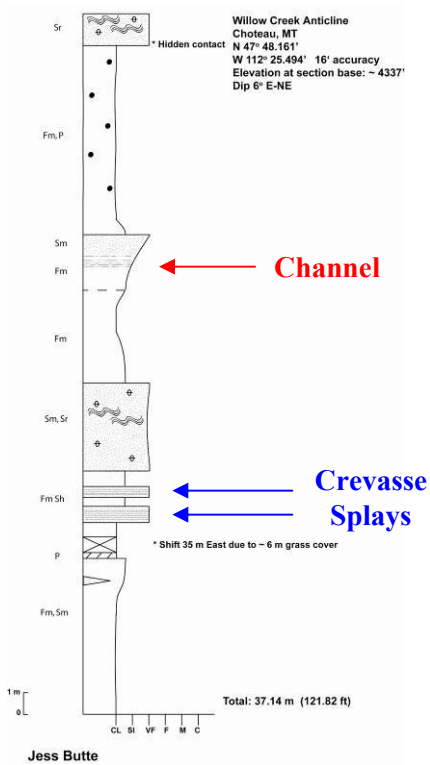

Figure 54: Examples of crevasse splay deposits at Jess Butte measured section site (denoted by blue arrows). In this example, the two interpreted crevasse splay (CS) deposits are followed by what is interpreted to be the formation of a new channel due to avulsion (recorded by thick sandstone and denoted by red arrow). Original sedimentary structures have been obscured due to bioturbation. (section location and key are located in Appendix A)

channel migration (Smith and Smith, 1980). However, Rust (1981) suggests that while floodplain vegetation may play an important role in stabilizing temperate zone

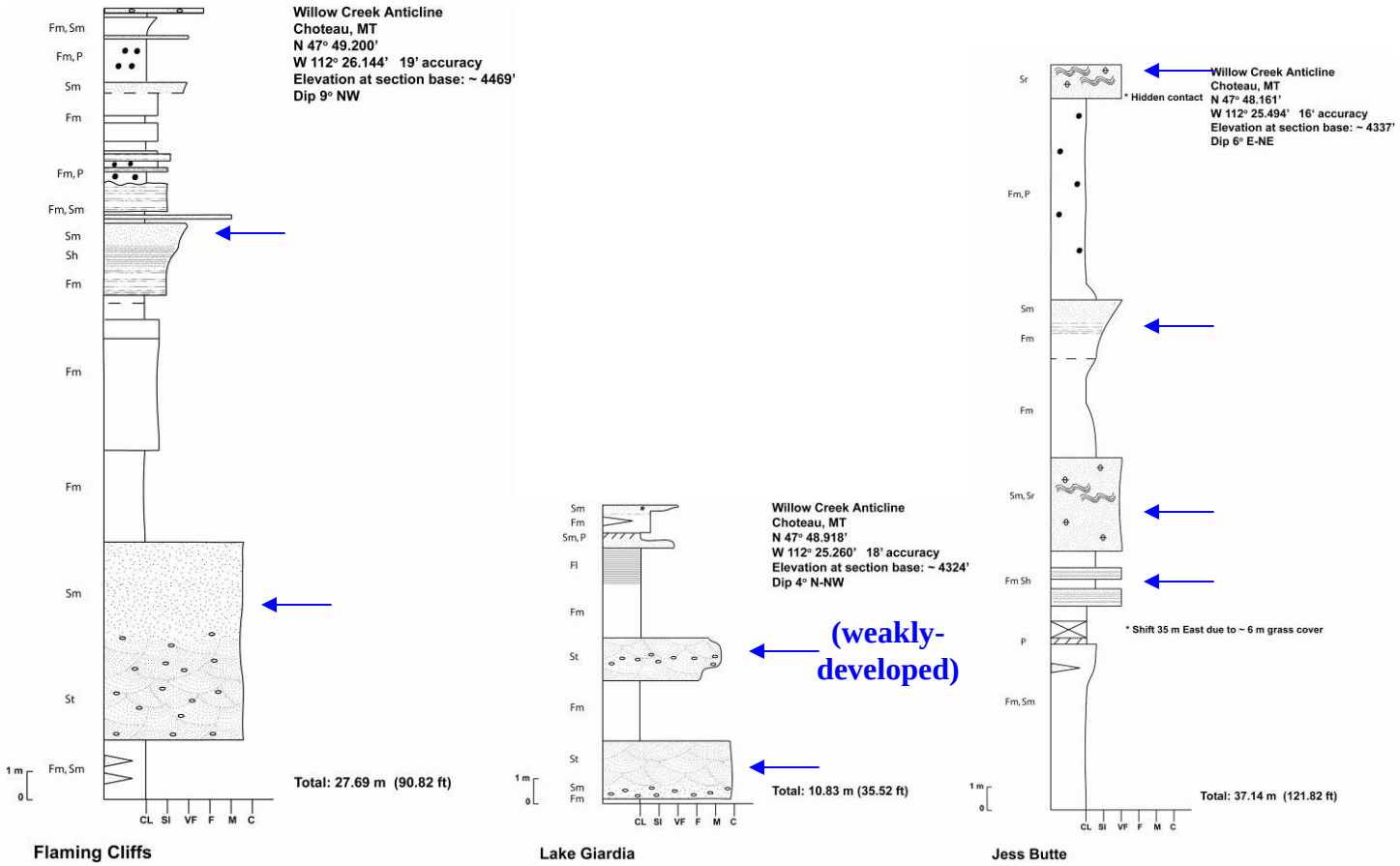

Figure 55: Examples of Willow Creek anticline measured sections showing weakly-developed upward fining trends. Blue arrows denote thick sandstones that do not show fining up trends (section locations and key are located in Appendix A)

anastomosing river systems, it may not be as important in arid zone systems due to the arid climate reducing plant growth. Rust (1981) does show evidence for a “modest” accumulation of plant material in arid zone systems, although it is mainly preserved as pedogenic rhizo-concretions rather than organic plant material. While some root traces can easily be seen in floodplain rocks of the Willow Creek anticline, Gavin (1986) showed they are most apparent when viewed under the microscope as pedotubules. Their presence is therefore more consistent with the characteristics of plant material preserved in arid-semi-arid zone anastomosing river system floodplains.

A more detailed sedimentological study and additional evidence for an interpretation of anastomosing rivers in the stratigraphically highest and lowest rocks of the Willow Creek anticline is provided by Gavin (1986). Width:thickness ratios of 4.1-6.6 for the stratigraphically lower fluvial deposits, and 5.9 and 7.1 for the stratigraphically higher fluvial deposits (as compared to Gavin (1986) with ratios of 3.8-2.9 for the stratigraphically lowest fluvial rocks and 4.8-6.7 for the stratigraphically highest fluvial rocks) are recorded in the Willow Creek anticline. These ratios are consistent with the low width:thickness ratios of anastomosing streams (Smith and Smith, 1980; Rust, 1981; Nadon, 1994). In addition, Gavin (1986) provides an overall sand:silt ratio of 0.9 for the stratigraphically lowest fluvial rocks and 0.9 for the stratigraphically highest fluvial rocks. This is consistent with high percentage of overbank fines as compared to channel and crevasse splay sands found in anastomosing river systems (Smith and Smith, 1980; Rust, 1981; Nadon, 1994).

Summary

In summary, the stratigraphically lowest and highest rocks exposed at the Willow Creek anticline display characteristics most consistent with an arid- to semi-arid-zone anastomosing fluvial system, with Cooper Creek in central Australia providing a good modern analogue. The fluvial system was characterized by predominantly ephemeral flow within a multiple interconnected channels characterized by vertical sand accretion and that occupied only a small portion of their floodplain. Figures 56 (A and B) show simplified diagrams illustrating of this depositional environment.

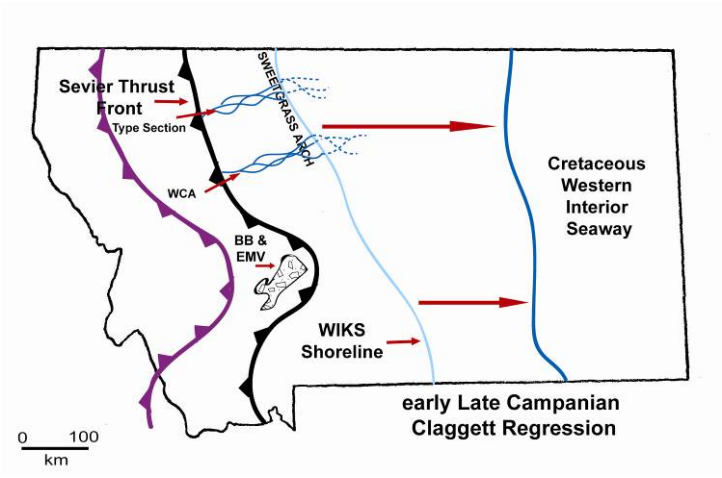

A.

Figure 56: A) Cartoon of interpreted environment of deposition for the stratigraphically lowest strata of the Two Medicine Formation at the Willow Creek anticline. The depositional environment was characterized by anastomosing streams and their associated floodplain deposits. Dashed lines represent possible gradual eastward expansion of anastomosing system as WIKS shoreline regressed east. WCA: Willow Creek anticline. BB: Boulder Batholith. EMV: Elkhorn Mountains Volcanics. Light blue line represents position of WIKS shoreline at start of Claggett Regression in “A” and at start of Bearpaw Transgression in “B”, while dark blue line represents position of WIKS at end of Claggett Regression in “A” (modified from Lillegraven and Ostresh, 1990).

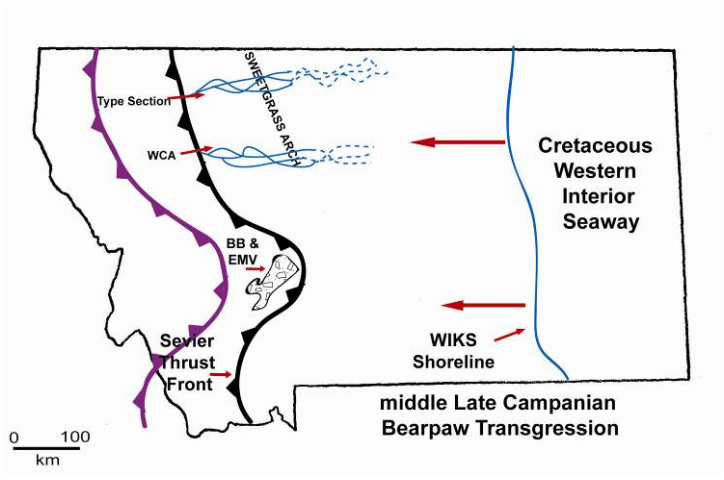

B.

Figure 56: B) Cartoon of interpreted environment of deposition for the stratigraphically highest strata of the Two Medicine Formation at the Willow Creek anticline. The depositional environment was characterized by anastomosing streams and their associated floodplain deposits. Red arrows denote direction of shoreline movement. WCA: Willow Creek anticline. BB: Boulder Batholith. EMV: Elkhorn Mountains Volcanics. Light blue line represents position of WIKS shoreline at start of Claggett Regression in "A" and at start of Bearpaw Transgression in "B", while dark blue line represents position of WIKS at end of Claggett Regression in "A" (modified from Lillegraven and Ostresh, 1990).

Ephemeral Fluvial Systems

Introduction. Ephemeral river systems are found in arid and semi-arid environments which are characterized by low annual precipitation, well-marked and prolonged dry seasons, a net annual moisture deficit, and a flashy stream regime (Tandon et al., 1997). As a result, ephemeral streams generally display short periods of flow following local and intense rainfall, alternating with long periods in which the channel is dry (Picard and High, 1973). Consequently, most ephemeral streams experience several flows of varying magnitude each year (Mabutt, 1977 in Dreyer, 1993). Both modern and ancient examples of ephemeral stream deposits have been documented (Picard and High,

1973; Mabutt, 1977; Rust, 1981; Olsen, 1989; Dreyer, 1993; Tandon et al., 1997; Gierlowski-Kordesch, 1998; Knighton and Nanson, 2000, 2001, 2002; Fagan and Nanson, 2004; Griffiths et al., 2006; Melchor et al., 2006; and many more).

Traditionally, ephemeral stream deposits have been described as alternations between reddish shales and thin, flat-based, and laterally extensive sandstones and conglomerates (Dreyer, 1993). However, there are other criteria for ephemeral stream deposits, and these are summarized by Dreyer (1993) based on the interpreted ephemeral fluvial system deposits of the Paleocene Esplugafreda Formation of the Tremp-Graus Basin in northern Spain (Figure 57).

Criteria for Ephemeral Stream Interpretation	**Applicable to Willow Creek Anticline deposits?**
Stacked, thin to moderately thick (0.1 – 1.7 m) beds in which normal grading is the most noticeable feature.	Yes, but normal grading is not always noticeable.
- Bases strewn with intraclasts, but only in the lower parts of the sandbodies are signs of deep scour common.	Yes
- Internally, beds are massive to parallel-bedded.	Yes
- Beds rarely display transitions to other sedimentary structures upward, suggesting rapidly declining flow power.	Yes, (although some transition is present)
The climate during deposition of strata was semi-arid, as indicated by the presence of well-oxidized floodplain fines, and the common occurrence of caliche.	Yes
Surfaces within sediments which signify a break in sedimentation (can be indicated by root traces, soil development, burrowing, dessication cracks, or deflation pavement)	Yes (root traces and soil development)
The formation has a very immature mineralogical composition and an immature textural maturity.	Compositionally immature-submature Texturally immature-submature
Levee and crevasse splay deposits are rarely developed along channel perimeters, suggesting low channel stability and/or that the channels were too short-lived to build up extensive channel-margin deposits.	Levee deposits rarely developed crevasse splays present

Figure 57: Criteria for ephemeral stream interpretation as presented by Dreyer (1993) (modified from Dreyer, 1993). These characteristics are also discussed in Spalletti and Pinol (2005).

Facies (Dreyer, 1993)	Characteristics (Dreyer, 1993)	Depositional Process (Dreyer, 1993)	Similar Lithofacies in (Spalletti and Pinol, 2005)	Similar Lithofacies in This Study
S1	Massive to diffusely horizontally bedded coarse-grained and pebbly sandstone. Normal graded beds 0.1-1.35 m thick.	Rapid deposition from both channelized and unconfined high-energy flows.	Massive sandstone (Sm), Horizontally-laminated sandstone (Sh)	Massive sandstone (Sm), Horizontally-bedded sandstone (Sh)
S3	Sheet-like beds displaying horizontal lamination in medium to coarse-grained beds. Up to 20 beds stacked in 0.5 – 6 m thick intervals. Root traces in upper parts.	Deposits from short-lived, unconfined flows (sheetfloods).	Horizontally-laminated sandstone (Sh)	Horizontally-bedded sandstone (Sh)
S6	Cross-bedded pebbly to medium-grained sandstone. Cosets and simple sets of limited lateral extent. Beds are 0.1 – 0.35 m thick and most common in the central parts of sandbodies. Trough and tabular cross-beds. Strong basal erosion.	Reflect the migration of bedforms along the bottom of channels. Also infilling of scours.	Trough cross-bedded sandstone (St)	Trough cross-bedded sandstone (St)
F1	1 – 10 m thick units in which pebbly to very-fine grained sandstones fine up into grey, yellow, and light red mudstone. Individual beds are 0.1 – 0.95 m thick and have strongly pedoturbated tops. Horizontal lamination and current ripples common.	Sediments deposited at the interface between channels/lobes and the floodplain. Represent proximal crevasse splays and suspended load overbank material.	Horizontally-laminated sandstone (Sh), Current-rippled sandstone (Sr), Massive mudstone (Fm), Paleosols (Fs)	Horizontally-bedded sandstone (Sh), Rippled-laminated sandstone (Sr), Massive mudstone (Fm), Pedogenic carbonate (P), Massive mudstone (Fm)
F5	Mudstones with caliche nodules in units up to 15 m thick. Red color dominates, also brown and orange. Moderate degree of caliche development. No primary structures.	Overbank material deposited some distance away from channels. All original features overprinted by soil processes. Consists of immature paleosols deposited on a well-drained semiarid floodplain.	Paleosols (Fs), Massive mudstone (Fm)	Pedogenic carbonate (P), Massive mudstone (Fm)
F6	Mudstones with large caliche concretions which have coalesced into hardpans. Reddish and purple colors dominate., with some color banding and mottling. Paleosol horizons in units up to 5 m thick. Large lateral extent.	Distal floodplain overbank material, strongly oxidized. All features overprinted by mature paleosol formation. Accumulated in areas that were cut off from sediment supply for long periods.	Paleosols (Fs), Massive mudstone (Fm)	Pedogenic carbonate (P), Massive mudstone (Fm), Carbonate-rich, color mottled massive mudstone (Fmc)?

Figure 58: Similar lithofacies found in this study and in Dreyer (1993) and Spalletti and Pinol (2005) (modified from Dreyer (1993) and Spalletti and Pinol (2005)).

In addition to the criteria listed in Figure 57, several studies of both modern and ancient ephemeral fluvial systems suggest that certain lithofacies, such as thin, horizontally-bedded sandstones, are common to, and are important characteristics of ephemeral fluvial deposits (Dreyer, 1993; Spalletti and Pinol, 2005). In studies of the Paleocene Esplugafreda Formation of the Tremp-Graus Basin in northern Spain, and the Upper Jurassic Tordillo Formation of the Neuquen Basin in Argentina, Dreyer (1993) and Spalletti and Pinol (2005) (respectively) noted and interpreted several lithofacies as ephemeral stream system deposits. Lithofacies very similar to many of Dreyer's (1993) and Spalletti and Pinol's (2005) are also found in deposits of the Two Medicine Formation exposed at the Willow Creek anticline, suggesting a similar depositional process in both areas. These similarities are summarized in Figure 58.

Thin, Horizontally-bedded Sandstones with Mudstone Rip-up Clasts. Most of the criteria for the recognition of ephemeral fluvial systems listed in Figure 57 can be found in the deposits of the Willow Creek anticline. First, these deposits contain numerous sandstone beds within the range listed (0.1 – 1.7 m), although normal grading is not always readily apparent. In addition, there is often no upward transition in sedimentary structures (Figure 59).

These thin sandstone beds are also commonly either massive as shown in Figure 59, or they can contain horizontal bedding and basal mudstone rip-up clasts as shown in Figure 60. These minor sandstone sheets with basal mudstone rip-up clasts and

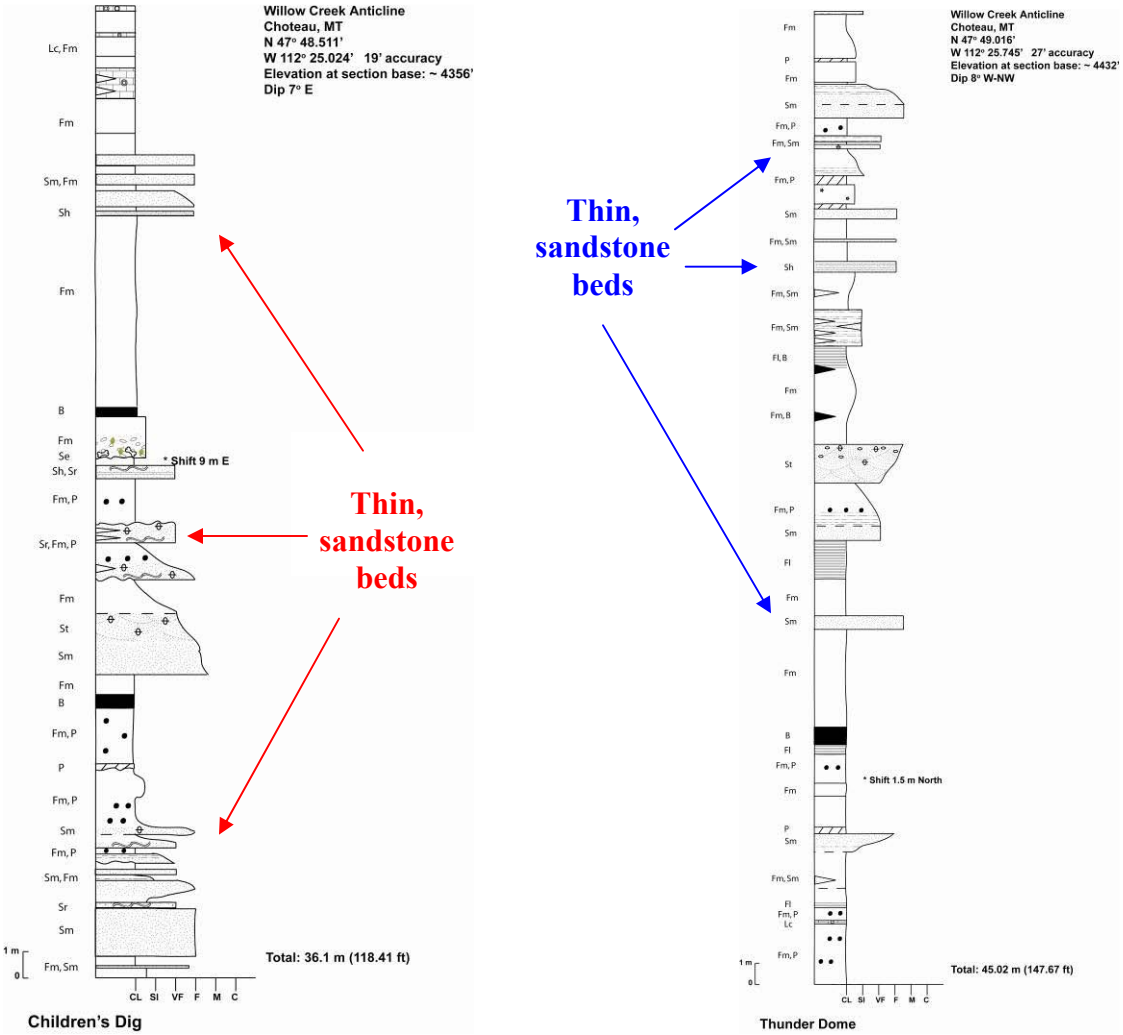

Figure 59: Measured sections from Children's Dig and Thunder Dome sites showing thin (< 1.7 m thick), repeating sandstone beds that sometimes show normal grading.

subsequent horizontally-bedded sandstone are also found in deposits of the Paleocene Esplugafreda Formation of Spain and the Upper Jurassic Tordillo Formation of Argentina, and are interpreted as the deposits of high energy tractional flows, most likely associated with rapid flooding and reworking of previously deposited muds (Dreyer, 1993; Spalletti and Pinol, 2005). The mudstone rip-up clasts may imply a local origin

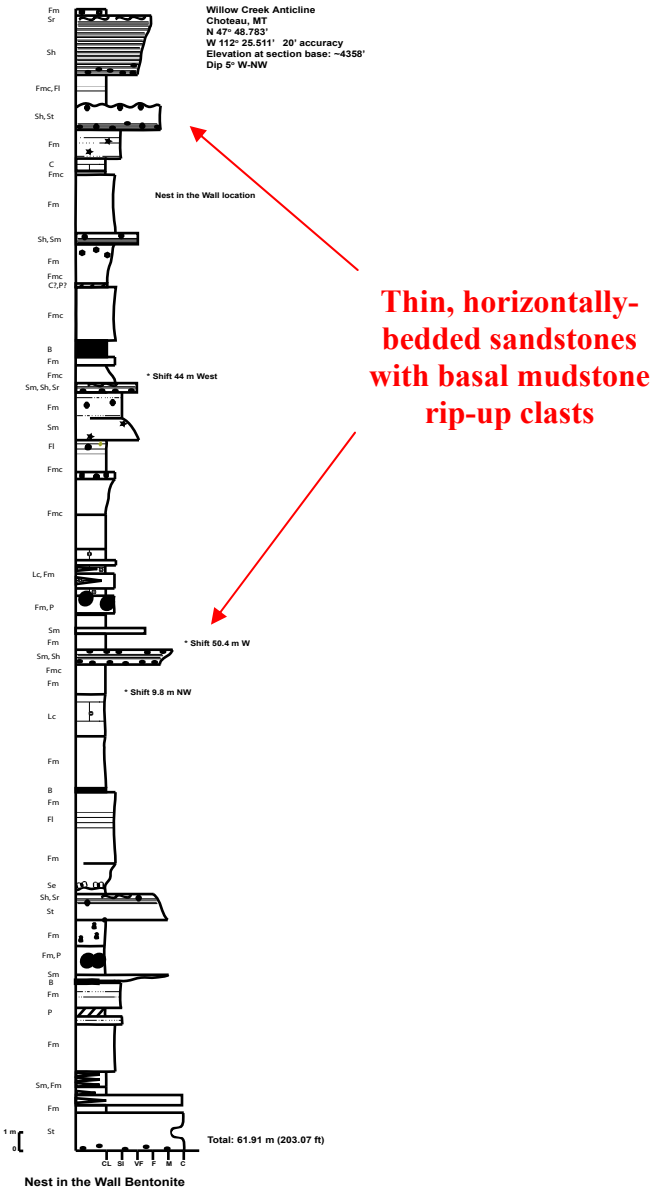

Figure 60: Measured section of Nest in the Wall Bentonite site showing thin, horizontally-bedded sandstones with basal mudstone rip-up clasts.

and the presence of a local erosion-dominated area located a short distance upstream, because mudstone clasts are naturally fragile and can therefore only be transported short distances before being destroyed (Spalletti and Pinol, 2005). In addition, the preferential

location of the mudstone clasts near the base of the sandstone layers may imply that the clasts were deposited from turbulent flows (Grecula et al., 2003; in Spalletti and Pinol, 2005).

Spalletti and Pinol (2005) attribute the widespread development of these tractional bedforms in fine-grained sandstone dominated successions to sudden and marked changes in flow conditions. The horizontal stratification present in the deposits is specifically attributed to sedimentation occurring in a moving layer of highly concentrated bedload material beneath a turbulent flow (Spalletti and Pinol, 2005). As previously stated, horizontally-bedded sandstones in predominantly fine-grained sandstones are common at the Willow Creek anticline as well, and are therefore interpreted to have formed and aggraded under upper flow regime plane bed conditions because of repeated generation and destruction of standing wave trains (Rahn, 1967; Blair, 1999, 2000; in Spalletti and Pinol, 2005).

Massive, Structureless Sandstones. Another lithofacies that is common to the three formations discussed in Figure 58 is massive, structureless sandstone beds. At the Willow Creek anticline, these sandstones can be found both as thin (< 2 m) or thick (up to 4 m) beds. Some of these beds at the Willow Creek anticline show evidence for extensive bioturbation and these beds therefore may have originally had sedimentary structures such as trough cross-bedding that was subsequently destroyed by later bioturbation. However, other massively bedded sandstones in the area do not contain evidence for bioturbation, and these sandstones are interpreted to have formed under

conditions of high rates of suspension settling from currents of moderate to high sediment concentration (Lomas, 1999; and Grecula et al., 2003; in Spalletti and Pinol, 2005

Semi-arid Climate. Using paleosols, Gavin (1986) provided a paleoenvironmental analysis of Willow Creek anticline deposits and determined that the area's climate was semi-arid (with rainfall < 500 mm/yr) during the entire interval of deposition of the Two Medicine Formation exposed in the area. In addition, both Gavin (1986) and this study found numerous pedogenic carbonates (both nodular and bedded) throughout Two Medicine Formation deposits in the area (see section on pedogenic carbonates at the end of this chapter). In the stratigraphically lower portions of the area, these pedogenic carbonates are associated with red, orange, and brown deposits, suggesting oxidized conditions (Collinson, 1996, p. 78). These pedogenic carbonates, as well as surfaces marked by root traces and bioturbation, also mark areas of breaks in deposition, which is another requirement of ephemeral stream systems (see section on pedogenic carbonates at the end of this chapter for further information and figures).

Textural and Compositional Immaturity, and Crevasse Splay Deposits. Dreyer (1993) also lists textural and compositional immaturity as characteristics of ephemeral stream deposits. Sandstones found at the Willow Creek anticline are consistent with this criteria as presented in Chapter 8 (please see Figure 46). Compositionally, sandstones are predominantly feldspathic litharenites and chert-arenites, and texturally are typically angular to subangular or subrounded, and poorly to moderately sorted. Consequently, sandstones in both the stratigraphically lower and upper fluvial and floodplain intervals

are both compositionally and texturally immature to submature. Finally, while levee deposits are not common in the area, crevasse splay deposits are present (see Figure 54, this chapter).

Other Lithofacies. The lithofacies found in the Paleocene Esplugafreda Formation of the Tremp-Graus Basin in northern Spain (Dreyer, 1993), and the Upper Jurassic Tordillo Formation of the Neuquen Basin in Argentina (Spalletti and Pinol, 2005) that were not found in Willow Creek anticline deposits, consisted mainly of conglomerate and pebbly sandstone facies. The Paleocene Esplugafreda Formation (Dreyer, 1993), the Upper Jurassic Tordillo Formation (Spalletti and Pinol, 2005), and the Two Medicine Formation were all deposited in foreland basin settings. Therefore, the presence of conglomerate facies in the Esplugafreda and Tordillo Formations may suggest that these formation may have been deposited closer to its sediment source (the uplifted thrust sheets), while the Two Medicine was deposited farther away from its sediment source (Sevier thrust belt).

Sandbody Width:Thickness Ratios. Also of importance, Dreyer (1993) found ephemeral fluvial channels with dominantly low width:thickness ratios (< 10), and which he classified as ribbons (*sensu* Friend et al., 1979). Dreyer (1993) notes that this dominance of low width:thickness ratios in an ephemeral setting contrasts with many previously published accounts of ancient ephemeral stream deposits, where sandbodies with mostly high width:thickness ratios (sheets) have been described or postulated (e.g. Steel, 1974; Tunbridge, 1981, 1984; Hubert and Hyde, 1982; Graham, 1983). However,

Friend et al. (1979), Allen et al. (1983), and Stear (1983) have shown that ancient ephemeral stream sandbodies can have a wide range of morphologies, varying from very narrow ribbons to kilometer wide sheets. Mabutt (1997) provides evidence that this same characteristic is also true in modern ephemeral streams. The presence of low width:thickness ratios in ancient ephemeral stream sandbodies is therefore further supported by Dreyer (1993). Major sandstone ribbons were also noted by Spalletti and Pinol (2005), although their width:thickness ratios were somewhat higher. Width:thickness ratios of 4.1-6.6 for the stratigraphically lower fluvial deposits, and 5.9 and 7.1 for the stratigraphically higher fluvial deposits (as compared to Gavin (1986) with ratios of 3.8-2.9 for the stratigraphically lowest fluvial rocks and 4.8-6.7 for the stratigraphically highest fluvial rocks) are recorded in the Willow Creek anticline. These ratios are consistent with the low width:thickness ratios of ephemeral streams (Smith and Dreyer, 1993).

Summary

In conclusion, the fluvial deposits of the Two Medicine Formation exposed at the Willow Creek anticline are interpreted as arid- to semi-arid zone ephemeral, anastomosing river systems. Flows in the area were most likely seasonal and typically ephemeral, and were characterized by episodic low-energy shallow sheetflooding, settlement from residual flood discharge, and prolonged periods of subaerial exposure and nondeposition (after Spalletti and Pinol, 2005). Cooper Creek, an ephemeral, anastomosing river system located in the Channel Country of Australia, provides a good

modern analogue for the fluvial systems of the Willow Creek anticline during the Campanian.

Lacustrine Deposits

The approximately 15 m (49.2 ft) thick lacustrine interval found in the Willow Creek anticline is characterized by interbedded limestones and dark colored mudstones. The limestones contain abundant charophyte fossils, which as described in the previous lithofacies section, and are indicative of shallow lakes (Gierlowski-Kordesch, 1998; Djamali et al., 2006). No evidence is recorded in the area for the presence of deep lakes. The interbedded nature of the limestone and mudstone suggests either that the edge of the lake was present in this area, or that the lake occasionally dried up (Figure 61). There are no evaporite minerals interbedded within the lacustrine deposits in this area, suggesting that the lake did not undergo rapid drying up periods, but instead may have merely fluctuated in size while remaining shallow in depth. The lack of evaporite minerals in an interpreted semi-arid setting (Gavin, 1986), might also be explained if the lake(s) formed under hydrologically open conditions that favored a relatively stable, near surface groundwater table (Djamali et al., 2006). If this were the case, then the lake(s) would have had inputs from groundwater and/or surface water which would have prevented the water from evaporating enough to precipitate evaporite minerals (Valero Garces et al., 1997).

At the Willow Creek anticline, the presence of the lithofacies association of carbonate-rich, color mottled massive mudstone (lithofacies Fmc) and light grey, well-

indurated carbonate (lithofacies C) stratigraphically above the lacustrine interval provides further evidence that groundwater tables in the area were rising and were likely near surface and oscillating in the area at the time of deposition of the charophytiferous limestone lithofacies (Lc) (Figure 61). This is because the presence of mottling (purple, green, and grey) in lithofacies Fmc (carbonate-rich, color mottled massive mudstone), and the presence of groundwater carbonate (lithofacies C: light grey, well-indurated carbonate) provide evidence for hydromorphic conditions in the area following the lacustrine interval suggesting that the groundwater table was most likely rising in the area throughout the lacustrine interval, and was probably near the surface during deposition of the lacustrine interval (Djamali et al., 2006).

Valero Garces et al. (1997) suggests that carbonate lakes develop in the topographic lows of the plain of anastomosing river systems, particularly in areas protected by levees because these areas are relatively protected from clastic inputs due to river flooding. This reduced clastic input allows carbonates to form in the lakes. These lakes tend to be small (several km^2), are generally shallow, and are filled with calcium-rich alkaline water (Valero Garces et al., 1997; Gierlowski-Kordesch, 1998; Djamali et al., 2006). Abundant charophyte fossils found in lacustrine sediments of the Willow Creek anticline suggest that the main source of calcium carbonate production was due to inorganic productivity by these plants.

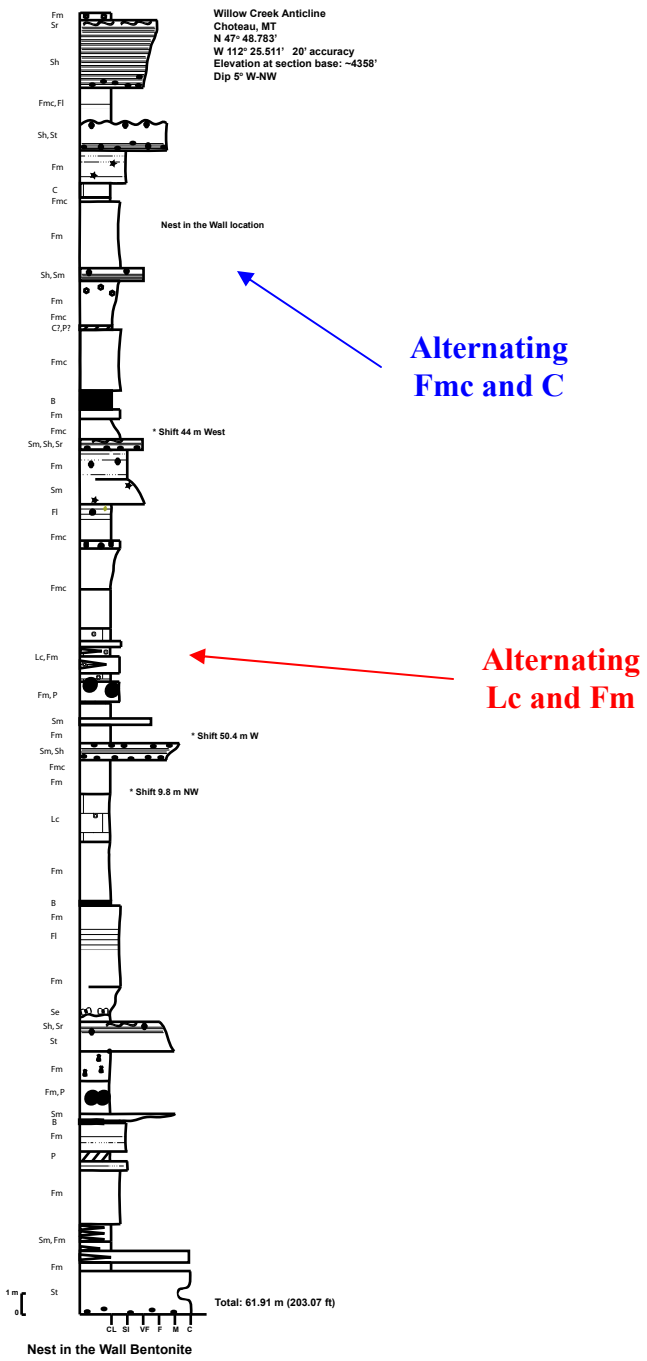

Figure 61: Measured section of Nest in the Wall Bentonite site showing interbedded charophytiferous limestone (lithofacies Lc) and massive mudstone (Fm), and alternating carbonate-rich, color mottled massive mudstone (lithofacies Fmc) and light grey, well-indurated carbonate (lithofacies C).

Ancient Analogues. The presence of lacustrine carbonates within a stratigraphic succession containing ephemeral river system deposits in an area receiving clastic sediment transported from an uplifted region is also consistent with other studies (Alonso-Zarza et al., 1992; Sanz et al., 1995; Valero Garces et al., 1997; Gierlowski-Kordesch, 1998; Gierlowski-Kordesch et al., 1991; Tanner, 2000; Djamali et al., 2006). A good ancient analogue for Two Medicine Formation lacustrine deposits in an ephemeral, anastomosing fluvial system setting is the Jurassic Shuttle Meadow Formation of the Newark Supergroup, Hartford Basin, USA (Gierlowski-Kordesch, 1998). Many of the lithofacies present in the Shuttle Meadow Formation are also present in the Two Medicine Formation of the Willow Creek anticline (summarized in Figure 62). Gierlowski-Kordesch (1998) interprets lithofacies Fr, Sr, Sh, and Fm in the Jurassic Shuttle Meadow Formation as representing an anastomosing alluvial plain system in an ephemeral setting with high accretion rates and with bedload sheetflooding as the dominant depositional mechanism, and provides the Channel Country drainage system of central Australia as an analogue. Lithofacies Pm (micritic carbonates with possible highly altered charophytes) occurs as two carbonate beds averaging 30 cm thick (Gierlowski-Kordesch, 1998), which is similar to the 3-4 carbonate beds averaging ~ 46 cm thick that occur at the Willow Creek anticline. Additionally, no evidence for a groundwater or spring source for the carbonate (e.g. “bizarre textures” such as dendrites, spherulitic crystals, etc. or stellate clusters) is present in lithofacies Pm. This is also true of lithofacies Lc (charophytiferous limestone) found at the Willow Creek anticline.

Lithofacies	Description	Present in Willow Creek Anticline Deposits?	Lithofacies Designation in This Study
Fr, Sr	Ripple cross-laminated muddy siltstones to sandstones	Yes	Ripple cross-laminated sandstone (Sr)
Fm	Massive siliciclastic mudstones	Yes	Massive mudstone (Fm)
Sh	Fine to medium-grained horizontally laminated sandstones	Yes	Horizontally-bedded sandstone (Sh)
Fl_3	Disrupted calcareous shales	Calcareous shales and mudstones are present, but are not "disrupted"	Carbonate rich, color mottled massive mudstone (Fmc)
Pm	Micritic carbonates with possible highly altered charophytes.	Yes	Charophytiferous limestone (Lc)

Figure 62: Similar lithofacies in the Jurassic Shuttle Meadow and Campanian Two Medicine Formation (lithofacies and description modified from Gierlowski-Kordesch, 1998).

Gierlowski-Kordesch (1998) interprets lithofacies Pm as representing the edge of a shallow freshwater carbonate lake or part of a small pond with vegetation and periodic exposure that was located in the distal environment of the Shuttle Meadow alluvial plain. Due to the numerous similarities between Shuttle Meadow Formation lithofacies Pm (micritic carbonates with possible highly altered charophytes) and Two Medicine Formation lithofacies Lc and their respective associated lithofacies, lithofacies Lc is also interpreted as having been deposited in a similar setting and via a similar mechanism. It should be noted however that while the local alluvial setting is interpreted to be similar, the regional tectonic setting for the two areas in which these formations were deposited is

different, as the Shuttle Meadow Formation was deposited in a rift basin, while the Two Medicine Formation was deposited in a retroarc foreland basin.

Summary

In summary, the charophytiferous limestone interval of the Two Medicine Formation at the Willow Creek anticline is interpreted as the edge of a shallow freshwater carbonate lake or part of a small pond with vegetation and periodic exposure that was located in the distal environment of the Two Medicine alluvial plain (Figure 63, 64).

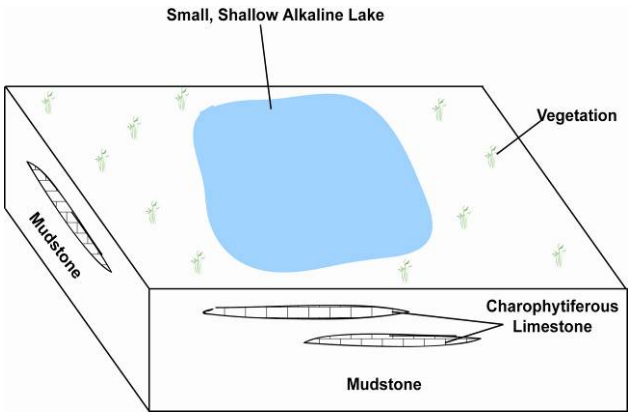

Figure 63: Simplified cartoon diagram of small, shallow alkaline lake depositional environment that is interpreted to have existed at the Willow Creek anticline.

Evidence for lakes at the same approximate time interval (~75.4 Ma at the type section and ~76.5 Ma at the Willow Creek anticline) during the Late Cretaceous is also recorded at the Two Medicine Formation type section 75 km (47 mi) to the north (Figure 21 in Appendix C). As a result, it is interpreted that during this time period the foredeep of the Sevier thrust belt foreland basin in Montana was characterized by a series of relatively

small, shallow, possibly hydrologically open lakes. These lakes may have been located on the plains between anastomosing river systems (Figure 64).

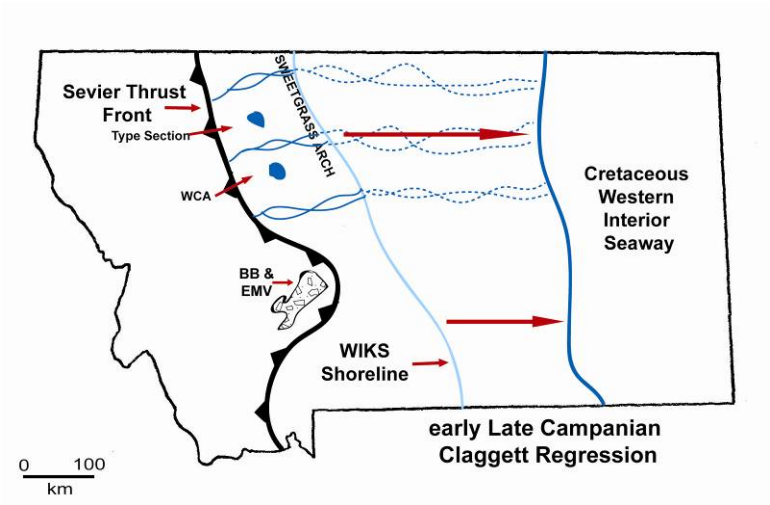

Figure 64: Cartoon of interpreted environment of deposition for the lacustrine strata of the Two Medicine Formation at the Willow Creek anticline. The depositional environment was characterized by shallow lakes in which carbonates of biologic origin accumulated. Anastomosing river systems may have been present in areas adjacent to those in which lacustrine sediments were accumulating. These lacustrine deposits were accumulating in the foredeep at the same time the WIKS was regressing to the east in the Claggett Regression. WCA: Willow Creek anticline. BB: Boulder Batholith. EMV: Elkhorn Mountains Volcanics. Light blue line represents position of WIKS shoreline at start of Claggett Transgression, while dark blue line represents position of WIKS at end of Claggett Regression (modified from Lillegraven and Ostresh, 1990). Red arrows denote direction of shoreline movement to east during the regression. Dashed lines represent possible gradual eastward expansion of anastomosing system as WIKS shoreline transgressed east.

Non-Lacustrine Carbonate Deposits

Two types of non-lacustrine carbonate deposits are present at the Willow Creek anticline: nodular to discontinuously bedded oxidized carbonate (lithofacies P) and a light grey, well-indurated carbonate (lithofacies C). As stated in Chapter 6, the nodular to discontinuously bedded oxidized carbonate (lithofacies P) is interpreted to be a pedogenic

carbonate. Pedogenic carbonates are calcitic soils that form above the water table in arid to semiarid oxidizing climates where floodplains are exposed to surface weathering processes for extended periods of time (thousands of years) (Miall, 1996, p. 127). This method of formation is in contrast to that of the light grey, well-indurated carbonate (lithofacies C) of the Two Medicine Formation, which is interpreted to be a groundwater carbonate deposit. Groundwater carbonate is a non-pedogenic form of calcrete (Khadkikar et al., 1998), and forms from rain infiltration leaching dissolvable ions downward during wet periods, and evaporation and capillary groundwater flow or carbon degassing concentrating ions as calcium carbonate near the ground surface during dry periods (Miall, 1996, p. 127; Khadkikar et al., 1998). These two types of non-lacustrine carbonate provide information regarding both the relative position of the water table and the nature of the fluvial floodplains during the time of Two Medicine Formation deposition at the Willow Creek anticline.

In order for pedogenic carbonates to form, the floodplains needed to be exposed to surface weathering processes for extended periods of time (thousands of years) (Miall, 1996, p. 127). Just as the nature of ephemeral river systems would allow floodplains to be exposed for long, uninterrupted time intervals, the aggradational nature of anastomosed river systems would also allow floodplains to be exposed in this way as long as the rate of floodplain sedimentation does not overwhelm the rate of pedogenesis (Kraus, 1999). As stated in the previous section, rocks of the Willow Creek anticline show evidence of periodic river avulsion. By causing channels to shift their position on the floodplain, avulsion can terminate sedimentation on a particular part of the floodplain

for periods of time approximating 10^3 years, which is an interpreted periodicity of avulsion as presented by Bridge and Leeder (1979) (in Kraus, 1999). The rate of sedimentation on Two Medicine floodplains in either an anastomosed or an ephemeral fluvial system may have been low enough to allow for pedogenesis to occur as a result of both autocyclic and allocyclic processes: lowered influx of sediment into the foredeep from the thrust belt to the west, stream avulsion, levees built up by anastomosed fluvial systems that protected the floodplain, lack of extensive lateral migration of anastomosed fluvial systems, and/or ephemeral nature of streams resulting in only periodic flooding. Anastomosed river systems and ephemeral river systems would therefore both have provided the area's floodplains with the long periods of exposure to surface weathering processes necessary for the formation of pedogenic carbonates.

At the Willow Creek anticline, pedogenic carbonates are present predominantly in nodular form in the stratigraphically lowest rocks, and are present predominantly as laterally discontinuous beds of coalesced nodules in the stratigraphically highest rocks (Figure 65). However, it should be noted that pedogenic carbonate also occurs in nodular form in the stratigraphically higher rocks, and rarely as discontinuous beds in stratigraphically lower rocks, so these forms are not stratigraphically restricted in their occurrence. It is only suggested that one form is more predominant in the separate fluvial intervals. This change in pedogenic carbonate form is attributed to the pedogenic carbonates of the stratigraphically higher rocks generally representing more mature soils relative to the stratigraphically lower pedogenic carbonate, as the layers in bed form

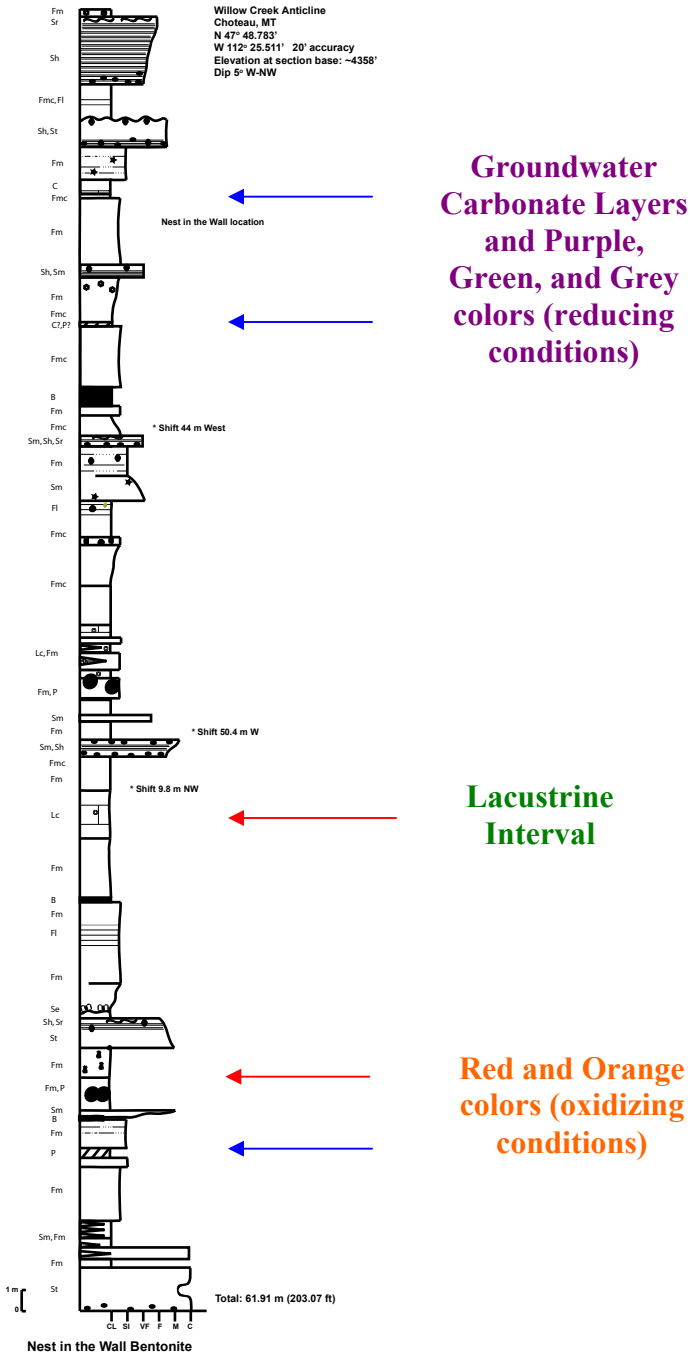

Figure 65: Measured section showing general change from nodular to bedded groundwater carbonate. Red arrows denote locations of nodular forms, while blue arrows denote locations of beds. (section location and key are located in Appendix A)

suggest that the pedogenic carbonate nodules had time to coalesce (Figure 65). This change was previously noted and attributed to this reason by Gavin (1986).

Additionally, the stratigraphically lower rocks exposed in the area are also characterized by red and orange hues, while stratigraphically higher portions of the sections are characterized by green, purple, and grey colors (Figures 66, 67). As discussed in the previous lithofacies section on pedogenic carbonates, color can be used as a rough indicator of both the drainage state of a floodplain and of the level of the water table (Collinson, 1996, p.78). Red colors can indicate relatively well- drained conditions on a floodplain and an oxidizing regime (Figure 66), while grey colors can indicate water-logged conditions and the presence of reducing pore water (Collinson, 1996, p. 78; Kraus, 1999), suggesting that the water table is closer to the surface (Figure 67). In addition to this change in color at the Willow Creek anticline, groundwater carbonate is mainly found in these stratigraphically highest fluvial and floodplain rocks (Figure 65), where it is primarily associated with carbonate-rich, color mottled massive mudstone (lithofacies Fmc). It is therefore interpreted that the stratigraphically lower rocks were deposited under predominantly oxidizing conditions when the local water table was relatively deep in the subsurface. In contrast, the presence of grey, green, and purple colors, mottling of these colors in carbonate-rich, color mottled massive mudstone (lithofacies Fmc), and the presence of groundwater carbonate intervals in this portion of the Willow Creek anticline exposures all suggest that the groundwater table was relatively higher, resulting in reducing conditions when these rocks were deposited, as

Figure 66: Outcrops of stratigraphically lower rocks exposed near the Egg Mountain area at the Willow Creek anticline Choteau, MT. These red colors may suggest relatively well-drained conditions and an oxidizing regime at the time of soil formation.

Figure 67: Outcrops of stratigraphically higher rocks exposed near the Egg Mountain area at the Willow Creek anticline Choteau, MT. These grey, purple, and green colors may suggest relatively poorer drainage conditions and a relatively higher water table at the time of soil formation.

compared to the stratigraphically lowest fluvial and floodplain rocks (Figure 65). This higher position of the water table is also supported by the presence of a relatively thick interval of lacustrine deposits indicating a raised base level (relative to the lowermost fluvial rocks located stratigraphically below these upper anastomosed fluvial and floodplain (Figure 65)).

CHAPTER 10

DISCUSSION OF RESULTS

Introduction

Two Medicine Formation outcrops exposed at the Willow Creek anticline record two important changes in stratigraphic architecture corresponding to base-level changes that occurred in the area during the time of sediment deposition. The first change, located just above the Museum of the Rockies TM-003 bonebed (Figures 26, 27 in Appendices D, E), records a shift from fluvial channel and floodplain deposits of anastomosing river systems to lacustrine carbonate and mudstone deposits. The second change, located stratigraphically up-section from these lacustrine deposits, is marked by a change from lacustrine carbonates to fluvial and floodplain deposits of anastomosing river systems (Figures 26, 27 in Appendices D, E). These deposits are discussed in greater detail below.

Change from Fluvial and Floodplain to Lacustrine Facies

Introduction

The age of the first change in stratigraphic architecture can be approximated as it occurs stratigraphically above a bentonite located above the TM-003 bonebed (Nose Cone bentonite (Figures 26, 27 in Appendices D, E). This bentonite, dated by U-Pb dating of zircons, yielded ages of 76.0 +/- 0.6 Ma and 77.0 +/- 0.7 Ma, with an average

age of approximately 76.5 Ma (USGS Denver Argon Geochronology Laboratory). Therefore, this change occurred no earlier than 76.5 Ma. Additionally, the 2.8 m (9.2 ft) of silty mudstone between the bentonite and overlying lacustrine carbonate/mudstone deposit suggests this change occurred later than 76.5 Ma. A similar change in stratigraphic architecture from fluvial and floodplain to lacustrine facies is seen at the Two Medicine Formation type section, and has been correlated to an ~ 75.4 Ma old bentonite in the Judith River Formation (upper discontinuity) (Rogers, 1994, 1995, and 1998).

This lacustrine interval preserved in Willow Creek anticline strata is approximately 14 m (45.92 ft) thick as recorded in the Nest in the Wall Bentonite measured section. This thickness is similar to that of the lacustrine interval found at the Two Medicine Formation type section where this interval is approximately 20 m (65.6 ft) thick.

Possible Autocyclic Cause

One possible simple way to explain the first change in stratigraphic architecture is that they mark a period where the ephemeral, anastomosing river system present in the area shifted out of the area of the Willow Creek anticline. This may have allowed lakes to form where river systems were once flowing because the shift in the position of the rivers may have allowed for clastic input into the area to drop to a low enough level to permit the formation of lakes. This mechanism would be autocyclic in nature, requiring no necessary changes in climate, relative sea level, or tectonics. The validity of this

possible cause will be evaluated along with the possible allocyclic causes in reference to the second change in stratigraphic architecture at the end of this chapter.

Possible Allocyclic Causes

Eustatic Sea Level Controls

This change from fluvial to lacustrine deposition records a base-level rise in the area of the Willow Creek anticline at the time these sediments were being deposited. In nonmarine areas, rising base level causes a rise in the position of the groundwater table, resulting in more poorly drained conditions that can eventually lead to the formation of lakes (Shanley and McCabe, 1994; Currie, 1997). In marine strata, rising base level results in the formation of flooding surfaces as the sea begins to transgress farther inland (Shanley and McCabe, 1994). This transgression ultimately culminates in the formation of a maximum flooding surface that marks the most landward position of the shoreline and that also is represented by the deepest water facies (Shanley and McCabe, 1994). A minor downlap surface, or marine flooding surface, is recorded in marine strata deposited globally ~ 76 Ma (Haq et al., 1987). In the nonmarine realm, a maximum flooding surface may be represented by lacustrine carbonates, reflecting propagation of a rising groundwater table inland from the shoreline (Shanley and McCabe, 1994).

However, during the period of time when this change in stratigraphic architecture was taking place, the WIKS was regressing to the east during the Claggett Regression (the Claggett Transgression ended approximately 79.6 Ma) (Rogers et al. 1993) (Figure 68). This regression would have had the effect of lowering base level rather than raising

it. The rise in baselevel recorded in Two Medicine deposits preserved at the Willow Creek anticline and at the type section is therefore not a reflection of changes in sea level, but rather of a different, overriding control (local-subregional tectonic subsidence within the foredeep) which was serving to raise baselevel at the time.

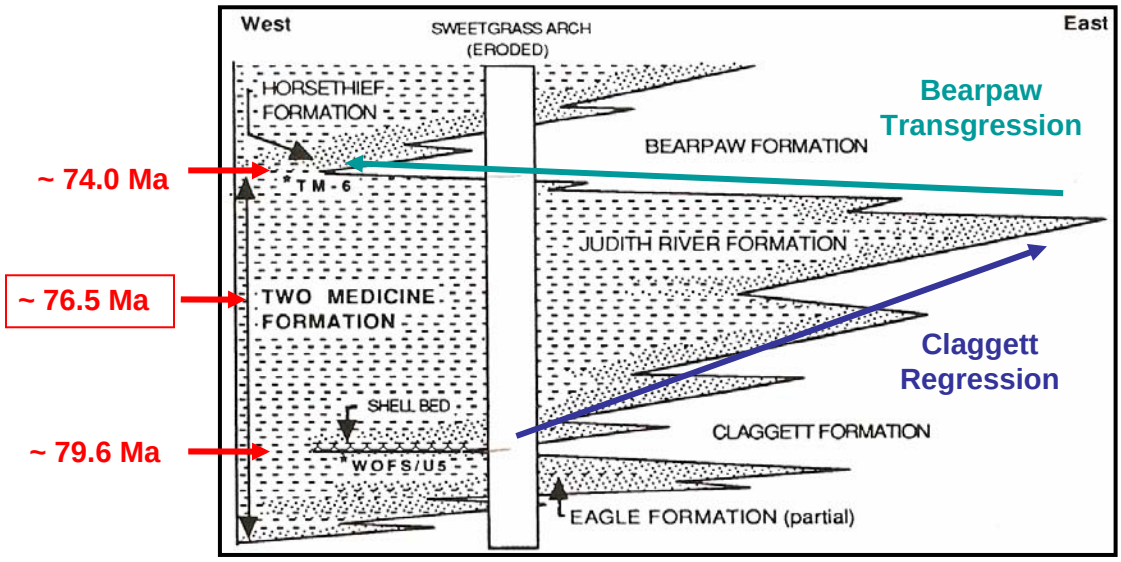

Figure 68: Schematic cross section showing interval of Two Medicine Formation deposition. 74.0 Ma and 79.6 Ma bentonite dates from Rogers et al. (1993). 76.5 bentonite date from this study. The changes in stratigraphic architecture at the Willow Creek anticline found in this study were most likely primarily controlled by local tectonics, rather than by changes in sea level. (modified from Rogers et al., 1993)

Tectonic Controls

Sedimentation in the Willow Creek anticline area was also subject to important tectonic controls during the Campanian. The primary tectonic controls consisted of two interrelated occurrences (Figure 7):

1. The Lombard-Eldorado thrust slab obtained maximum values of supercritical taper 76-74 Ma. Hinterland shortening occurred in conjunction with this until approximately 74 Ma. (Lageson et al., 2001)
2. Emplacement of the Boulder Batholith (80-70 Ma) and coeval eruption of the Elkhorn Mountains Volcanics (81-74 Ma). (Lageson et al., 2001)

The Lombard-Eldorado thrust slab forms one of the principal thrusts in the Helena salient, and is located to the southwest of the Willow Creek anticline and Two Medicine Formation type section areas (Figure 13). During the period of time in which the change in stratigraphic architecture is seen in both these areas, this thrust slab was being intruded by the Boulder Batholith and was also subject to coeval eruptions from the Elkhorn Mountains Volcanics (Lageson et al., 2001) (Figure 16). Together these related igneous events had the effect of adding a substantial amount of igneous rock (16-17 km (9.9-10.5 mi) thick) to the Lombard-Eldorado thrust slab over a relatively short interval of time (10 Ma) (Lageson et al., 2001). Hinterland contraction (shortening) was also occurring at this time, ending approximately 74 Ma (Lageson et al., 2001). The combined effects of the emplacement of the Boulder Batholith and eruption of the Elkhorn Mountains Volcanics, as well as hinterland shortening had the result of thickening the orogenic wedge to the point of supercritical taper between 76-74 Ma, and ultimately played an important role in causing the continued eastward motion of the Lombard-Eldorado thrust system between 74-70 Ma (Lageson et al., 2002).

During this interval of supercritical taper between 76-74 Ma, the orogen was subject to substantial loading due to weight added to the slab from the igneous events and

from shortening. As a response to this loading, the adjacent foreland basin to the east subsided rapidly, particularly in the foredeep region (Catuneanu et al., 1999) (Figure 69). The effect of rapid subsidence was to increase the amount of accommodation available in the foreland basin for sediment deposition, as well as to cause a rapid base-level rise that would have been most pronounced in the foredeep region (Catuneanu et al., 2000) (Figure 70).

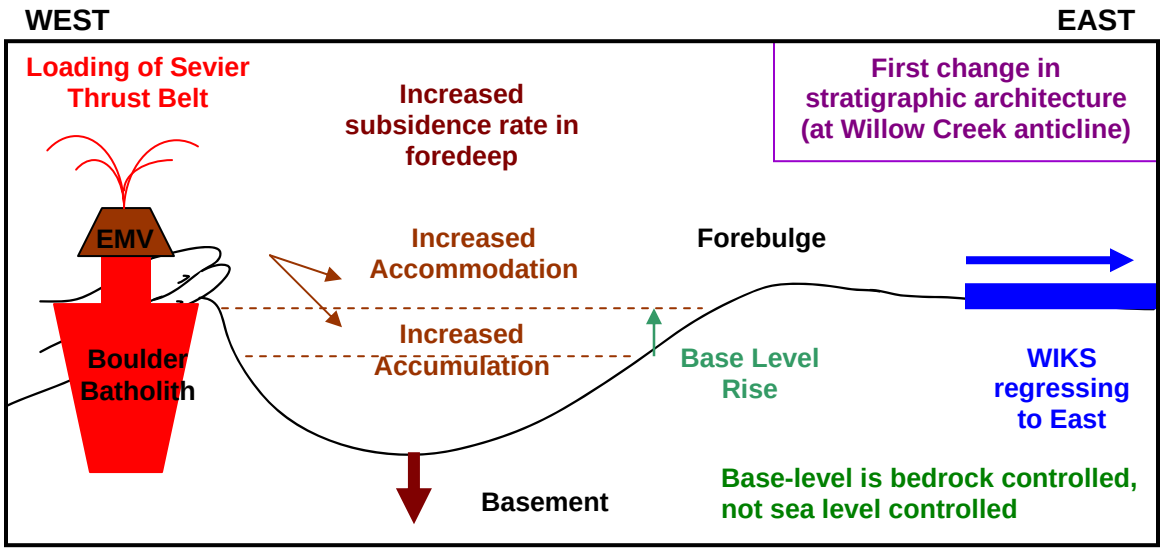

Figure 69: Cartoon cross section through Sevier Thrust Belt foreland basin. The emplacement of the Boulder Batholith and Elkhorn Mountains Volcanics would have caused further loading in the Sevier thrust belt, causing increased subsidence in the adjacent foreland basin, and particularly in the foredeep region, to the east. This would have caused a base level rise, which would have produced additional accommodation, as well as caused the water table to rise during the time of the first change in stratigraphic architecture. Additionally during this time, the WIKS was regressing to the east. Base-level is therefore bedrock controlled, not sea level controlled.

This rate of proximal subsidence may have been very high, as the foreland basin would have experienced the effects of both dynamic subsidence (large-scale lithospheric

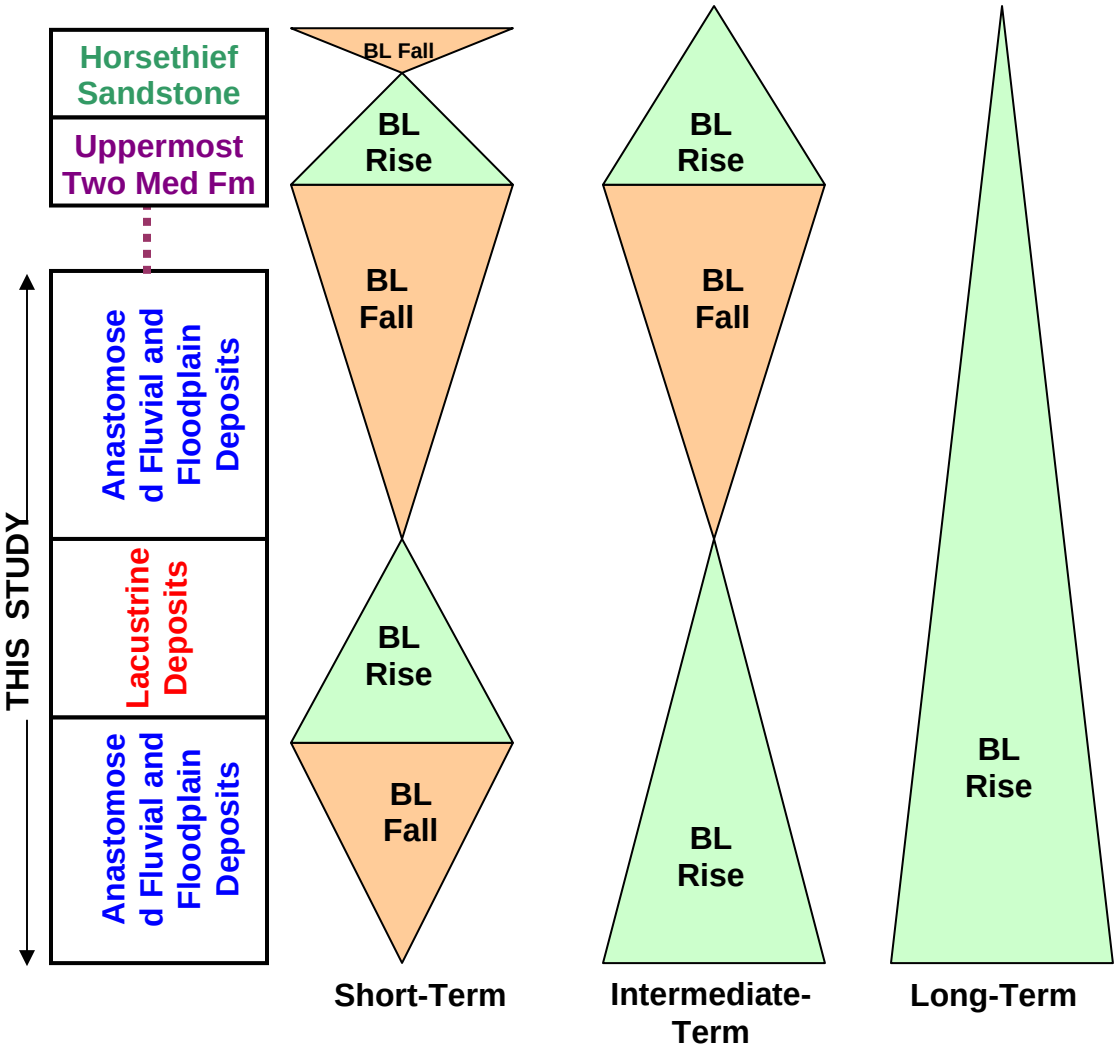

Figure 70: Simplified diagram of Two Medicine Formation depositional environment interpretations, and their associated base level energy cycles. The changes in stratigraphic architecture observed at the Willow Creek anticline are interpreted to be short-term in scale. The long-term scale is interpreted to represent an overall base level rise because this area was located in the foredeep of a foreland basin during deposition of Two Medicine Formation sediments. The Uppermost Two Medicine Formation and the Horsethief Sandstone have been added to the diagram to show the next set of base level cycle changes.

deflection in response to sublithospheric loading) as well as flexural tectonics (foredeep subsidence coeval with forebulge uplift as a result of orogenic loading) (Catuneanu et al., 1999). Therefore the rise in base level generated by these tectonic events would most certainly have effected Two Medicine Formation sedimentation as this formation was deposited in the foredeep adjacent to this thrust slab. Studies by Blair and Bilodeau (1988) suggest that the change to finer grained sedimentation above coarser grained deposits in a foreland basin reflect a syntectonic response of the system to thrusting in the orogen. The change to lacustrine and finer grained facies at the Willow Creek anticline is consistent with this interpretation, and may reflect a sedimentary syntectonic response to loading occurring in the wedge.

As discussed in chapter 4 of this thesis, Rogers (1998) attributed the formation of the upper discontinuity and the associated change in stratigraphic architecture found at the type section to an abrupt increase in accommodation in the Montana portion of the foreland basin, presumably related to flexural subsidence. Further Rogers (1998) gives an approximate $^{40}Ar/^{39}Ar$ bentonite date of ~ 75.4 Ma for a discontinuity of the Judith River Formation which he considers to be the lateral equivalent (to the east) of the upper discontinuity found that the Two Medicine Formation type section. Therefore, although a more precise date of the upper discontinuity is not possible because no bentonites have been found stratigraphically near the upper discontinuity at the type section, the timing of this change can at least be narrowed to having occurred some time between ~ 75.4 Ma and 74.1 +/- 0.7 Ma (from a dated bentonite located 130 m above the discontinuity). Both the change in stratigraphic architecture recorded at the Willow Creek anticline and

the change in stratigraphic architecture observed across the upper discontinuity at the Two Medicine Formation type section are interpreted to reflect the same driving processes, and are further interpreted to be a consequence of the achievement of supercritical taper in the Lombard-Eldorado thrust slab between 76-74 Ma. However, the difference in available dates for these changes at the two areas (~75.4 Ma for type section and ~76.5 Ma for the Willow Creek anticline) suggest that these two areas responded to this loading at progressively different times. This is interpreted to reflect the fact that the loading occurred in the Helena Salient, which is located closer to the Willow Creek anticline area, and therefore affected this area first (that is, at an earlier date) (Figure 71).

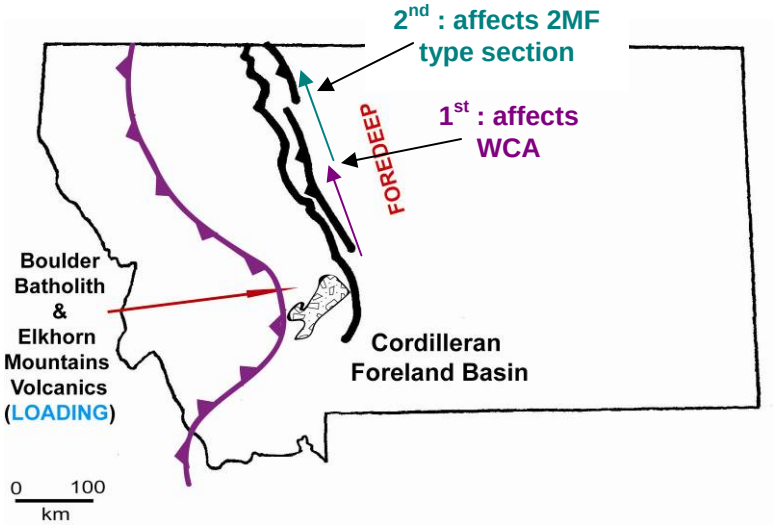

Figure 71: Generalized diagram of present day Montana showing the interpreted northward propagation of increased subsidence and stress from loading by the Boulder Batholith (denoted in its present position in the Helena Salient). Purple: Campanian position of Sevier fold and thrust belt; Black: present-day position.

Then the continued loading and its associated subsidence and stresses continued to propagate north through the foredeep, therefore not showing its effects at the Two

Medicine Formation type section (located approximately 75 km (47 mi)) to the north of the Willow Creek anticline) until a later date.

Climatic Controls

Approximately 76.5 - 75.4 Ma, global ocean bottom waters began to cool (Huber et al., 2002). However, this was only the very beginning of a change in climate that would eventually lead to the cooling and draining of epicontinental seaways as expressed in the Bearpaw Regression (Catuneanu et al., 1999; Huber et al., 2002). Therefore, the initial cooling of ocean bottom waters would not have had a great effect on sea level until later in the Campanian, making it an unlikely control on foreland basin stratigraphy. No other major changes in global or local climate are recorded for this period of time during the Campanian (Figure 7). In addition, Gavin (1986), using paleosols of the Willow Creek anticline as a proxy for climate, concludes that while there may have been a slight increase in precipitation during deposition of the rocks of the Willow Creek anticline, this increase was not enough to change the regional climate significantly, and it therefore remained semi-arid throughout the interval recorded. Climatic controls therefore did not play an important role in causing the change in stratigraphic architecture observed at either the Two Medicine Formation type section or the Willow Creek anticline.

Summary

The change in stratigraphic architecture recorded in Two Medicine type section and Willow Creek anticline strata is interpreted to be primarily a response to loading in the Lombard-Eldorado thrust slab to the southwest approximately 76-74 Ma. This

loading would have caused subsidence in the adjacent foredeep, causing base level to rise, and resulting in a change to lacustrine sedimentation in areas of the foredeep. Additionally, this change occurred during the Claggett Regression of the WIKS, when the WIKS western shoreline was moving eastward. The change in stratigraphic architecture is therefore not interpreted to be related to a sea level change because the regression of the sea would have caused a base level fall, not a base level rise, as would be needed to produce lacustrine units. Finally, despite the initiation of cooling in ocean bottom waters, no major changes in global climate are recorded for the period of time in which this architectural change is observed, and as a result, climatic controls did not play an important role in causing the observed change in stratigraphic architecture. Further, both the change in stratigraphic architecture recorded at the Willow Creek anticline and the change in stratigraphic architecture observed across the upper discontinuity at the Two Medicine Formation type section are interpreted to reflect the same driving processes, and are further interpreted to be a consequence of the achievement of supercritical taper in the Lombard-Eldorado thrust slab between 76-74 Ma. However, the difference in available dates for these changes at the two areas (~75.4 Ma for type section and ~76.5 Ma for the Willow Creek anticline) suggest that these two areas responded to this loading at progressively different times. This is interpreted to reflect the fact that the loading occurred in the Helena Salient, which is located closer to the Willow Creek anticline area, and therefore affected this area first (that is, at an earlier date). Then the continued loading and its associated subsidence and stresses continued to propagate north through the foredeep, therefore not showing its effects at the Two Medicine Formation type

section (located approximately 75 km (47 mi)) to the north of the Willow Creek anticline) until a later date.

Change from Lacustrine to Fluvial and Floodplain Facies

Introduction

The second change in stratigraphic architecture observed at the Willow Creek anticline consists of a change from lacustrine carbonates/shales to fluvial and floodplain facies of an anastomosing river system (Figures 26, 27 in Appendices D, E). In the Nest in the Wall Bentonite measured section (Figure 26, 27 in Appendices D, E), this change occurs approximately 36.61 m (120.1 ft) up from the base of the section. A possible surface is recorded at this position in the form of a poorly developed groundwater carbonate layer with root traces. It is important to note however that although groundwater carbonate layers are abundant throughout the stratigraphic sections measured at the Willow Creek anticline, it is impossible to accurately correlate them over long distances as most are discontinuous and as the axis of the anticline running through the area has been eroded away. Therefore, while the groundwater carbonate layer preserved at 36.61 m (120.1 ft) up-section in the Nest in the Wall Bentonite measured section may represent a surface associated with the change in architecture, it is not necessarily continuous over the entire Willow Creek anticline (Figures 26, 27 in Appendices D, E). The change in stratigraphic architecture is however, observed throughout the area of the Willow Creek anticline addressed in this study, and therefore this change in architecture may not always be associated with a surface, but rather with a

period of transition. The relative age of this architectural change can be loosely estimated using the afore mentioned Nose Cone bentonite, dated to approximately 76.5 Ma. The 17.18 m (56.4 ft) of strata between the bentonite and the change in architecture suggests that this change occurred much later than 76.5 Ma (Figures 26, 27 in Appendices D, E). A second age control estimate can be made using the stratigraphic position of this change in stratigraphic architecture in relation to the stratigraphic position of the Horsethief Sandstone. The Horsethief Sandstone stratigraphically overlies the Two Medicine Formation in the Pine Butte area located approximately 6 km (3.7 mi) to the northwest of the Willow Creek anticline study area. Outcrops exposed in this area record the transition from nonmarine deposits of the Two Medicine Formation to shallow marine deposits of the Horsethief Sandstone, and are stratigraphically above the upper Two Medicine Formation deposits found at the Willow Creek anticline. Deposition of the Horsethief Sandstone and associated Bearpaw Shale were dated to approximately 74.1 Ma via $^{40}Ar/^{39}Ar$ dating of bentonites (Rogers et al., 1993). Therefore, the change in stratigraphic architecture observed at the Willow Creek anticline occurred sometime after 76.5 Ma and before 74.1 Ma.

A similar change in stratigraphic architecture from lacustrine to fluvial and floodplain deposition is recorded in strata at the Two Medicine Formation type section, although the age of this change is also unknown (Rogers 1994, 1995, and 1998). The change has to have occurred before 74.1 Ma however, as this marks the approximate arrival of Bearpaw deposits of the WIKS into western Montana (Rogers et al., 1993).

Possible Autocyclic Cause

One possible simple way to explain the first change in stratigraphic architecture is that they mark a period where the ephemeral, anastomosing river system present in the area shifted back into the area of the Willow Creek anticline from a different adjacent area. This renewed presence of the river system in the area may have brought an influx of clastic sediments into the area that was too high to sustain the presence of lakes. This mechanism would be autocyclic in nature, requiring no necessary changes in climate, relative sea level, or tectonics. The validity of this possible cause will be evaluated along with the possible allocyclic causes in reference to the second change in stratigraphic architecture at the end of this chapter.

Possible Allocyclic Causes

Eustatic Sea Level Controls

This change to fluvial and floodplain deposition records a base-level fall in the area of the Willow Creek anticline at the time these sediments were being deposited. In nonmarine areas, falling base level causes a lowering in the position of the groundwater table, resulting in better drained conditions that can eventually lead to the formation of paleosols, as well as to the reestablishment of fluvial systems in areas once occupied by lakes (Shanley and McCabe, 1994; Currie 1997). In marine strata, falling base level results in the formation of sequence boundaries as sea level begins to fall (Shanley and McCabe, 1994). Sequence boundaries, although always associated with sea level falls in

marine strata, are not often recorded in nonmarine strata, especially in areas proximal to thrust sheets (i.e. foredeep) (Posamentier and Allen, 1993). This is because areas such as the foredeep are undergoing a relatively continuous and high sedimentation rate, and as such are not likely to record depositional hiatuses (Posamentier and Allen, 1993). When sequence boundaries do form in foreland basin nonmarine strata, they are usually discontinuous and most likely to form in the distal areas of the foreland basin, away from the thrust front (often on the forebulge) (Posamentier and Allen, 1993). As a result, a sequence boundary developed in distal regions of a foreland basin may have a correlative conformity in more proximal parts of the basin.

The second change in stratigraphic architecture occurred sometime after deposition of the lacustrine interval which occurred after ~ 76.5 Ma and before 74.0 Ma (date of uppermost Two Medicine Formation near Horsethief transition (Rogers et al., 1993)). This timing therefore places this change in architecture either in the final stages of the Claggett Regression or in the initial stages of the Bearpaw Transgression (Figure 68). If the change occurred during the final stages of the Claggett Regression, then the baselevel fall recorded in Two Medicine Formation deposits at both the Willow Creek anticline and the type section would be consistent with a falling WIKS sea level. However, given the fact that the first change in architecture at both areas was tectonically controlled with no apparent sea level influence, it is most likely that the second change in architecture was also tectonically controlled. If the change in architecture occurred during the Bearpaw Transgression, then the base level fall recorded in Two Medicine Formation strata at both the Willow Creek anticline and at the type section is not

consistent with the rise in baselevel that a WIKS transgression would have produced. Again, there must have been a different, overriding control (tectonics) on baselevel in both of these areas in order to explain the change in stratigraphic architecture.

Tectonic Controls

Orogenic unloading associated with periods of tectonic quiescence is a tectonic mechanism that can initiate a base level fall (Catuneanu et al., 1999). During times of tectonic quiescence, the cessation of thrusting prevents no new material from being added to a thrust slab via shortening. At the same time isostatic rebound of the slab and erosion of the slab surface takes place, decreasing the amount of loading experienced by the slab, and resulting in a decrease in the amount of accommodation being created in the adjacent foreland basin (Catuneanu et al., 2002). As a consequence of the reduced accommodation, base level begins to fall (Figure 70, 72).

As mentioned previously in this chapter, the Lombard-Eldorado thrust slab was actively thrusting during the time of Two Medicine Formation deposition. The change in stratigraphic architecture recorded in Willow Creek anticline strata is interpreted to represent a base level fall associated with a period of tectonic quiescence in the Sevier thrust belt (Figure 21 in Appendix C). Movement on the LEH thrust slab to the west of the Willow Creek anticline and type section areas did not occur until approximately 74 Ma (Sears, 2001), therefore making the movement of the Lombard-Eldorado thrust the more important tectonic control on deposition with the foredeep prior to 74 Ma.

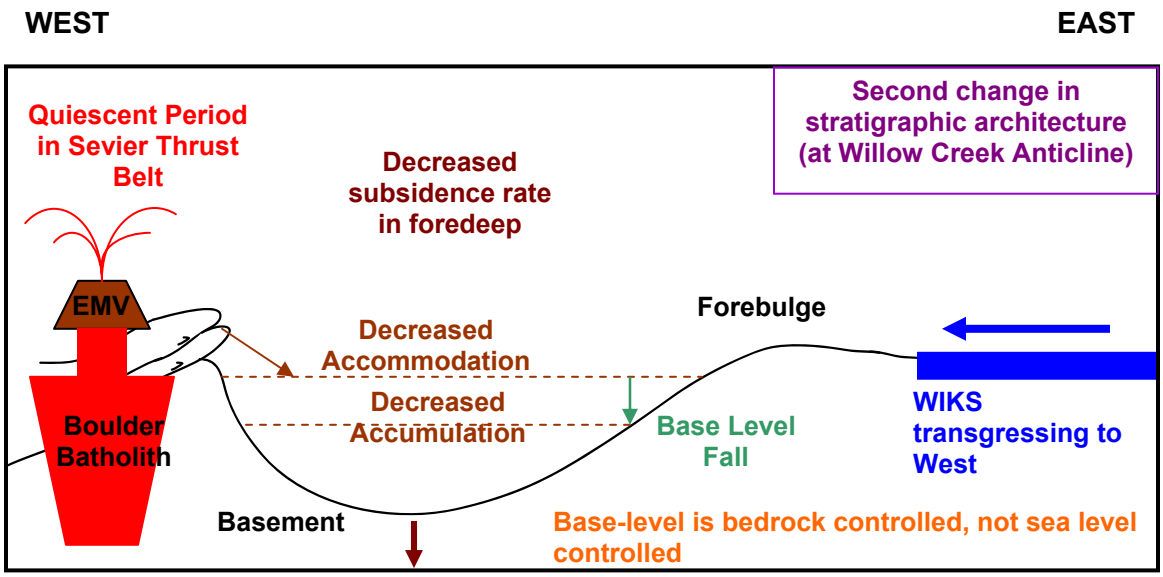

Figure 72: Cartoon cross section through Sevier Thrust Belt foreland basin. A period of quiescence in the Sevier thrust belt would have caused a decrease in the subsidence rate in the adjacent foreland basin. This would have caused a base level fall, which would have decreased accommodation, as well as caused the water table to fall during the time of the second change in stratigraphic architecture. Additionally during this time, the WIKS was transgressing to the west. Base-level is therefore bedrock controlled, not sea level controlled.

As stated in the previous section discussing the tectonic influence on the first change in stratigraphic architecture, the difference in age dates for the first change suggests that the area now known as the Willow Creek anticline generally responded to loading by the Boulder Batholith in the Helena Salient before the type section responded because of the former's closer proximity to the Helena Salient. It is therefore suggested that the second change in stratigraphic architecture may also have occurred at a slightly earlier time at the Willow Creek anticline, than at the Two Medicine Formation type section. This however cannot be confirmed at this time due to a lack of radiometric dates for this interval. All that can be said is that in both areas it occurred after the first change

in stratigraphic architecture and before ~74.1 Ma (the uppermost bentonite date of the Two Medicine Formation in northwestern Montana which occurs just before the deposits of the Bearpaw Transgression (Horsethief Sandstone and Bearpaw Shale) in this area.

Summary

The change in stratigraphic architecture recorded in Two Medicine type section and Willow Creek anticline strata is interpreted to be primarily a response to a period of quiescence in the Lombard-Eldorado thrust slab. This period of quiescence would have caused a reduction in accommodation and a related base level fall in the adjacent foreland basin that was manifested in a change in stratigraphic architecture in the foredeep in response. Also, this change occurred during the Claggett Regression or during the initial stages of the Bearpaw Transgression of the WIKS, when the WIKS western shoreline was moving eastward. It is unlikely that either the regression or transgression played a role in the architectural changes observed in the foredeep since base level controls of the foredeep are more likely to be a function of hinterland tectonics and bedrock base level controls on the forebulge. Finally, despite the initiation of cooling in ocean bottom waters, no major changes in global climate are recorded for the period of time in which this architectural change is observed, and as a result, climatic controls did not play an important role in causing the observed change in stratigraphic architecture. Further, as stated in the previous section discussing the tectonic influence on the first change in stratigraphic architecture, the difference in age dates for the first change suggests that the Willow Creek anticline generally responded to loading by the Boulder Batholith in the

Helena Salient before the type section responded because of the former's closer proximity to the Helena Salient. It is therefore suggested that the second change in stratigraphic architecture may also have occurred at a slightly earlier time at the Willow Creek anticline, than at the Two Medicine Formation type section. This however cannot be confirmed at this time due to a lack of radiometric dates for this interval. All that can be said is that in both areas it occurred after the first change in stratigraphic architecture and before ~74.1 Ma (the uppermost bentonite date of the Two Medicine Formation in northwestern Montana which occurs just before the deposits of the Bearpaw Transgression (Horsethief Sandstone and Bearpaw Shale) in this area.

Autocyclic Versus Allocyclic Causes

As previously stated, both autocyclic and allocyclic causes may be invoked to explain the changes in stratigraphic architecture present in the Two Medicine Formation at the Willow Creek anticline. However, while autocyclic processes were most likely operating at one scale, the two changes in stratigraphic architecture noted in this study were most likely due to allocyclic causes. Four factors that are not consistent with an autocyclic interpretation, but that support an allocyclic interpretation are: 1) the area's location in an actively deforming retroarc foreland basin in front of the Sevier thrust belt, 2) the change from overall oxidizing to overall reducing conditions found in the area suggesting a rising groundwater table through time, and 3) the scarcity of thick lacustrine deposits in other stratigraphic intervals of the Two Medicine Formation both at the Willow Creek anticline and in other areas, and 4) the presence of a lacustrine unit at

similar stratigraphic level and time unit in the Two Medicine Formation at the Two Medicine Formation type section.

CHAPTER 11

SIGNIFICANCE TO DINOSAUR PALEONTOLOGY

The Willow Creek anticline is famous for its paleontological findings relating to dinosaur embryos, juvenile dinosaurs, and dinosaur nesting behavior (e.g. Horner and Makela, 1979; Horner, 1982, 1983, and 1984; Horner and Weishampel, 1988; Hirsch and Quinn, 1990; Varricchio and Horner, 1993; Chin and Gill, 1996; Varricchio et al., 1999) (Figure 73). Consequently, it is an important site to put into a chronostratigraphically

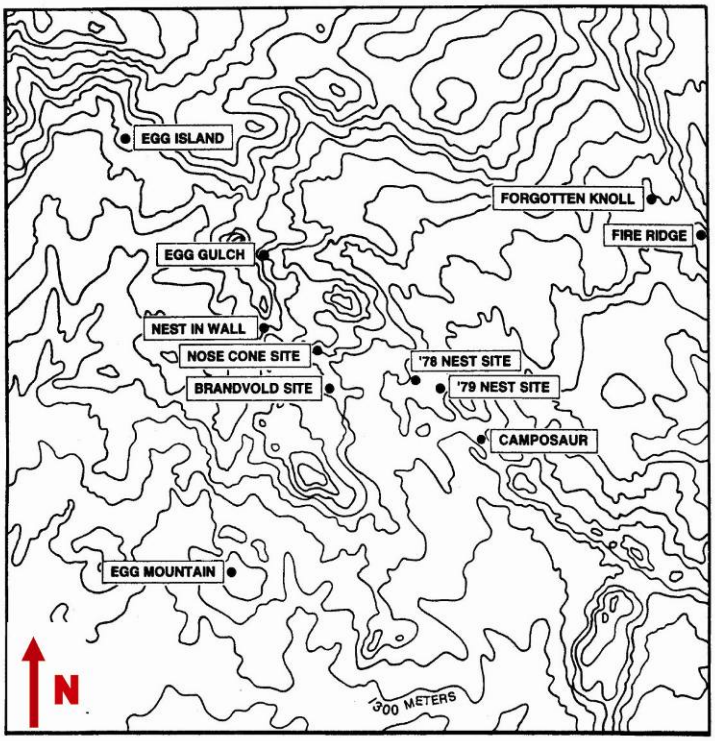

Figure 73: Location of dinosaur nests in the Egg Mountain area at the Willow Creek anticline near Choteau, MT. Map area = 10.4 km^2. Locations plotted on USGS Watson Flats 1:24,000 Quadrangle. (modified from Horner, 1988)

significant framework. The new U-Pb bentonite dates of 76.0 +/- 0.6 Ma and 77.0 +/- 0.7 Ma (average 76.5 Ma) for the Nose Cone bentonite (Appendix A), and 76.9 +/-0.5 Ma for the Justin's Peak bentonite (USGS Denver Argon Geochronology Laboratory) provide a relative age for these nests. While the eroded nature of the Willow Creek anticline makes it difficult to determine the exact stratigraphic distribution of dinosaur nests, the presence of the bentonite bed stratigraphically above the TM-003 bonebed provides a somewhat laterally traceable bed that can be used to separate nests of different ages. The Nest in the Wall, Egg Island, and Egg Mountain nest sites are located stratigraphically above both the bonebed and the dated bentonite, and are therefore younger than approximately 76.5 Ma (Figures 26, 27 in Appendices D, E). The '79 Nest Site is located between the Nose Cone bentonite and the Justin's Peak Nest Site and therefore is between 76.9 +/- 0.5 Ma and ~ 76.5 Ma (Figure 26 in Appendix D). The '78 Nest Site is located stratigraphically below the Justin's Peak bentonite, and is therefore older than 76.9 +/- 0.5 Ma (Figures 26, 27 in Appendices D, E). The Nose Cone, Branvold, and Camposaur sites (representing the TM-003 bonebed) can also be relatively dated as older than 76.5 Ma, but younger than 76.9 +/- 0.5 Ma (Figures 26, 27 in Appendices D, E).

The position of the '78 and '79 nest sites below the change in stratigraphic architecture from ephemeral, anastomosed fluvial and floodplain to lacustrine facies and of the Nest in the Wall nest site found above the change in stratigraphic architecture from lacustrine to ephemeral, anastomosed fluvial and floodplain places these nests within strata recording relatively lower accommodation as compared to the higher accommodation strata within which the Egg Island and Egg Mountain nest sites are

recorded (Figures 26, 27 in Appendices D, E). Although the lacustrine strata record the highest degree of accommodation for deposition of the Two Medicine in the area at this time, the lower accommodation strata were also deposited during a period of significant (albeit relatively less) accommodation due to the area's proximity to the Sevier trust blt. In addition, extensive preservation of the Nose Cone, Brandold, and Camposaur sites (TM-003 bonebed, an event bed of undetermined origin) (Figures 26, 27 in Appendices D, E) suggests that increasing accommodation in the area (due to loading in the Sevier Thrust Belt to the west) during this event may have played a significant role in its extensive preservation.

These findings are consistent with a study in the Hell Creek Formation of eastern Montana (Flight, 2004) in which exceptional dinosaur remains are found in strata reflecting higher accommodation rates. High accommodation rate is important in preserving dinosaur bones and nests because it increases the likelihood of their being preserved due rapid burial with less chance of sediment reworking. This is in contrast to periods of time characterized by increased erosion and sediment bypass due to lowest accommodation (Shanley and McCabe, 1994). As a result, if dinosaur material is found during times of extremely low accommodation, it is more likely to be disassociated and reworked (Rogers and Kidwell, 2000).

CHAPTER 12

SIGNIFICANCE TO THE MANSON IMPACT EVENT

Also present in Willow Creek anticline, is Museum of the Rockies dinosaur bonebed TM-003, which is comprised almost exclusively of hadrosaurid dinosaurs (Horner and Gorman, 1988). This bonebed is one of several present in the Two Medicine Formation of western Montana; however, it is anomalous in its mechanism of formation, as it is the only bonebed that has not been interpreted to be drought-induced (Rogers, 1990 and 1993; Varricchio and Horner, 1993). The questionable cause for the generation of this bonebed has led to many hypotheses regarding its origins (Lorenz, 1981; Schmitt et al., 1998). One interpretation that has been offered attempts to relate the Cretaceous Manson impact to the formation of the bonebed. The Manson impact event occurred approximately 74.1 +/- 0.1 Ma ($^{40}Ar/^{39}Ar$) when the eastern shore of the Cretaceous Western Interior Seaway was struck by a southeast approaching bolide approximately 2 km (1.2 mi) in diameter (Izett et al., 1993; Schultz and Anderson, 1996). The timing of this impact and the southeastern trajectory of the bolide have led to the hypothesis that an impact of this size might have generated a tsunami which could have traveled across the Western Interior Seaway and resulted in the formation of the bonebed following landfall on the western shores of the seaway. Among other attempts at possible correlation, present studies are attempting to trace and correlate an unconformity present in the Manson impact crater with discontinuities of the same age present along the inferred path of destruction caused by the meteorite impact (i.e. from Iowa northwest

to Montana). The presence of discontinuities in the Two Medicine Formation, and specifically in the Willow Creek anticline, is therefore important for use as chronological indicators in potentially correlating Montana discontinuities to the unconformity within the Manson impact crater.

The new U-Pb date from the bentonite located stratigraphically above the TM-003 bonebed constrains the bonebed age to older than approximately 76.5 Ma (Figures 40, 41 in Appendices D, E). This date suggests that the TM-003 bonebed is too old to be associated with the Manson impact, and that the impact event is more likely equivalent to a stratigraphically higher portion of the Two Medicine Formation, and possibly the base of the overlying Horsethief Sandstone.

CHAPTER 13

SUMMARY

The Upper Cretaceous Two Medicine Formation preserved at the Willow Creek anticline is characterized by two major changes in stratigraphic architecture. The first change from ephemeral, anastomosing fluvial and floodplain deposits to lacustrine deposits represents an increase in accommodation due to a relative base-level rise, and is interpreted to reflect the transition from a period of relatively lower accommodation to a period of higher accommodation. Based on a new U-Pb bentonite date, this change occurred no earlier than 76.5 Ma, and the 2.8 m (9.2 ft) of silty mudstone between the bentonite and the first lacustrine carbonates/mudstone deposit suggests that this change occurred later than 76.5 Ma.

This change is interpreted as a response primarily to loading in the Lombard-Eldorado thrust slab located to the southwest approximately 76-74 Ma. Additionally, this change occurred during the Claggett Regression of the WIKS, when the WIKS western shoreline was moving eastward. The change in stratigraphic architecture is therefore not interpreted to be related to a sea level change because the regression of the sea would have caused a base level fall, not a base level rise, as would be needed to produce lacustrine units. Additionally, despite interpreted initiation of cooling in ocean bottom waters (Huber et al., 2002), no major shifts in global climate are recorded for the period of time in which this architectural change is observed. In addition, no major shifts in regional climate occurred during this time (Gavin, 1986). As a result, climatic controls

are not interpreted to play an important role in causing the change in stratigraphic architecture. Further, both the change in stratigraphic architecture recorded at the Willow Creek anticline and the change in stratigraphic architecture observed across the upper discontinuity at the Two Medicine Formation type section are interpreted to reflect the same driving processes, and are further interpreted to be a consequence of the achievement of supercritical taper in the Lombard-Eldorado thrust slab between 76-74 Ma. However, the difference in available dates for these changes at the two areas (~75.4 Ma for type section and ~76.5 Ma for the Willow Creek anticline) suggest that these two areas responded to this loading at progressively different times. This is interpreted to reflect the fact that the loading occurred in the Helena Salient, which is located closer to the Willow Creek anticline area, and therefore affected this area first (that is, at an earlier date). Then the continued loading and its associated subsidence and stresses continued to propagate north through the foredeep, therefore not showing its effects at the Two Medicine Formation type section (located approximately 75 km (47 mi)) to the north of the Willow Creek anticline) until a later date.

The second change from lacustrine to ephemeral, anastomosing fluvial and floodplain deposits represents a decrease in the rate of accommodation creation and an associated relative base-level fall, and is interpreted to reflect the transition from a period of high accommodation to a period of relatively lower accommodation. The change is interpreted as a response primarily to a period of quiescence in the Lombard-Eldorado thrust slab. Also, this change occurred during the Claggett Regression or during the initial stages of the Bearpaw Transgression of the WIKS, when the WIKS western

shoreline was moving eastward. It is unlikely that either the regression or transgression played a role in the architectural changes observed in the foredeep since base level controls of the foredeep are more likely to be a function of hinterland tectonics and bedrock base level controls on the forebulge. Additionally, in regard to climate controls, there is no evidence to suspect any differences from those described for the first architectural change. Further, as stated in the previous section discussing the tectonic influence on the first change in stratigraphic architecture, the difference in age dates for the first change suggests that the Willow Creek anticline generally responded to loading in by the Boulder Batholith in the Helena Salient before the type section responded because of the former's closer proximity to the Helena Salient. It is therefore suggested that the second change in stratigraphic architecture may also have occurred at a slightly earlier time at the Willow Creek anticline, than at the Two Medicine Formation type section. This however cannot be confirmed at this time due to a lack of radiometric dates for this interval. All that can be said is that in both areas it occurred after the first change in stratigraphic architecture and before ~74.1 Ma (the uppermost bentonite date of the Two Medicine Formation in northwestern Montana which occurs just before the deposits of the Bearpaw Transgression (Horsethief Sandstone and Bearpaw Shale) in this area.

Correlation between the Willow Creek anticline and the Two Medicine Formation type section areas provides additional support for using nonmarine sequence stratigraphy to correlate strata within a Cretaceous nonmarine retroarc foreland basin. Dinosaur nests and the TM-003 bonebed at the Egg Mountain area of the Willow Creek anticline can now be relatively dated as older than 76.5 Ma ('78 and '79 nests and TM-003 bonebed)

and younger than 76.5 Ma (Nest in the Wall nest site and Egg Mountain and Egg Island). These nests and the bonebed were preserved during a period of generally high accommodation in which the lowermost and uppermost deposits record relatively lower accommodation (3 sites) with respect to the very high accommodation recorded by the middle lacustrine interval (2 sites). Increasing accommodation may have played a role in preserving the extensive TM-003 bonebed. The exceptional preservation of dinosaur embryos, juvenile dinosaurs, and dinosaur nests at the Willow Creek anticline may serve as another indicator of an accommodation increase in the area of the Willow Creek anticline during deposition of the Two Medicine Formation.

The new U-Pb date from the bentonite located stratigraphically above the TM-003 bonebed constrains the bonebed age to older than approximately 76.5 Ma (Figures 40, 41 in Appendices D, E). However, while this date suggests that the TM-003 bonebed is too old to be associated with the Manson impact, this bentonite was dated using the U-Pb shrimp method, while the Manson impact was dated using the $^{40}Ar/^{39}Ar$ methods, and as a result, these dates are not directly comparable because they were not dated using the same dating techniques. However, the new date of 76.5 Ma at the Willow Creek anticline does provide an initial step towards future work addressing the relationship of the TM-003 bonebed and the Cretaceous Manson impact. Future work is therefore needed to determine the cause and method of deposition for this bonebed.

REFERENCES CITED

Alonso-Zarza, A.M., Calvo, J.P., and M.A. Garcia del Cura, 1992, Palustrine sedimentation and associated features – grainification and pseudo-microkarst – in the Middle Miocene (Intermediate Unit) of the Madrid Basin, Spain: Sedimentary Geology, v. 76, p. 43-61.

Allen, P.A., Cabrera, L., Colombo, F., and A. Matter, 1983, Variations in fluvial style on the Eocene-Oligocene alluvial fan of the Scala Dei Group, SE Ebro Basin, Spain: Journal of the Geological Society of London, v. 140, p. 133-146.

Arthur, M.A., Dean, W.E., and S.O. Schlanger, 1985, Variations in the global carbon cycle during the Cretaceous related to climate, volcanism, and changes in atmospheric CO_2: *in* The Carbon cycle and atmospheric CO_2: variations Archean to present, Sundquist, E.T. and W.S. Broecker, eds.: Geophysical Monograph, v. 32, p. 504-529.

Barron, E.J., 1983, A warm, equable Cretaceous: the nature of the problem: Earth Science Reviews, v. 19, p. 305-338.

Barron, E.J. and W.M. Washington, 1984, The role of geographic variables in explaining paleoclimates; results from Cretaceous climate model sensitivity studies: Journal of Geophysical Research, v. 89, p. 1267-1279.

Barron, E.J., Peterson, W.H., Pollard, D., and S. Thompson, 1993, Past climate and the role of ocean heat transport; model simulations for the Cretaceous: Paleoceanography, v. 8, p. 785-798.

Berner, R.A., 1994, Enriched: GEOCARB II; A revised model of CO_2 over Phanerozoic time: American Journal of Science, v. 294, p. 56-91.

Blair, T.C., 1999, Sedimentary processes and facies on the waterlaid Anvil Spring Canyon alluvial fan, Death Valley, California: Sedimentology, v. 46, p. 913-940.

Blair, T.C., 2000, Sedimentology and progressive tectonic unconformities of the sheetflood-dominated Hell's Gate alluvial fan, Death Valley, California: Sedimentary Geology, v. 132, p. 233-262.

Blair, T. C. and W. L. Bilodeau, 1988, Development of tectonic cyclothems in rift, pull-apart, and foreland basins: Sedimentary response to episodic tectonism: Geology, v. 16, p. 517-520.

Bridge, J.S., and M.R. Leeder, 1979, A simulation model of alluvial stratigraphy: Sedimentology, v. 26, p. 599-623.

Boggs Jr., S., 2001, Principles of Sedimentology and Stratography Third Edition, Prentice Hall, 726p.

Catuneanu, O., Sweet, A.R., and A.D. Miall, 1999, Concept and styles of reciprocal stratigraphies: Western Canada foreland basin: Terra Nova, v. 11, p. 1-8.

Catuneanu, O., Sweet, A.R., and A.D. Miall, 2000, Reciprocal stratigraphy of the Campanian-Paleocene Western Interior of North America: Sedimentary Geology, v. 134, p. 235-255.

Chin, K. and B. D. Gill, 1996, Dinosaurs, dung beetles, and conifers: Participants in a Cretaceous food web: Palaios, v. 11, p. 280-285.

Cobban, W.A., 1955, Cretaceous rocks of northwestern Montana: Billings Geological Society, 6th Annual Field Conference Guidebook, p. 107-119.

Church, K. D., and Coe, A. L., 1988, Processes controlling relative sea-level change and sediment supply: *in* Coe, A. L. ed., The sedimentary record of sea-level change: Cambridge University Press, Cambridge, 288pp.

Collinson, J. D., 1996, Alluvial Sediments: *in* Reading, H. G., ed., Sedimentary Environments: Processes, Facies, and Stratigraphy: Blackwell Science, 688p.

Currie, B.S., 1997, Sequence stratigraphy of nonmarine Jurassic-Cretaceous rocks, central Cordilleran foreland-basin system: Geological Society of America Bulletin, v. 109, p. 1206-1222.

DeCelles, P.G., 2004, Late Jurassic to Eocene evolution of the Cordilleran thrust belt and foreland basin system, western U.S.A.: American Journal of Science, v. 304, p. 105-168.

DeConto, R.M., Brady, E.C., Bergengren, J., and W.W. Hay, 2000, Late Cretaceous climate, vegetation, and ocean interactions: *in* Huber, B.T., MacLeod, K.G., and S.L. Wing, eds., Warm climates in Earth history: p. 275-296.

Djamali, M., Soulie-Marsche, I., Esu, D., Gliozzi, E., and R. Okhravi, 2006, Palaeoenvironment of a Late Quaternary lacustrine-palustrine carbonate complex: Zarand Basin, Saveh, central Iran: Palaeogeography, Palaeoclimatology, Palaeoecology, v. 237, p. 315-334.

Dreyer, T., 1993, Quantified fluvial architecture in ephemeral stream deposits of the Esplugafreda Formation (Palaeocene), Tremp-Graus Basin, northern Spain:

Special Publication of the International Association of Sedimentologists, v. 17, p. 337-362.

Fagan, S.D. and G.C. Nanson, 2004, The morphology and formation of floodplain surface channels, Cooper Creek Australia: Geomorphology, v. 60, p. 107-126.

Flight, J. N., 2004, Sequence stratigraphic analysis of the Fox Hills and Hell Creek Formations (Maastrichtian), eastern Montana, and its relationship to dinosaur paleontology: M.S. Thesis, Montana State University, 148p.

Folk, R. L., 1962, Spectral subdivision of limestone types, in Ham, W. E. (ed.), Classification of carbonate rocks: American Association of Petroleum Geologists Memoir 1, p. 62-84.

Francis, J.E. and I. Poole, 2002, Cretaceous and early Tertiary climates of Antarctica: evidence from fossil wood: Palaeogeography, Palaeoclimatology, Palaeoecology, v. 182, p. 47-64.

Friend, P.F., 1983, Towards the field classification of alluvial architecture or sequence: *in* Collinson, J.D. and J. Lewin, eds., Modern and Ancient Fluvial Systems: Special Publication of the International Association of Sedimentologists 6, Blackwell, Oxford, p. 345-354.

Gavin, W., 1986, A paleoenvironmental reconstruction of the Cretaceous Willow Creek anticline dinosaur nesting locality: North Central Montana: M.S. Thesis, Montana State University, 148pp.

Gibling, M. R. and D. J. Bird, 1994, Late Carboniferous cyclothems and alluvial paleovalleys in the Sydney Basin, Nova Scotia: Geological Society of America Bulletin, v. 106, p. 105-117.

Gierlowski-Kordesch, E.H., 1998, Carbonate deposition in an ephemeral siliciclastic alluvial system: Jurassic Shuttle Meadow Formation, Newark Supergroup, Hartford Basin, USA: Palaeogeography, Palaeoclimatology, and Palaeoecology, v. 140, p. 161-184.

Gierlowski-Kordesch, E., Gomez, Fernandez, J.C., and N. Melendez, 1991, Carbonate and coal deposition in an alluvial-lacustrine setting: Lower Cretaceous (Weald) in the Iberian Range (east-central Spain): Special Publication of the International Association of Sedimentologists, v. 13, p. 109-125.

Gill, J. R. and W. A. Cobban, 1973, Stratigraphy and geologic history of the Montana Group and equivalent rocks, Montana, Wyoming, and North and South Dakota: U. S. Geological Survey, Professional Paper 776, 37 pp.

Grecula, M., Flint, S.S., Wickens, H.V., and S.D. Johnson, 2003, Upward-thickening patterns and lateral continuity of Permian sand-rich turbidite channel fills, Laingsburg Karoo, South Africa: Sedimentology, v. 50, p. 831-853.

Griffiths, P.G., Hereford, R., and R.H. Webb, 2006, Sediment yield and runoff frequency of small drainage basins in the Mojave Desert, U.S.A.: Geomorphology, v. 76, p. 232-244.

Hancock, J.M. and E.G. Kauffman, 1979, The great transgressions of the Late Cretaceous: Journal of the Geological Society of London, v. 136, p. 175-186.

Haq, B. U., Hardenbol, J., and P. R. Vail, 1987, Chronology of fluctuating sea levels since the Triassic: Science, v. 235, p. 1156-1167.

Hirsch, K. F. and B. Quinn, 1990, Eggs and eggshell from the Upper Cretaceous Two Medicine Formation of Montana: Journal of Vertebrate Paleontology, v. 10, p. 491-511.

Horner, J. R., 1982, Evidence of colonial nesting and site fidelity among ornithischian dinosaurs: Nature, v. 297, p. 675-676.

Horner, J. R., 1983, Cranial osteology and morphology of the type specimen of *Maiasaura peeblesorum* (Ornithischia: Hadrosauridae), with discussion of its phylogenetic position: Journal of Vertebrate Paleontology, v. 3, p. 29-38.

Horner, J. R., 1984, The nesting behavior of dinosaurs: Scientific American, v. 250, pp. 130-137.

Horner, J. R.,1988, Roadside geology field guide Bozeman to the Willow Creek anticline: Field Guide to the Two Medicine Formation and Willow Creek anticline of North Central Montana: Museum of the Rockies, Montana State University, 18pp.

Horner, J. R. and J. Gorman, 1988, Digging Dinosaurs. Harper Collins, New York, 210 pp.

Horner, J. R. and R. Makela, 1979, Nest of juveniles provides evidence of family structure among dinosaurs: Nature, v. 282, 296-298.

Horner, J. R. and D. B. Weishampel, 1988, A comparative embryological study of two ornithischian dinosaurs: Correction: Nature, v. 332, p. 256-257.

Huber, B.T., Norris, R.D., and K.G. MacLeod, 2002, Deep sea paleotemperature record of extreme warmth during the Cretaceous Period: Geology, v. 30, p. 123-126.

International Commission on Stratigraphy, 2004, International Stratigraphic Chart.

Izett, G. A., Cobban, W. A., Obradovich, M. J., and M. J. Kunk, 1993, The Manson impact structure: $^{40}Ar/^{39}Ar$ age and its distal impact ejecta in the Pierre Shale in southeastern South Dakota: Science, v. 262, p. 729-732.

Jeletzky, J.A., 1971, Marine Cretaceous biotic provinces and paleogeography of western and arctic Canada: Geological Survey of Canada Paper 70-22, 92p.

Jordan, T.E., 1981, Thrust loads and foreland basin evolution, Cretaceous, western United States: American Association of Petroleum Geologists, v. 65, p. 2506-2520.

Kauffman, E.G., 1977, Geological and biological overview: Western Interior Cretaceous Basin: The Mountain Geologist, v. 14, p. 75-99.

Khadkikar, A.S., Merh, S.S., Malik, L.S., and L.S. Chamyal, 1998, Calcretes in semi-arid alluvial systems: formative pathways and sinks: Sedimentary Geology, v. 116, p. 251-260.

King, J.T., 1997, Facies analysis of the Volcaniclastic Two Medicine Formation, Wolf Creek, Montana: M.S. Thesis, The University of Montana, 54p.

Knighton, A.D. and G.C. Nanson, 2000, Waterhole form and process in the anastomosing channel system of Cooper Creek, Australia: Geomorphology, v. 34, p. 101-117.

Knighton, A.D. and G.C. Nanson, 2001, An event-based approach to the hydrology of arid zone rivers in the Channel Country of Australia: Journal of Hydrology, v. 254, p. 102-123.

Knighton, A.D. and G.C. Nanson, 2002, Inbank and overbank velocity conditions in an arid zone anastomosing river: Hydrologic Processes, v. 16, p. 1771-1791.

Kraus, M.J., 1999, Paleosols in clastic sedimentary rocks: their geologic applications: Earth-Science Reviews, v. 47, p. 41-70.

LaBranche, J.V., 1999, Sedimentary deposits and processes of the Late Cretaceous Adel Mountain volcaniclastic apron, west-central Montana: M.S. Thesis, Montana State University – Bozeman, 115pp.

Lageson, D.R., Schmitt, J.G., Horton, B.K., Kalakay, T.J., and B.R. Burton, 2001, Influence of Late Cretaceous magmatism on the Sevier orogenic wedge, western Montana: Geology, v. 29, p. 723-726.

Legarreta, L., Uliana, M.A., Lorotonda, C.A., and G. R. Meconi, 1993, Approaches to nonmarine sequence stratigraphy – theoretical models and examples from Argentine basins: Proceedings of Institut Francais du Petrole, Conference on Exploration and Production: Subsurface Reservoir Characterization from Surface Observations, April 12-17, 1992, Scarborough, England. Publ. IFP, Technip, p. 125-143.

Lerbekmo, J.F., 1963, Petrology of the Belly River Formation, southern Alberta Foothills: Sedimentology, v. p. 54-86.

Lillegraven, J.A. and L.M. Ostresh, Jr., 1990, Late Cretaceous (earliest Campanian/Maastrichtian) evolution of western shorelines of the North American Western Interior Seaway in relation to known mammalian faunas: *in* Bown, T.M. and K.D. Rose, eds., Dawn of the Age of Mammals in the northern part of the Rocky Mountain Interior, North America: Geological Society of America Special Paper 243, p. 1-30.

Lomas, S.A., 1999, A Lower Cretaceous clastic slope succession, Livingston Island, Antarctica: sand-body characteristics, depositional processes and implications for slope apron depositional models: Sedimentology: v. 46, p. 477-504.

Lorenz, J. C., 1981, Sedimentary and tectonic history of the Two Medicine Formation, Late Cretaceous (Campanian), northwestern Montana: Ph.D. Thesis, Princeton University, 215pp.

Lorenz, J. C. and W. Gavin, 1984, Geology of the Two Medicine Formation and the sedimentology of a dinosaur nesting ground: Montana Geological Society 1984 Field Conference Guidebook: 175-186.

Mabutt, J.A., 1977, Desert Landforms, MIT Press, Cambridge, 340 pp.

MacLeod, K.G. and B.T. Huber, 1996, Reorganization of deep ocean circulation accompanying a Late Cretaceous extinction event: Nature, v. 380, p. 422-425.

Makaske, B., 2001, Anastomosing rivers: a review of their classification, origin, and sedimentary products: Earth-Science Reviews, v. 53, p.149-196.

Martinson, V.S., Heller, P.L., and W.E. Frerichs, 1998, Distinguishing middle Late Cretaceous tectonic events from regional sea-level change using foraminiferal data from the U.S. Western Interior: Geological Society of America Bulletin, v. 110, p. 259-268.

Martin, A. J., 2001, Evidence for insect nesting and its paleoenvironmental significance in the Two Medicine Formation (Late Cretaceous), Choteau, Montana: PaleoBios, v. 21, p. 88.

McLean, J. R. and T. Jerzykiewicz, 1978, Cyclicity, tectonics and coal, : some aspects of fluvial sedimentology: *in* the Brazeau-Paskapoo formations, Coal Valley area, Alberta, Canada, *in* Miall, A. D., ed., Fluvial sedimentology: Canadian Society of Petroleum Geologists, Memoir 5, p. 441-468.

Melchor, R.N., Bedatou, E., de Valais, S., and J.F. Genise, 2006, Lithofacies distribution of invertebrate and vertebrate trace-fossil assemblages in an Early Mesozoic ephemeral fluvio-lacustrine system from Agentina: Implications for the Scoyenia ichnofacies: Palaeogeography, Palaeoclimatology, Palaeoecology, v. 239, p. 253-285.

Miall, A. D., 1996, The Geology of Fluvial Deposits: Sedimentary facies, basin analysis, and petroleum geology: New York: Springer.

Miggins, D., USGS Denver Geochronology Laboratory, personal communication, 24 October 2006.

Mollard, J.D., 1973, Airphoto interpretation of fluvial features: *in* Fluvial Processes and Sedimentation: Proceedings of the Hydrological Symposium, Natural Resources Council of Canada, p. 341-380.

Munsell Soil Color Chart, 2000, GretagMacbeth, New York.

Nadon, G. C., 1994, The genesis and recognition of anastomosed fluvial deposits; data from the St. Mary River Formation, Southwestern Alberta, Canada: Journal of Sedimentary Research, Section B, v. 64, 451-463.

Nanson, C.G., Rust, B.R., and G. Taylor, 1986, Coexistant mud braids and anastomosing channels in an arid-zone river: Cooper Creek, central Australia: Geology v. 14, p. 175-178.

Olsen, H., 1989, Sandstone-body architectures and ephemeral stream processes in the Dinosaur Canyon Member, Moenave Formation (Lower Jurassic), Utah, U.S.A.: Sedimentary Geology, v. 61, p. 207-221.

Olsen, T., Steel, R., Hogseth, K., Skar, T., and S.L. Roe, 1995, Sequential architecture in a fluvial succession: Sequence stratigraphy in the Upper Cretaceous Mesaverde Group, Price Canyon, Utah: Journal of Sedimentary Research, V. B65, p. 265-280.

Peck, R. E., 1957, North American Mesozoic Charophyta: U.S. Geological Survey Professional Paper 249-A, 44pp.

Picard, M.D. and L.R. High Jr., 1973, Sedimentary Structures of Ephemeral Streams: Developments in Sedimentology 17, Elsevier, Amsterdam, 223 pp.

Pimentel, N.L., Wright, V.P., and T.M. Azevedo, 1996, Distinguishing early groundwater alteration effects from pedogenesis in ancient alluvial basins: examples from the Palaeogene of southern Portugal: Sedimentary Geology, v. 105, p. 1-10.

PiPujol, M.D. and P. Buurman, 1994, The distinction between ground-water gley and surface-water gley phenomena in Tertiary paleosols of the Ebro basin, NE Spain: Palaeogeography, Palaeoclimatology, Palaeoecology, v. 110, p. 103-113.

Posamentier, H. W., Jervey, M. T., and P. R. Vail, 1988, Eustatic controls on clastic deposition I – Conceptual framework: Society of Economic Paleontologists and Mineralogists Special Publication 42, p. 109-124.

Posamentier, H. W. and G. R. Allen, 1993, Siliciclastic sequence stratigraphic patterns in foreland ramp-type basins: Geology, v. 21, p. 455-458.

Rahn, P.H., 1967, Sheetfloods, streamfloods, and the formation of sediments: Annals of the American Association of Geography, v. 57, p. 593-604.

Retallack, G. J., 1990, Soils of the Past: An introduction to paleopedology, Unwin Hyman, 520pp.

Roberts, A. E., 1972, Cretaceous and early Tertiary depositional and tectonic history of the Livingston area, southwestern Montana: U.S. Geological Survey Professional Paper 526-C, 120pp.

Roberts, E. M., 1999, Sedimentology, taphonomy, and alluvial sequence stratigraphy of the Lower Two Medicine Formation (Campanian) near Choteau, Montana: M.S. Thesis, The University of Montana, 80 pp.

Rogers, R. R., 1990, Taphonomy of three dinosaur bone beds in the Upper Cretaceous Two Medicine Formation of northwestern Montana: Evidence for drought-related mortality: Palaios, v. 5, p. 394-413.

Rogers, R. R., 1993, Systemic patterns of time-averaging in the terrestrial vertebrate record: a Cretaceous case study. i*n* Kidwell, S. M. and A. K. Behrensmeyer, eds., Taphonomic approaches to time resolution in fossil assemblages, Paleontological Society Short Courses Paleontology, v. 6, p. 228-249.

Rogers, R. R., 1994, Nature and origin of through-going discontinuities in nonmarine foreland basin strata, Upper Cretaceous, Montana: Implications for sequence analysis: Geology, v. 22, p. 1119-1122.

Rogers, R. R., 1995, Sequence stratigraphy and vertebrate taphonomy of the Upper Cretaceous Two Medicine and Judith River Formations, Montana: Ph.D. Thesis, 400 pp.

Rogers, R. R., 1998, Sequence analysis of the Upper Cretaceous Two Medicine and Judith River Formations, Montana: Nonmarine response to the Claggett and Bearpaw marine cycles: Journal of Sedimentary Research, v. 68, p. 615-631.

Rogers, R.R., Swisher III, C.C., and J.R. Horner, 1993, 40Ar/39Ar age correlation of the nonmarine Two Medicine Formation (Upper Cretaceous), northwestern Montana, U.S.A.: Canadian Journal of Earth Science, v. 30, p. 1066-1075.

Rogers, R. R. and S. M. Kidwell, 2000, Association of vertebrate skeletal concentrations and discontinuity surfaces in terrestrial and shallow marine records: A test in the Cretaceous of Montana: The Journal of Geology, v. 108, p. 131-154.

Rust, B.R., 1981, Sedimentation in an arid-zone anastomosing fluvial system: Cooper's Creek, central Australia: Journal of Sedimentary Petrology, v. 51, p. 745-755.

Sanz, M.E., Alonso-Zarza, A.M., and J.P. Calvo, 1995, Carbonate pond deposits related to semi-arid alluvial systems: examples from the Tertiary Madrid Basin, Spain: Sedimentology: v. 42, p. 437-452.

Schmitt, J. G., Horner, J. R., Laws, R. R., and F. Jackson, 1998, Debris-flow deposition of a hadrosaur-bearing bone bed, Upper Cretaceous Two Medicine Formation, Northwest Montana: Journal of Vertebrate Paleontology v. 18 (Supp 3), 76A.

Schultz, P. H. and R. R. Anderson, 1996, Asymmetry of the Manson impact structure: Evidence for impact angle and direction: Geological Society of America Special Paper 302, p. 397-417.

Schumm, S. A., 1993, River Response to baselevel change: Implications for sequence stratigraphy: The Journal of Geology, v. 101, p. 279-294.

Schumm, S.A., Erskine, W.D., and J.W. Tilleard, 1996, Morphology, hydrology, and evolution of the anastomosing Ovens and King Rivers, Victoria, Australia: Geological Society of America Bulletin, v. 108, p. 1212-1224.

Schumann, R.R., 1989, Morphology of Red Creek Wyoming, an arid region anastomosing channel system: Earth Surface Processes and Landforms, v. 14, p. 277-288.

Sears, J.W., 2001, Emplacement and denudation history of the Lewis-Eldorado-Hoadley thrust slab in the northern Montana Cordillera, USA: Implications for steady-state orogenic processes: American Journal of Science, v. 301, p. 359-373.

Semeniuk, V. and T.D. Meagher, 1981, The geomorphology and surface processes of the Australind-Leschenault Inlet coastal area: Journal of the Royal Society of Australia, v. 64, p. 33-51.

Shanely, K. W. and P. J. McCabe, 1989, Sequence-stratigraphic relationships and facies architecture of Turinian-Campanian strata, Kaiparowits Plateau, south-central Utah: American Association of Petroleum Geologists Bulletin, v. 73, p. 410-411.

Shanely, K. W. and P. J. McCabe, 1991, Predicting facies architecture through sequence stratigraphy – An example from the Kaiparowits Plateau, Utah: Geology, v. 19, p. 742-745.

Shanely, K. W. and P. J. McCabe, 1993, Alluvial architecture in a sequence stratigraphic framework: A case history from the Upper Cretaceous of southern Utah, USA, *in* Flint, S. and I. Bryant, eds., Quantitative modeling of clastic hydrocarbon reservoirs and outcrop analogues: International Association pf Sedimentologists Special Publication 15, p. 21-55.

Shanely, K. W. and P. J. McCabe, 1994, Perspectives on the sequence stratigraphy of continental strata: American Association of Petroleum Geologists Bulletin, v. 4, p. 544-568.

Smith, D.G., 1973, Aggradation of the Alexandra-North Saskatchewan River, Banff Park, Alberta: in M. Morisawa, ed., Fluvial Geomorphology: Proceedings of the 4th Annual Geomorphology Symposium, Binghampton, p. 201-219.

Smith, D.G., 1983, Anastomosed fluvial deposits, modern examples from western Canada: *in* Collinson, J.D. and J. Lewin, eds., Modern and Ancient Fluvial Systems: International Association of Sedimentologists Special Publication v. 6, p. 155-168.

Smith, D.G., 1986, Anastomosing river deposits, sedimentation rates and basin subsidence, Magdelena River, Northwestern Colombia, South America: Sedimentary Geology, v. 46, p. 177-196.

Smith, A. E., 1998, Volcanism and associated sedimentation in a retroarc foreland basin: the Upper Cretaceous Two Medicine Formation of west-central Montana: M.S. Thesis, Montana State University, 170pp.

Smith, D.G. and P.E. Putnam, 1980, Anastomosed river deposits: modern and ancient examples in Alberta, Canada: Canadian Journal of Earth Sciences, v. 17, p. 1396-1406.

Smith, D.G. and N.D. Smith, 1980, Sedimentation in anastomosed river systems: examples from alluvial valleys near Banff, Alberta: Journal of Sedimentary Petrology, v. 50, p. 157-164.

Smith, D.G., Cross, T.A., Dufficy, J.P., and S.R. Clough, 1989, Anatomy of an avulsion: Sedimentology, v. 36, p. 1-23.

Smith, N.D., McCarthy, T.S., Ellery, W.N., Merry C.L., and H. Ruther, 1997, Avulsion and anastomosis in the panhandle region Okavango Fan, Bostwana: Geomorphology, v. 20, p. 49-65.

Southard, J.B. and L.A. Boguchwal, 1990, Bed configurations in steady unidirectional water flows. Part 2 Synthesis of flume data: Journal of Sedimentary Petrology, v. 60, p. 658-673.

Spalletti, L.A., and F.C. Pinol, 2005, From alluvial fan to playa: an Upper Jurassic ephemeral fluvial system, Neuquen Basin, Argentina: Gondwana Research, v. 8, p. 363-383.

Stear, W.M., 1983, Morphological characteristics of ephemeral stream channel and overbank splay sandstone bodies in the Permian Lower Beaufort Group, Karoo Basin, South Africa: *in* Collinson, J.D. and J. Lewin eds., Modern and Ancient Fluvial Systems: Special Publications of the International Association of Sedimentologists, Blackwell Scientific Publications, Oxford.

Stebinger, E., 1914, The Montana Group of northwestern Montana: U.S. Geological Survey Professional Paper 90-G, p. 61-68.

Stebinger, E., 1916, Geology and coal resources of northern Teton County, Montana: U.S. Geological Survey Bulletin 621-K, p. 117-156.

Stebinger, E., 1917, Stratigraphy of the Two Medicine Formation: *in* Gilmore, C.W. Brachyceratops, a Cerotopsian dinosaur from the Two Medicine Formation of Montana, with notes on associated fossil reptiles: U.S. Geological Survey Professional Paper 103, p. 1-3.

Talbot, M. R. and P. A. Allen, 1996, Lakes: *in* Reading, H. G., ed., Sedimentary Environments: Processes, Facies, and Stratigraphy: Blackwell Science, 688p.

Tandon, S.K., Sareen, B.K., Someshwar Rao, M., and A.K. Singhvi, 1997, Aggradation history and luminescence chronology of Late Quaternary semi-arid sequences of the Sabarmati basin, Gujarat, Western India: Palaeogeography, Palaeoclimatology, Palaeoecology, v. 128, p. 339-357.

Tanner, L.H., 2000, Palustrine-lacustrine and alluvial facies of the (Norian) Owl Creek Formation (Chinle Group), Four Corners Region, southwestern U.S.A.: implications for Late Triassic paleoclimate: Journal of Sedimentary Research, v. 70, p. 1280-1289.

Vail, P. R., 1987, Seismic Stratigraphy interpretation using sequence stratigraphy; Part 1, Seismic stratigraphy interpretation procedure: *in* Bally, A. W. ed., Atlas of Seismic Stratigraphy: American Association of Petroleum Geologists Studies in Geology 27, p. 1-10.

Vail, P. R., Mitchum, R. M., Todd Jr., R. G., Widmier, J. M., Thompson, S., Sangree III, J. B., Bubb, J. N., and W. G., Hatlelid, 1977, Siesmic stratigraphy and global changes of sea level, *in* Clayton, C. E. ed., Seismic stratigraphy – Applications to hydrocarbon exploration: American Association of Petroleum Geologists Memoir 26, Tulsa, Oklahoma, p. 49-212.

Valdes, P.J., 2000, Warm climate forcing mechanisms: *in* Warm climates in Earth history, Huber, B.T., MacLeod K.G., and S.L. Wing, eds.: p. 3-20.

Valero Garces, B. L., Gierdowski-Kordesch, E., and W. A. Bragonier, 1997, Pennsylvanian continental cyclothem development: No evidence of direct climatic control in the Upper Freeport Formation (Allegheny Group) of Pennsylvania (northern Appalachian Basin: Sedimentary Geology, v. 109, p. 305-319.

Van Wagoner, J. C., 1995, Sequence stratigraphy and marine to nonmarine facies architecture of foreland basin strata. Book Cliffs Utah, USA., *in* Van Wagoner, J. C. and G. T. Bertram, eds., Sequence stratigraphy of foreland basin deposits: American Association of Petroleum Geologists Memoir 64, p. 137-223.

Van Wagoner, J. C., Posamentier, H. W., Mitchum, R. M., Vail, P. R., Sarg, J. F. Loutit, T. S., and J. Hardenbol, 1988, An overview of the fundamentals of sequence stratigraphy and key definitions: Society of Economic Paleontologists and Mineralogists Special Publication 42, p. 39-45.

Varricchio, D. J. and J. R. Horner, 1993, Hadrosaurid and lambeosaruid bone beds from the Upper Cretaceous Two Medicine Formation of Montana: Taphonomic and biologic implications: Canadian Journal of Earth Sciences, v. 30, p. 997-1006.

Varricchio, D. J., Jackson, F., and C. N. Trueman, 1999, A nesting trace with eggs for the Cretaceous theropod dinosaur *Troodon formosus*: Journal of Vertebrate Paleontology, v. 19, p. 91-100.

Viele, G.W. and F.G. Harris III, 1965, Montana Group stratigraphy, Lewis and Clark County, Montana: American Association of Petroleum Geologists Bulletin, v. 49, p. 379-417.

Wescott, W. A., 1993, Geomorphic thresholds and complex response of fluvial systems – Some implications for sequence stratigraphy: American Association of Petroleum Geologists Bulletin, v. 77, p. 1208-1218.

Wright, V.P. and M.E. Tucker, 1991, Calcretes: an introduction, *in* Wright, V.P. and M.E. Tucker eds., Calcretes: International Association of Sedimentologists, Reprint Series 2, p. 1-22.

Wright, V. P. and S. B. Marriott, 1993, The sequence stratigraphy of fluvial depositional systems: The role of floodplain sediment storage: Sedimentary Geology, v. 86, p. 203-210.

APPENDICES

APPENDIX A

WILLOW CREEK ANTICLINE MEASURED SECTIONS

LOCATIONS

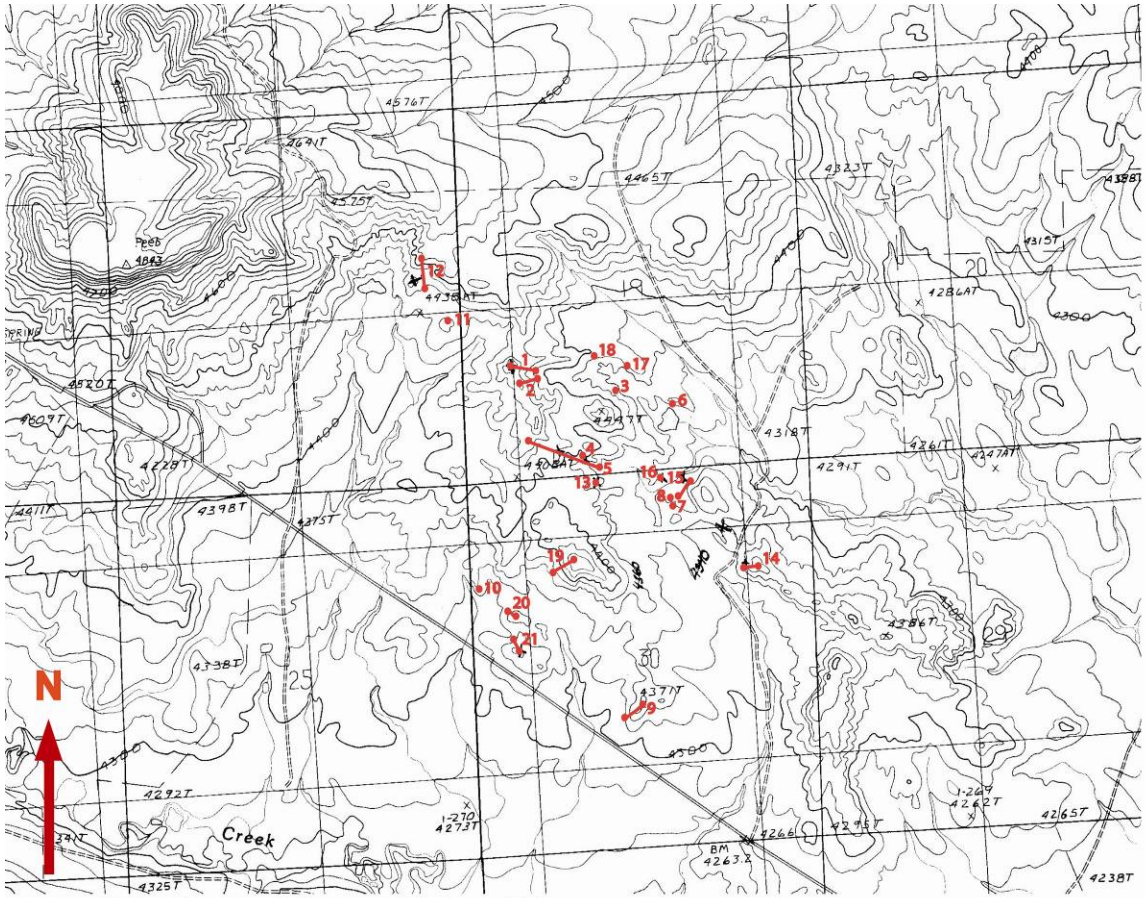

Willow Creek anticline near Choteau, MT
Blow-up of central portion of Watson Flats, MT Quadrangle
Scale 1:24,000
* Measured Sections shown in red

1: Thunder Dome
2: T.D. Bentonite
3: Pete's Pupa Peninsula
4: Nose Cone 2
5: Nest in the Wall Bentonite
6: Lake Giardia
7: Justin's Peak
8: Josh's Hill
9: Jess Butte
10: Frans Site
11: Egg Island
12: Flaming Cliffs
13: Branvold Site
14: Children's Dig
15: '78 Nest
16: '79 Nest
17: Fault Mountain 1
18: Fault Mountain 2
19: Egg Mountain C
20: Egg Mountain B
21: Egg Mountain A

KEY

- Clay/ Mudstone/ Silty Mudstone
- Siltstone
- Sandstone
- Trough Cross-Bedded Sandstone
- Charophytiferous Limestone
- Groundwater Carbonate
- Bentonite Bed
- Pedogenic Carbonate Layer

- Parallel Lamination/ Bedding
- Wave Ripple Lamination
- Interfingering Layer
- Pedogenic Carbonate Nodule
- Mudstone Rip-up Clasts
- Siltstone/ Sandstone Clasts
- Pupal Case Casts
- Root Traces
- Burrows
- Organics
- Seed Casts

- Vertebrate Fossils
- Invertebrate Fossils
- Egg Shell
- Charophyte Fossils

CL Clay-size Particles

SI Silt-sized Particles

VF Very Fine-grained Sandstone

F Fine-grained Sandstone

M Medium-grained Sandstone

C Coarse-grained Sandstone

Bed Contacts:

- Sharp, Planar
- Sharp, Irregular Erosional
- Gradational

Lithofacies:

B	Bentonite layer
C	Light grey, well-indurated carbonate
Fm	Massive mudstone, siltstone
Fmc	Carbonate-rich, color mottled massive mudstone
Fl	Laminated sandstone, siltstone, and mudstone
Lc	Charophytiferous limestone
P	Nodular to discontinuously-bedded oxidized carbonate
Sh	Horizontally-bedded sandstone
Sm	Massive, structureless sandstone
Sp	Carbonate cemented sandstone with pupal cases
Sr	Ripple cross-laminated sandstone
St	Trough cross-bedded sandstone

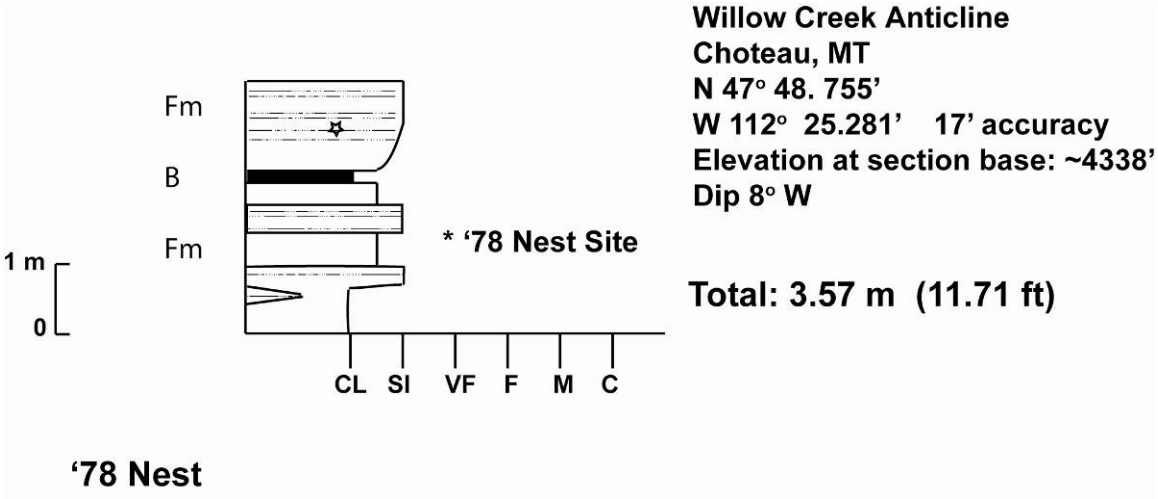
Willow Creek Anticline
Choteau, MT
N 47° 48. 755'
W 112° 25.281' 17' accuracy
Elevation at section base: ~4338'
Dip 8° W
Fm
B
Fm
* '78 Nest Site
Total: 3.57 m (11.71 ft)
1 m
0
CL SI VF F M C
'78 Nest

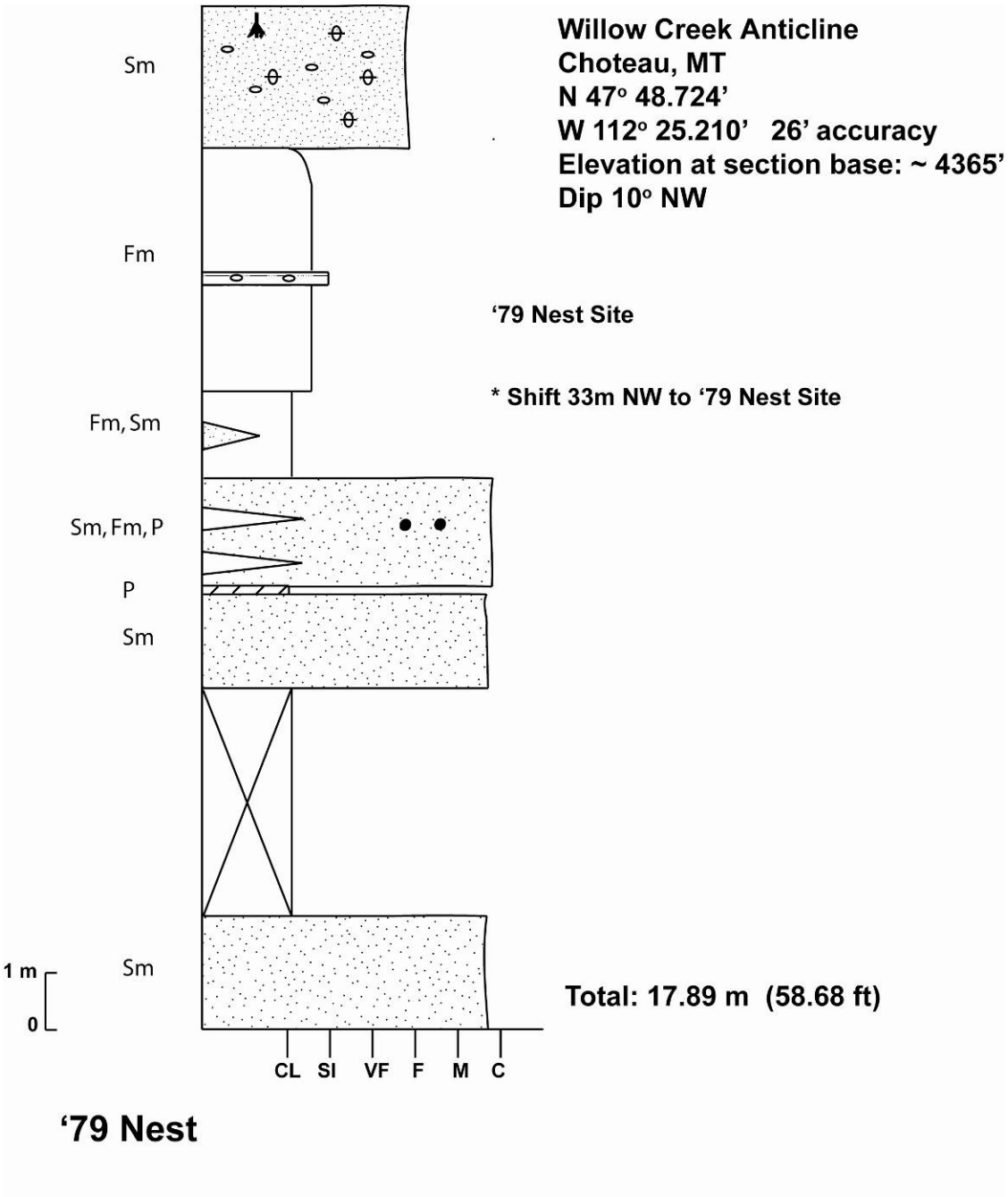
Willow Creek Anticline
Choteau, MT
N 47° 48.724'
W 112° 25.210' 26' accuracy
Elevation at section base: ~ 4365'
Dip 10° NW
'79 Nest Site
* Shift 33m NW to '79 Nest Site
Sm
Fm
Fm, Sm
Sm, Fm, P
P
Sm
Sm
1 m
0
Total: 17.89 m (58.68 ft)
CL SI VF F M C
'79 Nest

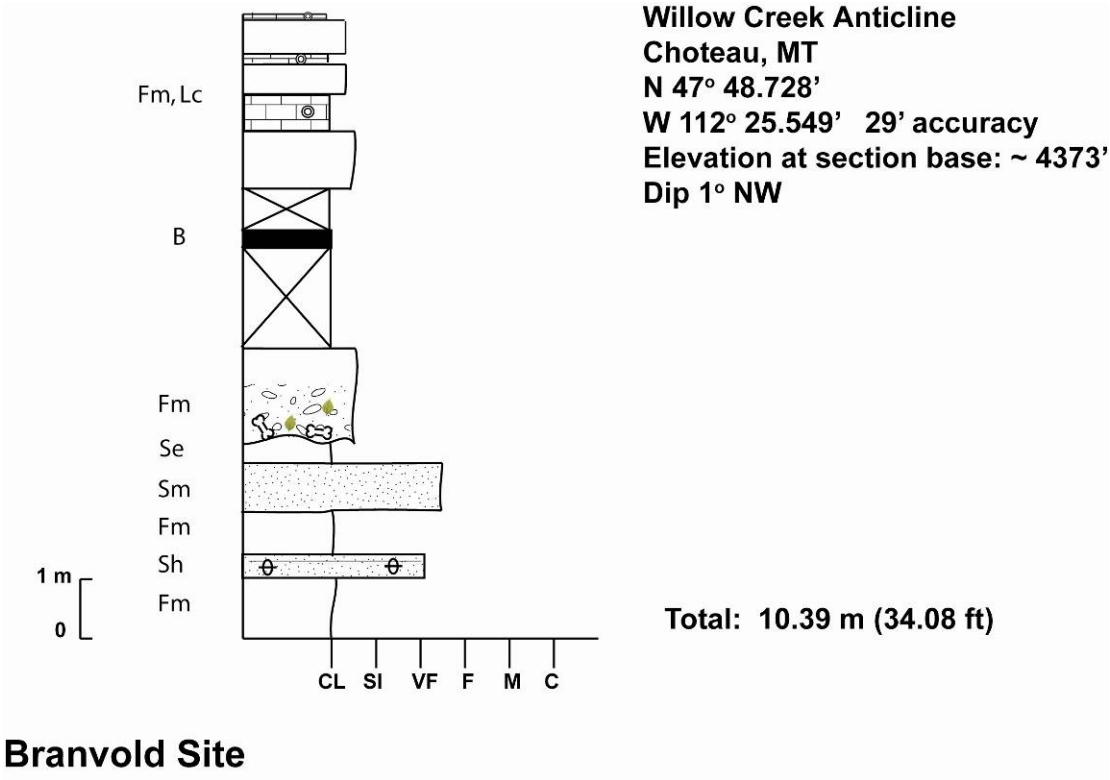
Willow Creek Anticline
Choteau, MT
N 47° 48.728'
W 112° 25.549' 29' accuracy
Elevation at section base: ~ 4373'
Dip 1° NW
Fm, Lc
B
Fm
Se
Sm
Fm
Sh
Fm
1 m
0
CL SI VF F M C
Total: 10.39 m (34.08 ft)
Branvold Site

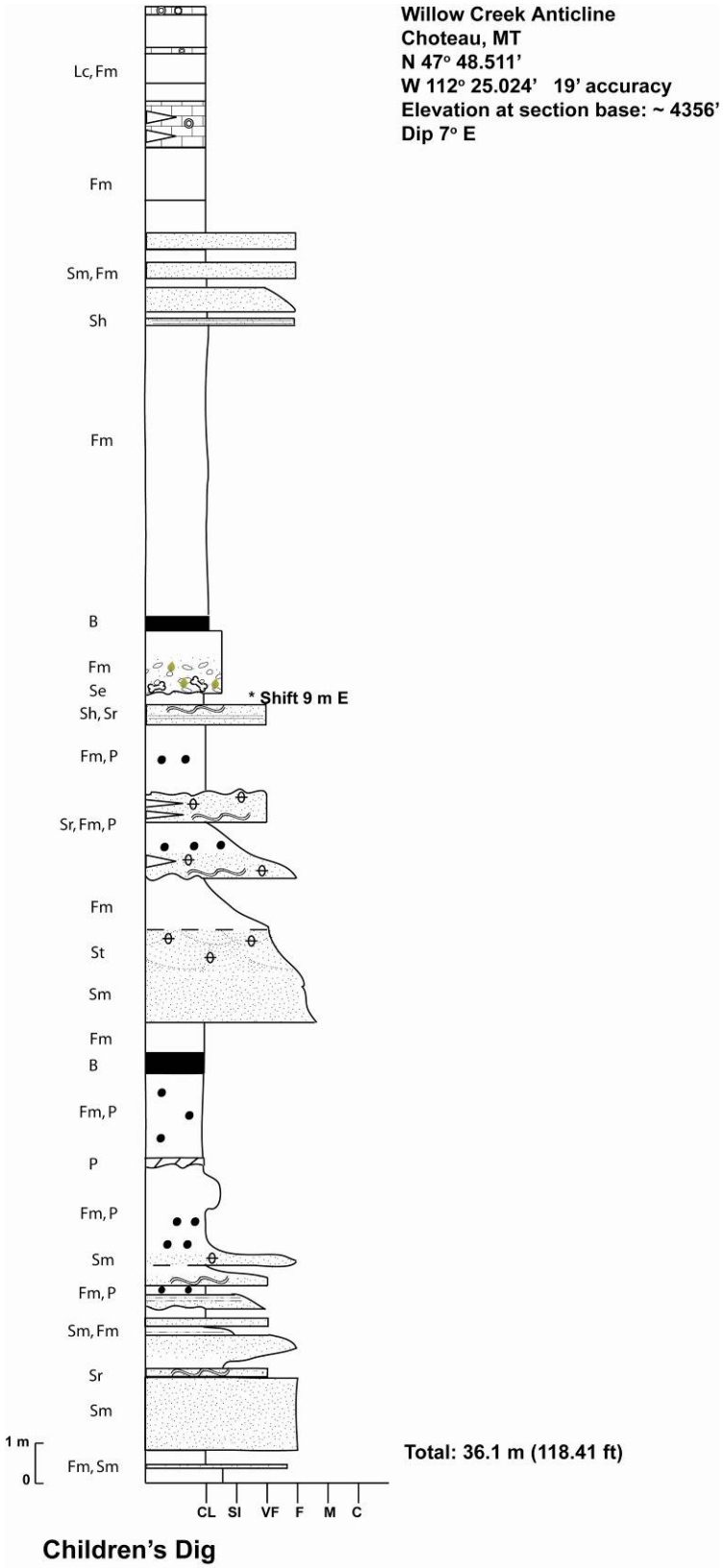
Willow Creek Anticline
Choteau, MT
N 47° 48.511'
W 112° 25.024' 19' accuracy
Elevation at section base: ~ 4356'
Dip 7° E
Lc, Fm
Fm
Sm, Fm
Sh
Fm
B
Fm
Se
Sh, Sr
* Shift 9 m E
Fm, P
Sr, Fm, P
Fm
St
Sm
Fm
B
Fm, P
P
Fm, P
Sm
Fm, P
Sm, Fm
Sr
Sm
Fm, Sm
1 m
0
Total: 36.1 m (118.41 ft)
CL SI VF F M C
Children's Dig

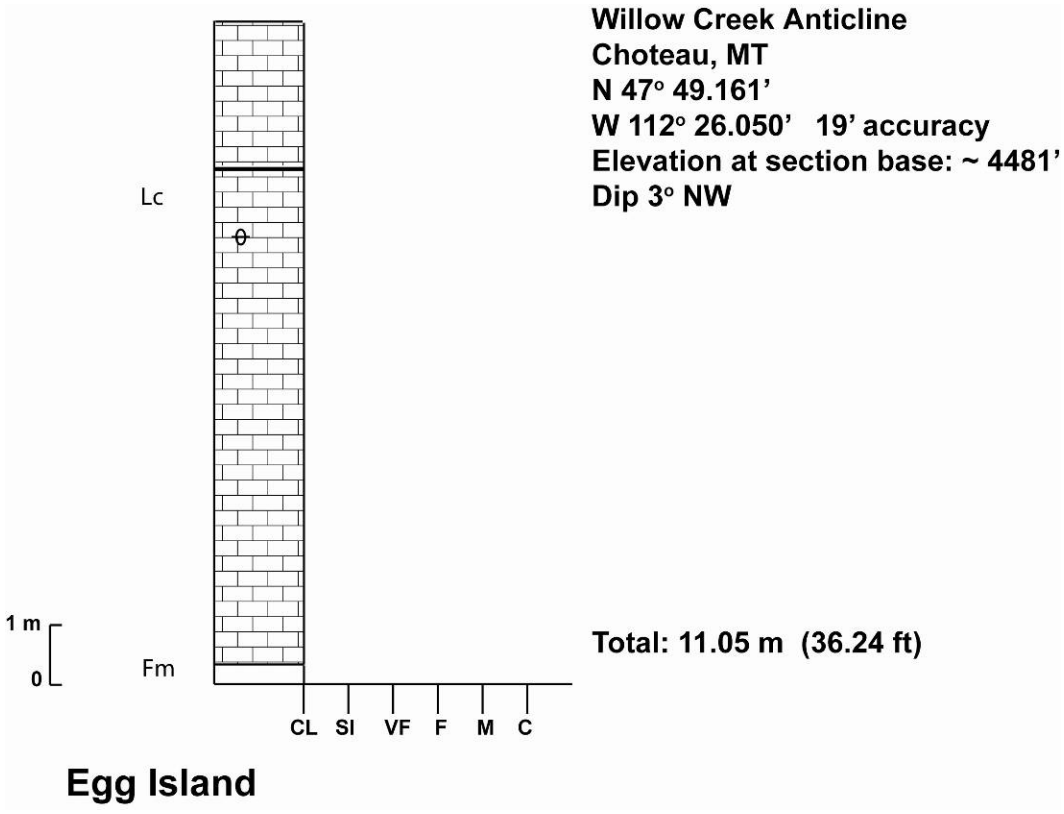
Willow Creek Anticline
Choteau, MT
N 47° 49.161'
W 112° 26.050' 19' accuracy
Elevation at section base: ~ 4481'
Dip 3° NW
Lc
Fm
1 m
0
Total: 11.05 m (36.24 ft)
CL SI VF F M C
Egg Island

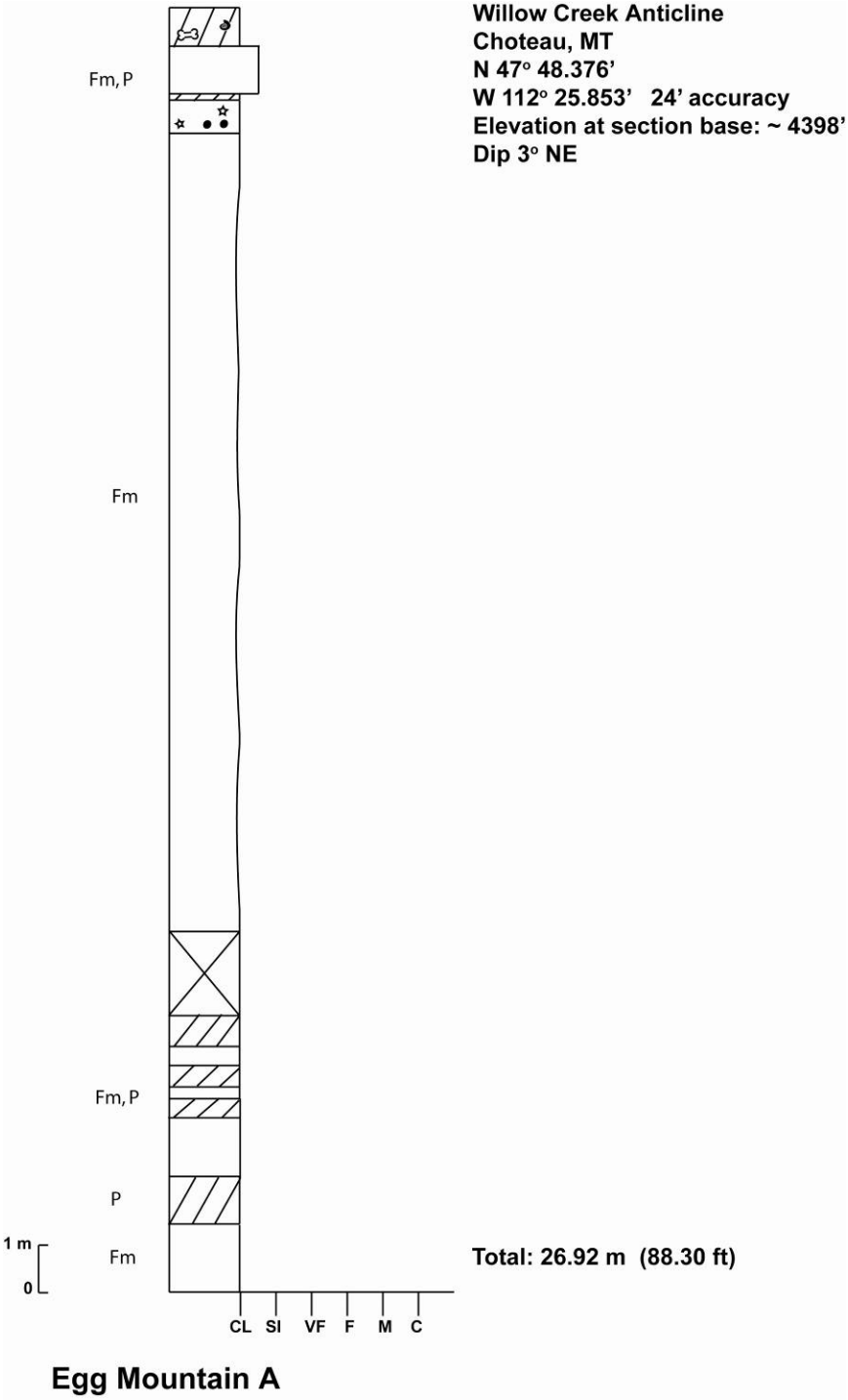

Egg Mountain A

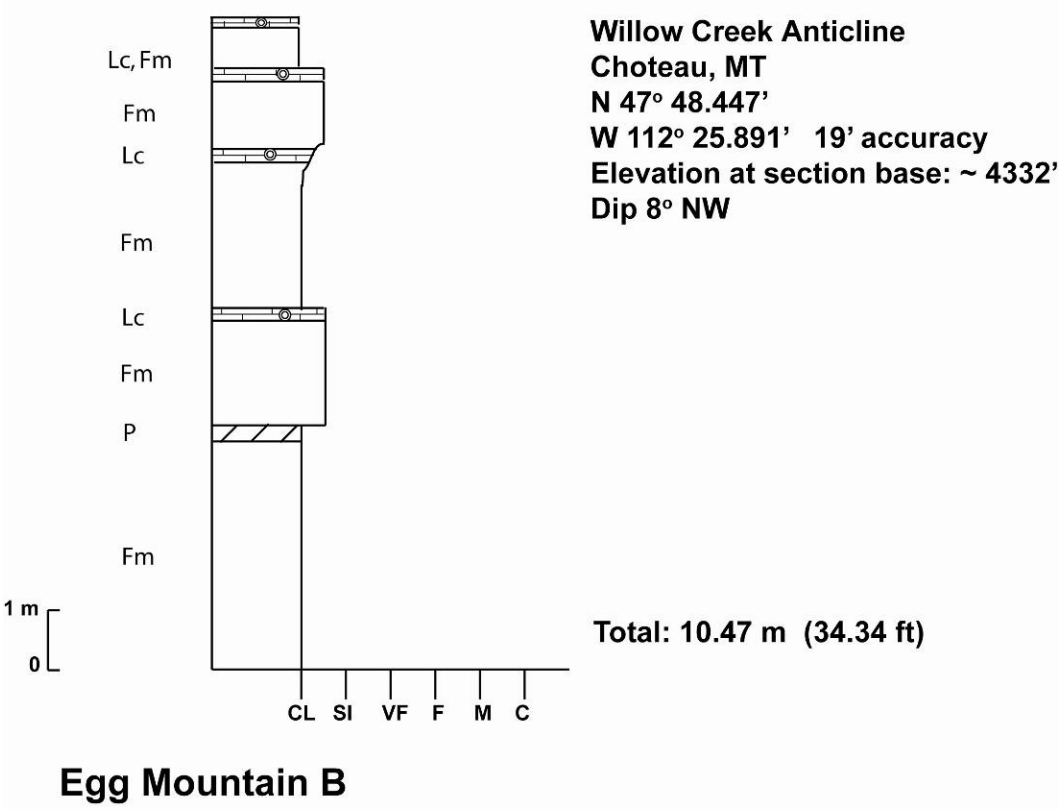
Lc, Fm
Fm
Lc
Fm
Lc
Fm
P
Fm
1 m
0
CL SI VF F M C
Willow Creek Anticline
Choteau, MT
N 47° 48.447'
W 112° 25.891' 19' accuracy
Elevation at section base: ~ 4332'
Dip 8° NW
Total: 10.47 m (34.34 ft)
Egg Mountain B

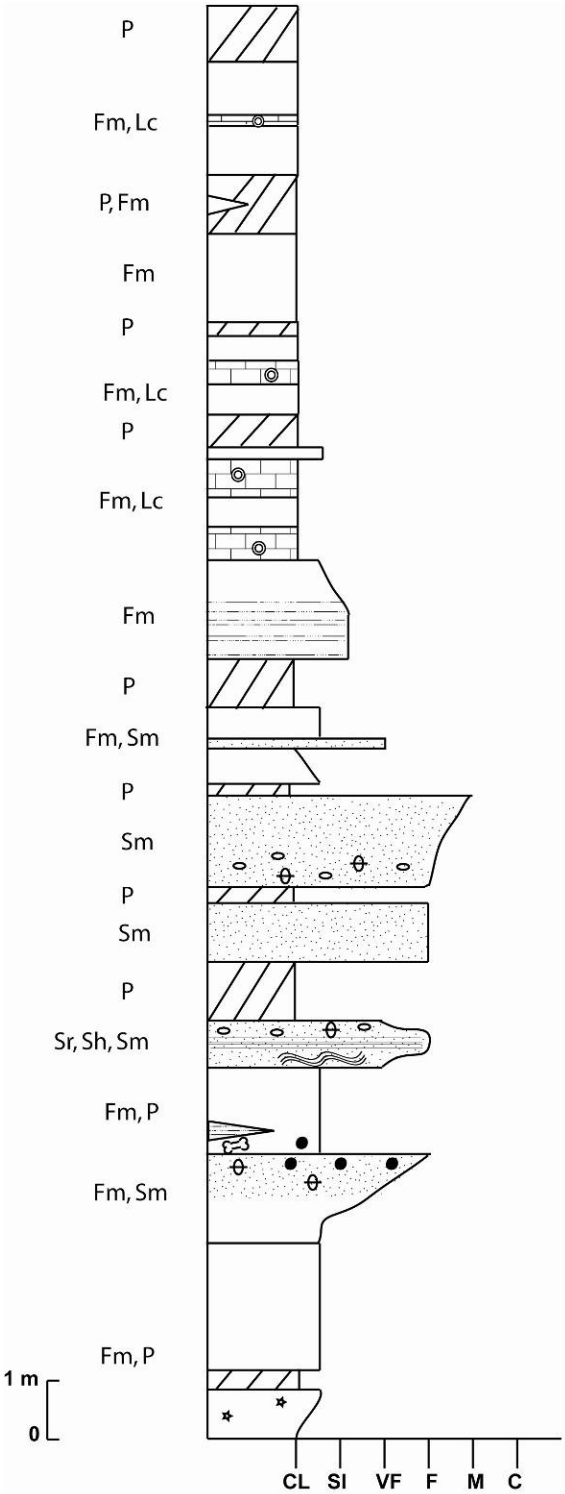

Willow Creek Anticline
Choteau, MT
N 47° 48.539'
W 112° 25.715' 27' accuracy
Elevation at section base: ~ 4363'
Dip 11° SW

Total: 24.20 m (79.38 ft)

Egg Mountain C

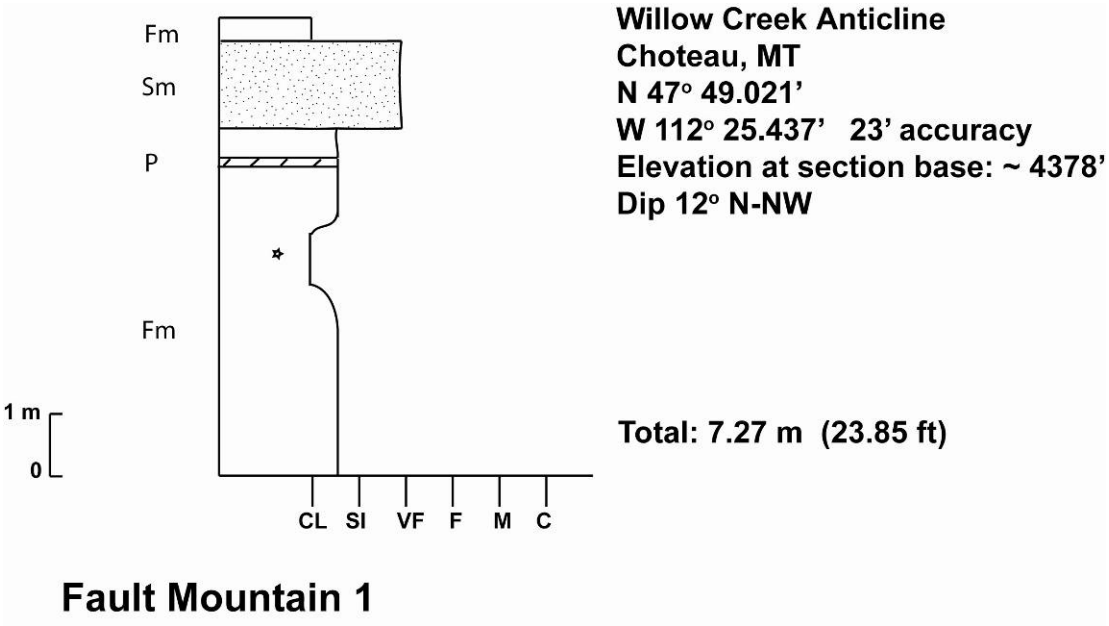
Fm
Sm
P
Fm
1 m
0
CL SI VF F M C
Willow Creek Anticline
Choteau, MT
N 47° 49.021'
W 112° 25.437' 23' accuracy
Elevation at section base: ~ 4378'
Dip 12° N-NW
Total: 7.27 m (23.85 ft)
Fault Mountain 1

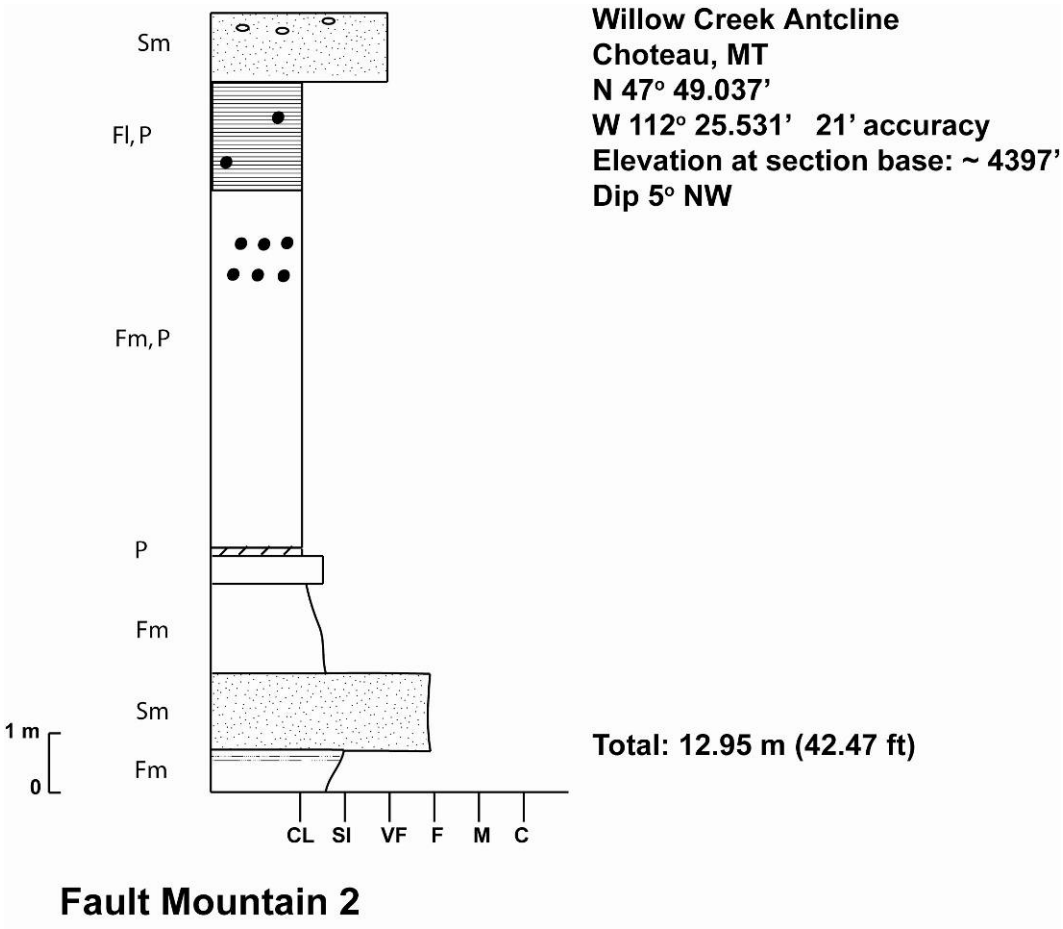
Willow Creek Antcline
Choteau, MT
N 47° 49.037'
W 112° 25.531' 21' accuracy
Elevation at section base: ~ 4397'
Dip 5° NW
Sm
Fl, P
Fm, P
P
Fm
Sm
Fm
1 m
0
CL SI VF F M C
Total: 12.95 m (42.47 ft)
Fault Mountain 2

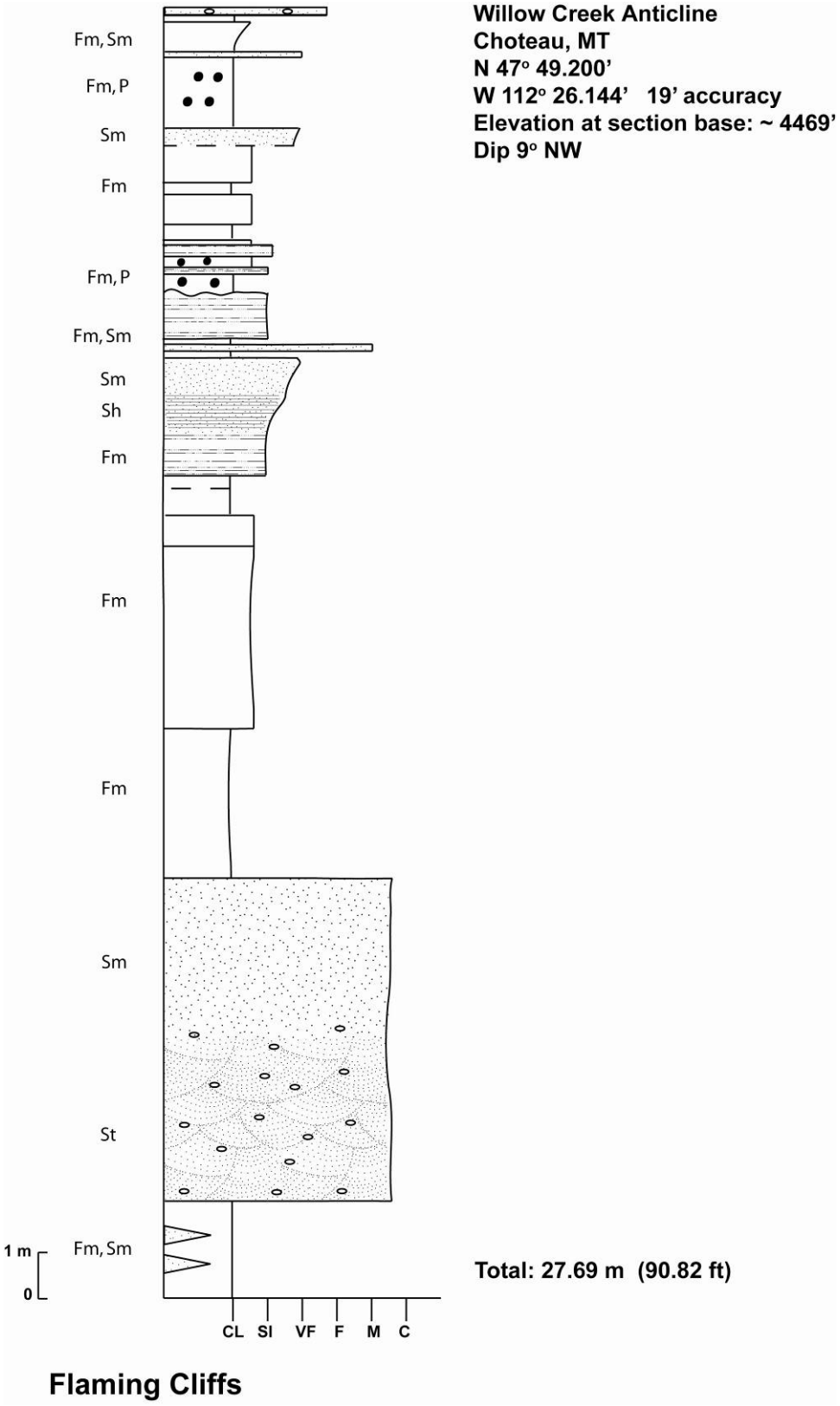
Willow Creek Anticline
Choteau, MT
N 47° 49.200'
W 112° 26.144' 19' accuracy
Elevation at section base: ~ 4469'
Dip 9° NW
Fm, Sm
Fm, P
Sm
Fm
Fm, P
Fm, Sm
Sm
Sh
Fm
Fm
Fm
Sm
St
Fm, Sm
1 m
0
CL SI VF F M C
Total: 27.69 m (90.82 ft)
Flaming Cliffs

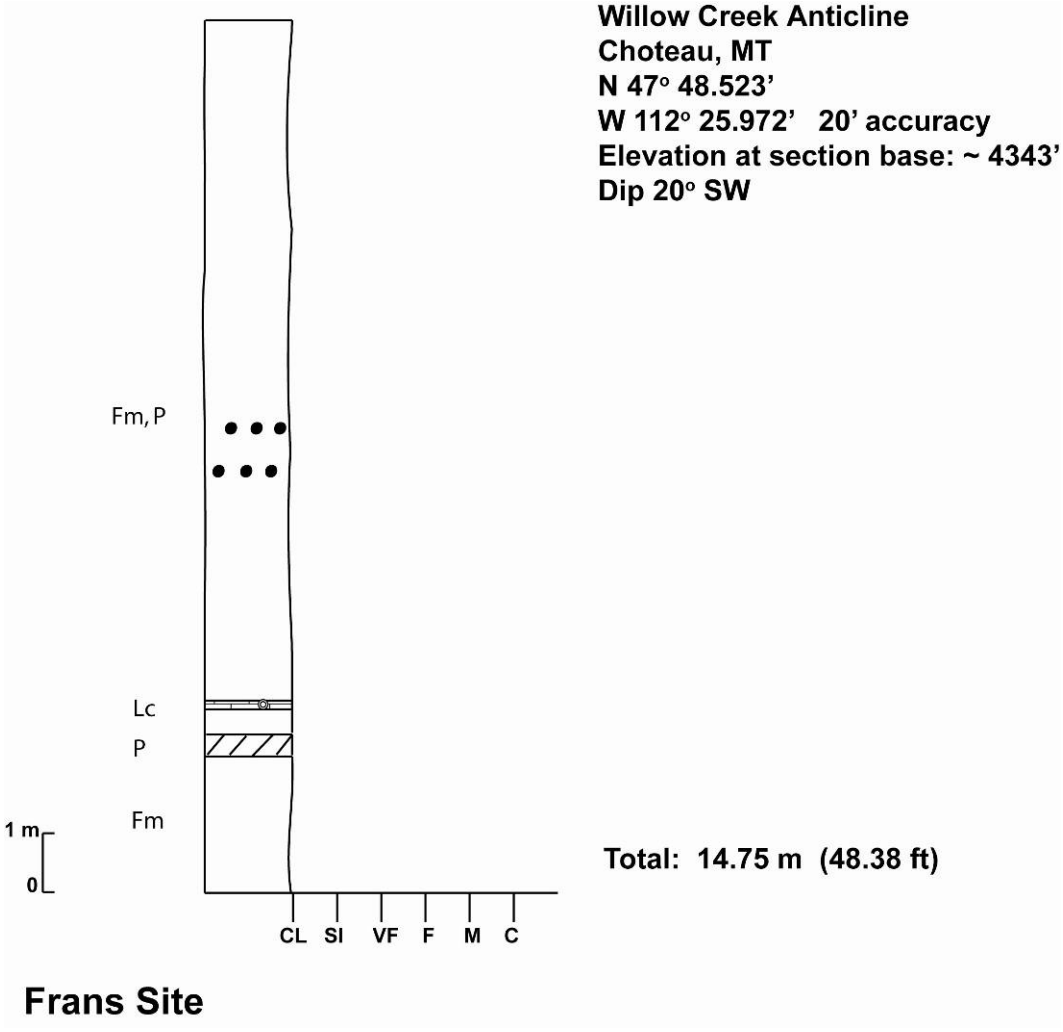
Willow Creek Anticline
Choteau, MT
N 47° 48.523'
W 112° 25.972' 20' accuracy
Elevation at section base: ~ 4343'
Dip 20° SW
Fm, P
Lc
P
Fm
1 m
0
CL SI VF F M C
Total: 14.75 m (48.38 ft)
Frans Site

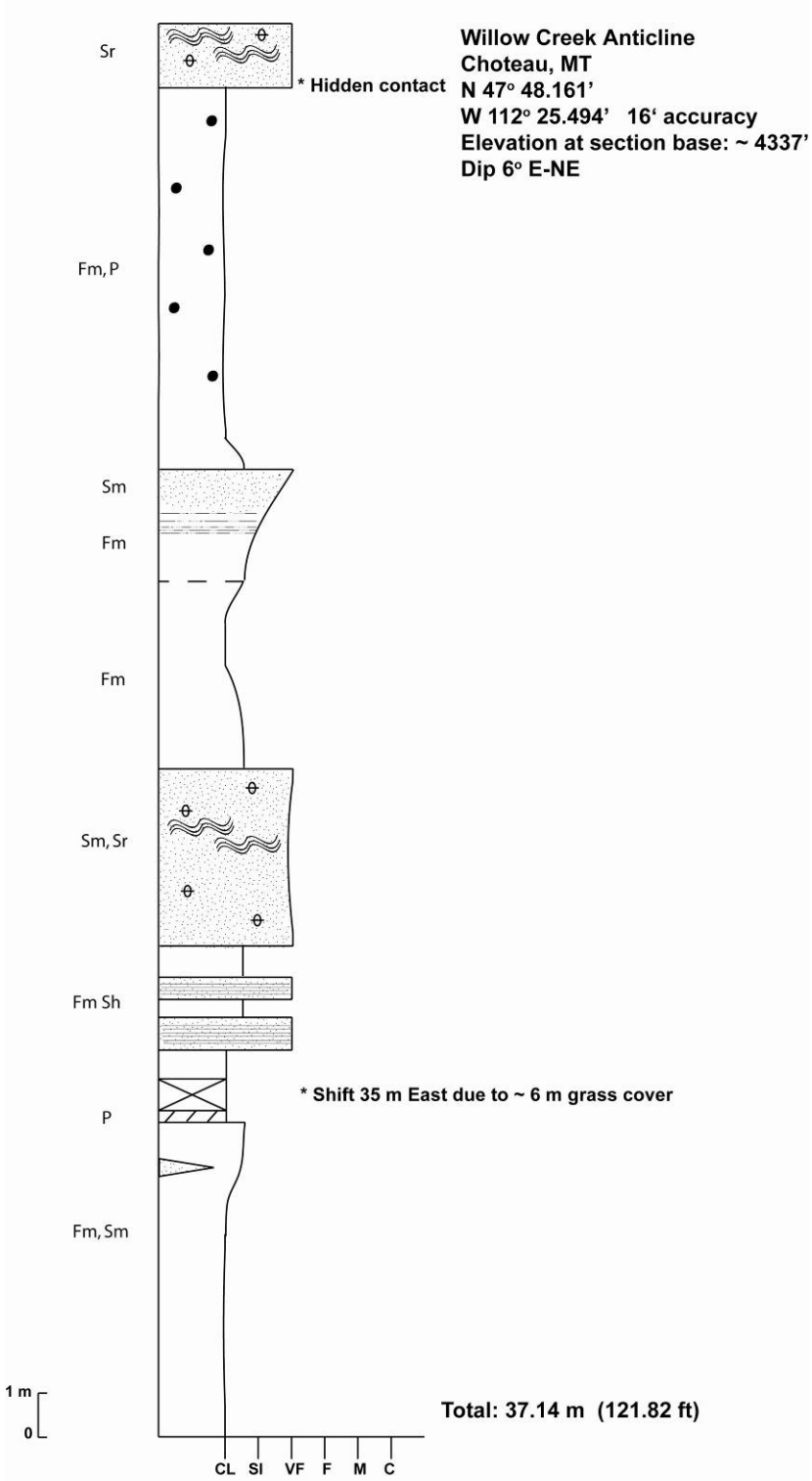
Willow Creek Anticline
Choteau, MT
N 47° 48.161'
W 112° 25.494' 16' accuracy
Elevation at section base: ~ 4337'
Dip 6° E-NE
Sr
* Hidden contact
Fm, P
Sm
Fm
Fm
Sm, Sr
Fm Sh
* Shift 35 m East due to ~ 6 m grass cover
P
Fm, Sm
1 m
0
Total: 37.14 m (121.82 ft)
CL SI VF F M C

Jess Butte

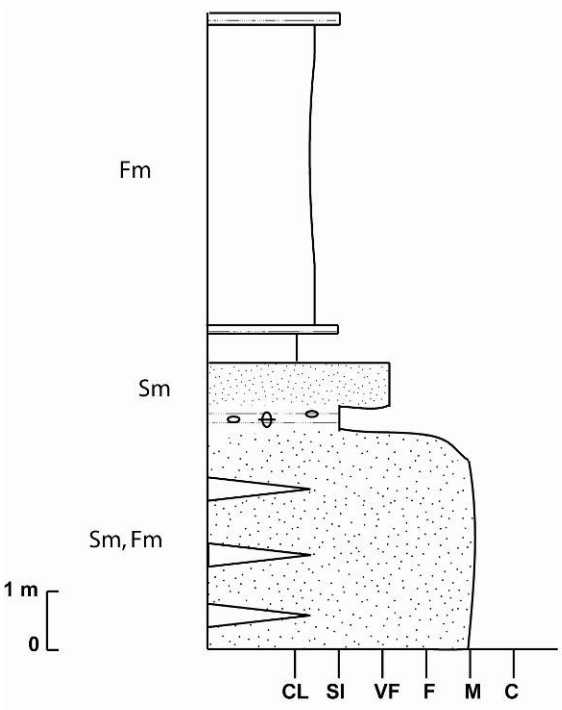

Willow Creek Anticline
Choteau, MT
N 47° 48.696'
W 112° 25.274' 18' accuracy
Elevation at section base: ~ 4326'
Dip 8° W

Total: 10.87 m (35.65 ft)

Josh's Hill

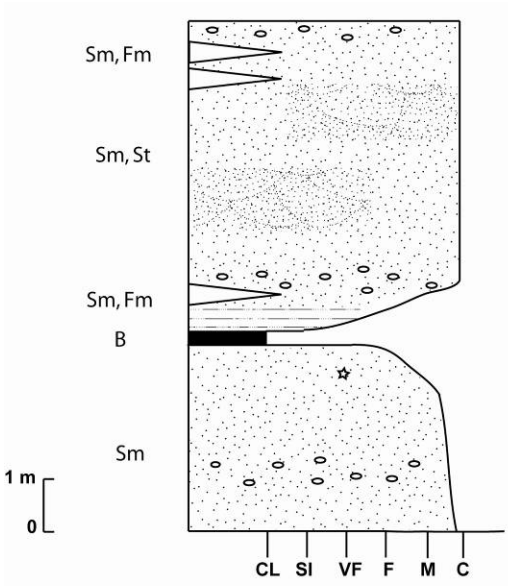

Willow Creek Anticline
Choteau, MT
N 47° 48.683'
W 112° 25.258' 23' accuracy
Elevation at section base: ~ 4372'
Dip 12° W-NW

Total: 9.29 m (30.47 ft)

Justin's Peak

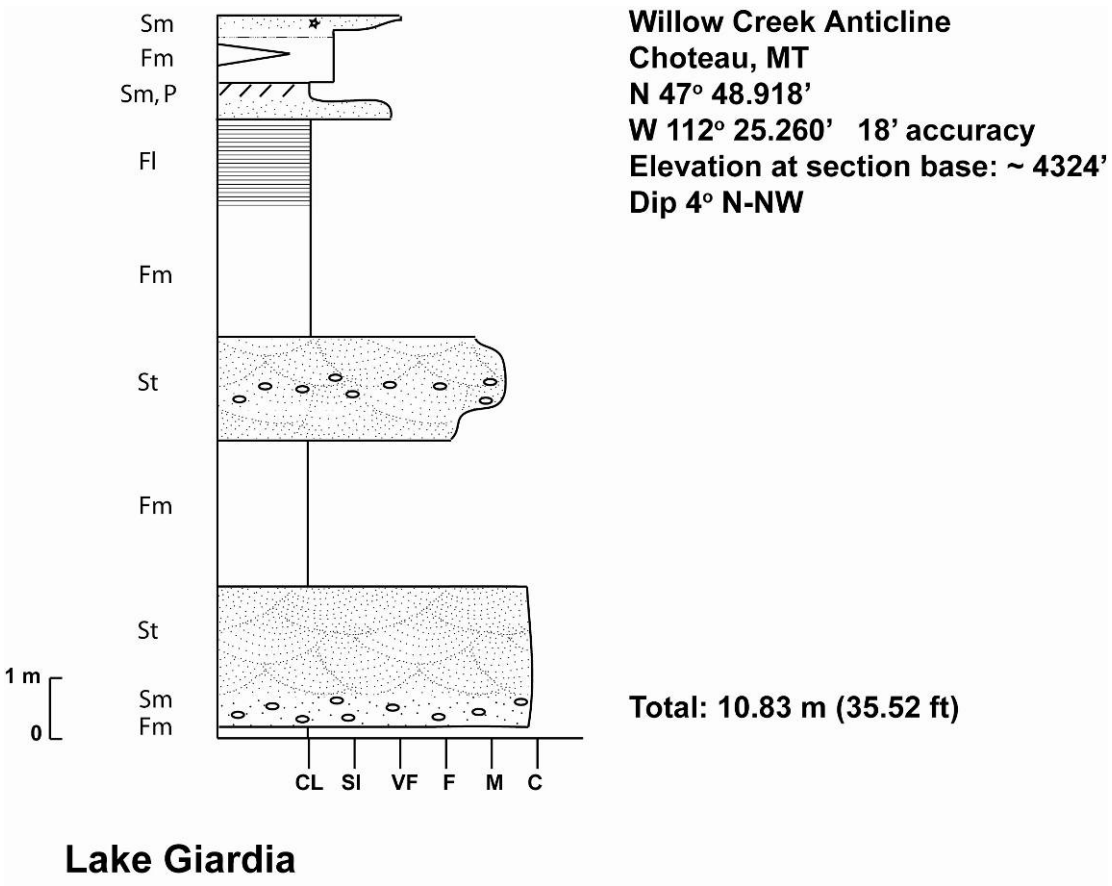
Sm
Fm
Sm, P
Fl
Fm
St
Fm
St
Sm
Fm
1 m
0
CL SI VF F M C
Willow Creek Anticline
Choteau, MT
N 47° 48.918'
W 112° 25.260' 18' accuracy
Elevation at section base: ~ 4324'
Dip 4° N-NW
Total: 10.83 m (35.52 ft)
Lake Giardia

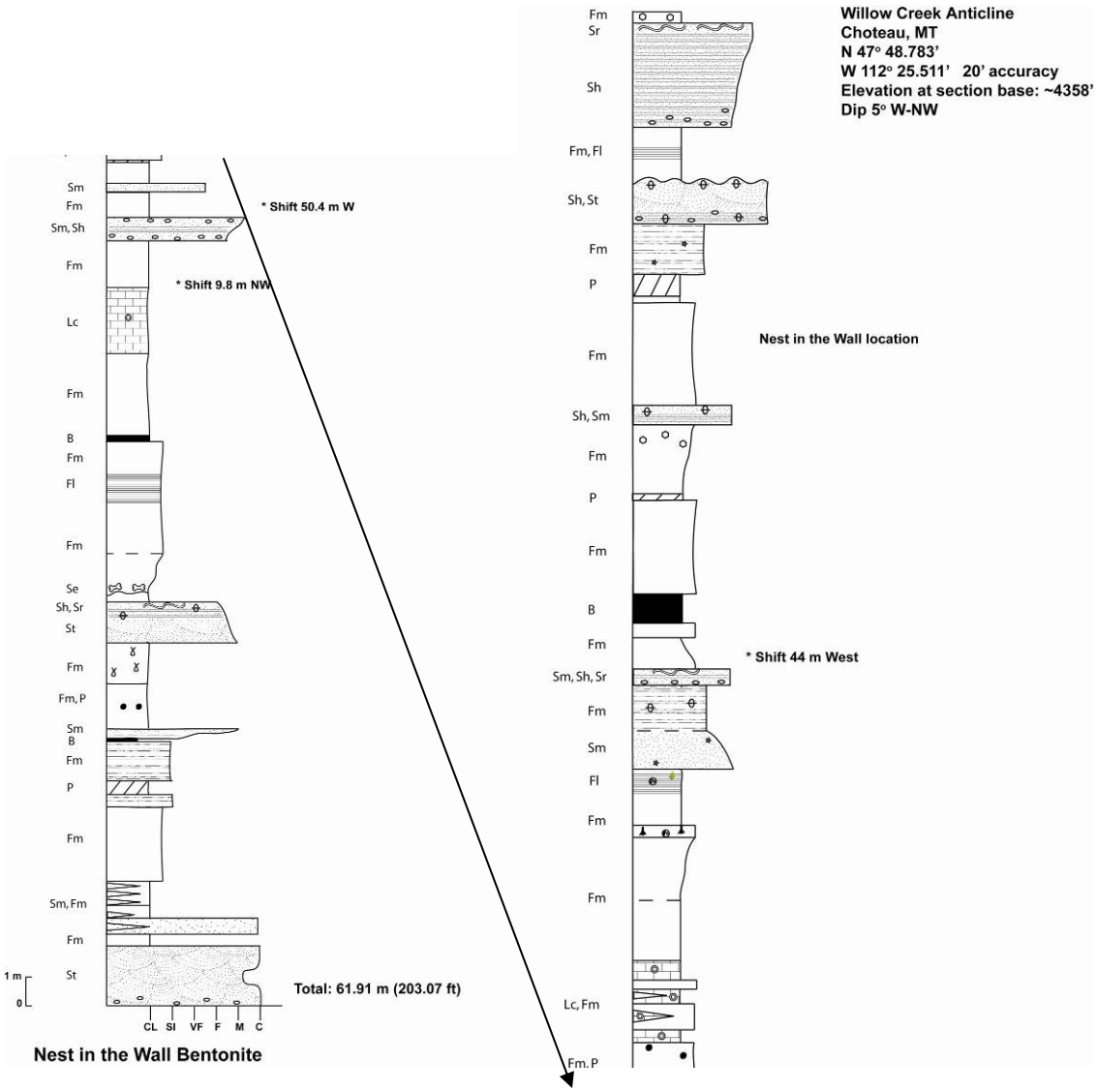
Willow Creek Anticline
Choteau, MT
N 47° 48.783'
W 112° 25.511' 20' accuracy
Elevation at section base: ~4358'
Dip 5° W-NW
Nest in the Wall location
* Shift 44 m West
* Shift 50.4 m W
* Shift 9.8 m NW
Total: 61.91 m (203.07 ft)
CL SI VF F M C
1 m
0
Nest in the Wall Bentonite

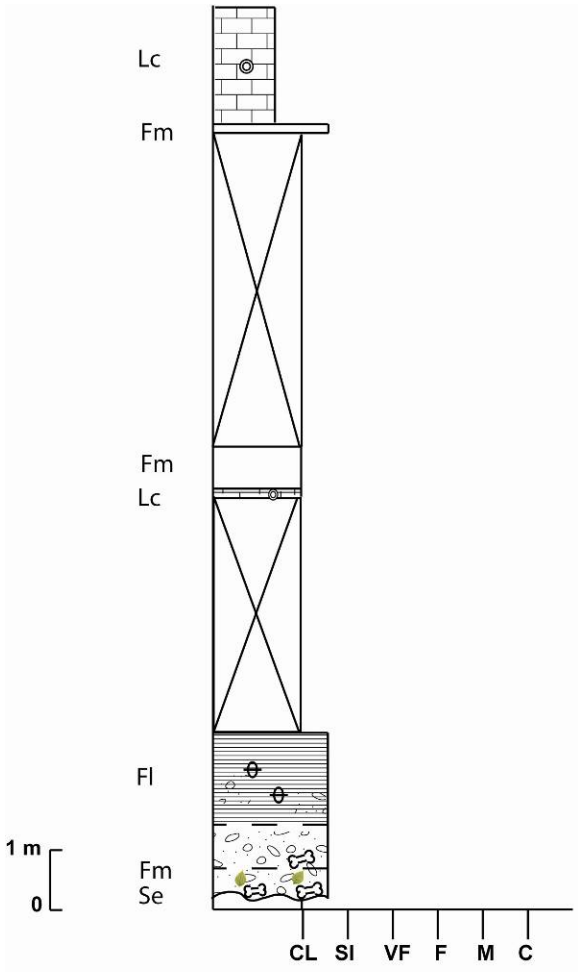

Willow Creek Anticline
Choteau, MT
N 47° 48.812'
W 112° 25.577' 17' accuracy
Elevation at section base: ~ 4382'
Dip 3° W

Total: 14.88 m (48.81 ft)

Nose Cone 2

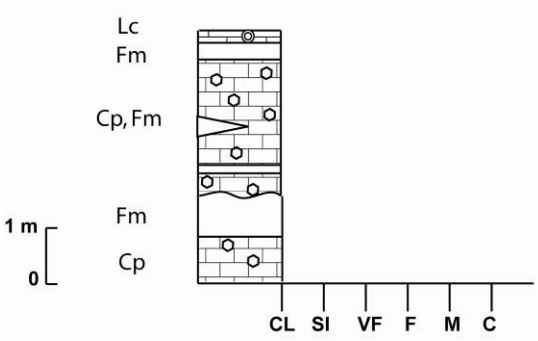

Willow Creek Anticline
Choteau, MT
N 47° 48.962'
W 112° 25.450' 16' accuracy
Elevation at section base: ~ 4378'
Dip 11° NW

Total: 4.47 m (14.66 ft)

Pete's Pupa Peninsula

\

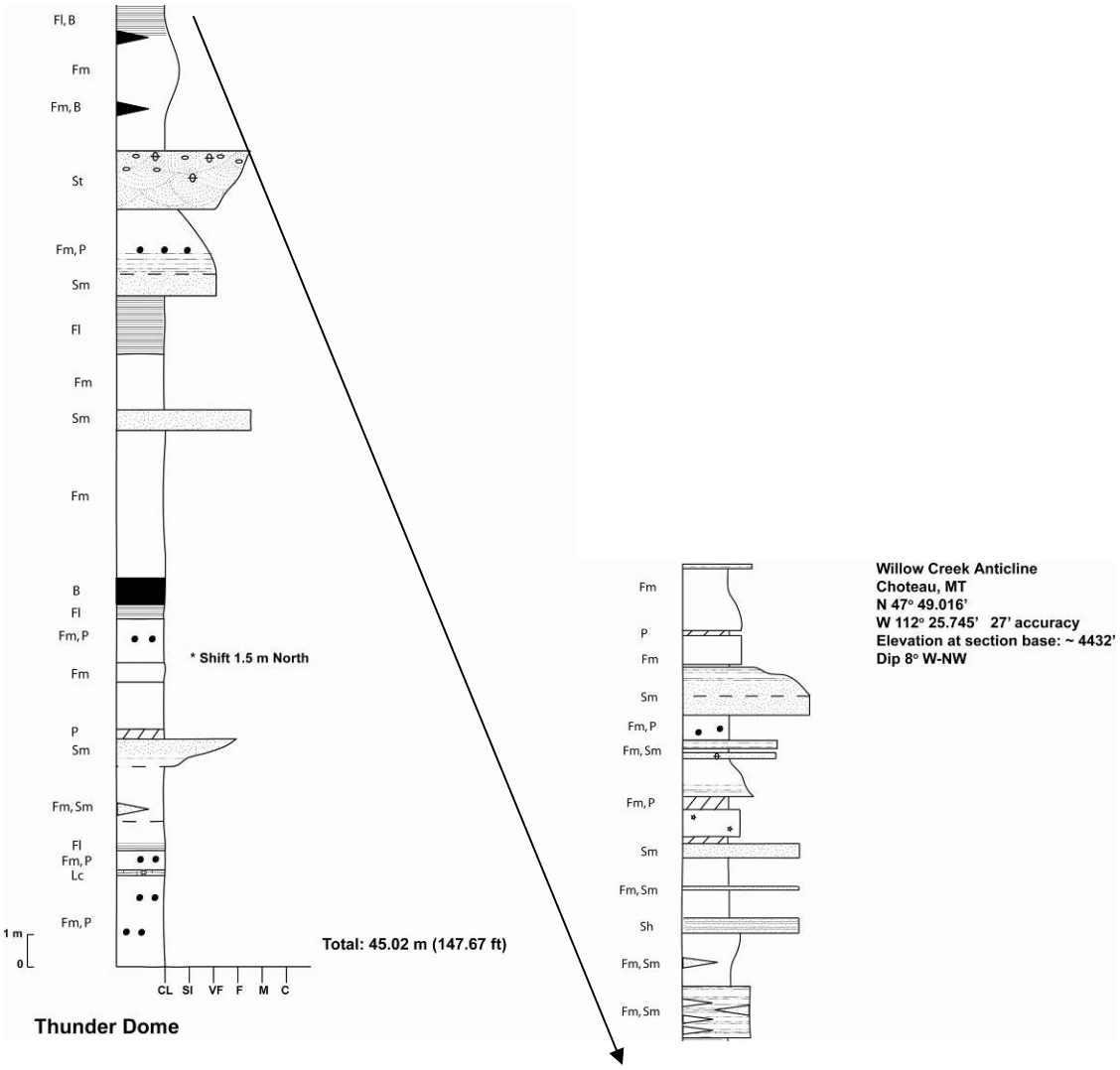
Fl, B
Fm
Fm, B
St
Fm, P
Sm
Fl
Fm
Sm
Fm
B
Fl
Fm, P
Fm
P
Sm
Fm, Sm
Fl
Fm, P
Lc
Fm, P
1 m
0
* Shift 1.5 m North
Total: 45.02 m (147.67 ft)
CL SI VF F M C
Thunder Dome
Fm
P
Fm
Sm
Fm, P
Fm, Sm
Fm, P
Sm
Fm, Sm
Sh
Fm, Sm
Fm, Sm
Willow Creek Anticline
Choteau, MT
N 47° 49.016'
W 112° 25.745' 27' accuracy
Elevation at section base: ~ 4432'
Dip 8° W-NW

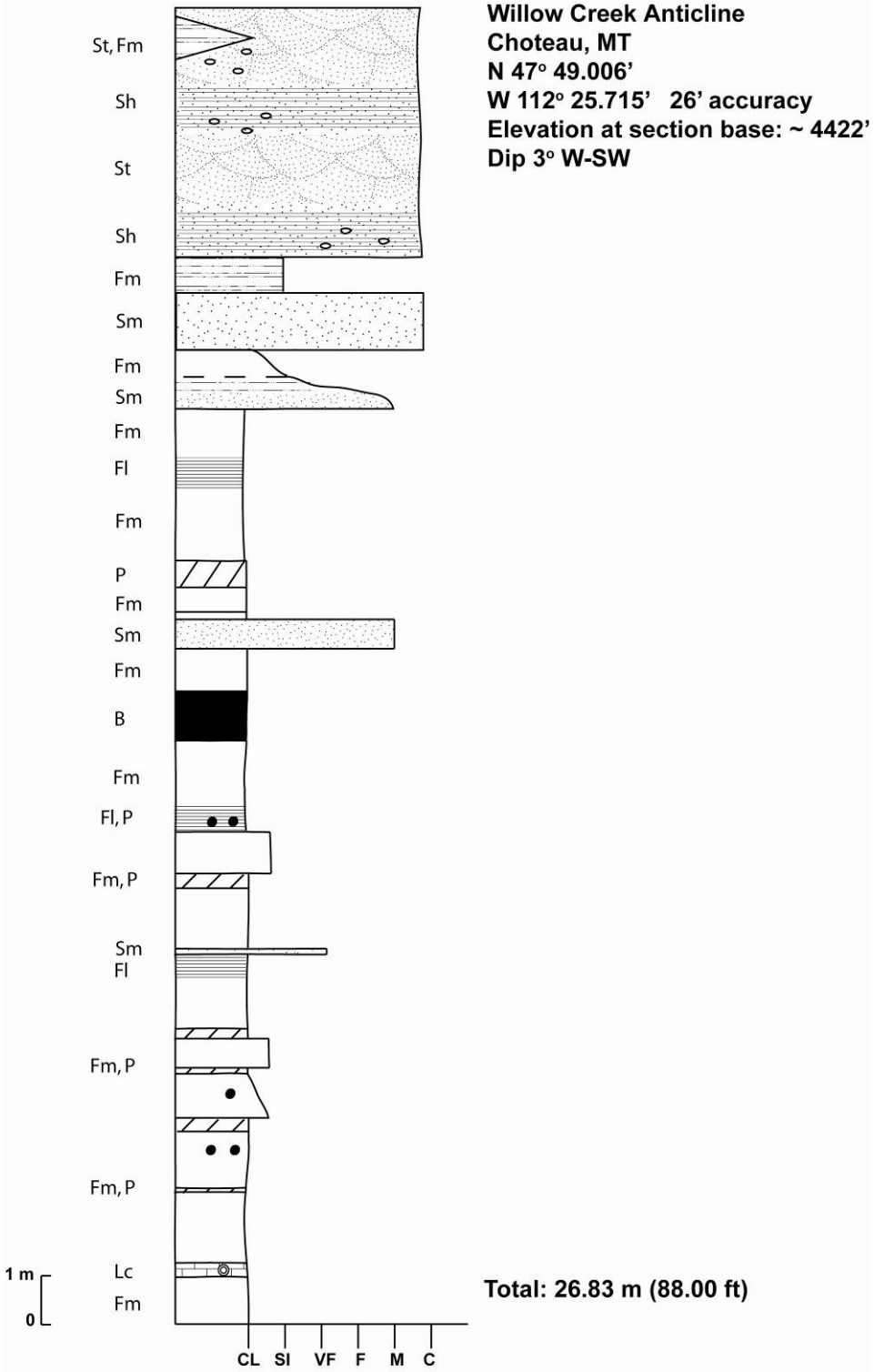

Thunder Dome Bentonite

APPENDIX B

MEASURED SECTION DESCRIPTIONS

1. ’78 NEST

Willow Creek Anticline, Choteau, MT
N 47° 48.755’ W 112° 25.281’ 17’ accuracy
Elevation at base of section: ~ 4338 ft
Dip 8° W

Unit	Thickness (m)	Total Thickness (m)	Unit Description	Unit Color (Munsell, 2000)	Upper Contact
1	0.68	-	Interbedded red-brown mudstone and light gray with a little brown sitlstone/very fine sandstone. Mudstone is prominent at base then sandstone more prominent at top starting at 0.6m (coarsening up)	6/3 10R	Sharp
2	0.27	0.95	Pedogenic carbonate. Equivalent of Josh’s Hill. Forms resistant bench.	4/2 10R	Sharp
3	0.45	1.40	Red brown mudstones grading to gray red brown silty mudstone. Some small lenses of very fine sandstone. Where the ’78 Nest was taken out.	5/3 10R	Grades into Unit 4
4	0.40	1.80	Light gray to medium gray siltstone with calcite precipitation veins. Forms resistant ledge above Unit 3. Where the ’78 Nest marker stake is. Some rusty weathering.	8/1 10YR	Sharp
5	0.30	2.10	Red brown silty mudstone, maybe a little sandy.	5/2 10R	Sharp
6	0.17	2.27	White and light red bentonite layer? Very hard and indurated; doesn’t look like the other bentonites seen in the area. Lots of large biotite grains. Only a thin lense is present and it pinches to the north and south. Forms a resistant bench.	5/2 10R	Sharp
7	0.70	2.97	Red brown silty mudstone grading to light gray very silty mudstone weathered siltstone at base. Piece of eggshell in float (Maiasaur?)	5/2 10R	Sharp
8	0.60	**3.57 (11.7 ft)**	Unit 4 repeated. Forms resistant ledge.	8/1 2.5Y	-

2. ’79 NEST

Willow Creek Anticline, Choteau, MT
N 47° 48.724’ W112^{o} 25.210’ 26 ft accuracy
Elevation at base of section: ~ 4365 ft
Dip 10° NW

Unit	Thickness (m)	Total Thickness (m)	Unit Description	Unit Color (Munsell, 2000)	Upper Contact
1	2	-	Justin’s Peak Unit 1	-	Sharp
2	4	6	Covered Interval. Vegetation.	-	Sharp

3	1.65	7.65	Justin's Peak unit 1. Dip changes here to NE (going through middle of anticline).	-	Sharp
4	0.10	7.75	Nodular pedogenic carbonate layer; some coalesced. Forms cap of bench.	Pinks and browns	Sharp
5	1.9	9.65	Justin's Peak unit 3. At about 1m there is some pedogenic carbonate present and here the sandstone is more indurated. Some interbedded purple red mudstone forming thin layers under where the sandstone forms a more indurated layer.	5/2 10R	Sharp
6	1.5	11.15	Interbedded mudstone and sandstone. Starts with 1 m thick purple red mudstone forming low angle slope. Then light gray very fine-grained sandstone forms a resistant bench 25 cm thick. Followed by more mudstone. Top of mudstone is very hard; possibly early stages of pedogenic carbonate formation.	5/2 10R	Sharp
-	-	-	CHANGE 33 m NW TO '79 NEST SITE SECTION	-	-
7	1.87	13.02	Purple gray silty mudstone alternating with light green grey silty mudstone. Forms low angle slope. Slope is covered with sandstone weathered from above. '79 Nest is in this layer and partially next to it, too.	7/1 10R and 7/10Y Gley 1	Sharp
8	0.22	13.24	Siltstone with mud clasts. Siltstone is gray and mud is mottled purples and greens some pieces are dark. Forms a resistant ledge; Fizzes…could be a stage in pedogenic carbonate fm.	8/10Y Gley 1	Sharp
9	2.15	15.39	Med green gray/purple color changes to med purple/dark gray silty mudstone. Less silty as go up. Slope covered in sandstone pieces weathered from above.	6/10Y Gley 1 and 5/1 10R	Sharp
10	2.5	**17.89 (58.7 ft)**	Light gray salt and peppery fine well sorted, subangular sandstone. Biotite grains are larger (medium). Purple mudstone rip-up clasts 1-2 cm thick and burrows 1-2 cm in diameter. Possible root trace. Calcite cemented.	8/N Gley 1	-

3. BRANVOLD SITE

Willow Creek Anticline, Choteau, MT
N 47° 48.728' W112^{o} 25.549' 29 ft accuracy
Elevation at base of section: ~ 4373 ft
Dip 1° NW

Unit	Thickness (m)	Total Thickness (m)	Unit Description	Unit Color (Munsell, 2000)	Upper Contact
1	1	-	Light to medium purple mudstone. Forms a low slope.	4/1 10R	Sharp
2	0.40	1.4	Lt gray subangular to subrounded, well sorted very fine sandstone. Turns more off tan as go up and then start to see more biotite and it seems to be concentrated in very thin	-	Sharp

			layers. Abundant burrows 0.5-3 cm in diameter. Slope covered in calcite float and blue calcite cemented dinosaur bone fragments 0.5-7 cm long. Calcite precipitation vein at base.		
3	0.70	2.1	Light to medium purple mudstone weathering to light to medium purple. Slope covered in calcite float and dinosaur fragments 0.5-7 cm long. Mudstone forms a lense pinching out to the East.	5/2 10R	Sharp
4	~0.80	2.9	Light gray/off-white and salt and peppery very fine-fine-grained sandstone.	-	Buried
5	0.30	3.2	Med-dark green clay. Can roll up into a ball...very "clayey". This layer is at the base of the bonebed and stops just before it. Some small organic specks in top. A little grayer in top 4-5 cm.	4/10GY at base and 5/10Y Gley 1 on top	Sharp
6	Siltstone: 0.20 1.4 to vegetation 1.4 silty mudstone	3.4 4.8	Light-med orange with possible light brown siltstone (might just be a big orange clast). Beginning at bonebed. Orange clasts approx. 3 cm in diameter, loosely consolidated and appear beginning with the bonebed and continue up to color change from light brown silty mudstone to light green. Bone fragments black to light blue and range in size, concentrated more at base but found up 0.18 m. Organics present. Color changes at 0.47m. Organics found up to color change but not after. Calcite precipitation veins run through vertically in silty mudstone. Some calcite precipitation in siltstone. Possible clasts of coarser grained in finer grained.	orange nodules 6/8 10/YR, brown 4/2 10YR, green 6/5 GY	Buried
7	1.7	6.5	Covered interval. Vegetation	-	-
8	0.30	6.8	Bentonite layer. Med-dark red brown mudstone weathering to light red/pink. Only a thin strip of this is exposed as the grass cover starts again.	5/2 10R	Buried
9	0.70	7.5	Covered interval. Grass	-	-
10	1	8.5	Medium gray with some light to medium green slightly silty mudstone. Forms a low slope. Start to see pink bones in float ranging from 2-7 cm.	5/5PB Gley 2	Sharp
11	0.60	9.1	Limestone. Very light, breaks into larger angular pieces.	Light gray	Sharp
12	0.50	9.6	Equivalent of Unit 10	4/1 10R	Sharp
13	0.15	9.75	Equivalent of unit 11	Light gray	Sharp
14	0.55	10.30	Equivalent of units 10 and 12	4/1 10R	Sharp
15	0.09	**10.39 (34.1 ft)**	Equivalent of units 11 and 13. Forms cap of section and hill.	Light gray	-

4. CHILDREN'S DIG

Willow Creek Anticline, Choteau, MT
N 47° 48.511' W112^{o} 25.024' 19 ft accuracy
Elevation at base of section: ~ 4356 ft
Dip 7° E

Unit	Thickness (m)	Total Thickness (m)	Unit Description	Unit Color (Munsell, 2000)	Upper Contact
1	0.35	-	Red brown silty mudstone. Very clayey	4/2 10R	Sharp
2	0.10	0.45	Light medium brown very fine sandstone. Clay in matrix, subangular to subrounded grains.	5/1 5YR	Sharp Irregular
3	0.35	0.80	Dark brown to black organic mud with stringers of sand (burrows?) of various thicknesses that run through out.	5/1 2.5YR	Inter-fingering
4	1.8	2.6	Off-white to light gray fine sandstone. Weakly cemented with calcite, well sorted subangular grains. Biotite and muscovite larger grains and very abundant.	8/N Gley 1	Sharp
5	0.20	2.8	Off-white to light gray very fine sandstone cemented with calcite. Well sorted, subangular to subrounded grains. Biotite and muscovite large. Some ripple cross bedding, burrows 1cm in diameter. Grading upwards to an off-white to light gray siltstone. Ledge former.	8/N Gley 1	Sharp
6	0.50	3.3	Medium to dark silty mudstone, calcitic, some pockets of sand. Grading upwards to light to medium grey fine-grained sandstone, calcitic, subangular to subrounded, well sorted.	6/N Gley 1	Sharp
7	0.30	3.6	Off-white to light gray very fine-grained sandstone. Well sorted, subangular to subrounded grains. Ripple cross lamination, well indurated.	7/N Gley	Sharp
8	0.20	3.8	Light gray siltstone. Calcitic. Grades up to red brown mottled silty mudstone.	7/N Gley	Sharp
9	0.20	4.0	Off-white to light gray very fine-grained sandstone. Calcite cemented, subangular, well sorted.	7/N Gley	Sharp
10	0.20	4.2	Medium to dark red brown mudstone	5/3 10R	Sharp Irregular
11	0.35	4.55	Grey tan siltstone to very fine-grained sandstone. Burrows less than or equal to 1cm in diameter, common. Ripple cross lamination towards top. One thin layer of mudstone interbedded (2cm thick).	-	Gradational
12	0.20	4.75	Red brown to dirty green mudstone, mottled, with possible pedogenic carbonate nodules (weakly cemented).	6/3 10R	Sharp
13	0.20	4.95	Light reddish brown very fine-grained sandstone, well cemented, some ripple cross lamination. Calcitic	-	Gradational

14	0.30	5.25	Greenish mudstone with red brown mottling, fines upward to claystone.	7/10Y Gley 1	Gradational
15	0.10	5.35	Green fine-grained sandstone moderately cemented. Small burrows. Nonresistant. Fines upward	-	Gradational
16	1.5	6.85	Red brown fissile mudstone, multiple layers of calcite nodules 3 cm max in diameter. Occasional green mottling.	4/1 10R	Gradational
17	0.80	7.65	Silty mudstone with high clay content. Med red brown at base to light red brown purpley with a higher silt content. Fines halfway up to a cleaner mudstone, purple red brown. Then fines to a claystone red-brown with green mottling. Some of the mottling is harder trending towards nodule fm.	4/1 10R	Sharp Irregular
18	0.20	7.85	Thick pedogenic carbonate horizon. Nodular. Forms a slight shelf on slope.	-	Sharp
19	2.1	9.95	Red brown mudstone with green mottling. Some small pedogenic carbonate nodules equal to or less than 1cm in diameter. Color changes to medium purple brown with green mottling. Slightly calcitic. Coarsening upwards over the last 0.5 m.	5/1 10R	Gradational
20	0.50	10.45	Red brown mudstone Possible Bentonite (equivalent to Justin's Peak?) with irregular nodular pedogenic carbonate horizon approx. 10cm from base. Nodules are mottled red brown and green	7/3 10R	Gradational
21	0.40	10.85	Dark purple brown mudstone.	5/1 10R	Gradational
22	0.35	11.20	Light to medium gray mudstone. Becomes slightly greenish and more indurated towards top.	4/N Gley 1	Sharp
23	2.3	13.50	White-off grey fine-medium-grained sandstone with occasional rusty staining on resistant horizon. Clean subrounded, well sorted, moderately cemented with calcite and with occasional cemented horizons. Well developed trough cross bedding in middle. Ripple cross lamination over upper meter and also a few vertical and horizontal burrows 1cm in diameter. Last m fine-grained sandstone. Resistant ledge former.	-	Gradational
24	1.25	14.75	Dark purple brown mudstone	6/1 10R	Sharp Irregular
25	0.30	15.05	Off-white to grey fine-grained sandstone, subangular, clean, well sorted, well cemented with calcite. Ripple cross lamination throughout. Abundant burrows1-2 cm in diameter. Ledge former, some burrows with sculpted sides.	-	Gradational
26	0.40	15.45	Muddy very fine-grained sandstone, grey brown. Grades to mudstone, dark purple brown. Very abundant burrows 1.5 cm in diameter. Fines over lower 5 cm. Then very fine sandstone, green gray, well cemented with a silty mudstone. Burrows towards top mixing it, abundant and throughout. Interbedded fine-very fine sandstone and mudstone.	-	Gradational
27	0.70	16.15	Dark purple brown mudstone with some pedogenic carbonate nodules 20 cm up from base (layer 15 cm thick). Color changes to medium red purple brown	5/1 10R	Sharp Irregular

28	0.70	16.85	Light gray interbedded very fine sandstone. Calcite cemented ledge former with rusty staining. Abundant ripple cross lamination best exposed in lower portion. 3 main sandstone units separated by thin (less than or equal to 5cm) light purple mudstone. Abundant burrows less than or equal to 2.5 cm in diameter horizontal and vertical. Dinosaur footprint sandstone casts 20-30cm depressed into lower mudstone.	-	Sharp
29	1.6	18.45	Medium grey carbonaceous mudstone with small white dots (calcite?). Clay rich grading upwards to green and purple brown mottled mudstone weathering to light gray. Pedogenic carbonate nodules horizons occur 1m from base. Green gray changes to light gray brown towards top. Fines to claystone above pedogenic carbonate.	5/N Gley 1	Sharp
30	0.50	18.95	Off-white to gray very fine-grained sandstone. Basal portion well cemented with calcite. 8 cm thick layer of interbedded mudstone. Ripple cross lamination in upper part. Sandstone thickens to N to 1.5m thick. Small pedogenic carbonate nodules/mud rip-up clasts at base. Some trough cross bedding near top. Dinosaur bones occur on upper surface with some partially imbedded (bonebed).		Exposed Surface
-	-	-	CHANGE 9 m TO EAST	-	-
31	0.25	19.20	Light gray mudstone (clay?) with small (1.5 cm) orange clasts and thin calcite veins. Possible base of bonebed.	6/10Y Gley 1	Sharp
32	0.60	19.80	Dark-med brown mudstone with abundant clay. Bone, pedogenic carbonate nodules, orange clasts 1-2 cm diameter, plant debris, silty orange clasts 8-9 cm long, calcite layers. Grades to light brown, then brownish gray with abundant organics.	6/3 10YR	Gradational
33	0.95	20.75	Light green mudstone, organics, but reduced in abundance from previous layer. Calcite veins. Pedogenic carbonate nodules 1-4 cm in diameters, in nodular horizon 11cm below upper contact.	7/15 GY Gley 1	Sharp
34	0.35	21.10	Off-white bentonite claystone (sampled for radiometric dates). Calcite veins	-	Sharp (slightly irregular)
35	2.3	23.40	Green-gray mudstone with calcite precipitation veins 0.25-1cm thick. Red brown clay occurs along fractures.	6/10GY Gley 1	Sharp
36	1.1	24.50	Light green gray silty claystone with purple-brown mottling. Calcite veins. Becomes hard and blocky up, forming thin resistant ridge (15 cm thick) near top. Thickness varies laterally.	6/N Gley 1	Sharp
37	3.8	28.30	Dark purple brown mudstone. Calcite veins. Coarsens upward over upper 20 cm.	4/1 10R	Sharp
38	0.15	28.45	Fine sandstone, subangular to subrounded. Ripple cross lamination at base. Upper portion shows horizontal bedding.	6/5 Gley 1	Sharp
39	0.15	28.60	Light brownish purple mudstone similar to Unit 37.	6/1 10R	Sharp
40	0.60	29.20	Light gray fine sandstone. Subangular to subrounded. Ledge former. Fines upward into a	6/5G Gley	Sharp

			light purple gray color and becoming less resistant.	1	
41	0.20	29.40	Purple brown mudstone.	6/1 10R	Sharp
42	0.40	29.80	Light gray fine sandstone. Subrounded to subangular.	6/5G Gley 1	Sharp
43	0.30	30.10	Purple brown mudstone similar to Units 37, 39, 41	6/1 10R	Sharp
44	0.40	30.50	Light to medium gray limestone with calcite growth along fractures. Very hard	5/N Gley 1	Sharp
45	0.30	30.80	Light purple gray well indurated mudstone.	5/1 10R	Gradational
46	0.50	31.30	Purple brown mudstone.	5/1 10R	Sharp
47	1.3	32.60	Dark chocolate brown mudstone weathering to small blocky pieces.	3/1 10R	Sharp Irregular
48	1.6	34.20	Nodular pedogenic carbonate layer. Multiple irregular beds 10-20cm thick interbedded with unit 47 mudstone 5-25 cm thick. Two pupal cases in float. Unit capped by 30 cm of mudstone.	-	Gradational
49	1.9	**36.1 (118.41 ft)**	Medium green gray mudstone. Nodular limestone layer 8 cm thick 0.85 cm up from base, and additional layer 24 cm thick 1.75 m from base. Limestone is charophytiferous.	5/5 GY Gley 1	-

5. EGG ISLAND

Willow Creek Anticline, Choteau, MT
N 47° 49.161' W112^{o} 26.050' 19 ft accuracy
Elevation at base of section: ~ 4481 ft
Dip 3° NW

Unit	Thickness (m)	Total Thickness (m)	Unit Description	Unit Color (Munsell, 2000)	Upper Contact
1	0.3	-	Dark gray black mudstone. Massive very well indurated. Some calcite crystals.	Dark gray black	Buried
2	8.3	8.6	Light gray limestone. Large calcite crystals. One burrow 2 cm in diameter.	Light gray	Sharp
3	2.45	**11.05 (36.24 ft)**	Light green gray limestone. Large calcite grains, and thick calcite precipitation.	Light green gray	-

6. EGG MOUNTAIN A

Willow Creek Anticline, Choteau, MT
N 47° 48.376’ W112^{o} 25.853’ 24 ft accuracy
Elevation at base of section: ~ 4398 ft
Dip 3° NE

Unit	Thickness (m)	Total Thickness (m)	Unit Description	Unit Color (Munsell, 2000)	Upper Contact
1	1.4	-	Dark purple mudstone. Forms low angle slope.	4/1 10R	Sharp
2	1	2.4	Pedogenic carbonate layer. Purple mud inclusions. Calcite precipitation veins.	Rusty	Sharp
3	1.2	3.6	Dark purple mudstone. Calcite precipitation veins.	4/1 10R	Sharp
4	0.40	4.0	Pedogenic carbonate layer.	Rusty	Sharp
5	0.25	4.25	Dark purple mudstone. Pinches out to S-SE.	4/1 10R	Sharp
6	0.45	4.70	Pedogenic carbonate layer.	Rusty	Sharp
7	0.40	5.10	Dark purple mudstone. Pinches out to S-SE.	4/1 10R	Sharp
8	0.65	5.75	Pedogenic carbonate layer.	Rusty	Buried
9	1.77	7.52	Covered interval. Vegetation.	-	Buried
10	16.8	24.32	Pedogenic carbonate. Sticking out of grass on hillside. In place. There could be lenses of mudstone or silty mudstone interfingering throughout. Dinosaur nest removed from top of section. Some eggshell present; some vertebrae found (float?). Calcite precipitation veins in pedogenic carbonate.	Rusty	Sharp
11	0.7	25.02	Light gray mudstone. Some parts more indurated than others (early stages of pedogenic carbonate formation?) Some loose eggshell. Small pedogenic carbonate lense at 0.33 m up from base of Unit 11.	6/10Y Gley 1	Sharp
12	0.10	25.12	Pedogenic carbonate layer.	Rusty	Sharp
13	1	26.12	Light gray silty mudstone.	5/10Y Gley 1	Sharp
14	0.80	**24.32 (88.30 ft)**	Pedogenic carbonate layer. Location of MOR-693 dinosaur nest. Off-white colored bone present in pedogenic carbonate. One small invertebrate shell present in pedogenic carbonate. Calcite precipitation veins.	Rusty	-

7. EGG MOUNTAIN B

Willow Creek Anticline, Choteau, MT
N 47° 48.447' W112^{o} 25.891' 19 ft accuracy
Elevation at base of section: ~ 4332 ft
Dip 8° NW

Unit	Thickness (m)	Total Thickness (m)	Unit Description	Unit Color (Munsell, 2000)	Upper Contact
1	3.8	-	Dark purple mudstone. Light pink bone in float (2cm long).	3/1 10R	Sharp
2	0.27	4.07	Pedogenic carbonate layer. Calcite precipitation veins.	Rusty	Sharp
3	1.75	5.82	Dark green gray silty mudstone.	4/N Gley 1	Sharp
4	0.12	5.94	Light gray limestone.	Light gray	Sharp
5	3.7	9.64	Light gray mudstone changing to silty mudstone. Calcite precipitation veins. Light pink bone in float (up to 5 cm long). Eggshell in float.	6/5G Gley 1	Sharp
6	0.12	9.76	Light gray limestone.	Light gray	Sharp
7	0.65	10.41	Light gray mudstone.	6/5G 1Gley	Sharp
8	0.06	**10.47 (34.34 ft)**	Light gray limestone.	Light gray	-

8. EGG MOUNTAIN C

Willow Creek Anticline, Choteau, MT
N 47° 48.539' W112^{o} 25.715' 27 ft accuracy
Elevation at base of section: ~ 4363 ft
Dip11^{o} SW

Unit	Thickness (m)	Total Thickness (m)	Unit Description	Unit Color (Munsell, 2000)	Upper Contact
1	0.85	-	Dark maroon mudstone grading to silty mudstone. One piece of light pink bone 3 cm long at base. Pieces of eggshell.	6/3 10R	Sharp
2	0.35	1.20	Pedogenic carbonate layer.	Rusty	Sharp
3	1.7	2.90	Light gray pink silty mudstone. Forms low slope.	6/2 2.5YR	Sharp
4	0.45	3.35	Pedogenic carbonate layer. Not continuous, but small ridge former.	Rusty	Sharp
5	1.52	4.87	Light maroon brown silty mudstone, followed by salt and pepper moderately sorted subangular to subrounded fine-grained sandstone with burrows 1 cm in diameter. Sandstone	7/1 2.5 Y	Sharp

			pinches out to E. One piece of light pink bone in float. Sandstone capped by nodular pedogenic carbonate layer at 0.73 m up from base		
6	0.30	5.17	Light maroon brown silty mudstone. Some pedogenic carbonate nodules at base. Lots of small pieces of light pink bone to the W, appear to be in place.	5/2 10R	Sharp
7	0.04	5.21	Light gray very fine-grained sandstone alternating with layers of maroon. Fines upward to a light gray siltstone	6/1 7.5YR	Gradational
8	1.1	6.31	Alternating light gray and light purple silty mudstone. Some calcite precipitation layers. Fines upward to a dark purple mudstone.	6/1/10R 5/1 2.5YR 5/2 10YR	Sharp
9	0.8	7.11	Light gray very fine sandstone. Forms a slight ridge. Possible ripples. Coarsens upward to moderately sorted, subrounded salt and peppery fine sandstone. Then fines up to light gray very fine sandstone. Some burrows 0.5-1 cm diameter.	8/N Gley 1	Sharp
10	1	8.11	Pedogenic carbonate layer. Large blocky pieces, interfingering with purple mudstone.	Rusty	Sharp
11	0.87	8.98	Salt and peppery fine sandstone. Large 2-3 cm burrows in float.	8/N Gley 1	Sharp
12	0.25	9.23	Pedogenic carbonate layer. Large blocky pieces and nodules.	Rusty	Sharp
13	1.55	10.78	Fine sandstone similar to unit 11. Burrows 2 cm diameter. Maroon mud clasts within sandstone 1 cm in diameter. Coarsens to salt and pepper subangular medium-grained sandstone. Pieces of light pink colored bone up to 4 cm long in float.	8/N Gley 1	Sharp
14	0.20	10.98	Pedogenic carbonate layer. Large blocky nodules loosely forming a layer.	Rusty	Sharp
15	0.60	11.58	Light red brown silty mudstone.	5/2/ 10R	Sharp
16	0.17	11.75	Light grey very fine sandstone. Forms resistant ledge.	8/N/Gley	Sharp
17	0.50	12.25	Dark maroon brown silty mudstone.	5/2/10R	Sharp
18	0.80	13.05	Pedogenic carbonate layer. Forms thin hard layer.	Rusty	Sharp
19	0.75	13.80	Tan siltstone to very fine sandstone.	7/1 5YR	Gradational
20	0.95	14.75	gray green silty mudstone	4/5PB Gley 2	Sharp
21	0.55	15.30	Gray green limestone.	Gray green	Sharp
22	0.50	15.80	Medium purple mudstone.	5/1 10R	Sharp
23	0.65	16.45	Unit 21 repeated.	Gray green	Sharp
24	0.20	16.65	Grey silty mudstone.	5/1 10R	Sharp
25	0.55	17.20	Pedogenic carbonate.	Rusty	Sharp
26	0.50	17.70	Grey purple mudstone.	5/1 10R	Sharp
27	0.40	18.10	Units 21 and 23 repeated.	Gray green	Sharp
28	0.40	18.50	Dark purple mudstone.	5/1 10R	Sharp

29	0.25	18.75	Pedogenic carbonate layer. Thick, blocky, forms resistant ledge. Some calcite precipitation.	Rusty	Sharp
30	1.5	20.35	Unit 28 repeated. Then changes to light grey mudstone.	5/1 10R	Sharp
31	1	21.35	Pedogenic carbonate layer. Interfingering dark purple mudstone.	Rusty	Sharp
32	0.85	22.20	Light gray mudstone. Some vegetation cover.	6/10Y Gley 1	Sharp
33	0.15	22.35	Groundwater carbonate layer. Large blocky, forms resistant ledge.	Rusty	Sharp
34	0.90	23.25	Grey brown mudstone.	6/10Y Gley 1	Sharp
35	0.95	**24.20 (79.38 ft)**	Pedogenic carbonate layer. Large blocky, forms resistant top ledge of section. Grass covered at very top.	Rusty	-

9. FAULT MOUNTAIN 1

Willow Creek Anticline, Choteau, MT
N 47° 49.021' W112^{o} 25.437' 23 ft accuracy
Elevation at base of section: ~ 4378 ft
Dip 12° N-NW

Unit	Thickness (m)	Total Thickness (m)	Unit Description	Unit Color (Munsell, 2000)	Upper Contact
1	2.75	-	Purple grey silty mudstone.	5/N/G/N Gley 1	Sharp
2	1.17	3.92	Purple mudstone with green mottling. Forms a resistant ledge. Dinosaur egg shell in float 1.5 cm in diameter.	4/1 10R	Sharp
3	1.0	4.92	Light grey silty mudstone.	7/10Y 1 Gley	Sharp
4	0.13	5.05	Pedogenic carbonate layer.	Rusty	Sharp
5	0.47	5.52	Light grey silty mudstone.	7/10Y Gley 1	Sharp
6	1.4	6.92	Salt and peppery very fine sandstone. Subangular grains. Calcite cemented.	7/1 2.5Y	Sharp
7	0.35	**7.27 (23.85 ft)**	Purple mudstone with light green mottling. Forms top of section	5/1 10R	-

10. FAULT MOUNTAIN 2

Willow Creek Anticline, Choteau, MT
N 47° 49.037' W112° 25.531' 21 ft accuracy
Elevation at base of section: ~ 4397 ft
Dip 5° NW

Unit	Thickness (m)	Total Thickness (m)	Unit Description	Unit Color (Munsell, 2000)	Upper Contact
1	0.7	-	Light grey silty mudstone grading up to siltstone.	6/5PB Gley 2	Sharp
2	1.3	2.0	Grey green fine sandstone. Forms hard ledge. Well sorted, subrounded. Calcite cemented. Some calcite precipitation layers.	6/N Gley 1	Sharp
3	1.5	3.5	Purple grey silty mudstone. Less silty near top.	5/1 2.5YR	Sharp
4	0.47	3.97	Light green silty mudstone with purple mottling. Thick and blocky.	5/10Y Gley 1	Sharp
5	0.08	4.05	Pedogenic carbonate nodular layer.	Rusty	Sharp
6	6.0	10.05	Alternating purple and green mudstone. Forms steep slope. Two pedogenic carbonate nodular layers near top, first at 4.8 m up from base and second at 5.35 m.	4/N Gley 1 5/N Gley 1	Sharp
7	1.8	11.85	Alternating purple and green shale. Some pedogenic carbonate nodules within.	4/1 10R 6/5G Gley 1	Sharp
8	0.38	12.23	Light grey very fine sandstone. Forms resistant ledge.	6/10Y Gley 1	Sharp
9	0.72	**12.95 (42.48 ft)**	Light grey very fine sandstone. Purple mud clasts 2 cm in layer approximately 2 cm thick on top.	7/10Y Gley 1	Sharp

11. FLAMING CLIFFS

Willow Creek Anticline, Choteau, MT
N 47° 49.200' W112° 26.144' 19 ft accuracy
Elevation at base of section: ~ 4469 ft
Dip 9° NW

Unit	Thickness (m)	Total Thickness (m)	Unit Description	Unit Color (Munsell, 2000)	Upper Contact
1	2.09	-	Purple brown mudstone with alternating bands of light gray and light purple. Two	6/5PB 2	Sharp

			interbedded, laterally short moderately sorted, subangular-subrounded sandstone lenses approximately 12 cm thick and located at 1.25 m and 1.8 m up from base.	Gley	
2	7	9.09	Light green medium to coarse-grained, poorly sorted, subangular to subrounded sandstone. Abundant purple and light green mudstone rip-up clasts present throughout, but mostly concentrated at the base thru middle, and ranging in 1mm-5cm in diameter. Trough cross bedding at base and thru middle.	5/5BG 2 Gley	Sharp
3	3.23	12.32	Dark purple to light brownish purple mudstone. Color changes from dark purple brown to grey-purple-brown with green mottling at 2.3 m up from base.	5/5PB Gley 2	Sharp
4	3.95	16.27	Off white-light gray silty mudstone (?). Very well indurated. Possibly containing volcanic glass. Color changes to purple grey in top.	7/N 1 Gley	Sharp
5	0.67	16.94	Green gray silty mudstone. Calcite precipitation veins present throughout. Thickness varies laterally. Upper contact marked by calcite precipitate layer 1 cm thick.	6/5G 1 Gley	Sharp
6	0.55	17.49	Dark purple mudstone. Calcite precipitation veins. Some green mottling. Possible slickensides.	6/1 10R	Gradational
7	0.28	17.77	Purple mudstone. Grades to light green color. Color change marked by calcite precipitation layer.	6/1 10R	Sharp
8	2.55	20.32	Off white to light gray siltstone coarsening upwards to very fine sandstone. Abundant large (0.5 mm) biotite grains. Near top sandstone present as very well indurated beds 1-5 cm thick separated by lenses of less indurated sandstone. Some mudstone rip-up clasts 1 cm in diameter present.	7/10Y 1 Gley	Sharp
9	0.12	20.44	Dark purple mudstone. Very well indurated. Some very fine to fine-grained sandstone clast inclusions 1-4 cm in diameter.	4/1 5YR	Sharp
10	0.15	20.59	Salt and peppery medium-grained angular to subangular sandstone.	8/1 5Y	Sharp
11	0.10	20.69	Unit 9 repeated.	4/1 5YR	Sharp
12	1	21.69	Off white to light gray siltstone. Some calcite precipitation veins. Possible soft sediment deformation at upper contact.	8/1 5Y	Sharp (Irregular)
13	0.40	22.09	Dark purple mudstone. Forms hard ridge. Two slightly siltier green beds interbedded within, and located at 18 cm and 30 cm up from base. 14 cm thick pedogenic carbonate layer present within unit.	5/1 10R	Sharp
14	0.15	22.24	Light gray-white siltstone.	6/N 1 Gley	Sharp
15	0.22	22.46	Light green gray silty mudstone forming resistant bench. Nodular pedogenic carbonate layer present within unit.	-	Sharp
16	0.25	22.71	Unit 14 repeated.	6/N 1 Gley	Sharp
17	0.08	22.79	Unit 15 repeated.	-	Sharp
18	0.30	23.09	Light purple to light green gray mudstone.	5/5PB 2	Sharp

				Gley	
19	0.65	23.74	Off-white to tannish gray silty mudstone. Calcite precipitation veins.	6/1 10YR	Sharp
20	0.22	23.96	Light gray mudstone.	-	Sharp
21	0.80	24.76	Light gray silty mudstone coarsening upwards to very fine-grained sandstone.	7/1 5YR	Sharp
22	0.40	25.16	Light gray very fine-grained moderately-well sorted, subangular sandstone. Calcite precipitation veins.	6/10Y Gley 1	Sharp
23	1.5	26.66	Light to medium purple mudstone with some light green mottling. Nodular pedogenic carbonate layer 85 cm up from base.	6/1 10R	Sharp
24	0.12	26.78	Light gray to off-white very fine-grained sandstone. Calcite cemented, ledge former.	8/N 1 Gley	Sharp
25	0.62	27.40	Light purple to light gray silty mudstone. Calcite precipitation veins. Upper contact marked by calcite precipitation layer.	7/5PB 2 Gley	Sharp
26	0.15	27.55	Dark purple mudstone. Very fissile.	3/1 10R	Sharp
27	0.14	**27.69 (90.82 ft)**	Light gray to off-white very fine-fine-grained moderately-well sorted, subangular sandstone. Some small holes present – possible eroded mud rip-up clasts.	7/N Gley 1	-

12. FRANS SITE

Willow Creek Anticline, Choteau, MT
N 47° 48.523' W112^{o} 25.972' 20 ft accuracy
Elevation at base of section: ~ 4343 ft
Dip 20° SW

Unit	Thickness (m)	Total Thickness (m)	Unit Description	Unit Color (Munsell, 2000)	Upper Contact
1	2.3	-	Grey, purple, green mudstone.	5/10G Gley 2	Sharp
2	0.35	2.65	Groundwater carbonate layer. Large and blocky.	Rusty	Sharp
3	0.4	3.05	Unit 1 interfingering into unit 2.	4/1 10R	Sharp
4	0.15	3.20	Rusty gray green limestone	Rusty gray green	Sharp
5	0.6	3.80	Unit 3 repeated and interfingering into unit 4.	4/1 10R	Sharp
6	0.15	3.95	Nodular groundwater carbonate.	Rusty	Gradational
7	2.8	6.75	Dark purple mudstone with interfingering nodular groundwater carbonate layers 4-7 cm thick. Carbonate sticks out as resistant rusty protrusions. First prominent carbonate layer at 1.75 m up from base, second at 2.1 m up from base.	4/1 10R	Gradational

8	8	**14.75 (48.38 ft)**	Dark purple mudstone. Bottom forms a low slope while top is steep. Top covered by grass. Light pink colored bone in float up to 3 cm in length.	4/1 10R	-

13. JESS BUTTE

Willow Creek Anticline, Choteau, MT
N 47° 48.161' W112^{o} 25.494' 16 ft accuracy
Elevation at base of section: ~ 4337 ft
Dip 6° E-NE

Unit	Thickness (m)	Total Thickness (m)	Unit Description	Unit Color (Munsell, 2000)	Upper Contact
1	7.1	-	Light grey mudstone, becomes siltier as go up. Lense of light grey very fine sandstone, thins to SE.	6/10G Gley 2	Sharp
2	0.25	7.35	Pedogenic carbonate layer of loose nodules approximately 9 cm in diameter.	Rusty	Sharp
3	6.0	13.35	Grass covered interval.	-	Sharp
			CHANGE 35.40 m TO EAST		Sharp
4	0.65	14.0	Purple mudstone, gets siltier as go up. Forms resistant layer.	4/2 10R	Sharp
5	0.74	14.74	Light grey very fine sandstone, well sorted, subangular, horizontally laminated.	7/1 2.5Y	Sharp
6	0.4	15.14	Reddish purple shale.	5.2 10R	Sharp
7	0.5	15.64	Light grey very fine sandstone, well sorted, subangular, horizontally laminated. Forms resistant ledge.	7/1 2.5Y	Sharp
8	0.7	16.34	Brownish purple shale.	6/1 10R	Sharp
9	4.0	20.34	Purple grey very fine sandstone. Forms resistant ledge. Some ripple marks in center of unit. Burrows 1-2 cm diameter.	7/10Y Gley 1	Sharp
10	2.3	22.64	Light grey silty mudstone, becomes less silty up unit and then become silty again.	6/1 7.5YR 5/2 10R	Gradational
11	1.9	24.54	Light purple grey silty mudstone	6/2 10R	Gradational
12	1.55	26.09	Light grey siltstone, becomes coarser up unit.	7/10Y Gley 1	Gradational
13	1.0	27.09	Light grey very fine sandstone.	7/10Y Gley 1	Sharp
14	8.6	35.09	Purple brown mudstone, becomes less silty up unit. Forms steep slope. Pedogenic carbonate and chert nodules present throughout.	7.3 2.5YR 6/3 2.5YR 5/2 2.5YR	Hidden
15	1.45	**37.14 (121.82 ft)**	Light grey very fine sandstone, subangular-subrounded. Burrows present 0.5 cm diameter. Ripple marks present.	7/2 2.5YR	-

14. JOSH'S HILL

Willow Creek Anticline, Choteau, MT
N 47° 48.696' W112^{o} 25.274' 18 ft accuracy
Elevation at base of section: ~ 4326 ft
Dip 8° W

Unit	Thickness (m)	Total Thickness (m)	Unit Description	Unit Color (Munsell, 2000)	Upper Contact
1	3.7	-	Salt and pepper medium-grained sandstone, well sorted, subrounded. Contains lenses of reddish brown mudstone. Some calcite precipitation layers near top.	8/N 1 Gley	Sharp
2	0.45	4.15	Reddish brown siltstone with some mud clasts and filled in burrows. Forms a hard resistant ledge.	8/N 1 Gley	Sharp
3	0.75	4.90	Grey green very fine-fine-grained sandstone, subangular to subrounded grains, moderately sorted.	7/10Y Gley 1	Sharp
4	0.47	5.37	Reddish brown mudstone.	5/3 10R	Sharp
5	0.15	5.52	Unit 2 repeated.	8/N 1 Gley	Sharp
6	5.25	10.77	Reddish brown silty mudstone.	5/2 10R 7/5PB 2 Gley	Sharp
7	0.10	**10.87 (35.65 ft)**	Light greenish grey siltstone. Calcite precipitation layers.	7/1 5YR	-

15. JUSTIN'S PEAK

Willow Creek Anticline, Choteau, MT
N 47° 48.683' W112^{o} 25.258' 23 ft accuracy
Elevation at base of section: ~ 4372 ft
Dip 12° W-NW

Unit	Thickness (m)	Total Thickness (m)	Unit Description	Unit Color (Munsell, 2000)	Upper Contact
1	3.52	-	Salt and pepper medium to coarse-grained sandstone. Moderately sorted, subangular, calcite cemented. One portion 7 cm thick is full of rip-up clasts 1-5 cm diameter. At 3.2 m up from base becomes finer grained to more of a siltstone. One piece of dinosaur egg shell in float.	Salt and pepper	Sharp
2	0.25	3.77	White and grey green bentonite layer.	Whitish	Sharp

				green	
3	0.6	4.37	Light grey silty mudstone, becomes coarser up unit turning to siltstone-very fine sandstone, subangular grains.	7/10Y Gley 1	Sharp
4	0.02	4.39	Purple mudstone.	5/1 10R	Sharp
5	4.9	**9.29 (30.47 ft)**	1st: Tan medium to coarse-grained sandstone, moderately sorted, angular to subangular grains; 1 cm thick. 2nd: Coarse-grained sandstone with very abundant green, purple, red, and white mud rip-up clasts 1 mm to 0.5 cm diameter; 18 cm thick. 3rd: Trough crossbedded medium to coarse-grained sandstone; 15 cm thick. 4th: Salt and pepper medium-grained sandstone. 5th: 4th sandstone becomes interfingered with reddish purple mudstone in lenses 7-10 cm thick. Top capped by rusty very fine-grained sandstone with purple red mud rip-up clasts 1 mm diameter.	Salt and pepper	-

16. LAKE GIARDIA

Willow Creek Anticline, Choteau, MT
N 47° 48.918' W112° 25.260' 18 ft accuracy
Elevation at base of section: ~ 4324 ft
Dip 4° N-NW

Unit	Thickness (m)	Total Thickness (m)	Unit Description	Unit Color (Munsell, 2000)	Upper Contact
1	0.2	-	Purple mudstone.	4/1 10R	Sharp
2	2.3	2.5	Green grey medium to coarse-grained trough cross bedded sandstone. Angular to subangular grains. Forms thick unit with trough cross-beds. Abundant purple and green mudstone rip-up clasts 2 mm-5 cm diameter. Clasts more abundant in base.	6/10Y Gley	Sharp
3	2.4	4.9	Purple mudstone.	4/1 10R	Sharp
4	1.7	6.6	Unit 2 repeated. Goes from fine to medium-grained sandstone to medium to coarse-grained sandstone to fine to medium-grained sandstone. All sandstone trough cross bedded. Purple mudstone rip-up clasts 2mm-5 cm diameter. More larger sized clasts and concentrated in the medium to coarse-grained section.	4/1 10R	Sharp
5	3.55	10.15	Purple mudstone with green mottling. Calcite precipitation layers throughout. Some portions thinly bedded (shale).	5/10G Gley 2 5/1 10R	Sharp
6	0.6	10.47	Light grey very fine-grained sandstone. Forms resistant ledge. Then a thin mudstone bed.	Light Grey	Sharp
7	1.0	11.75	Silty mudstone with calcite precipitation layers.	6/N Gley 1	Sharp
8	0.08	**10.83**	Light grey very fine sandstone. Subangular to subrounded grains. Forms hard cap on hill.	Light Grey	-

		(35.52 ft)	One piece of hadrosaur eggshell on top of hill.		

17. NEST IN THE WALL BENTONITE

Willow Creek Anticline, Choteau, MT
N 47° 48.783' W112^{o} 25.511' 20 ft accuracy
Elevation at base of section: ~ 4358 ft
Dip 5° W-NW

Unit	Thickness (m)	Total Thickness (m)	Unit Description	Unit Color (Munsell, 2000)	Upper Contact
1	2.05	-	Salt and pepper medium-coarse-grained trough cross bedded sandstone. Angular-subangular grains, moderately sorted. Some calcite precipitation grains. Pink and red mudstone rip-up clasts 1-5 cm diameter in bottom portion. From 1.15-1.33 m up from base, fine-medium-grained sandstone. Then coarsens slightly.	Salt and pepper	Sharp
2	0.4	2.45	Pinkish brown mudstone	5/2 10R	Sharp
3	0.55	3.0	Salt and pepper medium-coarse-grained sandstone. Moderately sorted, angular-subangular. Thin 3 cm thick layer of mudstone at 0.25 m up from unit base.	Salt and pepper	Sharp
4	0.42	3.42	Unit 2 repeated. Fine-medium-grained sandstone lense 25 cm thick at 0.2 m up from base.	5/2 10R	Sharp
5	0.07	3.49	Light gray siltstone-very fine sandstone. Some ripple cross lamination on top.	Light gray	Sharp
6	0.22	3.71	Unit 2 repeated.	5/2 10R	Sharp
7	0.09	3.8	Light gray very fine ripple cross laminated sandstone.	Light gray	Sharp
8	0.45	4.25	Unit 2 repeated. Three thin sandstone interbeds.	5/2 10 R	Sharp
9	2.54	6.79	Unit 2 mudstone repeated but a little siltier. Color changes to light green gray at top.	5/2 10R	Sharp
10	0.43	7.22	Light green gray very silty mudstone.	7/10Y Gley 1	Sharp
11	0.45	7.67	Pedogenic carbonate layer. Forms resistant bench.	Rusty	Sharp
12	1.35	9.02	Light grey siltstone.	7/10Y Gley 1	Sharp
13	0.07	9.09	Bentonite layer. Calcite precipitation layer at upper contact.	5/2 10R	Sharp
14	0.34	9.43	Light green gray silty mudstone coarsening up to light green medium sandstone.	7/10Y Gley 1	Sharp
15	1.53	10.96	Purple red mudstone. Nodular loose pedogenic carbonate layer at 0.95 m up from base.	6/2 10R	Sharp
16	1.4	12.36	Light red brown mudstone. Some calcite precipitation veins. Where seed casts are weathering out.	5/1 10R	Sharp

17	1.4	13.76	Salt and pepper medium-grained sandstone fining up to fine-grained sandstone. Trough cross bedding in coarser basal part. Ripples and planar bedding in top portions. Abundant burrows 1.5-2 cm diameter, 8 cm long.	7/10Y Gley 1	Sharp
18	1.63	15.39	Claystone changing to light brown/orange silty mudstone changing to light green silty mudstone. Some dinosaur bones (bonebed).	Light Brown Light Green	Sharp
19	3.83	19.22	Light green silty mudstone. Calcite precipitation veins. Goes from massive to thinly bedded then to massive.	7/5GY Gley 1	Sharp
20	0.21	19.43	Bentonite layer.	6/1 10R	Sharp
21	2.8	22.23	Light green gray mudstone. Color changes to light purple at 0.5 m up from unit base.	7/5GY Gley 1 5/1 10R	Sharp
22	2.27	24.50	Charophytiferous limestone.	Light green gray	Sharp
			CHANGE 9.8 m NW		
23	1.6	26.1	Salt and pepper fine to medium-grained horizontally bedded sandstone. Forms a resistant bench. Mudstone rip-up clasts 0.5-5 cm diameter found mainly in bottom portion. Then coarsens upward to light green salt and pepper medium to coarse-grained sandstone.	7/10Y Gley 1 4/5 PB	Sharp
24	0.8	27.05	Light purple mudstone changing to dark purple.	4/5 PB	Sharp
			CHANGE 50.4 m W		
25	0.85	27.9	Purple gray mudstone.	5/1 10R	Sharp
26	0.3	28.2	Gray very fine to fine-grained sandstone.	6/10PG Gley 2	Sharp
27	0.7	28.9	Unit 2 repeated.	5/1 10R	Sharp
28	0.09	28.99	Nodular pedogenic carbonate layer.	Rusty	Sharp
29	0.95	29.94	Grey silty mudstone. Some pedogenic carbonate nodules in top.	6/N Gley 1	Sharp
30	0.38	30.32	Charophytiferous limestone.	Light green gray	Sharp
31	0.8	31.12	Unit 29 repeated. Charophytiferous limestone layer at 0.53 m up from base.	6/N Gley 1	Sharp
32	0.73	31.85	Charophytiferous limestone. Then a thin bed of unit 31, then another layer of charophytiferous limestone. Then Light green silty mudstone.	Light green gray 7/10Y Gley 1	Sharp
33	0.6	32.45	Charophytiferous limestone.	Light green	Sharp

				gray	
34	1.85	34.3	Light purple mudstone.	5/5 PB	Gradational
35	1.93	36.23	Light green silty mudstone. Gets darker green as go up.	7/10Y	Sharp
36	0.38	36.61	Dark green sandy mudstone. Some sandy inclusions. Root traces in top portion.	6/10GY Gley 1	Sharp
37	0.9	37.51	Light green mudstone.	6/10 GY	Sharp
38	0.82	38.33	Light green/light purple mottled mudstone.	7/10GY 5/1 10R	Sharp
39	1.2	39.53	Light tan gray very fine horizontally bedded sandstone. Moderately sorted, subangular grains. Troodon eggshell in float.	Light gray tan	Sharp
40	1.33	40.86	Light grey siltstone. Forms a step. Possible burrows, 1cm diameter.	6/1 2.5 YR	Sharp
41	0.07	40.93	Light green/light purple mottled mudstone.	7/10GY 5/1 10R	Sharp
42	0.5	41.43	Light gray very fine sandstone. Mudstone rip-up clasts I cm diameter. Burrows 0.5-1cm diameter. Horizontal bedding and ripple marks on top.	Light gray	Sharp
43	0.39	41.82	Light brown silty mudstone.	6/1 10R	Sharp
44	0.45	42.27	Purple red mudstone. Some mottling.	6/1 10R	Sharp
			CHANGE 44 m WEST		
45	0.1	42.37	Light green mudstone.	7/5 GY	Sharp
46	0.45	42.82	Light brown silty mudstone.	7/1 10R	Sharp
47	0.9	43.72	Bentonite layer. Equivalent to bentonite in Thunder Dome bentonite section.	White	Sharp
48	2.87	46.59	Alternating light gray/purple silty mudstone.	6/N Gley 1 5/1 10R	Sharp
49	0.2	46.79	Groundwater carbonate layer.	Rusty	Sharp
50	2.12	48.91	Light gray mudstone. Pupal cases 3-4 cm long and abundant in float. Bone fragments 2 cm long. Calcite precipitation veins.	7/10Y 5/1 10R	Sharp
51	0.6	49.51	Salt and pepper very fine horizontally bedded to massive sandstone. Moderate-well sorted, subangular grains. Burrows 1-2 cm diameter in top.	Salt and pepper	Sharp
52	3.15	52.66	Light grey silty mudstone. Where Nest in the Wall dinosaur nest site is.	6/1 7.5 YR	Sharp
53	0.2	52.86	Purple/ green mottled mudstone.	6/1 10R	Sharp
54	0.67	53.53	Groundwater carbonate layer. Could possibly be limestone?	Rusty	Sharp
55	1.88	55.41	Light grey siltstone. Some pieces of dinosaur egg shell with bumps.	7/10 GY	Sharp
56	1.3	56.71	Salt and pepper fine to medium-grained sandstone. Forms resistant bench. Moderately sorted, subangular to subrounded grains. Horizontally bedded in bottom portion. Then trough cross bedded with very abundant mudstone rip-up clasts 0.5-1 cm diameter in base.	7/10Y Gley 1 White	Sharp Irregular

			Some burrows 1-2 cm diameter in top.		
57	1.65	58.36	Purple mudstone with some green mottling. Then thinly bedded mudstone. Then massive mudstone.	7/1 10R 7/10Y	Sharp
58	3.2	61.56	Light green very fine horizontally bedded sandstone. Small mudstone rip-up clasts 0.5 cm diameter abundant in base. Then grades to very fine to fine-grained horizontally bedded sandstone with thicker beds (~3 cm). Ripple marks in top portion.	6/10Y White	Sharp
59	0.35	**61.91 (203.07 ft)**	Medium purple mudstone. One pupal case in float Burrows in float 1-2 cm diameter.	7/1 10R	-

18. NOSE CONE 2

Willow Creek Anticline, Choteau, MT
N 47° 48.812' W112^{o} 25.577' 17 ft accuracy
Elevation at base of section: ~ 4382 ft
Dip 3°NW

Unit	Thickness (m)	Total Thickness (m)	Unit Description	Unit Color (Munsell, 2000)	Upper Contact
1	0.14	-	Basal clay layer in sharp contact with bonebed. Orange clasts 2-3 cm long and brown silty mudstone up to fist sized clasts.	Dark green/black	Sharp Irregular
2	0.46	0.6	TM-003 bonebed. Light brown silty mudstone with orange and white siltstone clasts 1-3 cm long. Abundant pieces of dinosaur bone 1-10+ cm long. Light brown color grades to light brownish green.	Light brown to Light brownish green	Sharp
3	0.73	1.33	Light green silty mudstone. Orange and white siltstone clasts present but not as abundant. One piece of bone 5 cm long found in light green silty mudstone a little above contact with unit 3. Calcite precipitation veins cutting across at sharp angles in light green silty mudstone.	Light green	Sharp
4	1.53	2.86	Light green thinly bedded silty mudstone. Burrows 7 cm long, 1 cm diameter. Orange staining on layers. Prominent bands of orange staining at: 0.57 m, 0.65 m, 0.85 m, and 1.08 m above unit base.	Light green	Buried under vegetation
5	3.92	6.78	Vegetation covered interval.	-	Sharp
6	0.13	6.91	Charophytiferous limestone layer.	Light green gray	Sharp
7	0.7	7.61	Dark gray purple mudstone.	3/N Gley 1	Buried under vegetation
8	5.2	12.81	Vegetation covered interval.	-	Sharp

9	0.15	12.96	Black silty mudstone.	4/N Gley 1	Sharp
10	1.92	**14.88 (48.81 ft)**	Charophytiferous limestone.	Light green gray	-

19. PETE'S PUPA PENINSULA

Willow Creek Anticline, Choteau, MT
N 47° 48.962' W112° 25.450' 16 ft accuracy
Elevation at base of section: ~ 4378 ft
Dip 11° NW

Unit	Thickness (m)	Total Thickness (m)	Unit Description	Unit Color (Munsell, 2000)	Upper Contact
1	0.8	-	Grey carbonate cemented sandstone. Forms resistant bench layer. Can't see the base. Contains abundant pupa cases 1cm x 2 cm. Weathers in large angular blocks.	6/1 10R	Sharp
2	0.72	1.52	Dark purple grey mudstone. Very fissile. Irregular sharp contact due to soft sediment deformation.	3/1 10R	Irregular Sharp
3	0.4	1.92	Unit 1 repeated. Abundant pupa cases. Forms resistant ledge.	6/1 10R	Sharp
4	0.15	2.07	Unit 2 repeated.	3/1 10R	Sharp
5	1.88	3.95	Units 1 and 3 repeated. Abundant pupa cases. Root traces and burrows 2 cm long. Interbedded repeat of unit 2 (3-5 cm thick).	6/1 10R	Sharp
6	0.3	4.25	Dark black mudstone. Very fissile.	4/N Gley 1	Sharp
7	0.22	**4.47 (14.66 ft)**	Light grey charophytiferous limestone. Forms resistant cap.	Light grey	-

20. THUNDER DOME

Willow Creek Anticline, Choteau, MT
N 47° 48.962' W112° 25.450' 16 ft accuracy
Elevation at base of section: ~ 4378 ft
Dip 11° NW

Unit	Thickness (m)	Total Thickness (m)	Unit Description	Unit Color (Munsell, 2000)	Upper Contact
1	2.8	-	Brown black mudstone. Two lenses of nodular pedogenic carbonate (at 1.3 m and 1.95 m above unit base).	2.5/5G Gley 1	Sharp
2	0.17	2.97	Charophytiferous limestone.	Light grey green	Sharp
3	0.60	3.57	Green grey mudstone. Lense of pedogenic carbonate nodules present.	6/5GY Gley 1	Sharp
4	0.9	4.47	Greenish purple thinly bedded mudstone. Some calcite precipitation layers.	5/10B Gley 2 5/5 PB	Gradational
5	1.55	6.02	Purple brown mudstone. Lense of very fine-grained sandstone at 1.21 m above base.	6/1 2.5 YR	Gradational
6	0.14	6.16	Unit 5 continued.	6/1 2.5 YR	Gradational
7	0.85	7.01	Light gray fine-grained sandstone.	Light gray	Sharp
8	0.3	7.31	Pedogenic carbonate layer	Rusty	Sharp
9	1.45	8.76	Purple brown mudstone grading to grey green color.	6/1 10R 6/10Y 1 Gley	Sharp
10	0.6	9.36	Purple green mudstone.	Purple green	Sharp
			CHANGE 1.5 m N		
11	1.35	10.71	Light grey green mudstone. Lense of pedogenic carbonate nodules at 1.1 m above base. Calcite precipitation layers parallel to beds.	6/5G Gley 1	Sharp
12	0.45	11.16	Purple thinly bedded mudstone. Calcite precipitation layers parallel to beds.	4/10B 5/5 BG	Sharp
13	0.8	11.96	Bentonite layer.	6/5 Gley 1	Sharp
14	4.55	16.51	Light green to purple mudstone. Calcite precipitation layers.	7/10GY 4/1 10R	Sharp
15	0.63	17.14	Light gray fine to medium-grained sandstone. Forms resistant ledge.	Light gray	Sharp

16	1.7	18.84	Green and purple mudstone. Calcite precipitation veins.	6/5 G 5/5 PB	Sharp
17	1.8	20.64	Alternating green and purple mudstone. Some mottling. Calcite precipitation layers.	6/5 G 5/10 G	Sharp
18	0.67	21.31	Light gray very fine sandstone.	7/N	Gradational
19	2	23.31	Light gray siltstone. Pedogenic carbonate layer at 0.85 m up from base.	6/N	Sharp
20	1.8	25.11	Gray green trough cross bedded very fine-grained sandstone. Coarsens up to trough cross bedded fine to medium-grained sandstone. Abundant burrows 1.5 cm diameter in top portion. Mudstone rip-up clasts 1 cm diameter in top.	6/5GY 6/10Y	Sharp
21	4.55	29.66	Purple reddish brown sitly mudstone and mudstone. Calcite precipitation layers. Two thin fingers possibly of bentonite	5/1 6/10Y 6/2 7/10Y	Sharp
22	1.7	31.36	Light gray siltstone. Some calcite precipitation veins. Lense of very fine sandstone at 0.8 m up from base.	7/10Y 6/5 PB	Sharp
23	0.75	32.11	Purple red mudstone.	5/2	Sharp
24	0.04	32.15	Light gray very fine sandstone.	7/1 2.5 YR	Sharp
25	0.95	33.10	Light gray silty mudstone	6/5 PB Gley 2	Sharp
26	0.5	33.60	Light gray fine-grained horizontally bedded sandstone.	7/N Gley 1	Sharp
27	0.9	34.50	Light purple mudstone with some green mottling.	5/1 10R	Sharp
28	0.11	34.61	Light gray fine-grained sandstone.	7/N Gley 1	Sharp
29	0.9	35.51	Light purple mudstone.	5/1 10R	Sharp
30	0.47	35.98	Light gray fine-grained sandstone.	7/N Gley 1	Sharp
31	0.23	36.21	Groundwater carbonate layer.	Rusty	Sharp
32	0.9	37.11	Light gray silty mudstone. Some small pieces of eggshell on surface (2-3 mm diameter).	6/5G Gley 1	Sharp
33	0.4	37.51	Groundwater carbonate layer.	Rusty	Sharp
34	1.25	38.76	Light gray siltstone fining up to purple mudstone.	6/1 5Y 6/10Y Gley 1	Sharp
35	0.2	38.96	Light gray very fine sandstone. Burrows 2cm diameter. Forms resistant ledge.	7/N Gley 1	Sharp
36	0.12	39.08	Light purple mudstone.	6/5PB Gley 2	Sharp
37	0.27	39.35	Light gray siltstone.	6/N Gley 1	Sharp

38	0.82	40.17	Light purple mudstone. Some small groundwater carbonate nodules.	5/1 10R	Sharp
39	0.63	40.80	Light gray fine to medium-grained sandstone.	7/N Gley 1	Sharp
40	0.95	41.75	Light gray very fine sandstone fining to siltstone.	6/10Y Gley 1	Sharp
41	0.09	41.84	Light purple mudstone.	5/1 10R	Sharp
42	0.95	42.79	Light gray silty mudstone.	6/10GY Gley 1	Sharp
43	0.15	42.94	Groundwater carbonate layer.	Rusty	Sharp
44	1.18	44.12	Light grey silty mudstone.	6/1 10R	Sharp
45	0.89	45.01	Light purple mudstone.	5/1 10R	Sharp
46	0.01	**45.02 (147.67 ft)**	Light gray siltstone. Root casts.	7/N Gley 1	-

21. THUNDER DOME BENTONITE

Willow Creek Anticline, Choteau, MT
N 47° 49.006' W112^{o} 25.715' 26 ft accuracy
Elevation at base of section: ~ 4422 ft
Dip 3° W-SW

Unit	Thickness (m)	Total Thickness (m)	Unit Description	Unit Color (Munsell, 2000)	Upper Contact
1	0.95	-	Purple mudstone.	Purple	Sharp
2	0.39	1.24	Charophytiferous limestone.	Light green gray	Sharp
3	1.45	2.69	Grey black mudstone.	Grey black	Sharp
4	0.09	2.78	Nodular pedogenic carbonate layer.	Rusty	Sharp
5	1.15	3.93	Light grey mudstone. Lense of pedogenic carbonate at 0.85 m up from base.	Light grey	Sharp
6	0.28	4.21	Pedogenic carbonate layer.	Rusty	Sharp
7	0.9	5.11	Light gray silty mudstone. Some pedogenic carbonate nodules and calcite precipitation.	Light gray	Sharp
8	0.13	5.24	Pedogenic carbonate layer.	Rusty	Sharp
9	0.6	5.84	Light green gray silty mudstone.	Light green gray	Sharp
10	0.20	6.04	Nodular pedogenic carbonate layer.	Rusty	Sharp
11	1.52	7.56	Light purple mudstone. Becomes bedded at top (1-3 cm thick beds). Some calcite	Light	Sharp

			precipitation layers.	purple	
12	0.12	7.68	Light gray very fine sandstone. Possible small ripple marks on top.	Light gray	Sharp
13	1.22	8.90	Light purple mudstone.	Light purple	Sharp
14	0.3	9.20	Nodular groundwater carbonate layer.	Rusty	Sharp
15	0.85	10.05	Light gray silty mudstone.	Light gray	Sharp
16	0.45	10.50	Light purple shale with green mottling. Nodular groundwater carbonate lense.	Light purple	Sharp
17	0.4	10.90	Purple mudstone with green mottling.	Purple	Sharp
18	0.99	11.89	Alternating dark purple and green mudstone.	Dark purple Green	Sharp
19	1	12.89	Bentonite layer.	White	Sharp
20	0.87	13.76	Alternating purple and green mudstone. (Unit 18 repeated)	Purple Green	Sharp
21	0.6	14.36	Off-white medium-grained sandstone. Massive.	Off white	Sharp
22	0.15	14.51	Light gray mudstone.	Light gray	Sharp
23	0.5	15.01	Purple and green mottled mudstone. Calcite precipitation layers.	Purple Green	Sharp
24	0.55	15.56	Groundwater carbonate layer.	Rusty	Sharp
25	1.7	17.26	Light gray green mudstone. Some calcite precipitation.	Light gray green	Sharp
26	0.6	17.86	Unit 25 becomes thinly layered purple shale with green mottling.	Purple Green	Sharp
27	0.8	18.66	Light green gray mudstone grading to purple.	Green gray Purple	Sharp
28	0.65	19.31	Salt and pepper medium-grained sandstone. Massive. Grades upward to a siltstone.	Salt and Pepper	Sharp
29	0.55	19.86	Light purple mudstone with green mottling. Some calcite precipitation.	Purple Green	Sharp
30	1.17	21.03	Light green medium to coarse-grained. Massive.	Light green	Gradational
31	0.7	21.73	Light green siltstone. Forms resistant ledge.	Light green	Sharp
32	5.1	**26.83 (88 ft)**	Light green medium to coarse-grained sandstone. Horizontally bedded at base then trough cross bedded. Then horizontally bedded again and then trough cross bedded again. Mudstone rip-up clasts 0.5-7 cm diameter at base. Lense of siltstone at top. Forms cap of ridge.	Light green	-

APPENDIX C

CORRELATION OF WILLOW CREEK ANTICLINE, TWO MEDICINE FORMATION TYPE SECTION, AND SEVEN MILE HILL AREA MEASURED SECTION DISCONTINUITIES

Figure 21: Correlation of Willow Creek anticline, Two Medicine Formation type section, and Seven Mile Hill area measured section discontinuities.

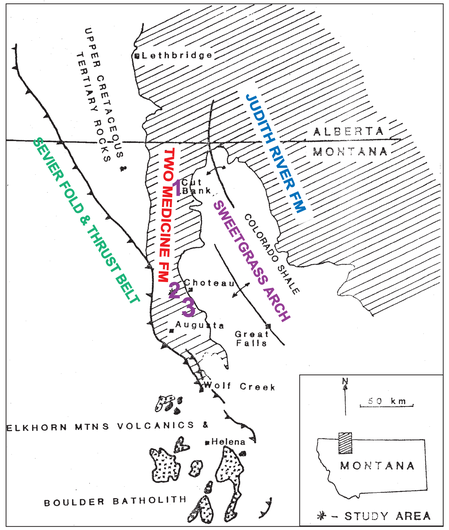

1: Two Medicine Formation Type Section
near Cut Bank, MT
75 km (47 mi) north of Willow Creek anticline
~90 km (56 mi) northwest of Seven Mile Hill area

2: Willow Creek anticline
19 km (12 mi) west of Choteau, MT
75 km (47 mi) south of Type Section
17 km (10.5 mi) northwest of Seven Mill Hill area

3: Seven Mile Hill area
9 km (6 mi) south of Choteau, MT
17 km (10.5 mi) southeast of Willow Creek anticline
~90 km (56 mi) southeast of Type Section

(Note: Measured sections are not to scale when sections in different areas are compared. Scale information for each is provided. Willow Creek anticline sections have been blown up relative to the other sections to show detail.)

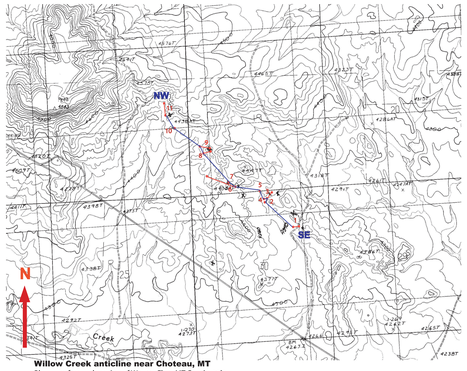

Willow Creek anticline near Choteau, MT
Blow-up of central portion of Watson Flats, MT Quadrangle
Scale 1:24,000
* Measured Sections shown in red
* SE-NW Cross Section shown in blue

1: Children's Dig
2: Justin's Peak
3: '78 Nest
4: Josh's Hill
5: '79 Nest
6: Nest in the Wall Bentonite
7: Nose Cone 2
8: Thunder Dome Bentonite
9: Thunder Dome
10: Egg Island
11: Flaming Cliffs

Topographic map and Key for Willow Creek anticline measured sections

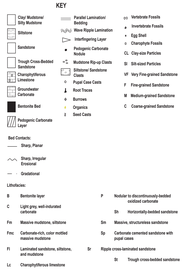

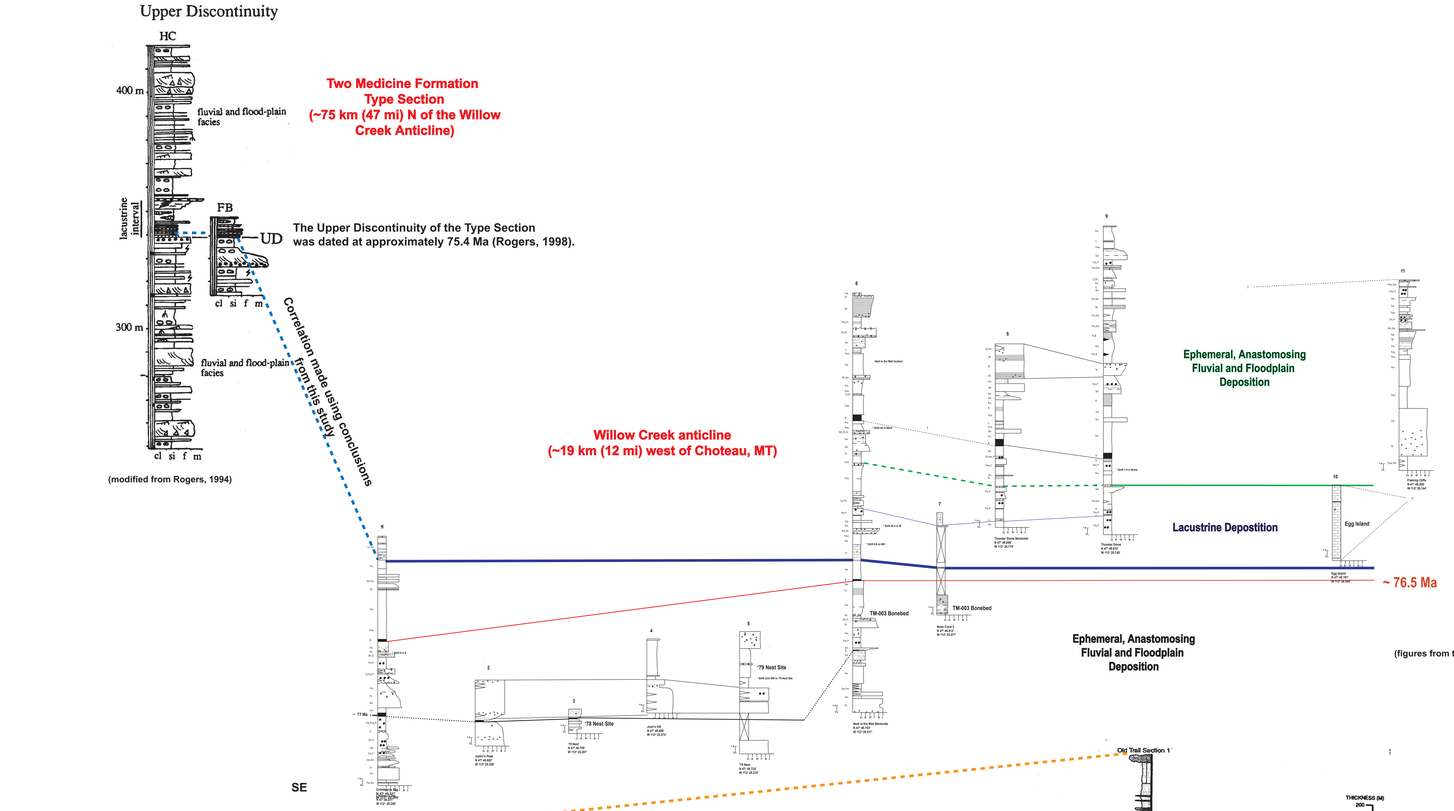

APPENDIX D

SE-NW STRATIGRAPHIC CROSS SECTION THROUGH MEASURED SECTIONS

APPENDIX D

Figure 26: SE-NW stratigraphic cross section through Willow Creek anticline measured sections.

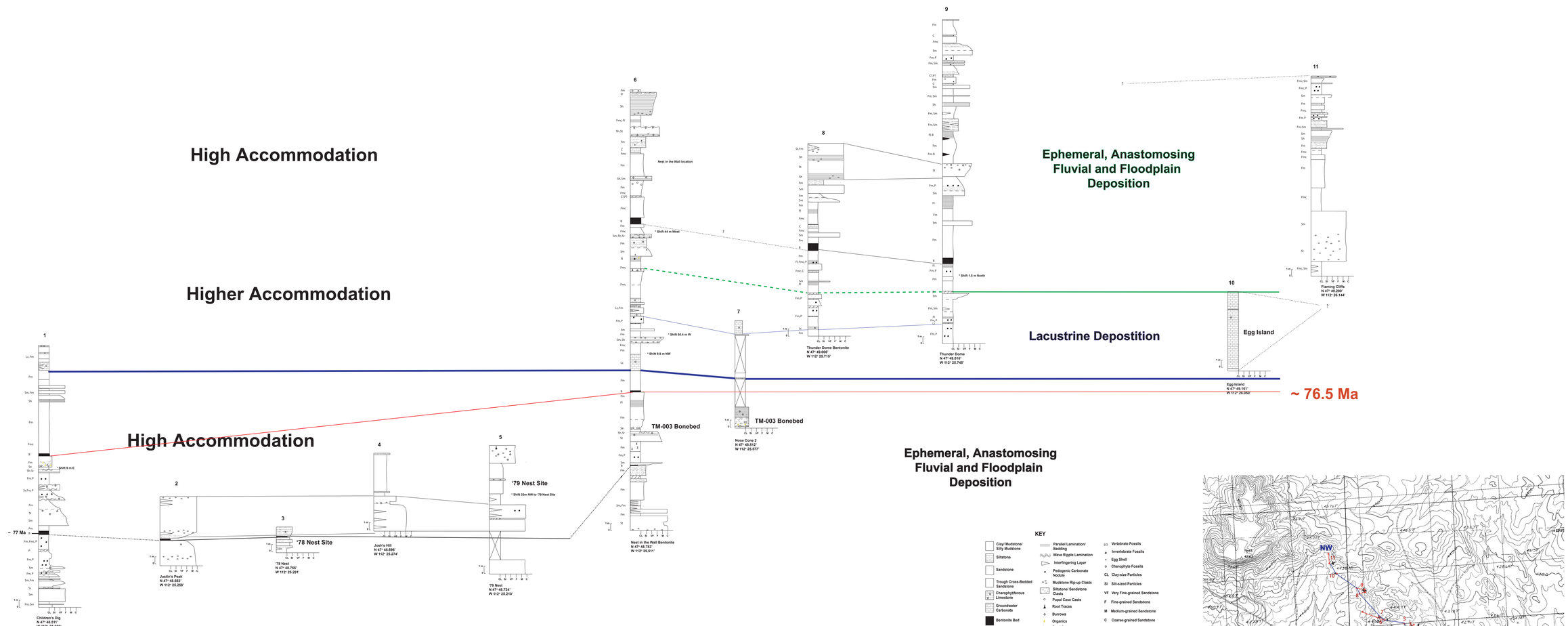

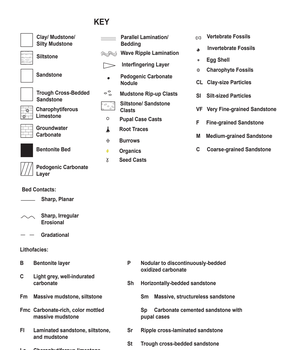

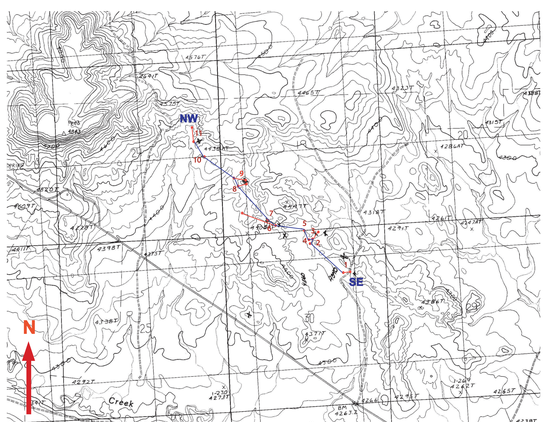

Willow Creek anticline near Choteau, MT
Blow-up of central portion of Watson Flats, MT Quadrangle
Scale 1:24,000
* Measured Sections shown in red
* SE-NW Cross Section shown in blue

1: Children's Dig
2: Justin's Peak
3: '78 Nest
4: Josh's Hill
5: '79 Nest
6: Nest in the Wall Bentonite
7: Nose Cone 2
8: Thunder Dome Bentonite
9: Thunder Dome
10: Egg Island
11: Flaming Cliffs

APPENDIX E

S/SW-N/NE STRATIGRAPHIC CROSS SECTION THROUGH MEASURED SECTIONS

APPENDIX E
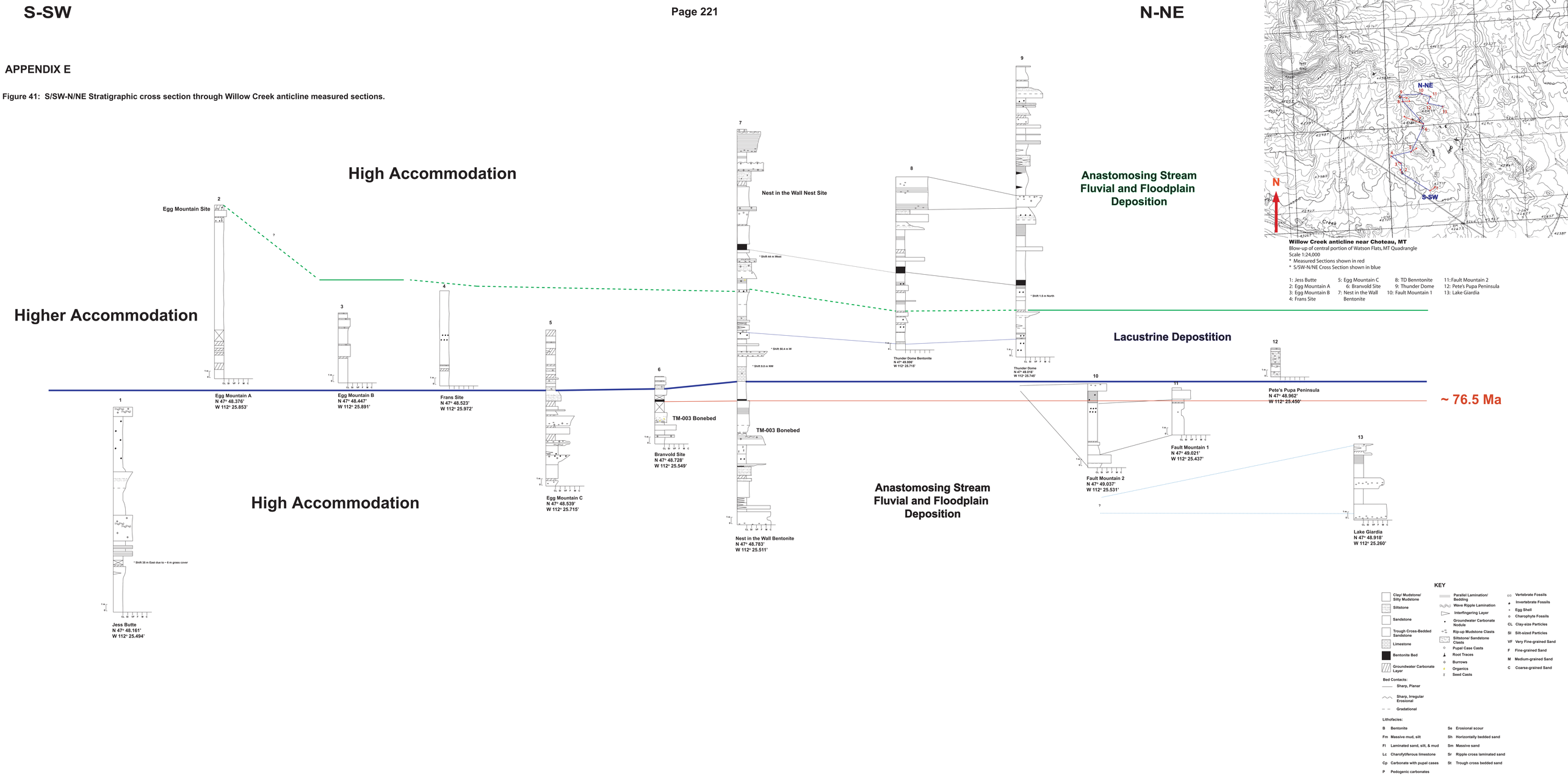
Figure 41: S/SW-N/NE Stratigraphic cross section through Willow Creek anticline measured sections.